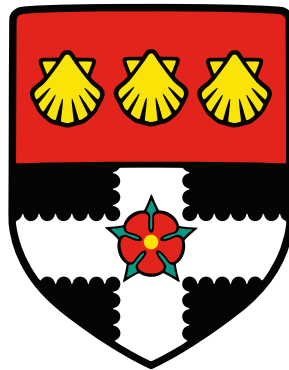# University of Reading

Department of Meteorology

School of Mathematical, Physical and Computational Sciences

Rethinking Reserve Power Systems using Meteorological Data

JAMES COLM FALLON

A thesis submitted for the degree of
Doctor of Philosophy
in Atmosphere, Oceans and Climate

September 2024

In the last 150 years, the world has warmed on average by just over 1 degree Celsius, and our atmosphere now contains concentrations of carbon dioxide that have not been equalled for millions of years. We are today perilously close to tipping points, that once passed will send global temperatures spiralling catastrophically higher. If we continue on our current path, we will face the collapse of everything that gives us our security; food production, access to fresh water, habitable ambient temperature, and ocean food chains. And if the natural world can no longer support the most basic of our needs, then much of the rest of civilisation will quickly break down. Please make no mistake, climate change is the biggest threat to security that modern humans face.

— David Attenborough
Broadcaster and natural historian, briefing the UN Security Council on the maintenance of international peace and security, 2021

We had hopes that rose as proudly
　　As each sculptured marble shrine;
And our prophets spake as loudly
　　As their oracles divine.
Grand resolves of giant daring,
　　Such as Titans breathed of old;
Brilliant aims their front uprearing,
　　Like a temple roofed with gold.

— Jane Wilde
A stanza from Ruins,
Poems by Speranza, 1864

DECLARATION

I confirm that this is my own work and the use of all material from other sources has been properly and fully acknowledged.

James C. Fallon

Acknowledgments

I am incredibly grateful to the Department of Meteorology at the University of Reading for hosting me as a doctoral student, to NERC for funding my studentship, and to BT Group plc. for providing additional CASE funding that has supported my work. I have benefited greatly from my PhD studentship received through the SCENARIO doctoral training partnership, with all of the fantastic teaching, support, and research that is a part of it.

I have been fortunate to benefit from the support and mentoring of my excellent supervisory team: PROF. DAVID BRAYSHAW, who has introduced me to the fascinating and rapidly evolving field of energy-meteorology research, expertly guiding me at every step; PROF. JOHN METHVEN, for meteorological, mathematical and academic insights; KJELD JENSEN (BT Research), for new perspectives, ideas, and statistics expertise throughout my research. Furthermore, I wish to thank LOUISE KRUG (BT Research) for brilliant ideas and enthusiasm and for providing input and feedback on each of my research papers and thank you to the rest of the team at BT Research. Thank you to DR. DAVID GREENWOOD (Newcastle) for expert knowledge in power systems, which has greatly supported this research, especially my third research chapter.

Many more people have been instrumental to my PhD, including my monitoring committee members, PROF. ANDREW CHARLTON-PEREZ and PROF. MICHAELA HEGGLIN, who ensured that my project stayed on track and whose lines of enquiry helped shape the direction that my research has taken.

I want to acknowledge the amazing Energy-Meteorology research group. In particular, thank you to both DR. HANNAH BLOOMFIELD (Newcastle) and DR. PAULA GONZALEZ (Met Office), for all of the encouragement when I first started my PhD and for extensive feedback, input, and kind support in our group meetings and events. Thank you also to IZZI ARIAIL, BEN

ABSTRACT

Critical infrastructure, such as telecommunications networks and hospitals, are typically required to have reserve power systems in place, mitigating power transmission failures. Energy consumption is often highly sensitive to weather conditions and seasonal variation. This thesis demonstrates how weather and climate information can support the efficient design and operation of reserve power systems, and the potential leverage of "surplus" reserve capacity to support the wider electricity network.

First, the weather sensitivity of infrastructure electricity load is characterised for a case study of GB telecommunications assets, with energy consumption well characterised in terms of Heating Degree Day and Cooling Degree Day demand. Having established a temperature-driven model of infrastructure electricity load, a framework for risk-sensitive system design is applied to re-analysis records of temperature to assess the weather and climate resilient design levels for reserve capacity. For GB-aggregate telecommunications assets, the summer peak in energy demand determines the reserve capacity installation requirement, whilst lower levels of energy consumption outside this period result in surplus capacity beyond what is required to maintain operations for the same length of time. This surplus capacity has the capability to support the wider grid during periods of stress.

In a second research chapter, the impact of a changing physical climate on the design and operation of reserve systems is assessed using data from the UK Climate Projections datasets. Focussing on the GB-aggregate telecommunications case study, an application of the Quantile Delta Mapping bias adjustment on climate models improves estimates of long-term variability and climate impact to modelled infrastructure electricity load. With this approach, simulation of climate-risk in models better represents regional internal variability than the limited sample of re-analysis observations, and using future projections shows that further in-

creases to installed capacity are necessary to maintain the tolerated level of risk in reserve systems.

Lastly, introducing models of GB national electricity generation capacity and demand alongside the models of infrastructure electricity load, the potential value of surplus capacity is estimated from the perspective of both the wider grid and the asset owner. Using surplus capacity to support the grid presents a win-win situation, with the Transmission System Operator able to benefit from low-cost capacity to improve system adequacy, and the reserve owner benefiting from new revenue streams for the services provided.

This thesis addresses rethinking the purpose of reserve power systems (currently used or planned) to protect infrastructure. Design decisions can be supported using re-analysis and climate model datasets in a framework for efficient decision-making that represents the underlying weather- and climate-risk. Whilst results relate to the specific case study of GB telecommunications assets, qualitatively similar behaviours are expected in other infrastructure with large backup requirements, including hospitals and data centres (the latter representing a rapidly growing global share of energy consumption), making this research more widely relevant.

With investment into battery energy storage already approaching a break-even point, dual purpose 'surplus' reserves could simultaneously benefit reserve owners (by offsetting the cost of reserve systems through new revenue streams) and can support the energy sector transition to highly-renewable energy supply by providing balancing services to the grid. Beyond the immediate scope of this research, these findings demonstrate the utility of weather and climate information in decision-making.

Authorship of Papers

This thesis is structured around three research papers. Each paper has been prepared for publication and is republished here with minor typographical alterations, reformatting, and revisions to text to improve the continuity within this thesis and avoid repetition. Alterations are summarised in each chapter's preface.

Supporting information is appended to each chapter, and the bibliographies have been gathered into a single thesis bibliography (Page 187). Datasets produced through this research work have been made freely available, with references given in Appendix A.

Publication I (Chapter 3)

The first paper has been published in the Royal Meteorological Society Journal of Meteorological Applications, and may be referenced with the following citation:

Fallon, J. C., Brayshaw, D. J., Methven, J., Jensen, K., Krug, L., 2023: A new framework for using weather-sensitive surplus power reserves in critical infrastructure. *Meteorological Applications*, *30(6), e2158*, https://doi.org/10.1002/met.2158

Estimated contribution: 80 %. JCF developed the conceptualisation and methodology alongside four co-authors to this publication. The analysis and manuscript were produced by JCF, with guidance and input from each co-author supporting this work. Two anonymous reviewers provided feedback on the submission.

vii

Publication II (Chapter 4)

The second paper has been prepared for Meteorological Applications (RMetS) and a manuscript is being prepared for submission. The following citation may be used:

Fallon, J. C., Brayshaw, D. J., Methven, J., Jensen, K., Krug, L., in preparation: Reserve Power Design in Future Climates: Bias Adjustment Approaches for Regional Climate Projections.

Estimated contribution: 80 %. JCF led the conceptualisation and methodology, supported by four co-authors to this publication. JCF conducted the analysis and write-up. All authors discussed the results and commented on the manuscript.

Publication III (Chapter 5)

The third paper has been prepared for Applied Energy (Elsevier), and a manuscript is being prepared for submission. The following citation may be used:

Fallon, J. C., Brayshaw, D. J., Methven, J., Greenwood, D., Jensen, K., Krug, L., in preparation: Weather-driven surpluses in backup energy stores: improving power system adequacy and unlocking the value of decarbonisation.

Estimated contribution: 80 %. JCF developed the methodology, with input from DG and all co-authors. JCF performed all analysis and wrote the manuscript. All authors discussed the results and commented on the manuscript.

Table of Contents

List of Figures

List of Tables

INTRODUCTION

All human civilisations have been affected by climate variability, including extreme weather and climate events. However, anthropogenic climate change is rapidly altering and destabilising the Earth climate. The present and future costs to society in mitigating and adapting to climate risk are driving an increased interest (and need) for the provision of weather and climate information used to support decision-making.

Despite the new and rapidly evolving challenges we now face, recent advances in meteorological observations, modelling, forecasting, and the provision of weather and climate services mean that we are better equipped now, more than ever before, to take climate action.

This thesis addresses the specific case of reserve power systems (used to protect high-value and critical infrastructure assets), with a focus on the specific case of Great Britain (GB) telecommunications service provider British Telecommunications PLC (BT). We demonstrate how state-of-the-art meteorological datasets can be used to support improved design and operation of reserve systems, and may contribute to new operational practices for dispatching *surplus* capacity (of reserve systems). The use of surplus capacity to support the wider grid can contribute to improved energy security and resilience, facilitating a transition to highly renewable energy generation.

1.1 Research Questions

A key challenge for critical infrastructure operators is to ensure that protected assets are resilient to weather and climate impacts, including mitigation of physical hazard risk and ensuring that services continue to operate in extreme situations. Reserve systems of critical infrastructure provide essential social and economic benefits (Guerrero et al., 2007; Chawla et al., 2018), and it is therefore imperative that weather and climate risk is appropriately understood and managed.

Reserve supplies are built to spend most time on standby, only providing electricity supply in unusual situations when the normal power supply is interrupted. These systems can be required to maintain expendable supplies to a provisioned number of days (CISA, 2022), and should therefore be designed with an installed energy capacity, E_{inst}, that can meet the anticipated energy consumption, E, over this period length (for example 5 days).

Infrastructure may experience significant weather-induced and seasonal variations in energy usage, resulting in *surplus* quantities, S, of reserve energy capacity outside periods of potential peak infrastructure electricity load:

$$S(t) = E_{\text{inst}} - E(t) \tag{1.1}$$

where E_{inst} is the installed reserve capacity, and $E(t)$ the anticipated energy consumption from time t to $t + n$ days.

Therefore, flexible use of reserve systems (when they are otherwise not in use) may offer benefits by providing services to the wider electricity network.

The practice of estimating demand for electricity based on weather conditions is well established (Taylor & Buizza, 2003), and in Chapter 3 we address a perceived gap in published literature for the application of these models to understand the weather-drivers of infrastructure electricity consumption, addressing the research question:

i Can weather-sensitive simulation of reserve power systems support resilient system design and furthermore characterise periods of surplus capacity?

Chapter 3 sees the application of the `MERRA-2` historical weather (re-analysis) as input to impact models of infrastructure electricity load. This practice improves upon estimates that would otherwise rely on a small sample of years to address these research questions. However, using re-analysis raises the question of whether the historically observed weather- and climate-variability sufficiently captures the true variability, and additionally the extent to which climate change may affect results.

Climate models simulate alternative realities of the weather spanning decades or centuries. In Chapter 4, `UKCP18` products are applied to the impact model of BT GB aggregate infrastructure electricity load. Focussing separately on the portion of the climate models representative of historic climate, and subsequently on future projections, we address the question:

ii To what extent can climate model simulations improve reserve power system design and quantify trends in surplus capacity?

The potential value of surplus capacity, to both the Transmission System Operator, and to owners of reserve systems is explored in Chapter 5, addressing the question:

iii Is it viable to (re)build reserve power systems to have a low carbon impact, paying for this investment through return of surplus power capacity to the wider grid?

National (GB) power system adequacy is assessed under different scenarios of utilising surplus capacity, indicating the benefit to the wider network. The potential benefits to asset owners is also assessed, using a simulation of and balancing service auctions in order to estimate income and return on investment potential.

1.2   Significance and Impact of this work

The transition to highly renewable power systems is creating a huge demand for providers of short term flexibility: for example 60 GW is anticipated to be required in the United Kingdom of Great Britain and Northern Ireland by 2030 (National Infrastructure Commission, 2023). Rethinking the purpose of reserve power systems presents a win-win opportunity, where low-cost surplus capacity (already required to be built but not always needed throughout the year) is made available to support system adequacy.

Chapters 3 to 4 establish novel uses of meteorological datasets that can support efficient design of reserve power systems, and quantify the potential use of surplus capacity. Chapter 5 is a practical assessment of how this surplus capacity can provide value to the wider electricity network (improving system adequacy), and to the reserve operator (through new revenue streams for services provided).

Stakeholders across sectors are increasingly paying attention to climate risk, and seeking to find co-benefits to de-carbonisation. We hope that this research highlights some of the methods and ideas that can support the use of weather and climate information to meet the challenges of the 21$^{\text{st}}$ century.

LITERATURE REVIEW

2.1 Introduction

The research conducted for this thesis leverages state-of-the-art energy, weather and climate datasets. The work's overarching aim is to support the safety and resilience of critical infrastructure in an optimised and cost effective approach. This work is interdisciplinary, drawing in particular from engineering and meteorological sciences.

We begin this literature review with an introduction to Energy Science (Section 2.1.1), data-driven modelling (Section 2.1.2), and energy-dependent infrastructure protected by reserve systems (Section 2.1.3). Section 2.2 covers in more detail the fundamentals of energy generation and transmission, the economics of energy, and the changes taking place within the energy sector, as renewable energy generation increases.

We apply some of the approaches to modelling demand in Chapters 3 and 4, to model infrastructure electricity demand (and therefore quantify the reserve energy capacity needed to meet a given risk-tolerance), with Chapter 3 first introducing this approach using re-analysis (Section 2.3.2.4), and Chapter 4 discussing how climate variability and projected climate change can be factored into the demand modelling methods (additionally using climate models — Section 2.3.2.5).

Sections 2.2.4 and 2.2.5 sets the foundation for Chapter 5, with a review of energy storage: challenges to quantifying the cost of storage, trade-offs presented by different available and

evolving technologies; and electricity market mechanisms: the design of energy markets and how the capacity market is used to address the adequacy problem, the growing role for demand flexibility. Building on Chapters 3 and 4, Chapter 5 aims to quantify the potential benefit of surplus capacity i) to the Transmission System Operator and ii) to the reserve owner.

Section 2.3 reviews some key applications of weather and climate information. In particular this section focuses on the use cases most relevant to the energy sector: covering topics from the understanding of synoptic scale weather that effects energy systems, to specially tailored provisions of weather and climate data.

Energy, and the science that supports operating complex modern energy systems, is an exciting and rapidly evolving field. This literature review aims to provide a comprehensive foundation to address the key research questions of this thesis (Section 1.1), while also providing relevant background to contemporary energy-meteorology.

2.1.1 ENERGY SYSTEMS LANDSCAPE

> *There is a fact, or if you wish, a law, governing natural phenomena that are known to date. There is no known exception to this law — it is exact so far as we know. The law is called conservation of energy; it states that there is a certain quantity, which we call energy that does not change in the manifold changes which nature undergoes. That is a most abstract idea, because it is a mathematical principle; it says that there is a numerical quantity, which does not change when something happens. It is not a description of a mechanism, or anything concrete; it is just a strange fact that we can calculate some number, and when we finish watching nature go through her tricks and calculate the number again, it is the same.*

Richard Feynman, *The Feynman Lectures on Physics*, 1961
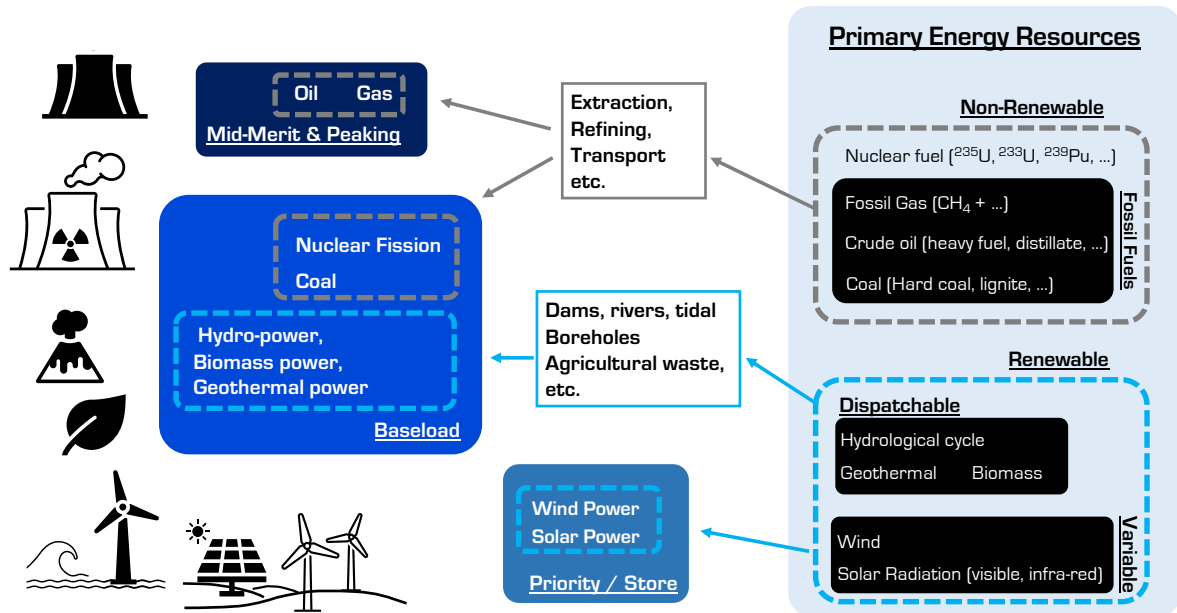
Figure 2.1: Schematic of primary energy resources used in electricity generation. Primary energy resources are naturally occurring sources of energy, that can be converted into useful work. Key considerations of energy sources are: abundance, accessibility, environmental impact, supply chain security, and economic constraints. The prioritisation of power generation sources is described by the Merit Order (peaking, mid-merit, baseload, and non-dispatchable generation), and is discussed in Section 2.2.5.

The First Law of Thermodynamics, alluded to by Richard Feynman in the preceding quotation, states that in a closed system energy is never created and neither is it lost. When a quantity of energy is converted between different forms, it is always conserved. Almost everything we do as living beings relates to the conversion of energy from one form to another, and so this law is fundamental to energy science.

However, our use of the word energy *generation* (and additionally, of *consumption*, *transmission*, …) is not meant in an exactly literal sense (which would invalidate the First Law); we are really referring to processes of useful energy conversion. Our interest lies in the extraction of useful energy from primary energy sources, the transportation of this energy to where it is needed, and ultimately, the application of this energy towards some purpose.

Energy often goes through many transformations before it becomes useful to us. Tracing this chain of conversions backwards will always lead to a form of primary energy, either renewable or non-renewable in nature.

The Second Law of Thermodynamics places a further limitation on energy conversion. This law can be expressed in terms of entropy: in a closed system, entropy will increase over time. This implies that in each process of energy conversion, the quantity of useful high-grade energy becomes more diluted.

Conventional sources of electricity generation (non-renewable resources in the categorisation of Figure 2.1), including coal, gas and nuclear plants, are all thermal power plants which convert generated heat into electrical energy via a turbine. In a conventional thermal power plant, a fluid drives a turbine that, in turn, produces a voltage. In 1824, Nicolas Carnot proved that the maximum possible efficiency of a heat engine (equivalent to an idealised conceptualisation of a thermal power plant) can be derived from the laws of thermodynamics[1], placing a limit on how much energy is extracted from the heat released in combustion or fission processes.

Some renewable energy sources, including windpower and hydropower, also operate on the basis of turbines (but instead of deriving energy from heat, useful energy is extracted from the kinetic energy of wind[2], or released water[3], respectively). Solar panels used in generating electricity operate on the basis of the Photovoltaic (PV) effect: closely related to the photoelectric effect, a material exposed to light generates a voltage and electric current. The maximum power output of solar panels is constrained by both the PV cell efficiency (typically around 20 % Green et al., 2024), and solar irradiance (affected by cosine of latitude and transient effects such as cloud cover).

Figure 2.2 shows global electricity production in recent decades. Electricity production is rapidly growing, reflecting increased energy electrification on top of increasing energy demand globally. In recent years, there has been a large growth in bioenergy, solar, and wind production (compared with negligible levels of production 30 years ago).

One thing that we might wish to know about a particular type of electricity generation (re-

---

[1]A heat engine operating in a closed cycle between two heat reservoirs has efficiency, η_C, dependent upon the ratio of absolute temperatures of the reservoirs: $\eta_C = 1 - T_2/T_1$. A derivation of this is given in Andrews and Jelley (2022, p. 52).

[2]The maximum efficiency of a wind turbine extracting kinetic energy from the wind is given by the Betz limit ($\eta_B = 16/27$), although in practice turbulence, misalignment, and other losses further degrade the efficiency.

[3]The power flow of a water turbine is controlled by dam headheight, and modern turbine designs achieve a power conversion efficiency above 90 % (Kumar et al., 2011).
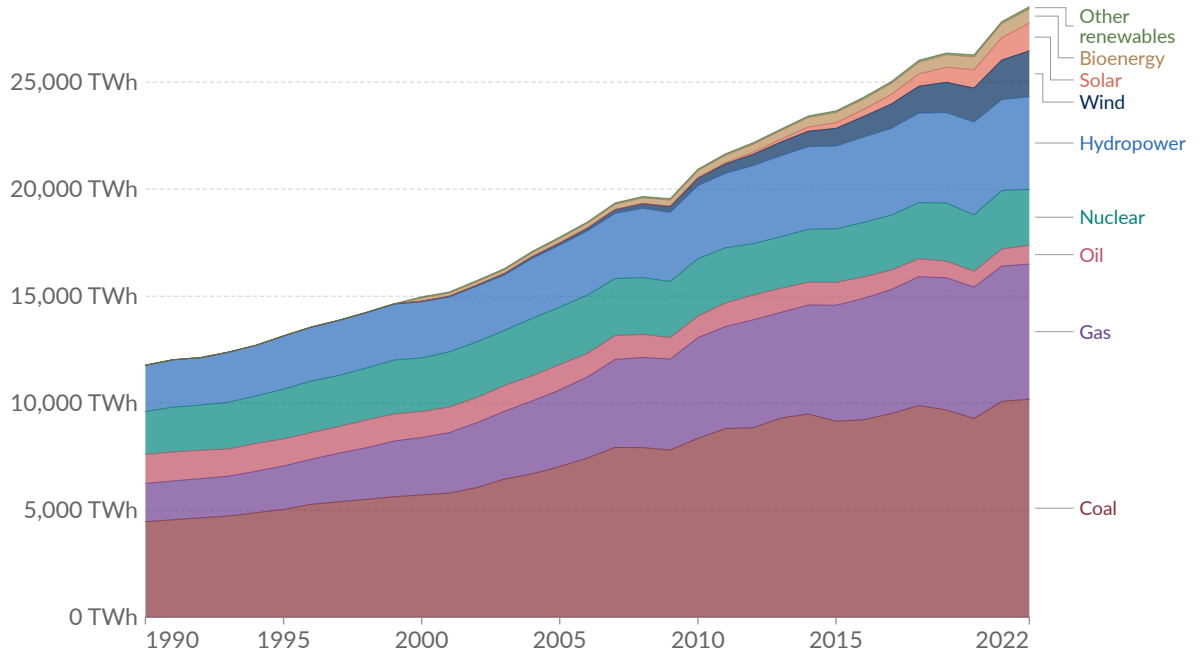
Figure 2.2: Electricity production by source, world total. Note: *Other renewables* includes waste, geothermal, wave and tidal. Source: Ember's Yearly Electricity Data; Ember's European Electricity Review; Energy Institute Statistical Review of World Energy. Figure reproduced from *Energy History*, OurWorldInData.org/energy (Ritchie et al., 2022) CC BY 4.0

newable or non-renewable) is its economic cost. A commonly used metric is Levelised Cost of Electricity (LCoE), the lifetime cost of building and operating some generation capacity (Department for Business, Energy & Industrial Strategy, 2020). Given the long timespan of energy investments, the LCoE is calculated at Net Present Value (NPV):

$$\text{Levelised Cost of Electricity} = \frac{\text{NPV of Total Expected Costs (£)}}{\text{NPV of Energy Generated (MWh)}} \tag{2.1}$$

where the NPV is the sum of a given quantity x_n for each year n reduced by discount rate D[4]:

$$NPV = \sum_n \frac{x_n}{(1+D)^n} \tag{2.2}$$

The costs of wind and solar energy have decreased significantly over the past decade. Fig-

---

[4]A discount rate is used to calculate the NPV of an investment to account for factors including opportunity cost, risk, and time value of money.
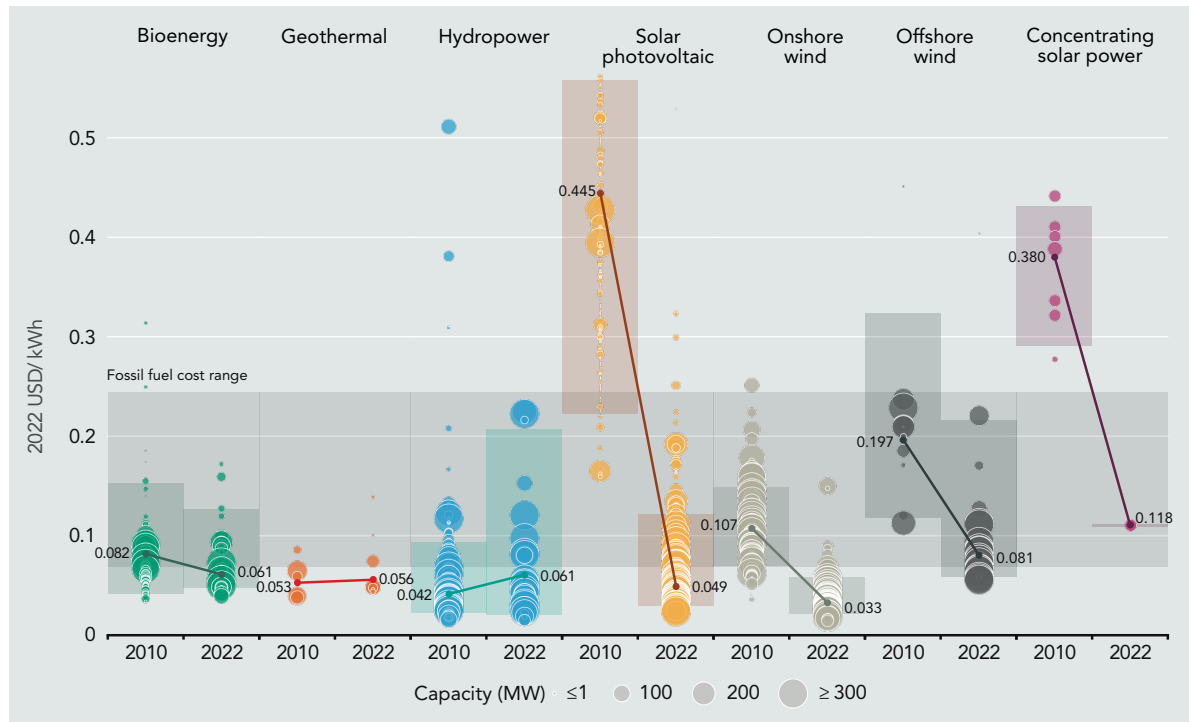
Figure 2.3: Global weighted average Levelised Cost of Electricity (LCoE) from newly com-
missioned, utility-scale renewable power generation technologies, 2010 to 2022. Thick lines
are the global weighted average LCoE value derived from the individual plants commissioned
in each year. Bands for each technology and year represent the 5th to 95th percentile bands for
renewable projects. (IRENA, 2023, Figure 1.2)

ure 2.3 shows the change in LCoE of utility-scale renewable power generation projects, from

2010 to 2022. A 90 % reduction in the global weighted average LCoE of solar PV has been

driven by declining module prices, attributed to a range of factors, including manufacturing

economies of scale and module efficiency gains (IRENA, 2023). Over the same period, the

global weighted average LCoE of onshore wind and offshore wind fell by 70 % and 60 %, re-

spectively.

These reductions bring the technologies into the range of being price-competitive with fossil

fuels. However, the large spread in LCoE values in Figure 2.3 (most notable for hydropower

and solar PV) are indicative of a flaw in the LCoE metric: it is a static measure of costs, and

whilst this reflects some useful information it has limitations.

The design and operation of energy systems is far from a trivial matter, and is indeed the

basis for an expansive and complex field of study: energy system modelling. The LCoE is

a good starting point for comparing and contrasting energy technologies, however, it does not take into account how the generation asset would interact within the constraints of the wider power system. Aldersey-Williams and Rubert (2019), show that LCoE can indicate a minimum required price for a project, but otherwise should not be seen as more than a rule of thumb guide for the actual total cost that would be observed.

Furthermore, the LCoE is also a purely monetary evaluation, whilst in practice power system design is a multi-attribute decision-making problem (Beccali et al., 1998; Pohekar & Ramachandran, 2004; Kaya & Kahraman, 2011; Ilbahar et al., 2019). A more complete evaluation of the value of a generation asset should incorporate an assessment of criteria beyond the direct economic cost, including environmental impact, social acceptability, land use, security, as well as the externalised economic impacts to power system adequacy and the energy market (discussed in Section 2.2.5).

The scope of energy science has expanded greatly over the past few centuries, responding to new technologies, societal challenges, and to political and economic policies. At present, electricity accounts for only 20 % of final energy consumption globally (up from 18 % in 2015). However, energy electrification is increasing, and meeting climate policy goals (that have at least in theory been adopted by various governments) will require electrification to advance significantly faster in coming years (IEA, 2024).

The limitations of metrics such as LCoE for decision-making motivates us to better understand the internal dynamics of power systems, and the relation to investments, risk, and decision-making. Section 2.2 expands on the key topics of energy science that will set the foundations for Chapters 3 to 4. The increasing sensitivity of energy systems to weather and climate is a key consideration for these types of decision-making, and we shall review the scope of weather and climate impacts to energy in Section 2.3.

2.1.2 DATA-DRIVEN IMPACT MODELS

> " *Philosophy is written in this great book open before our eyes: the universe. But one cannot understand it if first one has not learnt the language and become familiar with the characters in which it is written. It is written in the language of mathematics, and the characters are triangles, circles, and other geometric shapes, without which it is impossible to understand the word; without these one wanders a dark labyrinth in vain.* "

Galileo Galilei, *Il Saggiatore*, 1623

Mathematical models underpin our understanding of physics and the natural world, and whilst the models that we use may not always be as accurate as we may desire (for example, processes too complex for us to model may be parametrised and simplified), ultimately, models are successful because they are a representation of deeper underlying effects in our mathematical universe.

Generalised Linear Models (GLMs) and the broader category of Generalised Additive Models (GAMs) encompass many types of statistical model used in practice (Wood, 2017). For example, linear regression and logistic regression models are each a type of GLM (Nelder & Wedderburn, 1972).

GAMs are an extension of the Generalised Linear Model, with a linear predictor involving a sum of smooth functions of covariates. These models can incorporate functions for temporal smoothing, autocorrelated terms, and non-linear terms, as well as facilitate a changing state-space. The models used in this thesis generally fall under the category of GAMs, implementing complex non-linear or time-dependent transformations of variables.

The relations encoded in a model do not have to perfectly represent the real world: 'All models are wrong but some are useful' (George Box). And elaborating on this insight, Box provides

the example that whilst the ideal gas law is not exactly true for any real gas, it nonetheless 'frequently provides a useful approximation and furthermore its structure is informative since it springs from a physical view of the behaviour of gas molecules' (Box, 1979).

It is important to continually evaluate (and where possible) improve upon models. Hamilton et al. (2019) describe a common workflow for model evaluation in environmental science:

1. Identify project context (modelling purpose and problem characteristics)

2. Characterise the outcomes to assess

3. Select methods and evaluation criteria

4. Perform evaluation plan (consider criteria such as model credibility, legitimacy, accessibility, relevance, and impact)

Model evaluation can be conducted in the *model world*, or in a *real-world* context. The model world has some advantages: it is often cheaper and easier to conduct experiments, and allows for simulation of hypothetical scenarios and setups. However, it is also inherently limited, containing simplifications and assumptions that are only addressed with real-world practice. Models work best when there is a close relation to the real-world context (both in terms of accurately representing what is being modelled, and meeting the needs of the model users).

2.1.2.1 IMPACT MODELLING

The term "impact modelling" is somewhat specific to environmental and meteorological sciences and not so widely used outside these fields. As a specific application of statistical methods, the term refers to a method of '[translating] multivariate drivers into a univariate impact, which therefore simplifies event selection' (van der Wiel et al., 2020). Put another way, impact models are a predictive framework used to assess some scenario. We may formulate an impact model as such:

$$\Phi = \mathbf{F}(\mathbf{M}; \mathbf{F_0}) \qquad (2.3)$$
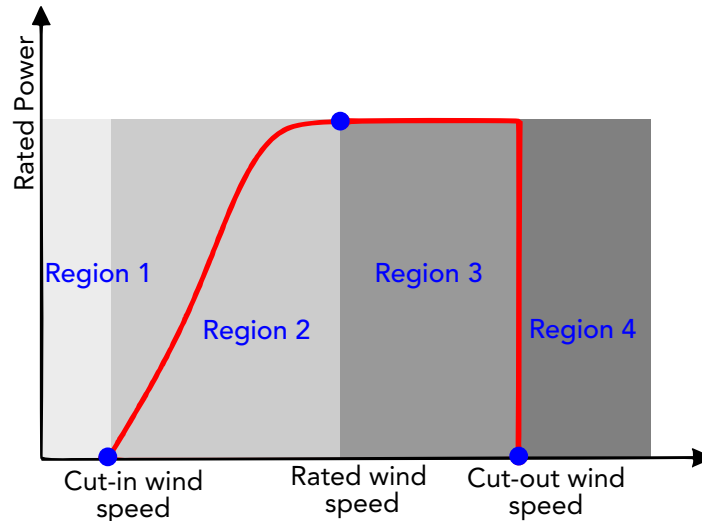
Figure 2.4: A typical wind power curve. Adapted from Wang et al. (2019, Figure 1), with permission from Elsevier.

for a quantitative impact, Φ (representing a set of actionable variables). Φ is determined through the action of a Generalised Additive Model, $\mathbf{F}$ (also known as a transfer function), acting on inputs $\mathbf{M}$. $\mathbf{M}$ could represent a set of time-series data inputs (such as meteorological variables). $\mathbf{F}_0$ is the model initial conditions.

Impact models may make use of a large number of exogenous variables (which may be gridded with latitudinal, longitudinal, or vertical coordinates), require downscaling variables, calibration, and other complex transformations to inputs. The transfer function, $\mathbf{F}$ can often take the simpler form of a GLM, but in some cases the transfer function may be more complex, for example containing non-linear responses to inputs, autoregressive terms, smoothing functions, etc.

In Figure 2.4, a simple example wind power curve can be used for an impact model converting wind speed into wind power potential. In Region 1 wind speeds are too low to drive the turbine. In Region 2, windpower output increases with the third power of Wind Speed. In Region 3, the power output is saturated, and in Region 4 curtailment prevents damage to the turbine.

The relation between windspeed and wind power potential displayed in Figure 2.4 is non-linear, and therefore any errors (systematic or aleatoric) experience a non-linear error propagation. Figure 2.5 demonstrates the asymmetric propagation of errors through the wind power curve,
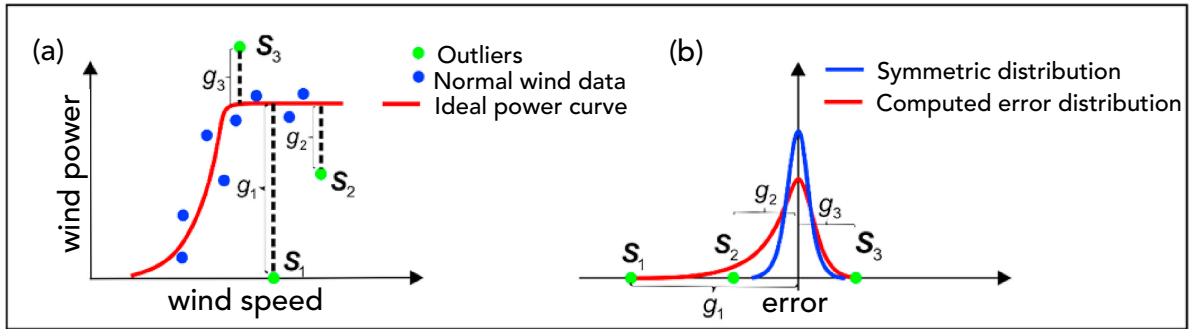
Figure 2.5: The relationship between outliers and error distribution. Adapted from Wang et al. (2019, Figure 16), with permission from Elsevier.

with three types of error outliers indicated (labelled with green markers, S_1, S_2 and S_3).

An initially small error can become magnified and the distortion in the shape of the error can lead to new systematic errors in the impact result. Some error can be reduced through suitable calibration of the model inputs (Gudmundsson et al., 2012; Hawkins et al., 2013; Siegert & Stephenson, 2019; Wang et al., 2019).

Whilst impact models can be developed to an arbitrarily high desired level of complexity, some types of uncertainty can be difficult to manage and foresee. Combinations of weather events that lie at the fringes of or beyond past climate knowns may induce hysteresis or persistent state changes leading to unexpected extreme impacts (M. D. Smith, 2011). Models may also become ineffective in the face of "black swan" events; events that are both exceedingly rare but of an extraordinary and disproportionate impact (Taleb, 2007).

Risk assessment and modelling in the energy sector has traditionally relied upon using recent years' data, limiting the representation of weather variability to only the events realised in those years and therefore missing the variability observed over multi-decade time periods (Craig et al., 2022), or relying on a subset *average* weather sample of 1 to 3 years (Bloomfield, Gonzalez et al., 2021). And despite an increasing number of climate model products, these products have seen insufficient uptake towards informing decisions and policy at sub-national scales (Singh et al., 2018).

However, there is a recent increased appreciation of the need to better represent weather variability. Long-term weather datasets, including re-analyses and climate models, are increasingly

being used in practice to inform impact modelling and risk assessment: for example, with the European Network of Transmission System Operators (ENTSO-E) mid-term adequacy assessments now use large re-analysis datasets in their simulations (ENTSO-E, 2019).

2.1.2.2 STOCHASTIC MODELS

A stochastic process describes a variable (or collection of variables) that evolves over time and involves a stochastic component (a random or pseudo-random component). An impact model may implement a stochastic component on top of its *deterministic* component (Φ, the part of the model where a given input corresponds to a known, calculable output), in order to represent missing effects and variability in the model. This stochastic model, Φ_{stoch} may be written:

$$\Phi_{\text{stoch}} = \mathbf{G}(\mathbf{M}; \mathbf{G}_0) \tag{2.4}$$

where $\mathbf{G}$ is a stochastic model (with potentially complex properties including state memory) and $\mathbf{M}$ is the collection of input variables (as in Equation (2.3)) and $\mathbf{G}_0$ the function initial state. The stochastic model must be computed repeatedly, generating many unique realisations. A sufficiently large collection of realisations can be used to compute results such as mean values or percentile likelihoods for a given deterministic input.

Some stochastic models are expressed as a multiplicative term acting on deterministic inputs:

$$\mathbf{G}(\mathbf{M}; \mathbf{G}_0) = \mathbf{F}((\mathbb{1} + \xi)\mathbf{M}; \mathbf{F}_0) \tag{2.5}$$

where $\mathbb{1}$ is the identity matrix, and ξ is a matrix of the stochastic components acting on $\mathbf{M}$.

Stochastic models have been applied to represent parameter uncertainty, for example, in Numerical Weather Prediction weather and climate model parametrisation schemes (Wilks, 2008; Palmer et al., 2009), and in correcting ensemble spread (van Leeuwen, 2020). In Buizza et al. (1999), multiplicative noise terms perturb the parametrised physics tendency of variables, in-

cluding wind components, temperature and humidity, with values of ξ drawn from the uniform distribution in the range $[-0.5, 0.5]$.

In Chapter 3, modelling the residual missing variability forms a crucial part of the analysis of modelled infrastructure electricity load, with benefits such as an improved estimation of the extreme values (and hence an appropriate value can be determined for the size of reserve energy capacity). This residual variability is represented with an additive stochastic term:

$$\Phi_{\text{stoch}} = \Phi + \varphi \tag{2.6}$$

with φ representing residual non-meteorological variability implemented as Gaussian noise with a one-day lag autocorrelation[5].

There are many ways of formulating stochastic models. Stochastic auto-correlation can be simulated in continuous variables using a lag component (Chatfield, 2003), as is the case for Chapter 3's implementation of Equation (2.6). There are also cases where this approach may not be feasible, for example, generator unavailability models used to model power outages and simulate the two-state process of power system components (Deakin et al., 2022). Since outcomes are dichotomous, a lag component won't work. However, a Markov-chain method is able to achieve the desired state-dependent effect (Zhang et al., 2016).

Stochastic models have many other applications in fields including economics (Dupačová et al., 2005), biology (Wilkinson, 2018), telecommunications (Brayshaw et al., 2020) and in energy: for example, stochastic processes are the basis of stochastic optimisation (also known as stochastic programming) which is used in capacity expansion planning problems to support the efficient design of power systems (Rezvan et al., 2013; Mavromatidis et al., 2018; Pickering & Choudhary, 2019).

---

[5]This form of impact model can equally be written in the matrix form of Equation (2.5), albeit with a more cumbersome notation: in this case, appending a unit column $\begin{pmatrix} 1 & 1 & \cdots & 1 \end{pmatrix}$ to $\mathbf{M}$ and allowing ξ to represent a sparse matrix with a column containing the values of φ aligned with the unit column of $\mathbf{M}$

2.1.3 INFRASTRUCTURE AND RESERVE SYSTEMS

> 66 *Unless we act now, the 2030 Agenda will become an epitaph for a world*
>
> *that might have been.*
> 99

António Guterres, *Secretary-General of the United Nations*, 2023

Infrastructures are basic essential services that support socio-economic development. International standardisation frameworks have adopted a common definition.

ISO/TC 292, CEN/TC 391: Infrastructure

Infrastructure (3.1.128): system of facilities (3.1.104), equipment and services needed for the operation of an organization (3.1.165)

Infrastructure can be categorised in many ways, for example, into publicly and privately owned assets; economic infrastructure and social infrastructure; 'hard' infrastructure (tangible, practical facilities and equipment such as roads and power systems) and 'soft' infrastructure (services such as financial and education systems) (Dyer et al., 2019).

2.1.3.1 INFRASTRUCTURE AND SUSTAINABLE DEVELOPMENT

The United Nations Sustainable Development Goals (SDGs) are a collection of 17 interconnected goals developed in a global partnership and are an urgent call for action by member states. 'They recognize that ending poverty and other deprivations must go hand-in-hand with strategies that improve health and education, reduce inequality, and spur economic growth — all while tackling climate change and working to preserve our oceans and forests.' (UN Department of Economic and Social Affairs, 2023).

The 7th and 9th SDGs relate closely to the research matter of this thesis:

SDG 7 To ensure access to affordable, reliable, clean and modern energy for all.

SDG 9 Towards building resilient infrastructure, to promote inclusive and sustainable industri-
alisation, and to foster innovation.

Without an immediate intervention to the SDGs, including Goal 7 (Energy) and Goal 9 (In-
frastructure), a projected middle-of-the-road development scenario sees only half of SDGs
being met by 2030, with 15 % of countries projected not to achieve any goals (as measured by
a reduced set of indicators, Moyer and Hedden (2020)).

Lack of access to modern energy contributes to hunger and indoor air pollution, among other
negative social and economic impacts (Sovacool, 2012; IEA, 2023b). International public fin-
ance for clean energy for developing countries continues to decline, whilst 675 million people
live in energy poverty (UN Department of Economic and Social Affairs, 2023).

Recent high inflation, energy price shocks, and supply chain disruption have contributed to
a slowing in manufacturing employment globally, and in least developed countries signific-
antly more investment is needed in advanced technologies, telecommunications, and lowering
carbon emissions to achieve Goal 9 by 2030 (Leal Filho et al., 2023).

2.1.3.2 CRITICAL INFRASTRUCTURE AND FACILITIES

Critical infrastructure (also known as *national infrastructure*) are the facilities, systems, and
networks of people and information that are essential for the functioning of a society and its
economy. These infrastructures are deemed critical because disruption or destruction of their
assets could have serious social consequences (public health and safety), detrimental economic
effects, or significant impacts on national security or the functioning of the state. (Department
of Homeland Security, 2013; Abbott et al., 2018; CPNI, 2021).

ISO/TC 268: Critical Infrastructure

Critical infrastructure (3.1): physical structures, facilities, networks and other
assets which provide services that are essential to the social and economic
functioning of a community or society

Governments are responsible for ensuring that critical infrastructure is resilient to risk, although this infrastructure is increasingly owned, administered and operated by private sector organisations (Pursiainen & Kytömaa, 2023).

In the UK, there are 13 defined national infrastructure sectors: Chemicals, Civil Nuclear, Communications, Defence, Emergency Services, Energy, Finance, Food, Government, Health, Space, Transport, Water (CPNI, 2021).

The definition of critical infrastructure varies by country; for example, the *Bundesamt für Sicherheit in der Informationstechnik (Federal Cyber Security Authority of Germany)* have adopted a similar definition to that of the UK government, but place a greater emphasis on information security and cyber threats. Other countries may not have any specific laws or regulations addressing the security and resilience of critical infrastructure at a national level, but it is common for governments to require that these types of assets undergo risk assessments and take sufficient measures to de-risk.

The implementation of critical infrastructure and attained levels of resilience in many least-developed countries remains distant from SDG targets. Many least-developed countries in Asia remain off target to meet the 2030 SDGs despite recent rapid economic growth and development (UN Department of Economic and Social Affairs, 2023).

The energy security of critical infrastructure is a vital aspect of ensuring resilience and reliability, and has many interdependencies with other critical infrastructure (Rinaldi et al., 2001). Regulations relating to the provision of energy security measures, such as putting in place reserve power systems, vary by country, and for large portions of the world population in low- and lower-middle income countries, much of the critical infrastructure that exists has unreliable electricity supply or no electricity access at all (WHO et al., 2023).

2.1.3.3 Reserve-Protected Infrastructure

Critical infrastructure and other infrastructure may be required to maintain expendable supplies up to a provisioned number of days. For example, the Cybersecurity and Infrastructure

Security Agency (of the United States Department of Homeland Security) define power resilience levels that infrastructure operators may want to incorporate into planning (CISA, 2022). These recommendations range from minimum protection guidance (Level 1) to maximum protections (Level 4):

1 Incorporates cost-effective best practices to maintain power in critical operations. Typically, expendable (e.g. fuel) supplies should be maintained for three days under "all hazards".

2 Further improved power resilience above Level 1's cost-effective practices. Typically, expendable supplies should be maintained for seven days under "all hazards".

3 Further improved power resilience above Level 2. Typically, expendable supplies should be maintained for around 30 days under "all hazards".

4 Systems should be implemented to ensure no unplanned downtime. Typically limited to the *most* critical infrastructure (including military, government).

Energy supply in present day reserve system fleets is dominated by fossil fuel generators, in particular diesel generation. These systems are known to have large CO_2 emissions, presenting a potential challenge to the decarbonisation aims of companies, and to country level Nationally Determined Contributions (NDCs).

In power systems with frequent outages, the cost of energy production and the resulting pollution from diesel generators can be many times greater than would be achieved from improved nationally distributed power production (Farquharson et al., 2018). In countries with reliable power systems, fossil fuel generators present lesser health and environmental hazards and there is little immediate economic incentive to reduce their use. Developing suitable long-term energy storage systems, which are affordable, reliable, and can guarantee energy security, is a necessary but challenging goal for reserve operators to address in coming years.

To address local pollution issues, and align with NDCs to emissions reductions, it will become increasingly important to phase out and replace legacy generation technology with clean

alternatives. Fuel substitutions, such as bio-diesel, offer marginal improvements (US EPA, 2014), but in the long term, it will be necessary to move to low and zero-emissions technologies, with some current and emerging energy storage technologies offering potential alternatives (see Section 2.2.4).

2.1.3.4   RESILIENCE, MITIGATION, ADAPTATION

Risk is the effect of hazard uncertainty on objectives (and how we manage it). In the context of evolving infrastructure and climate change, it is necessary to constantly monitor and update our understanding of risk to ensure that infrastructure is resilient. The Sendai Framework for infrastructure resilience (adopted by United Nations member states) aims to 'substantially reduce disaster damage to critical infrastructure and disruption of basic services, among them health and educational facilities, including through developing their resilience by 2030' (UN Office for Disaster Risk Reduction, 2022).

ISO/TC 292, CEN/TC 391: Risk & Resilience

Risk (3.1.215): effect of uncertainty on objectives (3.1.162)
Resilience (3.1.206): ability to absorb and adapt in a changing environment

---

The scope of risk and resilience refers to all kinds of risk, not just risk stemming from natural hazards. Risk registration may include categories for: terrorism; cyber risk; state threats; geographic and diplomatic risks; accidents and systems failures; natural and environmental hazards; human, animal and plant health; societal risks; conflict and instability (Cabinet Office (UK), 2023).

Two key challenges in mitigating risk in infrastructure are *complexity* and *uncertainty* (Hall et al., 2017). Complexity arises from the number of moving parts, and interconnectedness between sectors. Multi-hazard risk assessments and modelling approaches can be used to assess compounding risk in critical infrastructure (Kappes et al., 2012; Liu et al., 2016; Wells et al., 2022).

No system can achieve 100 % resilience — things will always go wrong. Cabinet Office (UK)

([2014](#)) define a list of *four R's* of critical national infrastructure resilience:

- **Resistance**: Direct physical protection of assets (such as flood defence)

- **Reliability**: Capability of infrastructure to maintain operations under extreme conditions (including winterisation of power infrastructure)

- **Redundancy**: The adaptability of an asset or network (for example, backup power supply)

- **Response and Recovery**: Ability to act quickly and resume critical functions following disruption

Implementations for resilience must balance these *four R's*, assessing components for their appropriateness and cost-effectiveness. Operators of critical infrastructure can increase the resilience of systems to extreme weather impacts using *i) appropriate preventive measures*, and additionally, operators may take action *ii) when an event is approaching*, with the aim of reducing its impact (Groenemeijer et al., [2015](#)).

2.1.3.5   RELATING CASE STUDY RESULTS TO OTHER INFRASTRUCTURE

Demand for digital services is rapidly increasing — from 2010 to 2023 internet traffic increased by 2400 %. Energy efficiency measures have helped to limit the growth in energy demand of data centres, which currently accounts for 1 % to 1.3 % of global electricity consumption and is projected to continuing growing in the near term (IEA, [2023a](#)).

Some smaller countries with expanding data centre markets are seeing much larger growth in the sector; for example, in Denmark data centre use is projected to increase 500 % by 2030, accounting for 15 % of electricity use, and in Ireland the demand could rise to 30 % by 2030 (IEA, [2023a](#); Ryan-Christensen, [2022](#)).

Given the increasing proportion of electricity consumption allocated to data centres, these should be a key focus for the potential application of the research conducted in this thesis,

alongside other sectors that also have access to large reserve systems (and potential periods of surplus capacity). The findings in this thesis could apply to many critical infrastructure sectors, including water treatment, healthcare, food, and government.

A case study of GB telecommunications infrastructure assets is examined in Chapters 3 to 5. Although results rely on models specific to British Telecommunications PLC (BT) infrastructure in studied regions, other infrastructure is known to exhibit qualitatively similar weather sensitivities, including data centres (Oró et al., 2015; Avgerinou et al., 2017) and hospital infrastructure (Burpee & McDade, 2014; Mustafa et al., 2021). Therefore, we expect many other types of infrastructure to exhibit analogous behaviours and for results to be relevant in these cases.
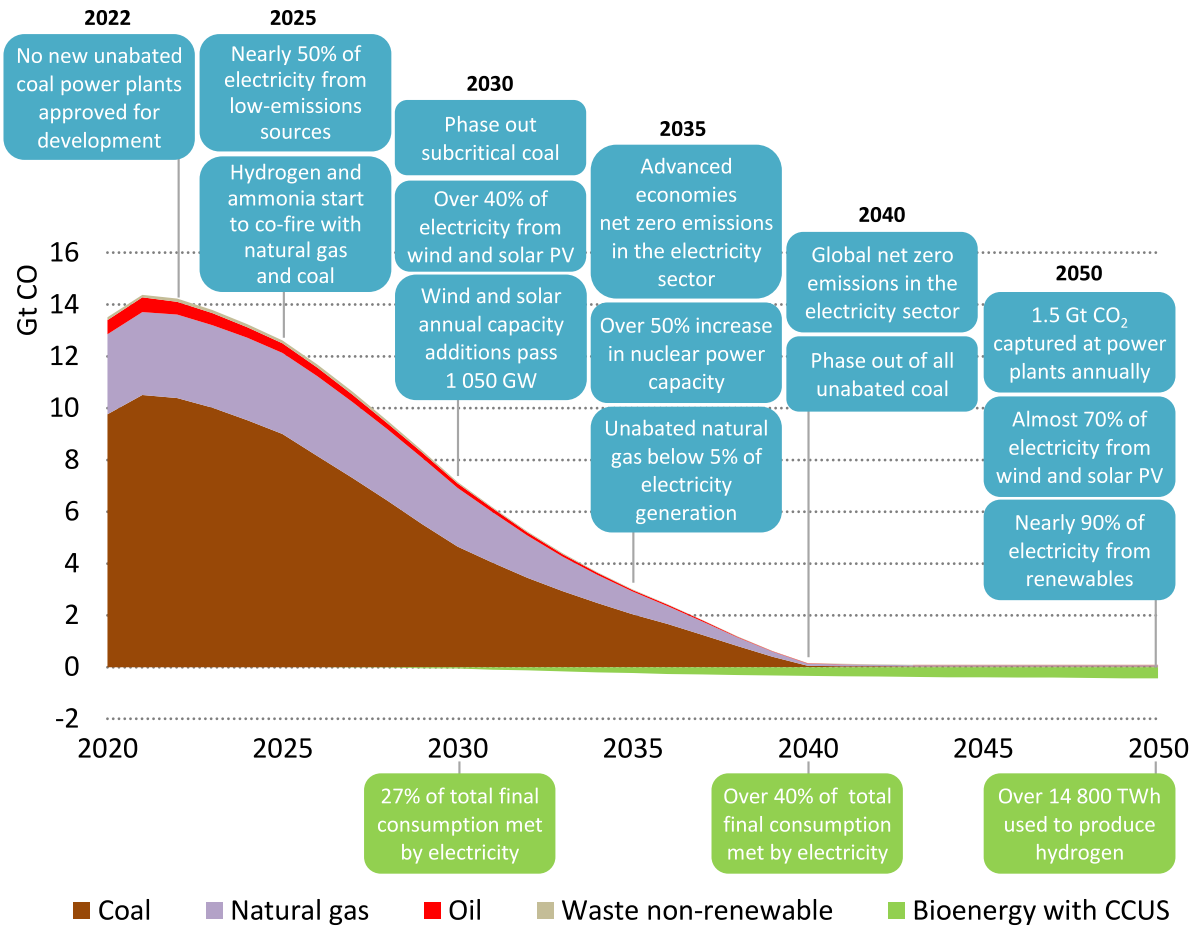
Figure 2.6: CO_2 emissions by source and key milestones in the electricity sector, in the IEA net-zero emissions scenario, 2020 to 2050. Note, CCUS is *carbon capture, utilisation and storage*. (IEA, 2022, Figure 3.9 CC BY 4.0).

2.2 The Future of Energy Systems

2.2.1 ELECTRICITY GENERATION

The electrification of energy and the increased use of renewable energy sources are changing the way that we think about power systems. Figure 2.6 shows a roadmap towards a decarbon-ised global electricity sector, with the share of renewables more than doubling by 2030 (to 60 %), and reaching almost 90 % in 2050 (supported by bioenergy, nuclear power, and fossil fuel generation with Carbon Capture, Utilisation and Storage).

The roles and challenges faced by power system operators are rapidly evolving, with a growing

use of variable generation, interconnectors (importing and exporting energy across national borders) to secure power, and Distributed Energy Resources increasingly used to assist balancing supply and demand. These terms are accurate for present-day GB, but this terminology has evolved over time and may differ in other locations.

Whilst conventional electricity generation is dispatchable, i.e. power output can be controlled and turned up or down to match demand, some renewable energy technologies including wind and solar power are not dispatchable. When non-dispatchable electricity sources are operating, the generated energy should receive priority for its use or placed into available energy stores, since the marginal cost is effectively zero. In an ideal scenario, energy generation will be secured from the sources which are cheapest to operate first (see discussion of the merit order effect in Section 2.2.5).

2.2.2 MODELLING ELECTRICITY CONSUMPTION

Attempting to characterise and model electricity demand is of great importance to a great number of stakeholders. For households, it can be important to track yearly, monthly, or even daily consumption of electricity in order to manage usage (and the associated costs). For Distribution System Operators (DSOs) and Electricity System Operators (ESOs), ensuring the security of energy supply requires tracking and forecasting consumption at timescales ranging from day-ahead markets to years ahead. At much shorter timescales (intra-day), supply and demand must be accurately balanced to ensure that correct grid frequency is maintained, and avoiding voltage drops on parts of the network.

A naïve model of electricity demand ($\hat{D}$) can be designed that persists the *observed* demand D to the subsequent timestep:

$$\hat{D}_t = D_{t-1} \tag{2.7}$$

The persistence model can in some situations perform remarkably well, since many of the conditions that may lead to suppressed or exaggerated levels of demand typically persist over

time.

More advanced models, still relying only on observations, can be implemented by analysing historical patterns, and a popular method is the modelling approach of Box et al. (2015): the ARIMA model.

$$\hat{D}_t = c + \sum_p \phi_p D_{t-p} + \sum_q \theta_q \epsilon_{t-q} \qquad (2.8)$$

The ARIMA model, without differencing[6], is composed of a constant (c), a linear combination of up to p lags (the autoregressive term $\sum_p \phi_p D_{t-p}$), and up to q lagged forecast errors (the moving average term $\sum_q \theta_q \epsilon_{t-q}$). In its most basic form, the ARIMA model can be reduced to a persistence model[7].

An extension of the ARIMA model, SARIMA, introduces additional autoregressive and moving average components to capture seasonality effects; including weekday and holiday effects, seasonal patterns, and diurnal cycle effects for data with sub-daily time intervals.

Given sufficient historical observations (ideally multiple years of data that encode seasonality), the ARIMA approach can perform exceedingly well for many purposes, including modelling or forecasting demand, and has been a popular tool in electricity price forecasting (Contreras et al., 2003). However, the use of weather forecasts for electricity demand forecasting can provide better predictions. De Felice et al. (2013), demonstrate that using temperature data obtained from Numerical Weather Prediction (NWP), considering both re-analysis and operational forecasts of gridded weather data, an improved model of electricity demand is constructed, which outperforms ARIMA alone at a lead time of 1 to 5 days in the context explored (i.e. demand forecasting over Italy).

The superior performance gained using weather forecasts arises from the substantial role temperature plays in affecting electricity demand levels (Houthakker & Taylor, 1970; Bessec &

---

[6]The differencing parameter d can be introduced, specifying how many times the original time series is differenced to achieve stationarity. With stationarity achieved, the ARIMA model is applied to the differenced timeseries.

[7]Achieved by setting $c = 0$, $\phi_1 = 1$, $\phi_p = 0 \ \forall p > 1$ and $\theta_q = 0 \ \forall q$.
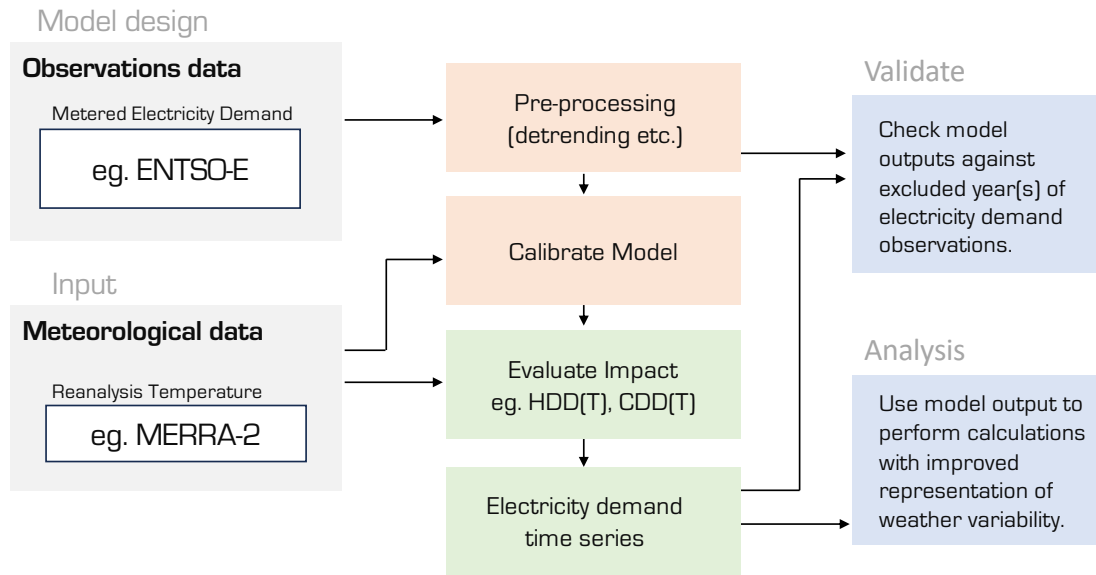
Figure 2.7: Demand modelling schematic: Meteorological inputs are used with electricity training data observations to construct a model for electricity demand (this could be at a national level, or targetting a specific subset of demand).

Fouquau, 2008; Thornton et al., 2016).

In Figure 2.7 we characterise a typical workflow for processing temperature data into a demand timeseries (as used in Chapter 3, Bloomfield et al. (2020), `MERRA-2 derived demand, wind and solar power`, etc.). The model can be constructed using national electricity demand, or focus on smaller scales, for example, modelling residential electricity demand in a restricted region or electricity demand corresponding to a specific industry.

The electricity demand response to temperature-sensitive assets, including cooling equipment, irrigation, refrigeration, space heating, etc., can be well modelled through the implementation of Heating Degree Day (HDD) and Cooling Degree Day (CDD) functions (McVicker, 1946; Billington, 1966; Hitchin, 1981; Taylor & Buizza, 2003).

Typically, these functions take the form of applying a linear function response to temperatures beyond a threshold range:

$$
\text{HDD}(T) = \begin{cases} T_{\text{HDD}} - T & \text{if } T < T_{\text{HDD}} \\ \\ 0 & \text{otherwise} \end{cases}
$$

$$
\text{CDD}(T) = \begin{cases} T - T_{\text{CDD}} & \text{if } T > T_{\text{CDD}} \\ \\ 0 & \text{otherwise} \end{cases}
$$

(2.9)

However, variations and alternative formulations of Equation (2.9) are relatively common. One can take a standard implementation of the degree days (and the pre-calculated coefficients), or alternatively, a better fit of coefficients or design of the function can be explored for a particular application. The correct model that represents national electricity demand is likely to look different to a model of residential demand, or electricity demand of a specific industry sector (as we shall see in the model of BT infrastructure developed in Chapter 3).

Variations in this style of workflow (Figure 2.7) can be used to model residential, infrastructure or regional/national electricity demand. For example, the degree day functions can be modified to use a building-adjusted internal temperature (a proxy for the temperature *feel-like* impact), accounting for solar irradiance, wind chill, humidity, and thermal inertia (Staffell et al., 2023). Non-meteorological effects such as day of the week and holiday day effects should also be accounted for (Bloomfield, Wainwright & Mitchell, 2022).

Residential cooling demand is sensitive to temperature and relative humidity (Maia-Silva et al., 2020). An alternative method for simulating cooling demand is the Enthalpy Latent Day, which accounts for humidity effects on air-conditioning demand (Hor et al., 2005). For heating-sensitive demand, variables including wind chill (combining temperature and wind thresholds) can improve demand models (Deakin et al., 2021).

Figure 2.8 demonstrates the processing steps used to model electricity demand (showing the case for France, although the same approach is used for 32 European countries), as implemented for the Copernicus Climate Change Service (C3S) Energy service. A generalised additive model uses detrended country-averaged daily temperature and calendar/holiday markers to train the model on 2010 to 2014 electricity observations (ENTSO-E load) and perform a model
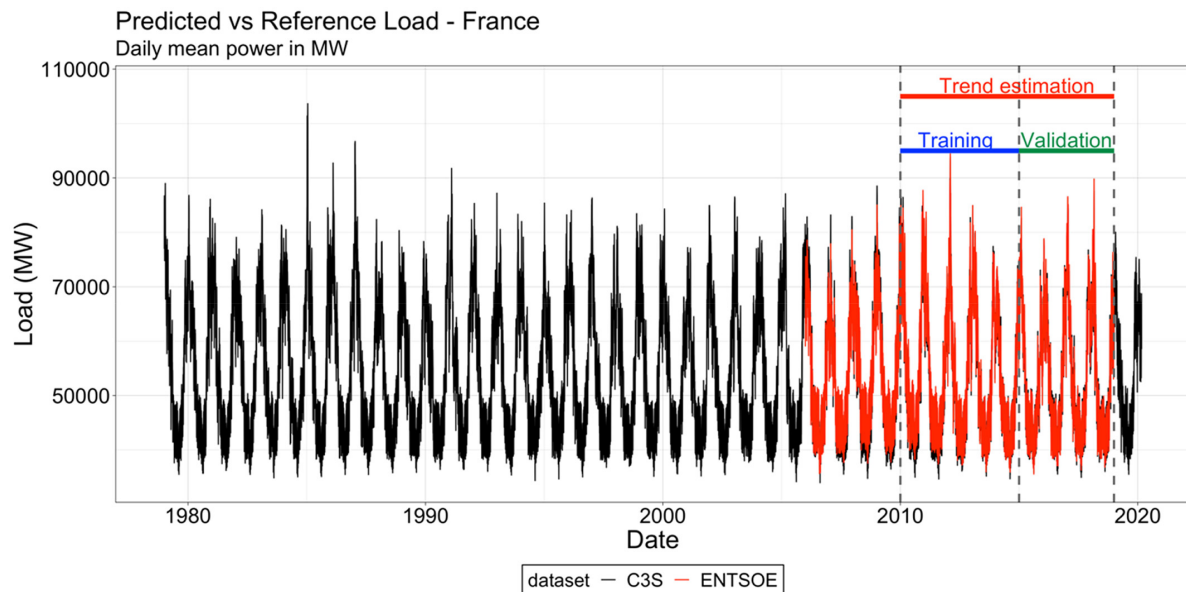
Figure 2.8: Model set-up steps for the case of France national electricity load, used in the EU C3S operational climate services for Energy. Load is expressed as the daily mean power demand (MW). The red curve corresponds to the ENTSO-E PS data. The black curve is the C3S-E reconstructed demand. The red, blue, and green horizontal lines represent the trend estimation, training, and validation period duration respectively. Figure republished from Dubus et al. (2023, Figure 3 CC BY 4.0).

verification over the period 2015 to 2018.

Figure 2.9 shows the validation results for four of the C3S models of national electricity demand. There is a very good fit in some regions between the ENTSO-E reference values, and the model reconstructed values of demand, with this skill benefiting from predictable seasonal, weekly, and daily calendar variations. Poorer results are observed in the UK, relating to quality issues in its ENTSO-E demand data European Commission Internal Energy Market, 2018

Modern predictive tools increasingly draw upon machine learning methods, including support vector machines and neural network approaches, to assign complex (e.g. non-linear) functions and weightings to the inputs (including meteorological observations and forecasts) to forecast electricity load (De Felice et al., 2015; Jasiński, 2020; Hong et al., 2023).

An important effect of models that may need to be considered is the represented variability. A model might have good predictability with respect to one or more inputs (for example, *perfectly* representing the demand-temperature impact), but it may fail to accurately represent
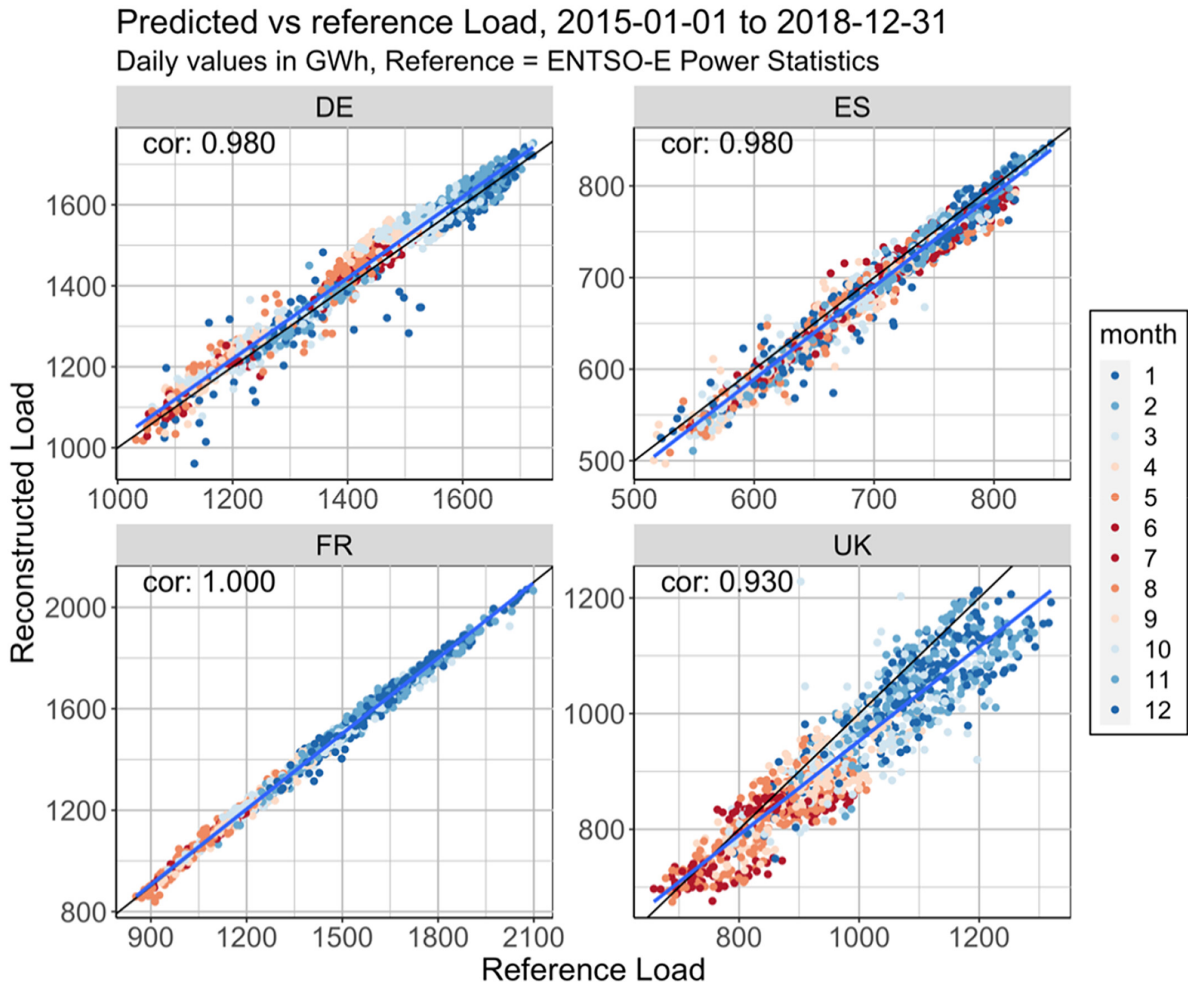
Figure 2.9: Scatter plots of simulated versus reference demand on the period 2015 to 2018 for four countries (Germany, Spain, France, United Kingdom), used in the EU C3S. Hue indicates the month (red for summer and blue for winter). Correlation coefficients are indicated on each panel. Diagonal black line indicates a 1:1 fit, and blue line is the linear fit. Figure republished from (Dubus et al., 2023, Figure 9 CC BY 4.0).

finer detail in the relation (e.g. diurnal variability or differences arising from downscaled vs. aggregated data). One source for a misrepresentation of variance can be the input timeseries. For example, using data at a 60 km resolution to model the electricity demand of a single residential unit will miss some of the finer-scale urban meteorology and downscaling effects. Electricity demand models can use downscaling methods to correct for some scale differences (Eskeland & Mideksa, 2010).

A model may instead perfectly represent the weather-induced response variability but fail to implement some unknown (perhaps even unknowable) effect — for example, accurately mod-

elling the electricity demand of a small village may depend upon the exact timings of individual people turning their kettles on, but this is in practice unknowable. We can use stochastic model to represent these kinds of pseudo-random effects (as in Section 2.1.2.2). In Chapter 3, modelling the residual missing variability forms a crucial part of the analysis of modelled infrastructure electricity demand, with benefits such as an improved estimation of the extreme values (and hence, an appropriate value can be determined for the size of reserve energy capacity).

In this thesis, we implement a degree-day stochastic model of infrastructure electricity demand for a case study (GB telecommunications). This model allows exploration of how infrastructure electricity demand would respond to a given temperature timeseries. In Chapter 3, we use re-analysis observations to simulate the extreme heating and cooling demand events that would have occurred to the present infrastructure had it experienced simulated historical weather events. Chapter 4 extends the model to a simulation of alternative historical and future climate scenarios, using climate model data.

2.2.3 Transmission of Electricity

Most energy generation resources will typically join a wider power system network (rather than supplying off-grid energy). A schematic of a power system network for a typical developed country is shown in Figure 2.10. At a national level, the Transmission System Operator (TSO) and ESO oversee the procurement of energy from different sources. Power is transmitted at a high voltage to a local area, where the Distribution Network Operator (DNO) and DSO oversee local distribution to industry and households.

The Joule-Lenz law states that the heating losses generated in cables shall equal the product of resistance (R) and square of current (I):

$$P_{\mathrm{loss}} = I^2 R \qquad\qquad (2.10)$$

At a given power output the voltage is inversely proportional to current, and hence from Equation (2.10), a reduction in heating losses is quadratic with voltage.
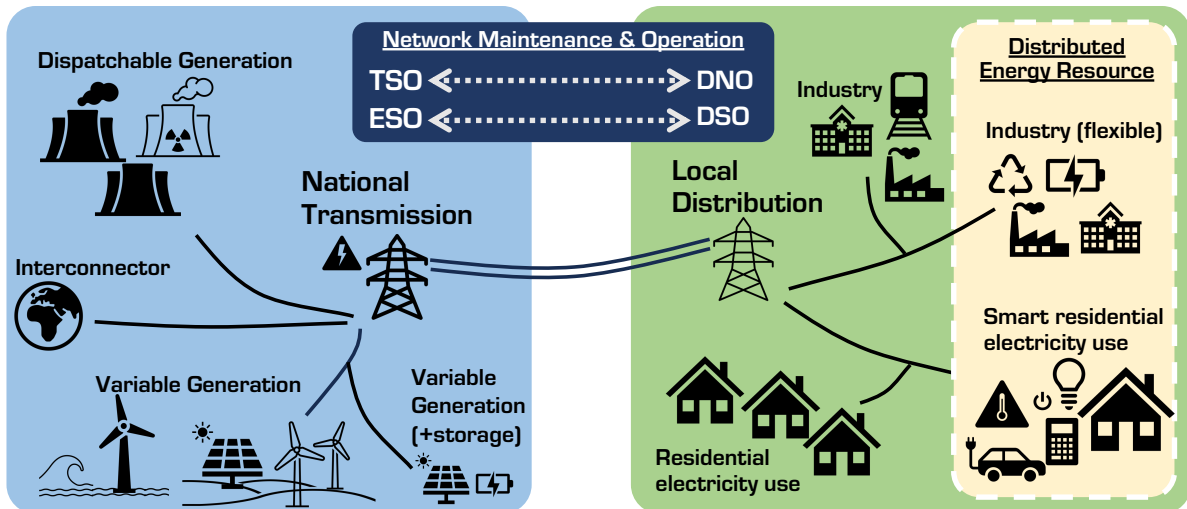
Figure 2.10: Power systems (also known as *electricity grids*) operate at local, national, and international scales. This schematic shows the interplay between a national power system network and local distribution network for a typical developed country. The Transmission System Operator (TSO) and Distribution Network Operator (DNO) are responsible for building and maintaining network infrastructure, whilst the Electricity System Operator (ESO) and Distribution System Operator (DSO) are required to balance supply and demand, ensuring ongoing stability and safety of the network. Distributed Energy Resources (DERs) can be called upon by the ESO and DSO to provide flex services.

Electrical power is typically transmitted from its point of generation (thermal power plant, renewable energy source, or otherwise) to a location where it is useful. To reduce the power losses that are incurred, transmission lines are operated at a high voltage, and may switch from Alternating Current (AC) to Direct Current (DC)[8]. Hence, it is common to see electricity transmission categorised by whether it is High Voltage or not, and whether it is AC or DC, with DC typically reserved for cross-border interconnectors.

A schematic of a modern day transmission network, is shown for national transmission (Figure 2.10) and regional distribution (Figure 2.11). This figure shows how the local distribution connected to homes and smaller industry users join up with national transmission, with substations of different scales in between. These substations are needed primarily to step down the high voltages used for long-distance transmission. If there are issues or interruptions to the power supply on one part of a network, a switch can be activated to connect the network

---

[8]The effective load of AC is less than DC at a given voltage, making AC less efficient at transmitting power over longer distances. However, DC lines are more complex to construct, requiring more expensive step-up and step-down transformers.
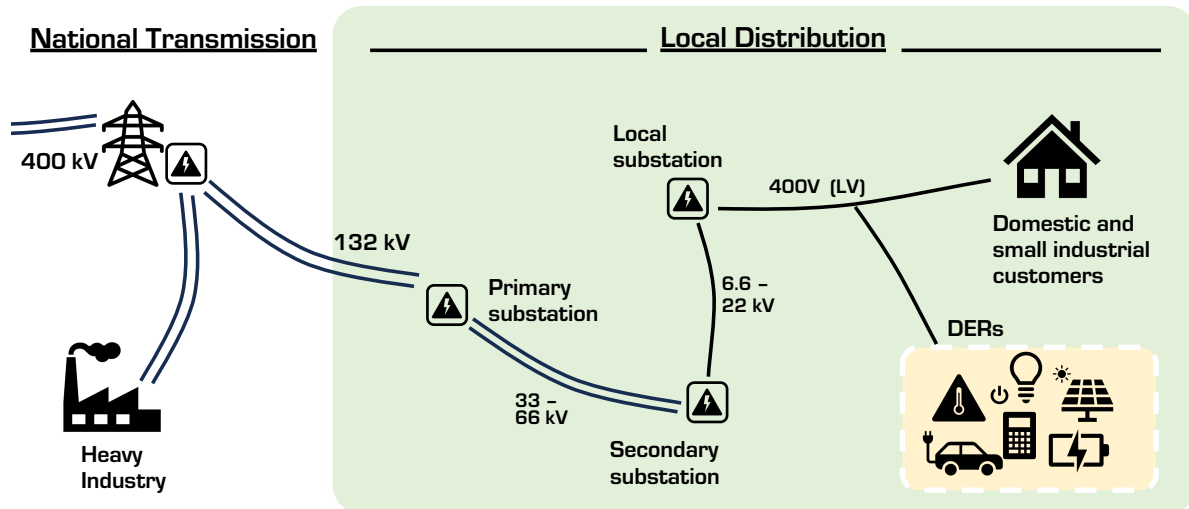
Figure 2.11: Local distribution network schematic, relating to the power network in GB. 132 kV lines are part of the national transmission network in Scotland, and part of the regional distribution network in England and Wales. Based on data from https://wiki.openstreetmap.org/wiki/Power_networks/Great_Britain.

up to a neighbouring substation ensuring that systems run reliably and with as little downtime as possible. Substations also protect infrastructure and equipment with circuit breakers and protection relays.

Local power distribution in GB is governed by two bodies, the Distribution System Operator (DSO) and the Distribution Network Operator (DNO). The DSO is a private company operating over a region of the country that is in charge of balancing the operational supply and demand on the network. The DNO is a separate private entity that is responsible for the network infrastructure. At a national level, the roles of the DSO and DNO are taken over by the national Electricity System Operator (ESO) and Transmission System Operator (TSO), respectively, (as shown in Figure 2.10).

International cooperation between the TSOs operating in different countries has led to the construction of substantial cross border networks. The UK TSO is a member of ENTSO-E, an association of European national TSOs. ENTSO-E was created as a result of an European Union (EU) legislative package on gas and electricity markets, which had examined issues in the integration between member state's power markets, and the transparency of market information. 40 member TSOs representing 36 countries participate in coordinating the operation of

the European electricity network, the largest interconnected electrical grid in the world.

From the local and regional scale, up to international cooperations, power system operators will need to ensure that infrastructure expands and evolves to support the future decarbonised energy system (Koolen et al., 2022; ENTSO-E, 2023). The UK TSO has set a target of connecting up to 50 GW of offshore wind capacity by 2030, which will require additional upgrades of onshore transmission infrastructure (Ofgem, 2022). Section 2.2.5 discusses the role of system operators in maintaining a reliable and secure power system and the policy decisions that could change the role of future system operators.

2.2.4 ENERGY STORAGE

We shall consider energy storage both in the context of purpose-built infrastructure to support TSOs in coping with peaks in electricity load (the demand-net-renewables, see Section 2.2.5.1), and in the context of reserve power supply for critical infrastructure. The utilisation of *surplus* reserve capacity explored in this thesis overlaps both of these contexts.

As we have discussed in Section 2.2.5, power system networks increasingly can benefit from balancing services to provide: energy stores (on the scale of minutes to months or years), frequency balancing (keeping grid frequency at a fixed value in a low inertia power system, Dreidy et al. (2017)) and other services. Different technologies of energy storage devices have the potential to offer one or more of these services to the wider grid.

The primary attributes considered in choosing an energy storage technology may include build cost, running cost, efficiency, environmental impacts, resource use, land use, suitability to site, carbon emissions, and fuel security of supply.

Storage devices have an analogous measure to the LCoE that gives a rule of thumb measure for their value, the Levelised Cost of Storage (LCoS) (Jülch, 2016; Schmidt et al., 2019):

$$\text{Levelised Cost of Storage} = \frac{\text{NPV of Annual Total Expected Costs (£)}}{\text{NPV of Energy Discharged (MWh)}} \tag{2.11}$$
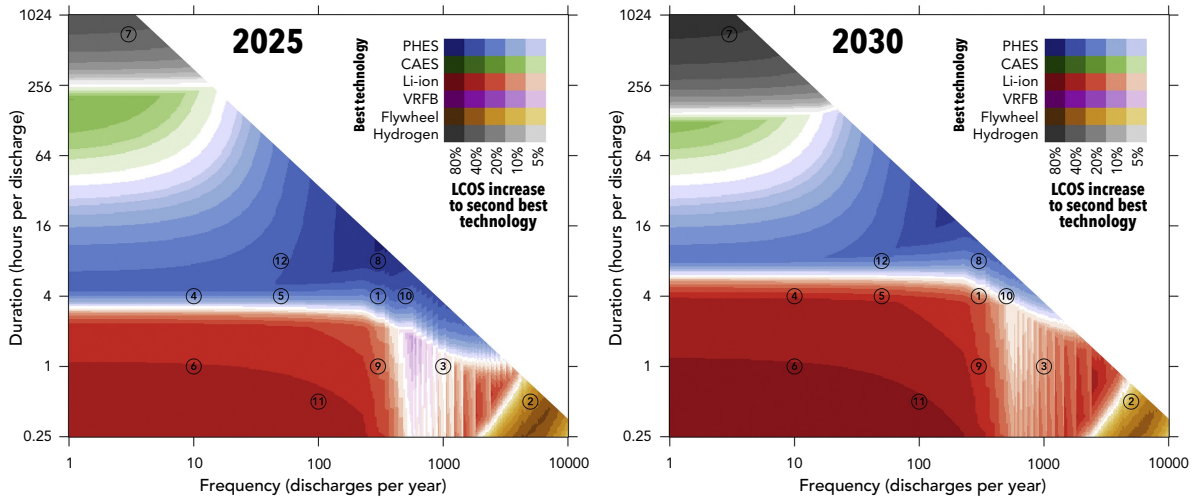
Figure 2.12: Technologies with lowest LCoS relative to discharge duration and annual cycle requirements. Circled numbers represent the requirements of 12 applications: 1, Energy Arbitrage; 2, Primary Response; 3, Secondary Response; 4 Tertiary Response; 5, Peaker Replacement; 6, Black Start; 7, Seasonal Storage; 8, Transmission and Distribution Investment Deferral; 9, Congestion Management; 10, Bill Management; 11, Power Quality; 12, Power Reliability. Colours represent technologies with lowest LCoS. Shading indicates how much higher the LCoS of the second most cost-efficient technology is, with darker areas indicating a strong cost advantage. Modelled electricity price is 50 USD $/MWh. Schmidt et al. (2019, Figure 3 (c-d)). Reprinted with permission from Elsevier.

where the calculation of NPV is given by Equation (2.2). As with the LCoE, the LCoS is only a rule of thumb guide for comparing costs (it does not factor in how the asset would interact with the dynamics of the power system network).

Schmidt et al. (2019, Figure 3), reproduced in Figure 2.12, shows the levelised cost of electricity storage in projected scenarios. Balancing service applications are marked on (labelled 1 to 12), and in most cases, Lithium-Ion (li-ion) batteries appear to offer the best value (as measured by LCoS), although pumped hydroelectric energy storage (PHES), vanadium reflex batteries (VRFB), and flywheels are competitive for some short-medium duration purposes, and compressed air energy storage (CAES) and hydrogen dominate the long-term storage scenarios.

The cost of li-ion batteries has fallen over the past decade. In 2022, production in China reached 5.5 TW h, and is projected to grow at a rate far outpacing demand (Dempsey & White, 2023). Longer duration batteries (for example, 8 h) have a lower capital cost, whilst shorter
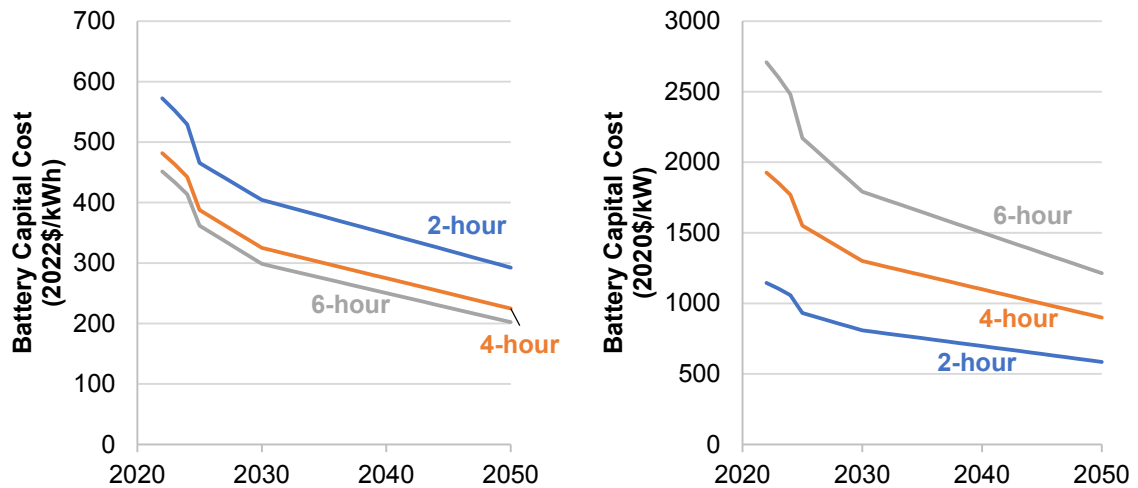
Figure 2.13: Cost projections for 2-, 4-, and 6-hour duration batteries using a mid cost projection. Left shows the values in USD $/kWh, while right shows the costs in USD $/kW. Reprinted from Cole and Karmakar (2023, Figure 5).

duration (faster discharge capability) batteries require significant investment into power components.

Recent years have seen large growth in electro-chemical and chemical energy storage, shown in Figure 2.14. Whilst compressed air energy storage has historically been the dominant chemical/electro-chemical energy store, in recent years the power capacity of battery technology, in particular li-ion battery, has surpassed this. Compressed air energy storage at present still accounts for the bulk of *energy* capacity (40 GW h compared to li-ion's 13 GW h in 2021).

Reserve power systems at present commonly depend on fossil fuel generators (diesel or fossil gas). Given the high cost of battery energy storage capacity compared to fossil fuel technologies, there is a pressing need for cheaper long-term energy stores to make up the bulk of energy capacity (even if higher cost batteries handle a portion of this) and it remains to be seen which technology can best fulfil this role, facilitating a transition to low emissions technologies at acceptable costs. Several blue-sky technologies may gain importance in coming years, such as *green ammonia*, a high energy density fuel that could be adopted for energy stores and transportation fuels (Royal Society, 2020).

In Figure 2.12, hydrogen energy storage is presented as the most efficient long duration energy
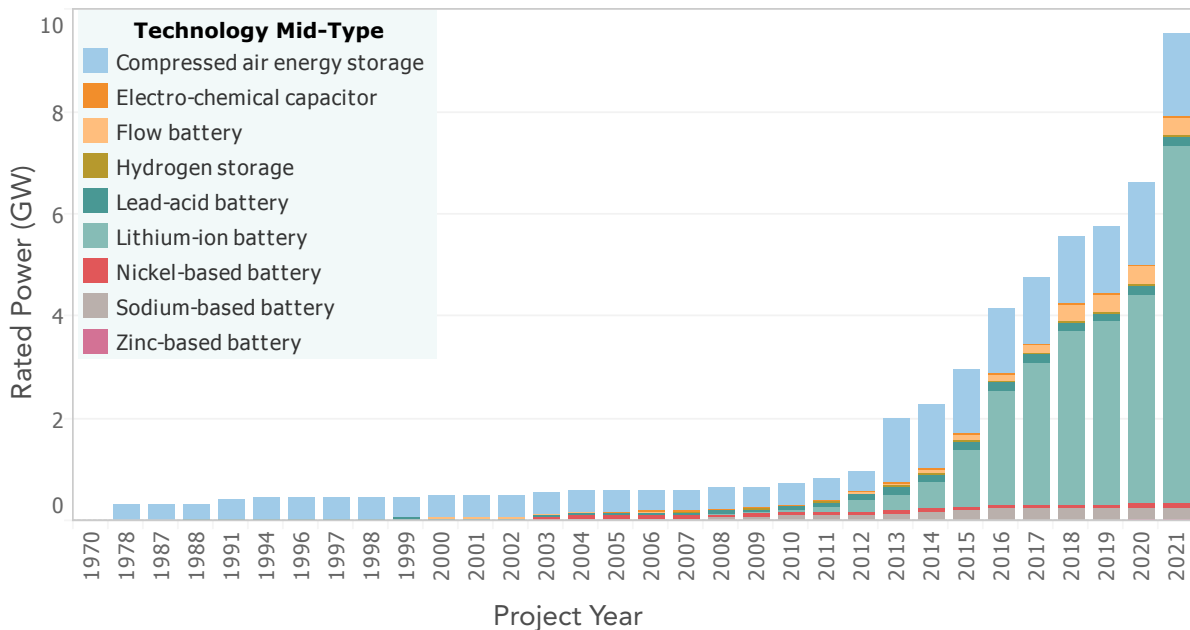
Figure 2.14: Cumulative sum of energy storage installations by year (restricted to electro-chemical battery and chemical energy storage technologies). Note: If the project commissioning date is not available in the database, the year represents either the constructed date or announced date. The projects for which the constructed/commissioned/announced date were not available have been omitted from the visualisation. Figure reproduced from Department of Energy: Global Energy Storage Database, NTESS (2022).

store. Hydrogen has the potential to play a significant role in decarbonising reserve systems, but there are significant barriers to overcome. *Green hydrogen* (produced through electrolysis) has the potential to be deployed in the near to mid-term, but is dependent on the abundance of low-carbon cheap energy generation to be economically viable Royal Society (2018). Thermo-chemical deployments reliant upon carbon capture and storage offer a lower cost alternative, but to become a low-emissions energy source are reliant on unproven future carbon capture technologies (Longden et al., 2022; Furbank, 2023).

A low-carbon replacement for reserve systems could be designed using a single individual technology (a long-term store), but a cost-optimal approach may implement two or more technologies to provide backup (integrating some short-term higher frequency energy storage alongside long-term). This could look like a hybrid hydrogen fuel cell + li-ion deployment, with hydrogen ensuring that the bulk energy needs are met, whilst li-ion batteries offer cheaper and immediate power supply for more frequent short-duration events.

The decreasing costs of battery energy storage combined with a rapidly growing need for balancing capacity means that battery systems have almost reached price parity for purpose built balancing services (IEA, 2019). Building a portion of the reserve system from battery energy storage offers potential benefits (reducing emissions, reducing energy consumption costs) and, combined with the potential role of surplus capacity, can offer additional benefits to the reserve operator and wider gird.

In the context of *surplus* capacity in reserve power systems, operating a portion of the reserve system for other purposes could reduce the cost of building some or all of the reserve from low-carbon technologies, allowing a phase-out of fossil fuel generators (Mustafa et al., 2021; Hansson, 2022). Chapter 5 assesses the potential benefits to reserve operators and the wider grid.

2.2.5 THE ELECTRICITY MARKET

2.2.5.1 POWER PRICE

The price of electrical power or energy delivery is typically expressed in value (currency) per unit energy used, for example £/MWh. The main costs of delivering energy from dispatchable generators is the combination of the fixed cost (relating to building and maintaining infrastructure regardless of the amount of power provided) and the variable operational cost (fuel cost per unit of output).

Energy market liberalisation, a process which began in the 1980s and has seen significant global adoption, may be characterised as the introduction of competition and the establishment of independent energy sector regulators (Jamasb & Pollitt, 2005). In liberalised energy markets, owners of generation capacity enter into an auction to supply power. Economic dispatch minimises the cost of electricity production, generally choosing the lowest cost generation capacity (except in cases where this is prevented or not optimal, for example due to transmission congestion). This results in a merit order structure, shown in Figure 2.15 (Cludius et al., 2014; Clò et al., 2015).
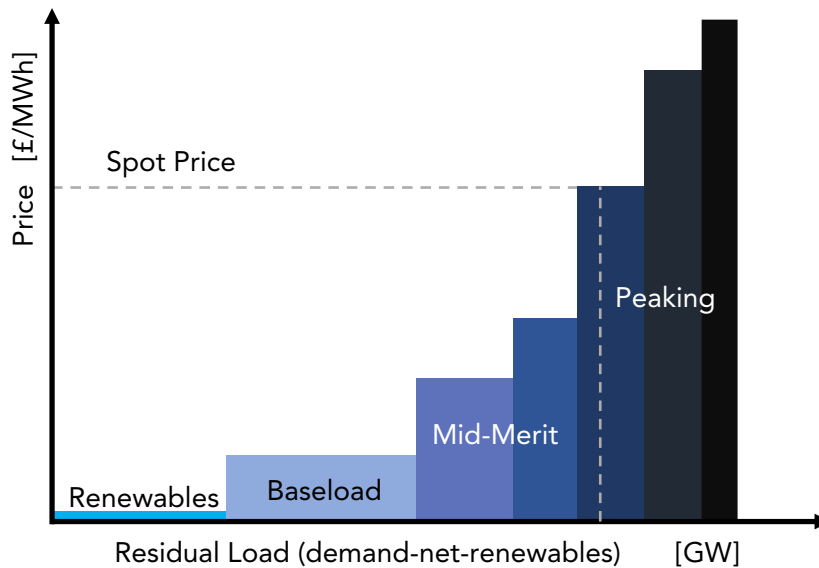
Figure 2.15: The merit order is a ranking of available sources of power generation. Energy market prices are sensitive to the merit order effect, depending on the level of energy demand to be met by dispatchable generation.

The merit order categories of generation refer to a relative trade-off between fixed and variable costs:

- Variable: Negligible variable operational costs, but power levels cannot be relied upon. Power should be used when available (and using any available interconnector and storage capacity for excess generation). Generally has a negligible marginal cost.

- Baseload: once built, these resources have a low operational cost and are therefore most economically viable when in near-constant use. Has a low negligible marginal cost.

- Mid-Merit: lower fixed costs but higher variable costs make these a good option to soften diurnal variability and manage high-load periods. As the name suggests, these have a medium marginal cost.

- Peaking: low fixed costs (sometimes subsidised) but high operational costs. Peaking capacity is vital to meet high-load events at short notice. Marginal costs can become very high.

In the case of variable generation, such as wind and solar power, the operational cost is neg-

ligible and often ignored. When renewable energy penetration is high, the merit order curve is shifted to the right and the spot price drops at times of high renewable energy production. In Germany, the effect of introducing more renewable generation capacity has had an average effect of reducing spot prices by 0.8 EUR €/MWh to 2.3 EUR €/MWh (Cludius et al., 2014).

However, the increased renewable energy penetration also sharpens the shape of the merit order curve (since other generation is less frequently called upon and therefore requires an increased revenue to remain profitable). This sharpening disincentivises additional renewable capacity, as the revenue to finance additional capacity will be reduced.

Responding to the increased merit-order impact of renewable energy generation capacity, energy policy approaches increasingly must address the issue of inter-seasonal weather variability, and prioritise diversifying renewable mixes to support low cost of supply market design (Coker et al., 2020). However, in principle, the 'energy-only' power market is well positioned to support highly renewable power generation, where power supply is composed mostly or entirely of renewable energy supply and energy storage resources (Antweiler & Müsgens, 2024).

2.2.5.2 CAPACITY MARKET

An important aspect of energy generation is the security of supply. Defining energy security is somewhat contextual (Kruyt et al., 2009), but relates to affordability, accessibility, acceptability and availability of the energy. An energy-only liberalised market has some inherent inefficiencies and has been criticised for not providing adequate incentives for investment into the security of supply (Cramton et al., 2013). Market mechanisms do not capture the cost of catastrophic blackouts (Joskow & Tirole, 2007), and lack mechanisms to encourage decarbonisation (Pollitt, 2012).

To address the issues with security of supply and capacity financing in an increasingly renewables dominated market (with the impacts of the merit-order effect), some energy regulators have introduced capacity market mechanisms (Kozlova & Overland, 2022). Implementations of a capacity market aim to encourage investment in existing capacity through
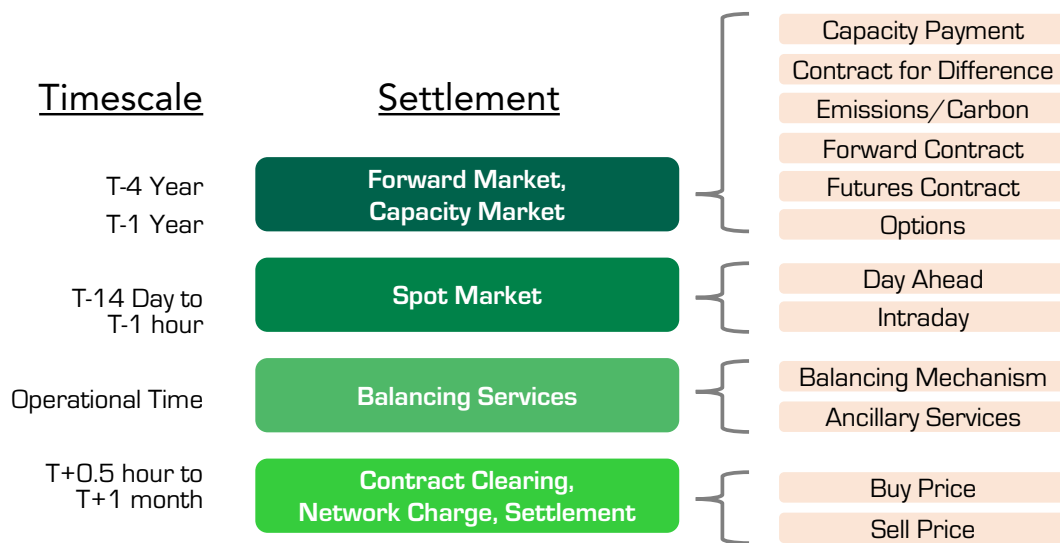
Figure 2.16: The UK Bilateral Electricity Trading and Transmission Arrangements, schematic categorising the timescale and contracts of different market settlements.

the additional revenue on top of energy revenue, and provide a commitment to new capacity providers through long-term contracts.

A capacity market can encourage continued investment in generating capacity by paying participants a rate for the power capacity offered (a 'quantity-based' implementation, as used in the UK market, (Cramton et al., 2013)). The only 'catch' for participants engaging in the capacity market is that capacity must be available to provide power for balancing supply and demand when necessary (although in practice it should not be necessary to actually call upon this commitment in a well functioning market).

Adequacy can be achieved through demand elasticity, operating reserves, strategic reserves, and power transmission between countries via interconnectors. These approaches can improve the adequacy problem, but as long as some demand remains inflexible, may not be able to fully eliminate structural issues in the energy market, and therefore even in an ideal environment a capacity market provides benefits (Cramton et al., 2013).

Liberalised markets have moved towards incentivising payments for capacity (the capacity market). This has improved security of supply, but has been criticised for unintentionally favouring peaking technologies (fossil fuels). The addition of variable wind and solar power

tends to depress energy market prices, leading to increased importance of capacity market payments, but this inadvertently favours capacity market payments towards peaking technologies, effectively discouraging investment into nuclear power and renewables (Mays et al., 2019).

An ongoing review into the GB capacity market is looking to adapt capacity payment mechanisms, to reflect the penetration of variable generation and support optimised levels of investment into energy storage. The current methodologies account for neither battery reliability or aging (Zachary et al., 2022). The UK proposal, Department for Energy Security & Net Zero (2023), proposes interventions such as *battery augmentation* to address the gradual loss of battery performance, and to address participation challenges faced by low-carbon projects and demand-side response participants.

2.2.5.3 ELECTRICITY FLEXIBILITY

A variety of mechanisms can be put in place to ensure power system adequacy. This takes place through transmission, electricity interconnectors, and market mechanisms that design for system adequacy as discussed above. However, an increasingly important and relied upon asset are Distributed Energy Resources (DERs) and balancing services.

National Grid ESO operates a large number of balancing services. These relate to arbitrage, electricity system restoration, frequency balancing, system security, operating reserve (National Grid ESO, 2024a).

In Chapter 5, we consider three services that reserve system owners could potentially participate in, using surplus capacity:

- Dynamic containment services control system frequency (keeping within the 1 % margin of 50 Hz). Initiation time is fast (0.5 s to 2 s), and the delivery duration is relatively short (15 min to 60 min). Payments are made through competitive bids.

- Reserve services are needed to meet imbalance between supply of energy and demand. Slow reserve operates bi-directionally to displace large losses on the system and recover

frequency to 50.0(2) Hz within 15 minutes. Activation time is a minimum of 30 min to 120 min. Payments are made through competitive bids.

- A new demand flexibility service has recently been trialled by National Grid ESO, for households and businesses to receive payments for shifting energy use outside of periods of peak demand. Participants are not committed to deliver the service (there is no penalty for non-participation). Businesses must offer a minimum 1 MW and in phase 1 to 6 trials receive a payment of 3000 GBP £/MWh for services delivered, although payments will become competitive in future. Unlike the other services discussed, the demand flexibility service excludes participation in the capacity market, and cannot participate in other balancing services.

The traditional operation of power system networks sees a unidirectional flow of energy; in Figure 2.10 this would be represented by power flowing from left to right and without the presence of DERs or variable generation/storage — i.e. from large generation assets (power stations), across the high-voltage transmission system before distribution to lower voltage sub-stations and energy users. In this model, the TSO has facilitated the operational power delivery ensuring reliability and stability of electrical power transmission across the grid, meeting the demand of DSOs who manage the local area distribution of electrical power.

However, the large penetration of renewable generation, and emergence of smart technologies that vary their consumption (DERs), has disrupted this model. Both DSOs and TSOs are having to facilitate the bi-directional flow of power across their networks, and in some market set-ups may operate their own DERs[9].

In Figure 2.17, common DERs are characterised in terms of siting (i.e. who is responsible for the asset) and the duration that energy can be delivered.

The EU-funded SmartNet project (SmartNet, 2019) has adopted a set of five co-ordination frameworks for the cooperation between DSOs and TSOs. These market models conceptualised in Gerard et al. (2018), are summarised below:

---

[9]In the UK, regulations prevent the TSO or DSOs from directly owning and operating DERs, which must instead be constructed by third-parties.
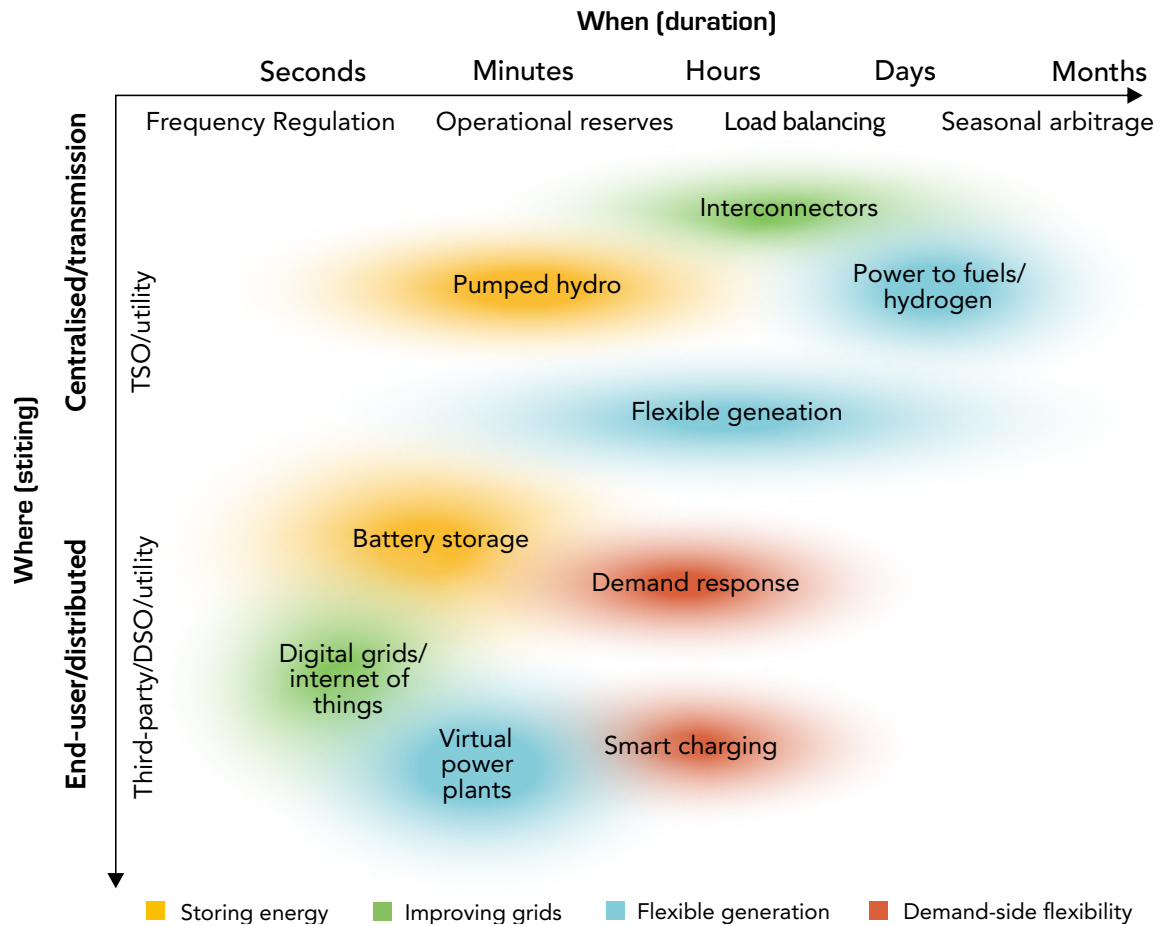
Figure 2.17: Growing needs for electricity flexibility can be met by DER options for flexibility. Expansion of electrification, distributed generation and variable renewables will further broaden the need and range of flexibility options. Figure adapted from IEA (2018, Figure 7.19 CC BY 4.0).

1. Centralised Ancillary Service Market Model — *A DER* aggregator places bids with the TSO *who is responsible for balancing.*

2. Local Ancillary Service Market Model — *A DER* aggregator places bids with the DSO, *who in turn places bids with the* TSO.

3. Shared Balancing Responsibility Model — *A DER* aggregator places bids with the DSO, *who shares a balancing responsibility with the* TSO.

4. Common TSO-DSO Ancillary Service Market Model — *A DER* aggregator places bids *on a coordinated* DSO/TSO *market.*

5. Integrated Flexibility Market Model — *Introduces the participation of both regulated parties (i.e.* DSOs *and* TSOs*) alongside commercial market parties to procure flexibility.*

Electricity markets may evolve to behave closely like one of the described models, or perhaps drawing on more than one approach (IRENA, 2020). The resulting framework will control who DER owners interact with, calculation for the priority of acquiring assets, and the prioritisation of local network constraints managed by DSOs vs. wider scale transmission constraints handled by the TSO. In the latter two frameworks, constraints on both the TSO and DSO transmission networks are resolved in a single mechanism, which in itself presents feasibility challenges and may also require third-party market operators to be established.

In the UK legacy implementation of the balancing market, services are acquired by the TSO, and have priority over the needs of the DSO, i.e. following the Centralised Ancillary Service Market Model (Item 1). However, trials are being conducted to involve DSOs to assist with distribution constraints (Edmunds et al., 2020). The Smart Systems and Flexibility Plan (Department for Business, Energy & Industrial Strategy & Ofgem, 2021) is an ongoing consultation set out to implement new rules for flexibility in markets. The cooperation between DSOs and National Grid Electricity Transmission is working towards implementing a set of primacy rules to resolve service conflicts (Department for Business, Energy & Industrial Strategy & Ofgem, 2022), and with the objective of promoting the efficient use of DERs.

2.3 Weather, Climate, and Energy

Weather and climate information is essential for safe, resilient and effective energy sector decision-making, whether considering small-scale individual needs up to utility-scale and international-scale cooperations.

Unprecedented extreme weather events are leading to new situations in energy production, consumption, and transmission that are difficult and costly to manage, require emergency interventions, and can have global impacts on energy prices (Añel et al., 2024). These impacts relate to risks from both physical hazards, and severe energy situations (such as energy drought, Dunkelflauten, etc.).

2.3.1 METEOROLOGICAL DRIVERS OF ENERGY

The relation between weather and production/consumption impacts is well understood and characterised through the application of weather patterns. Weather patterns are statistically determined patterns of variability that describe a large proportion of variance over a region (but are not necessarily connected with the dynamics of the system). The improved quality of weather observations and access to modern clustering algorithms (such as k-means) has enabled more accurate and consistent classification of circulation types in recent decades (Neal et al., 2016).

weather regimes, such as the Großwetterlage which represent 29 weather systems over Europe (Baur, 1949; Werner & Gerstengarbe, 2010), characterise different dynamical states of large-scale atmospheric circulation that a system may occupy for an extended period. The terms weather patterns and weather regimes are often used interchangeably, although the latter are typically larger in scale and describe a longer persisting state. We use "weather pattern" to refer to both classifications.

Weather patterns can be used to characterise the influence of meteorological variability on the energy sector. For each classification, the associated changes to wind and solar power produc-
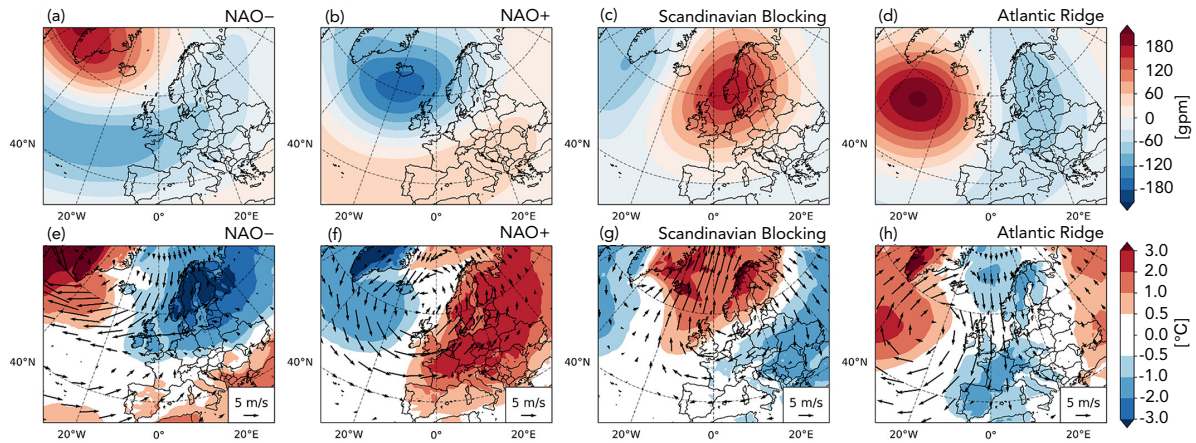
Figure 2.18: Composite fields of 500 hPa geopotential height anomalies (a—d) and 2 m temperature and 925 hPa wind speed anomalies (e—h) of the regimes. The anomalies are calculated relative to the 1981 to 2010 period. Reproduced from Rantanen et al. (2023), Creative Commons Attribution.

tion, and temperature-driven energy demand across neighbouring countries can be explored. The overall constraining effect on the grid may be considered in terms of the electricity load[10].

The key meteorological drivers of grid stress (in terms of the load) over Europe are commonly described in terms of the four winter Euro-Atlantic regimes introduced by Michelangeli et al. (1995) and Cassou (2008) (shown in Figure 2.18). Days with a blocked circulation pattern (such as the *Scandinavian Blocking* and *North Atlantic Oscillation (NAO) negative* regimes) lead to lower than expected renewable power production, and higher than normal energy demand (Grams et al., 2017; van der Wiel et al., 2019). For example, Figure 2.19 shows the effect of weather regimes on wind power production in Europe.

However, the 'average' effects characterised by patterns and regimes hide large variability within each weather regime, and the actual regional impacts that are experienced and dependent for example on regional transmission line capacities (Grochowicz et al., 2024).

The suitability of weather regimes is dependent on present climate systems broadly resembling their past state. Rantanen et al. (2023) show an asymmetric warming occurs in the four Euro-Atlantic weather regimes. For example, a faster warming rate in NAO− compared to winter averages and other regimes could lead to an overestimation of energy shortfall events

---

[10]The national electricity load is often considered as *demand-net-renewables*, to account for the negligible marginal cost of renewables.
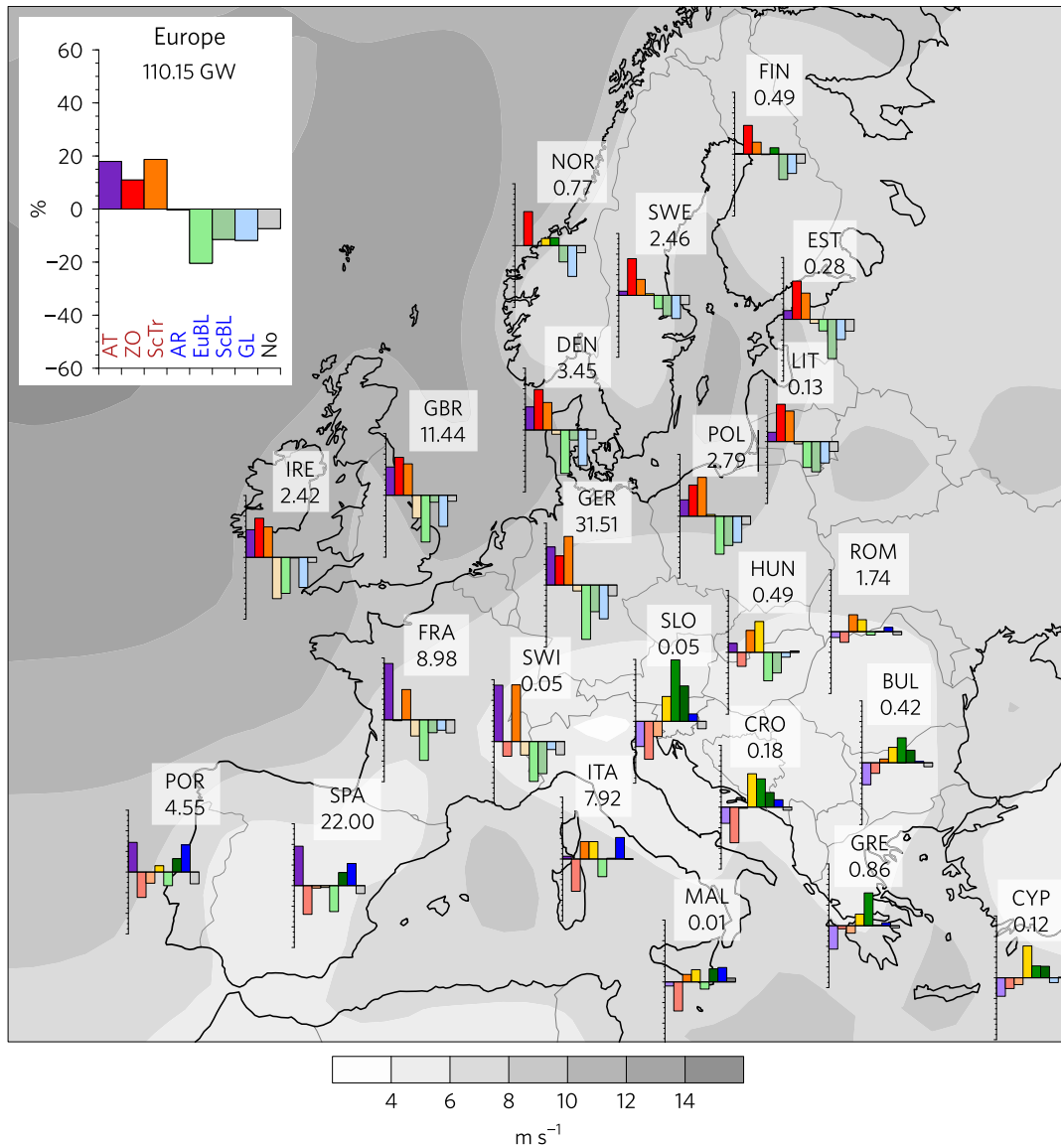
Figure 2.19: Weather Regime dependent change in wind electricity generation. Country-specific relative change of wind capacity factor during cyclonic regimes (red labels), blocked regimes (blue labels), and no-regime periods, shown as percent deviations from winter mean. Seven weather regimes are designed to capture year-round, large-scale flow variability in the Atlantic-European region. The cyclonic regimes are *Atlantic trough* AT, *zonal regime* ZO, *Scandinavian trough* ScTr, and the blocking regimes (*Atlantic ridge* AR, *European blocking* EuBL, *Scandinavian blocking* ScBL, *Greenland blocking* GL). Reproduced with permission from Nature, Grams et al. (2017, Figure 1).
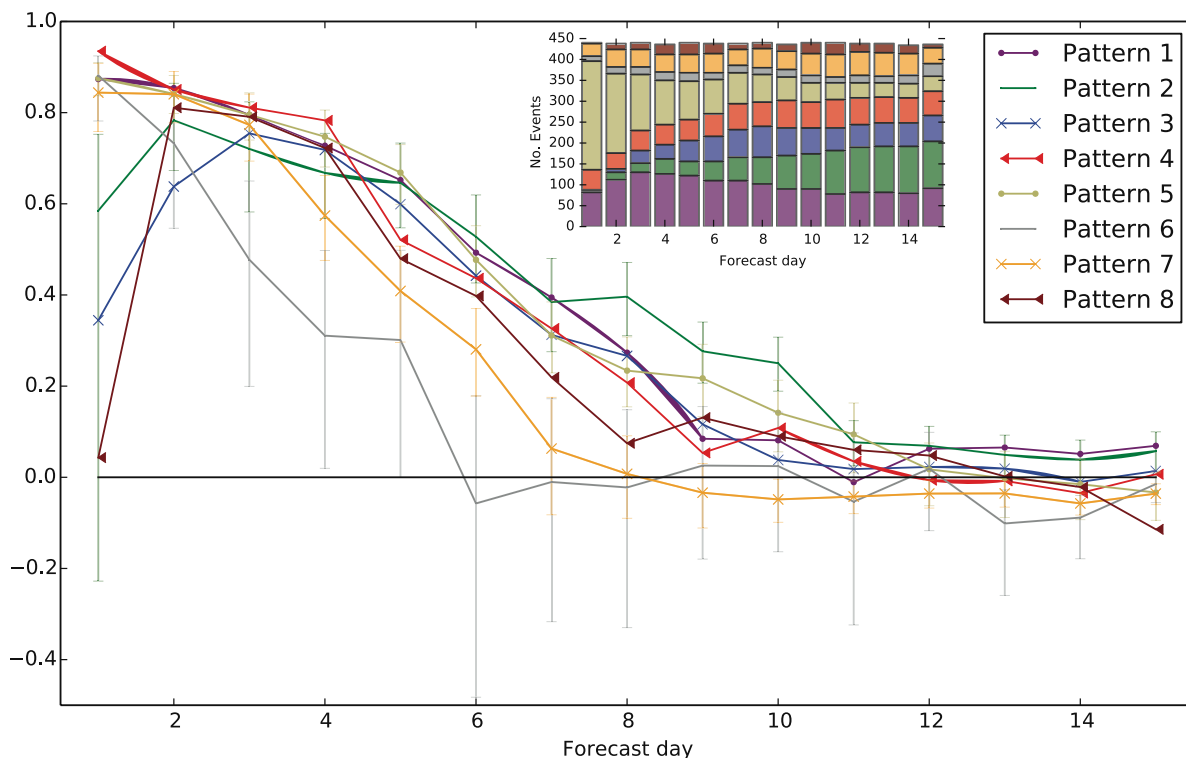
Figure 2.20: Brier skill scores for each of the UK Met Office eight weather patterns, for all forecasts initialised in Weather Pattern 5 (Scandinavian high). Confidence intervals at the 90 % level are shown by the vertical lines (for patterns 2, 5, 6, 7 only). Stacked probability plot shows the number of observations for each pattern at a given lead time, from the starting point of pattern 5 at day 0. Reproduced from, Neal et al. (2016, Figure 9).

associated with this regime.

Weather patterns (including weather regimes) remain a popular tool for categorising weather systems' impacts on energy, and forecasts (such as picture in Figure 2.20) are popular with many decision-makers (some discussion of this follows in Section 2.3.2.2 in the context of Sub-seasonal to Seasonal forecasts).

The Met Office (Met Office) 'Decider' tool implements a set of 30 patterns (alongside a smaller set of 8 patterns), reducing the complexity of forecast outputs into recognisable weather states that support users in anticipating impactful weather events at regional and country level scales (Neal et al., 2016). However, these patterns may not always be an optimal use of information, with targeted circulation types and gridded meteorological data offering more accurate predictive skill (at the cost of increased complexity) (Bloomfield, Brayshaw & Charlton-Perez, 2020).

2.3.2 Numerical Models of Atmosphere, Ocean, and Climate

At the turn of the 20th century, recognising that the evolution of the atmospheric state could be formulated as an initial value problem, meteorologists proposed that numerical models could be used to predict the weather (Abbe, 1901; Bjerknes, 1904), as long as two conditions are satisfied:

Bjerknes (1904) stated that two conditions must be satisfied to successfully predict future atmospheric states:

1. The initial atmospheric conditions must be characterised with a high accuracy

2. The physical laws describing the evolution of atmospheric states must be known

Following from these assumptions, Bjerknes divided the problem of NWP into three components: the observation component (collecting measurements of field variables such as temperature, pressure, and humidity), the diagnostic component (analysis of the present atmospheric state), and the prognostic component (using mathematical models to predict the evolution of the atmospheric state).

> *…the motion of large-scale systems is governed by the laws of conservation of potential temperature and potential vorticity and by the condition that the field of motion is in hydrostatic and geostrophic balance.*

Jule Gregory Charney, *On the scale of atmospheric motions*, 1948

The scale arguments described by Charney (1948) led to the first serious attempts at NWP Charney et al. (1950).

Another key advancement to NWP came from the discovery of the chaotic attractor and understanding how a set of deterministic equations describing the state of the atmosphere could

(a)   (b)

future climatology

forecast uncertainty
current climatology
forecast uncertainty
with model bias
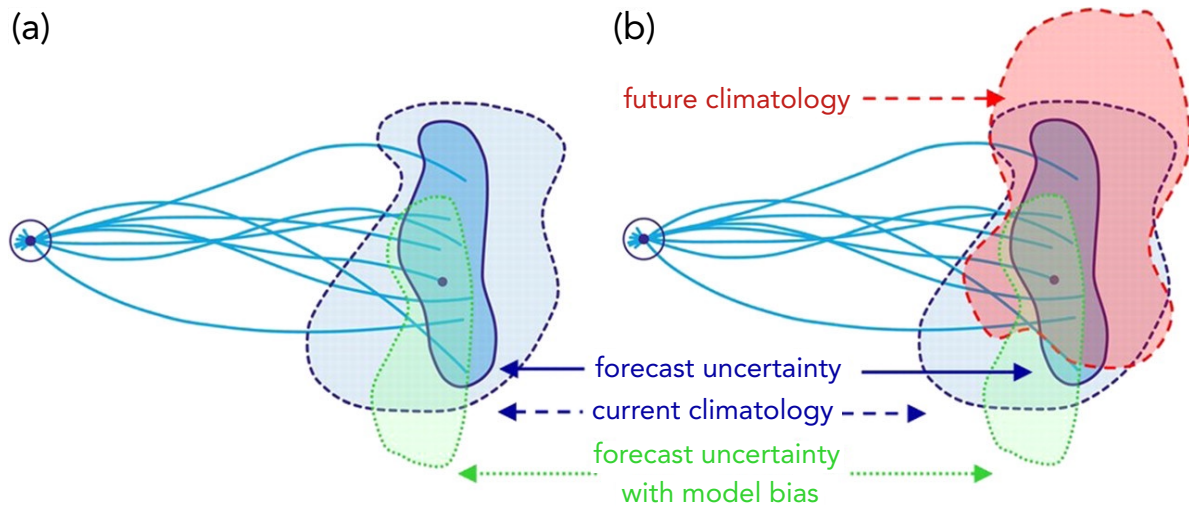
Figure 2.21: Schematic of ensemble prediction system on seasonal to decadal time scales, showing a) the impact of model biases and b) a changing climate. The uncertainty in the model forecasts arises from both initial condition uncertainty and model uncertainty. Slingo and Palmer (2011, Figure 8), CC BY.

result in chaotic behaviour (Lorenz, 1963). Weather and climate prediction (and the forecasting time horizons that lie in between) are a mixture of initial condition and boundary condition problems (Slingo & Palmer, 2011; Brayshaw, 2018). Modern forecasting techniques aim to *solve* an initial condition problem by implementing an ensemble, allowing for the model to simulate a range of plausible outcomes. However, at climate system timescales, the initial conditions are no longer relevant, and instead, it is a boundary condition problem that must be solved.

Figure 2.21 shows the effect of model-specific bias in the context of extended-range weather prediction: an ensemble forecast from a set of initial conditions leads to a spread in values at the later stage. Unlike short-range forecasting, model-specific biases grow more strongly, leading to forecast distribution biases (panel a). Additional bias arises due to the effect of climate change: calibrations are sensitive to the long-term trends present in observational data.

2.3.2.1   Short-range Weather Forecasting

Weather forecasts make use of NWPs initialised on the most recent weather analysis, and are used to predict future weather conditions up to several days in advance (usually 1 to 5 days —

beyond 7 days is considered the sub-seasonal range, see Section 2.3.2.2).

High-quality observations, four-dimensional variational (4D-Var) data assimilation, and improved physics parameterisation permits operational forecasts to provide predictions at very high resolutions and short time scales multiple times per day (Bauer et al., 2015).

Operational forecasts are produced by national weather centres, including the Met Office (UK), Japanese Meteorological Agency, US National Centers for Environmental Prediction, Deutscher Wetterdienst, Météo-France, and the multi-national European Centre for Medium-Range Weather Forecasts (ECMWF). These datasets are the most popular weather product accessed by large portions of the public, through TV forecasts, websites, and smartphone applications.

The state of weather systems is closely related to atmospheric pressure. The 500 hPa geopotential height (Z500) relates to the structure of the atmosphere at mid-levels. It is away from the surface and smooth (fluctuating at large scales), and therefore useful as a proxy variable for the general state of the atmosphere. Figure 2.22 shows how skill in predicting Z500 has evolved in recent decades.

Skill at lead times of 3, 5, 7, and 10 days has consistently increased in recent decades at a rate of about one day per decade (i.e. today's 6-day forecast is as accurate as the 5-day forecast ten years ago, Bauer et al. (2015)). The historic discrepancy between Global North and Global South skill caused by a difference in the distribution of observations has been closed.

2.3.2.2 Sub-seasonal to Seasonal Forecasts

Sources of predictability at timescales in between the traditional horizon of NWP and decadal predictability has been an area of great interest in recent years, spurred by growing demand from applications (Vitart & Robertson, 2018; Domeisen et al., 2022; Vitart & Takaya, 2021; Gonzalez et al., 2021; Tripathi et al., 2015; Brayshaw, Hoskins & Blackburn, 2011; Cassou, 2008; Lynch et al., 2014; Brayshaw, Troccoli et al., 2011).

Sub-seasonal to Seasonal (S2S) forecasts are run at longer timescales (and typically lower
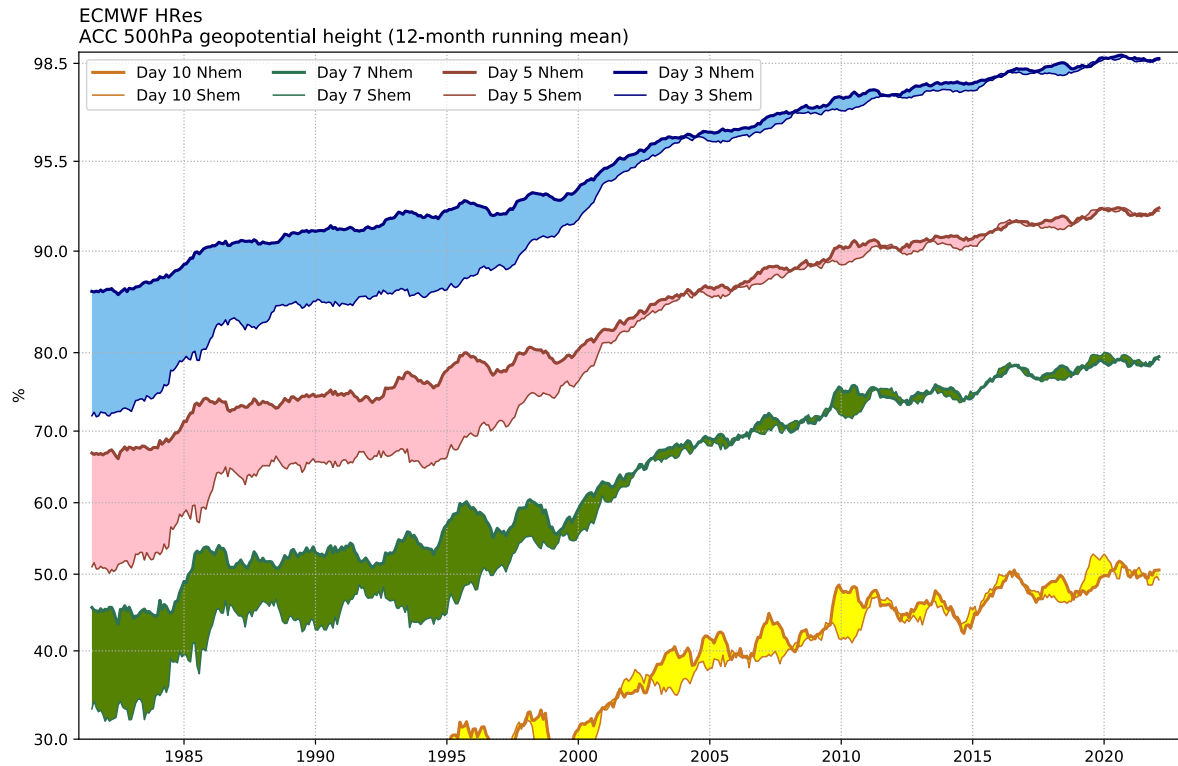
Figure 2.22: Time series of the annual running mean of anomaly correlations of 500 hPa height forecasts evaluated against the operational analyses for the period 2000 until 2022. Values are running 12 month average scores. Forecast lead-times in days ahead — 3 (blue), 5 (red), 7 (green) and 10 (yellow) — are shown for scores averaged over the northern extra-tropics (bold lines) and southern extra-tropics (thin lines). The shading shows differences in scores between the two hemispheres at the forecast ranges indicated. Currently 3-day, 5-day, 7-day, 10-day forecasts have attained approximately 98.5 %, 92 %, 80 %, 50 % anomaly correlation (ACC), respectively. ECMWF (2024) CC BY 4.0.

resolutions) than short-range forecasts. Both implement NWP of coupled atmosphere-ocean-land models. Modern *seamless* models, such as the Met Office Unified Model, can be used for prediction across both of these timescales with the aim of minimising differences between the configurations (Bush et al., 2020).

S2S forecasts are sensitive to evolving boundary conditions (shown in Figure 2.21), and therefore depend on long-lived precursor patterns and their teleconnections (Vitart, 2014), and other sources of slowly-evolving predictability (Figure 2.23).

Key sources of S2S skill in winter include the NAO (Lynch et al., 2014; Vitart, 2014; O'Reilly et al., 2017) Madden-Julian Oscillation (Cassou, 2008), the El Niño Southern Oscillation state (Bloomfield, Wainwright & Mitchell, 2022; Fröhlich et al., 2015), the Stratospheric Polar
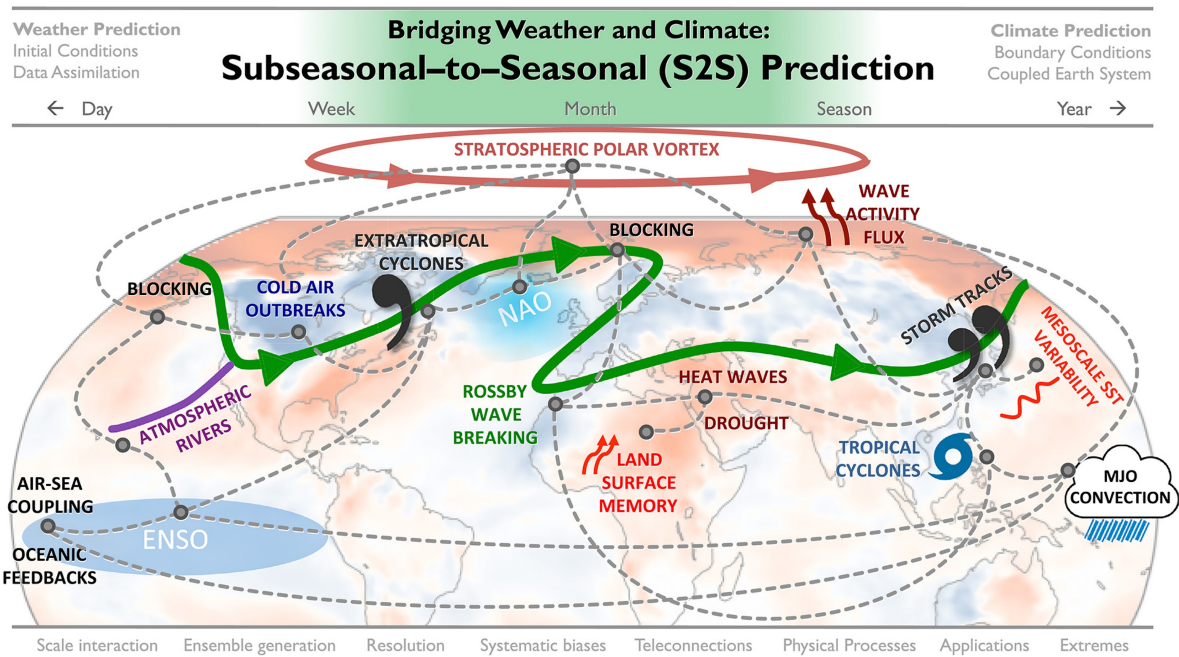
Figure 2.23: Schematic of key atmospheric phenomena and numerical modelling considerations needed to make accurate forecasts at the subseasonal-to-seasonal forecast time scale. Background coloured shading represents surface air temperature anomalies for February 2018, relative to the February average (1981 to 2010). Reproduced with permission from Wiley, Lang et al. (2020, Figure 1).

Vortex (Büeler et al., 2020; Tripathi et al., 2015; Lee et al., 2020), as well as from initial conditions, monitoring surface cover (land/sea ice).

White et al. (2017) and Domeisen et al. (2022) identify potential applications of S2S in: the humanitarian sector; public health; agriculture; water management; the maritime sector; energy. Figure 2.24 shows the connection between timescale and S2S weather-influenced decision-making.

S2S forecasts can be used to anticipate changes in renewable electricity weeks in advance (Soret et al., 2019), allowing the sector to take preparative action. This is reflected by fluctuations in market prices (Dorrington et al., 2020), and can facilitate TSOs and participants in the power network to reschedule energy use and storage.

Robust extended-range forecast products include the World Meteorological Organization S2S prediction project, the ECMWF's S2S forecast system, the North American Multi-Model Ensemble, and the Australian Bureau of Meteorology's S2S prediction.
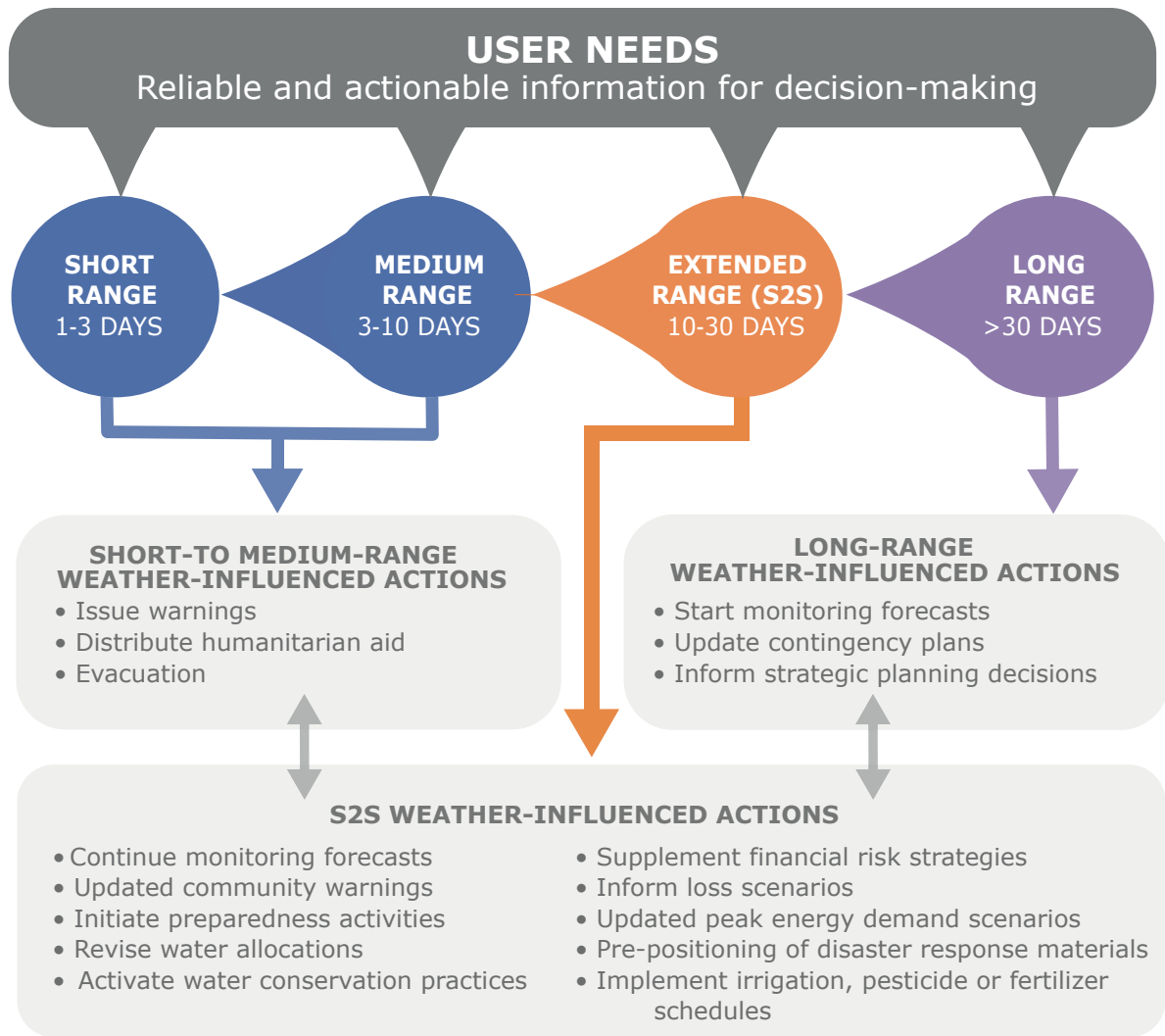
Figure 2.24: Schematic diagram highlighting the relationship between the subseasonal-to-seasonal (S2S) 'extended-range' forecast range and other prediction timescales. Actions are examples only and are not exclusive to a forecast range. White et al. (2017, Figure 1-b)

2.3.2.3   DECADAL FORECASTS

Beyond the timescale of S2S are seasonal to inter-annual, and seasonal to decadal forecasting timescales. Forecasts at these longer timescales are beginning to offer useful skill to many sectors including agriculture, infrastructure, climate-related health issues and water management (Hurrell et al., 2010; Meehl et al., 2021).

Predictability at these time scales is largely associated with the major modes of variability in the atmosphere-ocean system (including the transport of heat in oceans), and trends due to anthropogenic climate change. Recent advances in the use of decadal ensemble forecasts

(relying on many hundreds of ensemble members) are facilitating increased skill (D. M. Smith et al., 2020; Marcheggiani et al., 2023).

Published decadal forecast products include the Met Office's `DePreSys`, `NOAA` Decadal Climate Outlook, and the ECMWF Decadal Forecasting System.

2.3.2.4 METEOROLOGICAL RE-ANALYSES

A meteorological analysis is obtained from data assimilation of a wide variety of observations (satellite, ground-based, from aircraft …); the observations adjust a short-range background forecast produced by Numerical Weather Prediction, producing a best estimate of the current state of the atmosphere to use in the next forecast step. A re-analysis product applies this process to historic records of observations, producing a more homogeneous record of the past atmospheric state by using NWP to fill in the gaps in data. Popular re-analysis products include `ERA5` (Hersbach et al., 2020), `MERRA-2` (Gelaro et al., 2017), `JRA-55` (Kobayashi et al., 2015), `NCEP` (Kalnay et al., 1996).

Re-analysis datasets are an essential tool for modern meteorological research, and also commonly employed for many applications outside of meteorological science, in sectors including health, finance, and energy. Among the most frequently used weather variables are surface temperature, near-surface wind speed, humidity, and surface pressure.

We can only go back so far with re-analysis, since we are reliant upon observations. Observations have not been evenly distributed throughout history, and the majority of older records are located across industrialised Europe and along shipping routes. From the 1970s and 80s onwards, the proliferation of satellite observations has greatly improved global observations coverage and reconciled a gap between northern and southern hemisphere forecast skill (Bauer et al., 2015).

A case study of the 1903 Storm Ulysses is explored by Hawkins et al. (2023), with re-analysis pressure, windspeed, and observations indicated in Figure 2.25. Panel *d* shows large spread in the re-analysis ensemble members sea level pressure (more than 7 hPa standard deviation)
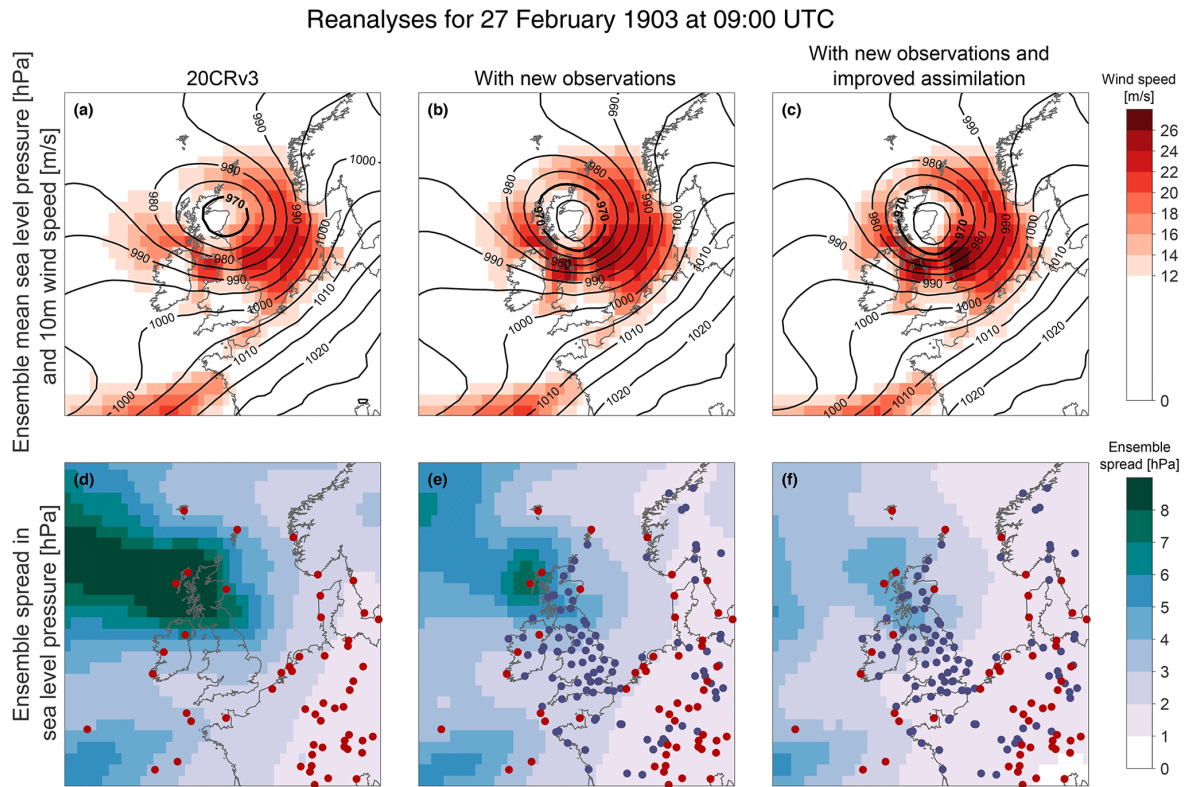
Figure 2.25: Reconstructing the atmospheric circulation during Storm Ulysses. Synoptic situation at 09:00 UTC on 27 February 1903. Isobars of sea level pressure (hPa, black contours) and wind strength at 10 m (m s^{-1}, red shading) from the ensemble mean of 80 reanalysis fields are shown from 20CRv3 and the two different experiments (top row, a–c). Standard deviation of the ensemble of sea level pressure reanalysis fields ("ensemble spread") for the same time (hPa, blue shading, bottom row, d–f). Locations with available surface pressure observations in 20CRv3 are shown as red dots, and new added observations in the experiments are shown as dark blue dots. Observations from both land stations and ships are shown, but there are very few available ship observations in this region at this time. Hawkins et al. (2023), CC BY 4.0.

in the North West. However, the re-analysis can constrain this uncertainty by assimilating a greater number of observations, with panel *e* showing a significant reduction in the ensemble member spread (down to below 5 hPa), and further reductions with improved assimilation in panel *f* (less than 3 hPa).

This case study shows how historic storms can be better modelled by rescuing old weather observation records. Furthermore, it showcases an important consideration for how we understand and use re-analyses: that weather re-analyses are a best attempt at re-creating past weather, but these models are not perfect — they are after all only models.

Therefore, it should not be taken for granted that re-analysis = truth. In particular, remote regions, and regions with complex surface structure (for example mountainous or urban) can provide challenges for re-analysis products. Additionally, whilst different re-analyses may agree at coarser temporal resolutions (monthly or daily), they may show quite different behaviours at sub-daily and hourly time resolutions.

Re-analyses are known to be unreliable for parameters relating to severe convection, due to poor representation of some rare and extreme convective environments. Although not perfect, modern re-analysis products, including `MERRA-2` and `ERA5`, have considerably improved representation of convective profiles compared to previous generations of re-analysis (Taszarek et al., 2021).

Results in this thesis depend on temperature (air temperature measured immediately above the surface), a variable that at the sampled spatial and temporal resolutions shows strong agreement across re-analysis and observations datasets (for example, see Appendix B).

2.3.2.5 Climate Models

Climate models are a representation of the Earth system, used to simulate historical or future climate conditions. The earliest climate models ('Energy Balance Models') implemented simple models of radiative equilibrium, cloud and ocean effects.

Subsequently, a one-dimensional radiative-convection model (Hansen et al., 1981; Jeevanjee et al., 2022) was used to compute temperature changes with altitude. The model calculated temperature-sensitive absorption coefficients at each pressure level, individually for the spectra of H_2O, CO_2, O_3, N_2O, and CH_4. Parameterisations for cloud and aerosol effects were explored, constraining large uncertainties present at the time. These models and successors have been recognised to have performed well at predicting climate sensitivity and projecting warming to the present day (Hausfather et al., 2020).

Building on the progress of energy balance models and radiative convective models, came the Global Climate Model (GCM) — which simulate physical processes. Initially, climate models
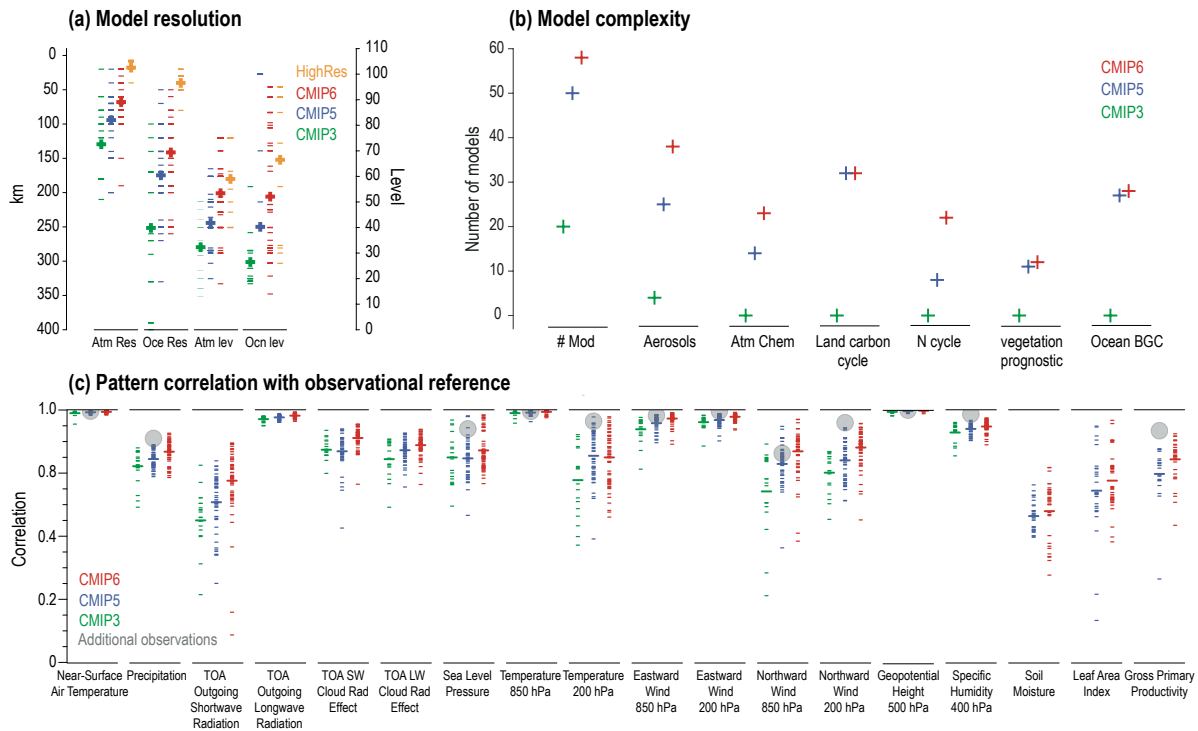
Figure 2.26: Present improvements in climate models in resolution (a), complexity (b) and representation of key variables 1980 to 1999 (c), from the Coupled Model Intercomparison Project Phase 3/5/6. Results are shown for individual CMIP3 (cyan), CMIP5 (blue) and CMIP6 (red) models as short lines, and ensemble averages (long lines). The correlations are shown between the models and the primary reference observational data set (from left to right: ERA5, GPCP-SG, CERES-EBAF, CERES-EBAF, CERES-EBAF, CERES-EBAF, JR-55, ERA5, ERA5, ERA5, ERA5, ERA5, ERA5, AIRS, ERA5, ESACCI-Soilmoisture, LAI3g, MTE). Grey circles indicate correlation between primary reference and additional observational data set. Chen et al. (2021, Figure TS.2)

were only designed as *atmosphere-only* or *ocean-only* models. The latest generation of climate models ('Earth System Models'), implement coupled land/ocean/atmosphere processes, and incorporate chemical, hydrological, cryosphere, and biosphere processes (Figure 2.26 panel b shows the increasing model complexity of modelled processes, and panel c the resulting improvements in modelling different physical processes). Climate models are applied to past, present, and future representations of the Earth system. With the advent of seamless models, many climate models now share their code base with weather prediction models (as is the case for the Met Office Unified Model).

Advances in model implementation, and in available computing power, facilitate running climate models at increasingly high resolution: early GCMs were limited to 500 km grid resolu-

tion, whilst recent generation GCMs (e.g. CMIP5 and CMIP6) are typically 150 km or higher resolution, shown in Figure 2.26 panel a. Higher resolution models allow access to higher resolution model outputs, but coarser scale outputs may also benefit from the improved representation of smaller scale processes. For example, Moreno-Chamarro et al. (2022) find multiple benefits to increasing model resolution (such as ocean-eddy and coastal wind systems representation), resulting in a reduction in ocean surface temperature biases. The improved process representation at a higher resolution should achieve better bias reduction in meteorological variables, therefore requiring less severe calibration when used in impact modelling.

The computational cost of climate models is a trade-off between resolution, physical complexity, and computational feasibility (number of model years and ensemble size). Our uncertainty in near-term projections of climate change is dominated by model uncertainty (parametric uncertainty and model formulation) and to a lesser degree, internal variability (Brayshaw, 2018; Hawkins & Sutton, 2009).

A logical next step towards constraining the dominant uncertainty in climate models is to further increase resolution — and Regional Climate Models (RCMs) achieve this by downscaling a GCM product (or less commonly an observations-based dataset) over a limited area. The CORDEX downscaling experiment is a collaborative effort to produce RCMs over each continent (including Antarctica), increasing the number of modelled scenarios and supporting the exploration of uncertainty (Giorgi et al., 2009; Rummukainen, 2016). In Chapter 4, RCMs from the UK Climate Projections (UKCP18) are used instead of GCM outputs, as these models demonstrate superior historical empirical adequacy as measured through the model ability to reproduce surface temperature, precipitation, and AMOC[11] strength (Pacchetti et al., 2021).

Beyond the constraints presented by model resolution and computing power, which induce some level of systematic bias, climate models reflect only our best effort in defining Earth system boundary conditions, transient orography, parametrisation of physical processes. Uncertainty in climate change projections has traditionally used multi-model ensembles, where different model assumptions are put to the test (Slingo & Palmer, 2011). However, producing

---

[11]AMOC: Atlantic Meridional Overturning Circulation, the main current system in the Atlantic ocean.

high resolution GCM and RCM runs, spanning decades (or centuries), for multiple ensemble members is computationally expensive, and without producing a very large number of model runs, it is difficult to reach a robust risk assessment.

Perturbed Physics Ensembles (PPEs) offer a more targeted exploration of the main source of model uncertainty (i.e. the uncertainty in representing different physical processes). Instead of exploring the uncertainty from differences in model implementation (resolution, time-stepping scheme, etc.), PPEs intentionally perturb the most poorly constrained model parameters related to key physical processes. The UKCP18 climate models, used in Chapter 4, include a collection of 15 PPEs (Lowe et al., 2018). Model 'emulators' are additionally used by Lowe et al. (2018) and elsewhere, as a computationally inexpensive approach to further sample parameter uncertainty.

Although the focus in Chapter 4 is on RCM PPE models, there are many ongoing efforts to constrain other key sources of variability, including internal variability. Multi-model ensembles and Perturbed Physics Ensembles should not be treated in the probabilistic sense that we use operational weather forecast ensembles — it is assumed that each ensemble is an equally plausible realisation rather than deviations about a single 'most plausible' model.

Large ensemble simulations, using a single model under the same physics and external forcing (and slightly perturbed initial conditions), are used to study uncertainties arising from internal climate variability. Since only one set of model physics is implemented, it is possible to take statistical measurements across the collection of ensemble members. These are of particular importance to the study of compound events and extreme event attribution (Thompson et al., 2017; Bevacqua et al., 2023).

2.3.2.6 CLIMATE CHANGE PROJECTIONS

Climate projections are simulations of the Earth's future climate — typically run until 2100. At multi-decade timescales and further into the future, the uncertainty presented by future emissions scenarios becomes a main source of uncertainty.

Climate models generally represent projected emissions using the Representative Concentration Pathways (RCPs), or the newer system of Shared Socio-economic Pathways (SSPs). RCPs describe the different levels of CO_2 and other greenhouse gases in terms of a defined level of radiative forcing (commonly RCP 2.6, 4.5, 6.0 and 8.5 W m^{-2}), and are designed to be used to measure climate sensitivity. The SSPs propose socio-economic narratives that represent plausible emissions pathways towards decarbonisation (or further fossil-fuelled development).

Actually using the outputs from climate models for some purposes requires a careful consideration of the types of uncertainty being represented and sampled, and understanding the assumptions and simplifications that models have taken. To use climate model outputs in an impact model, we must account for differences in the model configuration compared to the observations used (grid size and type, time step). Climate models, as with any Numerical Weather Prediction model, exhibit biases (e.g. (Kennedy-Asser et al., 2021)), and we must consider where biases may affect results and correct for this — Chapter 4 explores several methods that correct for bias in modelled infrastructure electricity load and reserve energy systems.

The UKCP18 land projections (Figure 2.27) used in Chapter 4 use results from the Met Office global climate model, HadGEM3-GC3.05, as well as a set of climate models from CMIP5. Downscaling models are produced covering Europe (the RCMs) for the HadGEM models, and a novel addition of Convection Permitting Models is produced at a 2.2 km resolution for the UK region HadGEM models (Lowe et al., 2018; Met Office Hadley Centre, 2019).

Outputs from UKCP18 are available as gridded data, or in the form of probabilistic projections. The probabilistic projections offer an interesting option, combining the outputs of HadGEM and CMIP models, and using emulators to further explore the parameter space. However, the presented probabilities are not presented with thorough physical interpretation of model outputs, and offer no method for correcting potential model biases (Pacchetti et al., 2021).
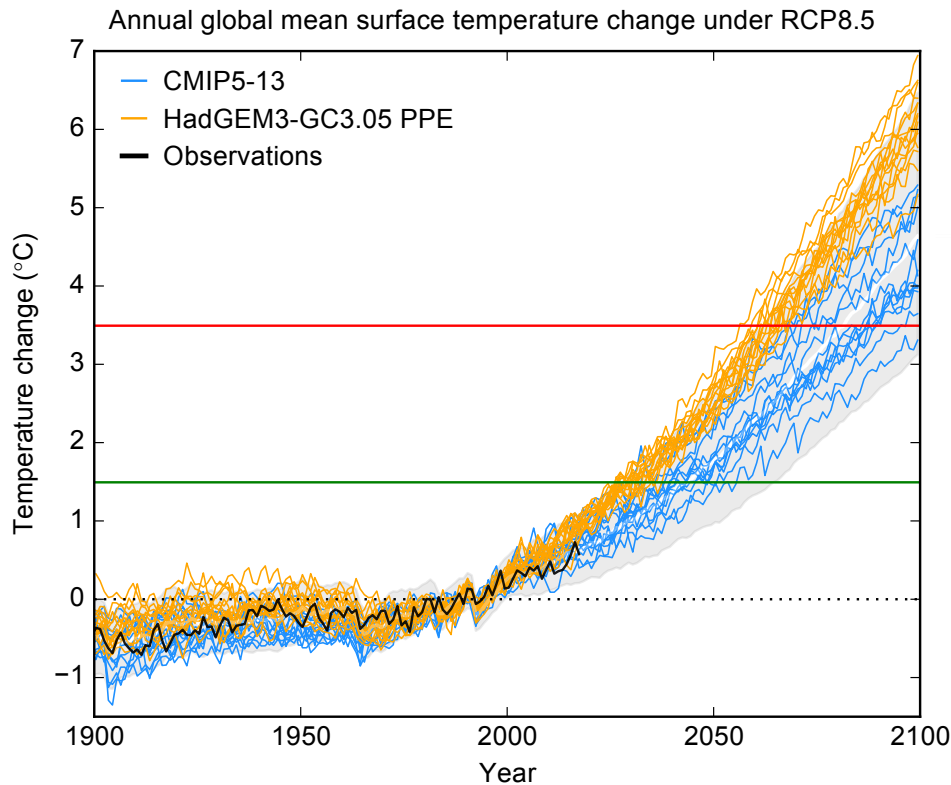
Figure 2.27: Historical and future changes in annual global mean surface temperature, from 1900 to 2100, relative to a 1981 to 2000 baseline. The RCP8.5 emissions scenario is applied from 2005 onwards. Probablistic projections shown shaded grey. CMIP5 models shown in light blue, and Met Office GC-3.05 models shown in orange. Observations (black) are derived from HadCRUT4. The green and red lines show $2\,°C$ and $4\,°C$ above pre-industrial baseline (1850 to 1900). Lowe et al. (2018, Figure 2.13). Crown copyright 2018, the Met Office.

2.3.3 WEATHER AND CLIMATE SERVICES FOR ENERGY

There is a growing awareness among individuals and organisations of risks arising from climate change, and the need to anticipate and manage weather risks across a broad range of timescales. However, the sheer size, number, and complexity of available datasets in itself presents a barrier to access and make use of all the available information.

As we have uncovered, there are an overwhelmingly large number of meteorological datasets. Some of these relate to simulations or observations of historic weather events, whilst other datasets might for example forecast future weather or explore hypothetical scenarios. Artificial intelligence models are likely to play an increasingly important role adding to the set of available tools to forecasting weather and anticipating high-impact weather events (Chantry
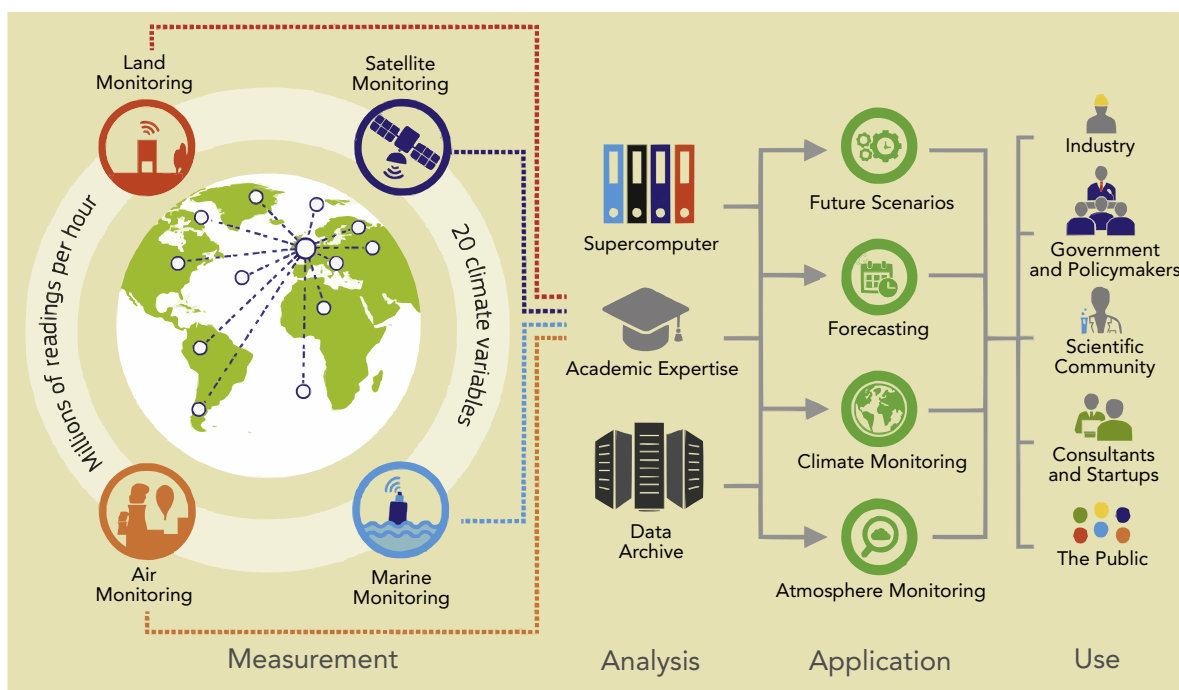
Figure 2.28: Components of the Copernicus Climate Change Service (C3S) implementation: measurement, analysis, application, and use. Buontempo et al. (2020, Figure 1), CC BY NC ND

et al., 2021; Charlton-Perez et al., 2024), and facilitating complex modelling such as pollution monitoring at neighbourhood scales (Kamigauti et al., 2024).

Climate services are 'the provision and use of climate data, information and knowledge to assist decision-making' (World Meteorological Organization, 2023). Climate services is often used to refer to the combined scope of weather and climate services.

There may not always be a clear distinction between a climate dataset and a service (sometimes a climate service may be used simply as a portal to download data), but climate services are intended to deliver more than just raw information. This *extra* value can take the form of pre-processing, user-friendly interfaces, and Application Programming Interfaces, making climate information 'useful, useable and used' (Findlater et al., 2021). Furthermore, climate services must be credible and trusted by decision-makers.

There is a current imbalance between the production of useful scientific products, and the practical uptake of climate services; there is a need to enhance the interactions between science and decision-making, with improved science translation, relationship building, question

framing, setting expectations for what services can achieve (Jacobs & Street, 2020). Furthermore, for policymakers there is a need for standards and validation of climate services, to avoid poor-quality services and misunderstanding/misrepresentation/misues of climate information (Hewitt et al., 2021).

A workshop held in 2020 with over 80 international participants from the "energy" and "climate" research communities was held to identify scientific challenges associated with modelling energy systems climate risk (Bloomfield, Gonzalez et al., 2021). Sources of uncertainty in meteorological datasets are not always well addressed by common practice techniques, which include:

- modelling the energy system impact of multi-decadal climate variability

- calibrating re-analysis data

- post-processing climate model simulations

- error propagation in decision modelling

- epistemic uncertainties in climate projections

Furthermore, energy models and data are not always accessible or credible. The inputs needed to run and design energy models (such as generation data, transmission design, etc.) are not always publicly available and can present inconsistencies (Dubus et al., 2023). For power system modellers, weather and climate many not be the largest uncertainty. Meteorological uncertainties are instead just one of a whole host of uncertainties that affect analysis of power systems. Energy modellers also face uncertainties from technological changes, policy, and other socio-economic factors.

Climate services, applied in the energy sector, agriculture, and else where, have the opportunity to communicate robust and unified datasets to users. These services should be tailored to meet user needs, and ensure that the appropriate weather and climate information is well communicated. Services including Copernicus Climate Change Service (C3S), NASA Prediction

of Worldwide Energy Resources Data Access Viewer (POWER DAVe), World Energy Meteorology Council Teal tool, and Horizon 2020 Sub-seasonal to Seasonal forecasts for Energy (S2S4E) project demonstrate the potential for trusted energy climate services (Bessembinder et al., 2019; Bloomfield, Brayshaw, Gonzalez & Charlton-Perez, 2021a; Hegyi et al., 2024; Dubus et al., 2023; Boorman et al., 2022).

2.4 Summary

Present-day fleets of reserve power systems are dominated by fossil fuel generators (often using diesel or fossil gas fuels). Low-emissions energy storage technologies, including li-ion batteries and hydrogen fuel cells present potential alternatives, but with significant upfront investment cost compared to legacy technologies. Reserve power systems are widely deployed to provide resilience for infrastructure, but this economic barrier to replacing legacy systems represents a challenge to infrastructure owners aiming to reach decarbonisation targets.

Static metrics (such as Levelised Cost of Electricity) for cost of investment and operation cannot reflect the complexities and dynamics of modern power systems (Section 2.1.1). Therefore, we have introduced impact modelling using meteorological inputs and discussed methods for model evaluation (Section 2.1.2). This modelling can support the efficient and resilient design and operation of reserve power systems in critical infrastructure (Section 2.1.3).

Next, Section 2.2 serves as an overview of the modern and evolving energy landscape, covering various important technical, economic, and regulatory aspects of the structure of power system networks and electricity markets. Section 2.3 introduces key meteorological background covering the dynamical processes that drive the energy sector, and the Numerical Weather Prediction methods and datasets that are essential tools for understanding energy-meteorology impacts.

The research chapters build on this multi-disciplinary collection of literature, bringing together some of the latest methods and datasets, and focusing on the practical application towards reserve power systems and critical infrastructure. With this background, we can address the central research theme: designing resilient reserve power systems and rethinking and repurposing these systems to unlock added benefits from decarbonisation.

A New Framework for Using Weather-Sensitive Surplus Power Reserves in Critical Infrastructure

This chapter addresses the research question: *Can weather-sensitive simulation of reserve power systems support resilient system design and characterise periods of surplus capacity?* (Thesis RQ i). The contents of this chapter have been adapted from an original research paper, published in the journal of Meteorological Applications (RMetS), available with the reference:

Fallon, J. C., Brayshaw, D. J., Methven, J., Jensen, K., Krug, L., 2023: A new framework for using weather-sensitive surplus power reserves in Critical Infrastructure. *Meteorological Applications, 30(6), e2158*, https://doi.org/10.1002/met.2158

Changes to this work include minor typesetting alterations and assigning new reference numbers to be consistent with the thesis. The original introduction and research challenges have been replaced with a shorter introduction below, to avoid repetition within the thesis. An accompanying dataset has been published at the Reading Research Data Archive (see *Telecoms Electricity Load Model (Re-analysis)*, Appendix A).

3.1   Introduction

Reserve power systems and critical infrastructure have been discussed in Chapters 1 and 2. A reserve power system may be subject to regulation, for example ensuring that expendable supplies can be maintained for a provisioned number of days (CISA, 2022). If heating or cooling is involved, energy consumption may be strongly influenced by prevailing weather conditions and seasonality.

Whilst weather-driven models of energy demand are well established (for example Taylor and Buizza, 2003), and there is literature on climate change impacts to backup energy storage (Weber et al., 2018), we address a perceived gap in published literature for the application of meteorological data to understanding drivers of critical infrastructure demand, making linkage to weather and climate risk to the reserve power infrastructure and wider grid.

An impact model for infrastructure electricity load (used here and in Chapters 4 and 5) is constructed and some potential applications are explored (Section 3.3). This model represents the national (and regional) electricity load of British Telecommunications PLC (BT) building demand, including server rooms and offices, characterised by heating and cooling demand. Whilst the electricity load model represents critical infrastructure (specifically the case study of BT), findings are considered more widely applicable to other sectors including data centres and hospitals. Thesis RQ i is divided into three sub-questions:

RQ i.1 To understand and quantify how the total reserve energy capacity required for the GB telecommunication system is impacted by differing levels of risk tolerance. (Sections 3.5.2 and 3.5.3)

RQ i.2 To assess and understand how the total reserve energy capacity varies seasonally and hence to identify periods and quantities of surplus capacity available, given an expressed risk tolerance. (Sections 3.5.4 to 3.5.6)

RQ i.3 To understand how the availability of surplus capacity relates to supply stress on the wider electricity network. (Section 3.5.7)
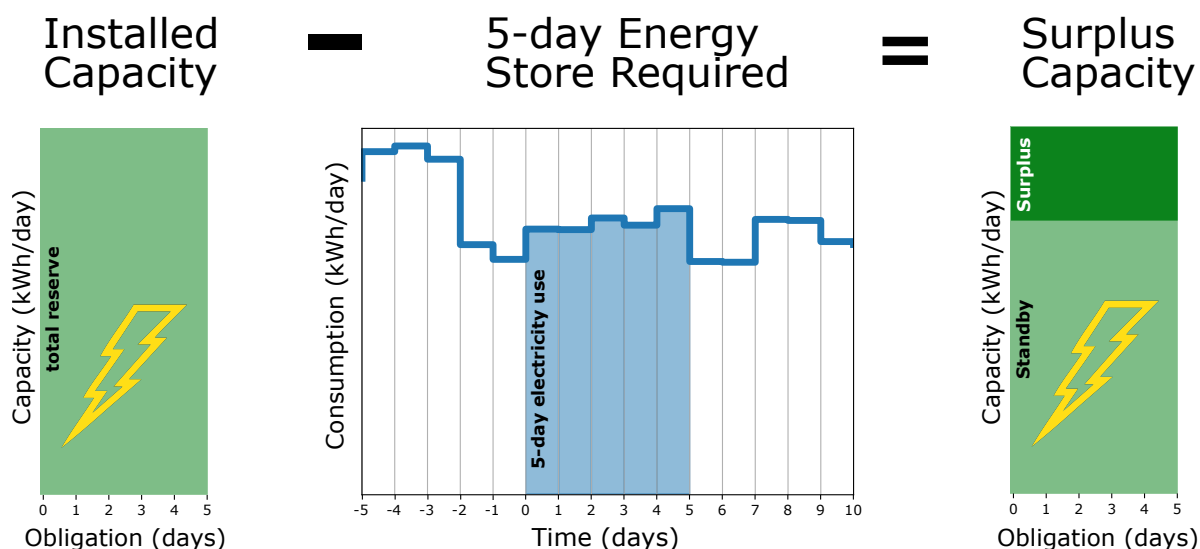
Figure 3.1: Schematic demonstrating the concept of surplus capacity, in the specific case of a 5-day reserve commitment. A critical infrastructure system has a fixed capacity of installed reserve (shown left shaded light green, height given in units of capacity per day, and width in the delivery obligation time). Outside of the periods with very high infrastructure demand, the 5-day consumption (light blue) is some amount less than the installed capacity, leaving a portion of "surplus" (dark green). If this surplus can be accurately anticipated, it may be utilised for other purposes without compromising the N-day reserve delivery commitment.

Using the weather-driven electricity load model applied to 41 years of weather data, a novel framework is introduced to quantify levels of risk[1] associated with a built energy capacity in a reserve system (RQ i.1).

Furthermore, acknowledging the financial and technological challenges of decarbonising and modernising reserve power systems, we explore "surplus" capacity (introduced in Chapter 1 and described in the schematic Figure 3.1). Surplus capacity may support both the security and decarbonisation of the wider grid, whilst offsetting some of the installation costs of the reserve power supply technology itself Mustafa et al., 2021.

We quantify periods of surplus capacity (RQ i.2), and its relation to periods of stress on the wider grid (RQ i.3).

---

[1]i.e. the risk that the provisioned 5 or N day target for backup supply is unmet due to a spike in heating- or cooling-driven demand.

3.2   Datasets

We develop a temperature-driven model of telecommunications service provider BT infrastructure electricity demand, based on data[2] spanning 2016 to 2020. For context, BT use just under 1 % of UK electric grid energy, whilst overall healthcare electricity consumption in the UK is just under 0.5 %[3]. The model's key features reflect those observed in the metered infrastructure demand datasets: weekday patterns driven by human behaviour and day-to-day variability largely explained by cooling power requirements. Analyses are conducted at both regional and national aggregate levels, with regions corresponding to the 14 British Distribution Network Operator (DNO) geographic zones (National Grid ESO, 2020).

In this section we describe the datasets used, specifically: BT electricity consumption data (Section 3.2.1), temperature records (Section 3.2.2), and nation-wide electricity consumption and renewable generation (Section 3.2.3).

3.2.1   INFRASTRUCTURE ELECTRICITY DEMAND

Metered infrastructure electricity demand data is shown in Figure 3.2-a (quality control has removed unphysical readings). Data is anonymised to preserve sensitive information. The significant features are an overall downward trend related to operational energy efficiency improvements over time, substantial peaks in the summer (in particular, due to increased cooling requirements for network equipment locations), and smaller increases in the winter months due to heating requirements. There is also a weekday pattern in infrastructure demand, with weekends being slightly lower than the workdays (on average by 1 %), as seen in Figure 3.2-b. The impact of weekday variability to total infrastructure metered demand measured in each region is between 2.5 % to 4.9 %.

In the present context, we seek to understand and model the impact of meteorological drivers

---

[2]BT `meter readings` have been kindly provided by BT and are not publicly available.

[3]Estimates based on data from Watson (2022), Short et al. (2015) and Department for Business, Energy & Industrial Strategy (2022)
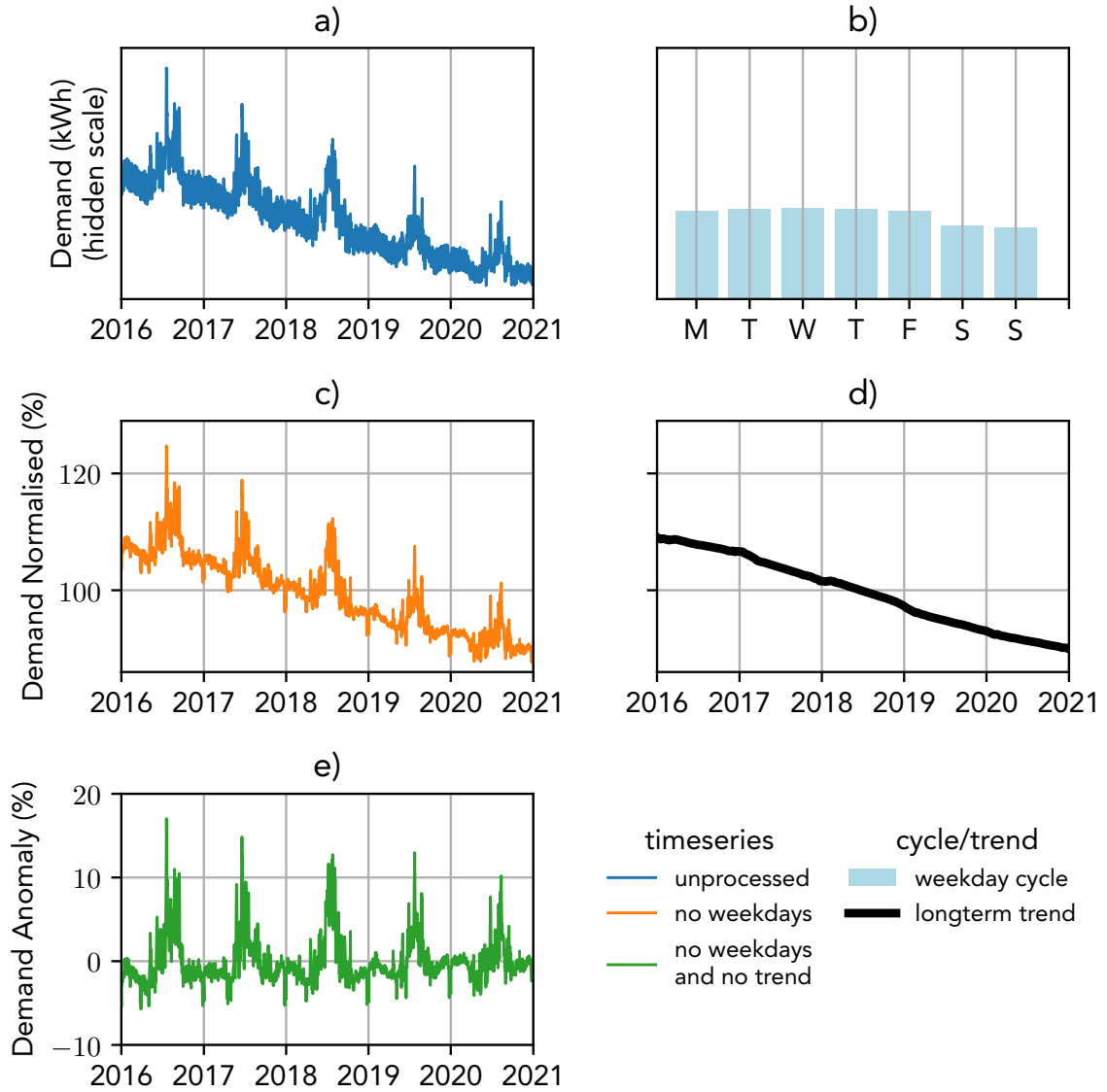
Figure 3.2: Processing steps for BT metered infrastructure demand, depicted for national data. Steps are reproduced at a regional level. Panels show: (a) Quality controlled data D. (b) Weekday pattern D_{weekday} is identified from a. (c) Normalised infrastructure demand (the result of dividing out b from a). (d) Longterm trend c_{trend} is identified from c. (e) Anomaly normalised infrastructure demand (longterm trend d is subtracted from c) uses the symbol $\mathcal{D}$ and forms the basis for analysing the infrastructure demand response to temperature.

on BT's consumption. It is therefore desirable to remove the effects of long-term technological and behavioural trends and patterns such as the day-of-the-week effect. This process is described in Figure 3.2 and Equation (3.1):

$$\mathcal{D}(t) = \frac{D(t)}{D_{\text{weekday}}(t)} - c_{\text{trend}}(t) \tag{3.1}$$

The anomaly normalised infrastructure demand $\mathcal{D}$, a function of time t (daily resolution), is calculated by dividing infrastructure demand D (shown in Figure 3.2-a) by weekday pattern D_{weekday} (shown in Figure 3.2-b) and then subtracting the longterm trend c_{trend} (shown in Figure 3.2-d).

Sensitivity tests showed that static values for D_{weekday} (as opposed to seasonally or annually evolving values) were sufficient in capturing day-of-the-week fluctuations in infrastructure demand.

Longterm infrastructure demand trend c_{trend}, calculated as the 1-year centred window running mean, is believed to result from operational energy efficiency improvements. In most regions c_{trend} evolves gradually and continuously. Three out of the fourteen regions contain discontinuous changes related to faster energy efficiency improvements.

3.2.2 TEMPERATURE

The MERRA-2 global weather reanalysis (Gelaro et al., 2017) is used as a source for temperature timeseries[4]. Daily gridded 2m air temperature data is converted into regional timeseries by averaging over a latitude-longitude box for each DNO zone (Figure 3.3). The resulting regional temperature data, T, is used in model fitting (2016–2020), and later as input to simulated infrastructure demand (1979–2020).

---

[4]Daily temperature timeseries for the gridboxes defined in Figure 3.3 are not sensitive to the choice of reanalysis. For example, ERA5 and MERRA-2 outputs are highly correlated. However, a model incorporating additional meteorological variables (for example windspeed, precipitation) may require further consideration on the choice of reanalysis product.
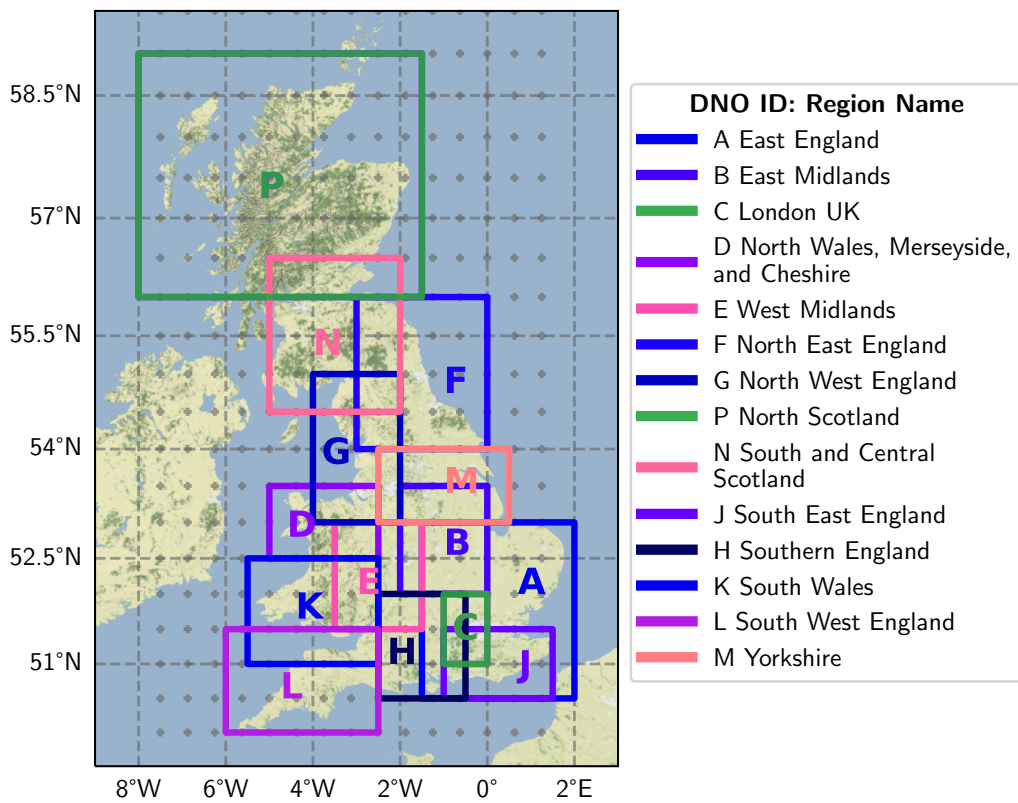
Figure 3.3: Gridboxes used to extract Temperature (2m) from `MERRA-2`, for the 14 DNO zones. Re-analysis gridpoints are displayed as dots, with $0.50° \times 0.625°$ spacing (latitude $\times$ longitude resolution). Zone averages of temperature are calculated by weighting by the square of land-sea fraction for intersecting grid-points. Boundary co-ordinates are given in supporting information Table S3.1
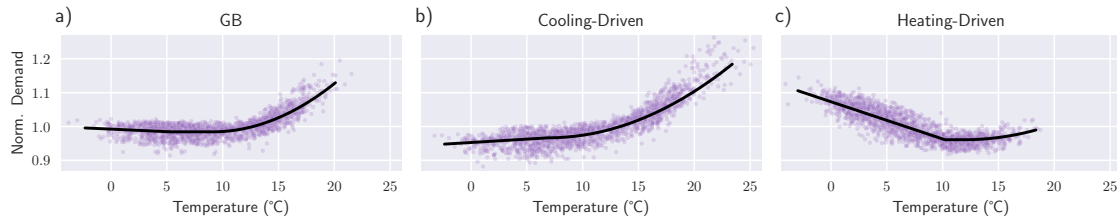
Figure 3.4: BT daily metered infrastructure demand (reconstructed to 2020 trend), in the three case study regions: GB, Cooling-Driven (London) and Heating-Driven (North Scotland). Values are normalised to remove weekday effects. Black curves indicate deterministic model fit.

3.2.3 GB-AGGREGATED GRID DEMAND-NET-WIND

The Transmission System Operator controls the transport of electricity on the wider electricity network, and in GB is served by National Grid Electricity System Operator. From Bloomfield, Brayshaw and Charlton-Perez (2020) and Bloomfield et al. (2016) we use reanalysis-derived grid demand and windpower. The demand-supply impact of weather and climate on the power system is the electricity grid demand minus windpower generation. These nationally aggregated daily variables are implemented with a single model realisation, derived from MERRA-2 data spanning 1979–2017, and without weekday varying component or residual noise. An analogous approach is taken in modelling weather-driven infrastructure electricity consumption in Section 3.3. We assume an installed windpower capacity of 24.5 GW in 2020 (Spry, 2023).

3.3 Weather-Driven Model of Infrastructure Electricity Demand

Figure 3.4 shows the metered infrastructure demand to temperature response. Panel a presents the typical pattern seen in most BT regions: warmer temperatures increase infrastructure demand above a threshold (approximately 10 °C), consistent with the need for cooling equipment dominating BT's overall energy usage nationally. In panel b, the region displayed (London) shows a particularly strong cooling response and no detectable heating response. In

one region, Northern Scotland, there is a markedly contrasting behaviour with cooler temperatures (below 10.2 °C) and differences in infrastructure temperature-sensitivity causing increased infrastructure demand, consistent with the dominance of office heating in energy usage. Elsewhere, the Heating Degree Day (HDD) effect is of much less significance than the Cooling Degree Day (CDD) effect, but in most regions has at least a measurable impact. In all cases, it is noted that there is some spread in the temperature-demand relationship, indicative of other factors impacting infrastructure demand (and explored further in Section 3.4).

Infrastructure electricity demand is modelled with Heating and Cooling Degree Days (Taylor & Buizza, 2003). Our degree day functions take input of regional daily timeseries of temperature ($T(t)$) and are defined in Equation (3.2):

$$
\begin{aligned}
\mathrm{HDD}(T) &= \begin{cases} T_{\mathrm{HDD}} - T & \text{if } T < T_{\mathrm{HDD}} \\ 0 & \text{otherwise} \end{cases} \\
\mathrm{CDD}(T) &= \begin{cases} T - T_{\mathrm{CDD}} & \text{if } T > T_{\mathrm{CDD}} \\ 0 & \text{otherwise} \end{cases}
\end{aligned}
\tag{3.2}
$$

In each region, these functions are used in fitting a new model of $\mathcal{D}$ by ordinary least squares. In each case, we allow the model to select terms which are up to quadratic in HDD and CDD, and we neglect terms which are shown to be negligible (using stepwise regression). In each case, the optimal fit identified either matches the form of Equation (3.3), or in some cases this form was detected as one of multiple fits whose error metrics are consistent. For simplicity, we then impose all models to take the form of linear HDD and quadratic CDD:

$$
\mathcal{D}(T) = \mathcal{D}_0 + \alpha_{\mathrm{HDD}} \times \mathrm{HDD}(T) + \alpha_{\mathrm{CDD}} \times \mathrm{CDD}(T)^2
\tag{3.3}
$$

The degree day functions are as defined in Equation (3.2), and $\mathcal{D}(T)$ is the modelled infrastructure demand. Intercept $\mathcal{D}$ and co-efficients for the three different regional models studied in detail are given in Table 3.1. Three regions are selected to represent distinct temperature-

Region	T_{HDD} °C	T_{CDD} °C	$\mathcal{D}_0$%	α_{HDD} %°C^{-1}	α_{CDD} %°C^{-2}
GB	5.3	9.1	-1.58	0.15	0.12
Cooling-Driven	6.9	6.9	-3.36	-0.2	0.08
Heating-Driven	10.2	11.95	-3.91	1.1	0.07

Table 3.1: Degree day threshold parameters (°C). The thresholds determine the extent of the *heating* and *cooling* degree day domains. The infrastructure demand when not in either heating or cooling regime has value $\mathcal{D}_0$ (%). The heating and cooling responses are further characterised by gradients, α_{HDD}, α_{CDD}, measured in units, %°C^{-1}, and %°C^{-2} respectively. Regions shown are GB, Heating-Driven (North Scotland) and Cooling-Driven (London), as in Figure 3.4, and a complete dataset covering all regions is given in supporting information Figure S3.1 and Table S3.2

demand sensitives. Whilst "North Scotland" has a strict geographical significance for BT (i.e. the data has a correspondence to real infrastructure installed across that region), the characteristic behaviour may be entirely relevant for a completely different type of infrastructure installed elsewhere, which could be, for example, a hospital in South Wales, or an office in North England, depending on the temperature-demand relation present. The three "regions" are chosen to give as wide a representation as possible of different behaviours of infrastructure electricity consumption. Henceforth, to make it clear that these case studies should be considered for their specific temperature-demand behaviours, we refer to the regions as "Cooling-Driven" (London), "Heating-Driven" (North Scotland), and "GB" (the sum total over subregions, reflecting a combination of heating and cooling behaviours, with behaviour broadly representative of other subregions).

Parameter uncertainty ranges are calculated by a random bootstrap sampling of daily infrastructure demand. The variation in temperature thresholds (T_{HDD} and T_{CDD}) calculated from sampling is below $1\,°C$, whilst gradient parameters vary by less than $10\,\%$ of their respective mean values[5].

---

[5]Bootstrap sampling was conducted by creating new 5–year timeseries based on the grid demand data 2016 to 2020, and randomly re-sampling the years. A bootstrap size of 41 was used. Further tests limiting the data to a 3-year window at the start/end (i.e. 2016 to 2018 and 2018 to 2020) showed parameters consistent and within the uncertainty range of the full 5-year version, indicating that despite long term trends in the mean energy use, the weather-sensitivity was consistent.

3.4   Stochastic Weather-Driven Model of Infrastructure Electricity Demand

The models introduced in Section 3.3 are deterministic, i.e. for a known set of weather conditions, there is a singular estimate of the infrastructure demand $\mathcal{D}$. As noted in Section 3.3, there is a spread in the temperature-demand relationship. The output from the deterministic model can be interpreted as the expected $\mathcal{D}$ for a given set of weather conditions. The actual $\mathcal{D}$ which would be recorded on such a day may be either higher or lower than this expected value due to 'other factors' which are not being expressly modelled. In some cases such factors may be weather related — e.g. additional variables such as humidity or wind speed — or from non-weather-related sources. However, no additional meteorological- or calendar-related impacts were detected in the BT consumption dataset.

The reduced variability in (deterministic) modelled $\mathcal{D}$ alters the probability distribution of demand, especially significant near the extreme tails. In the context of estimating reserve requirements it is therefore useful to represent the effect of these 'other factors' stochastically. We introduce a first-order autoregressive stochastic term, which encompasses the missing variability. A pseudo-random, normally distributed first-order autoregressive timeseries is constructed for the *residual* infrastructure demand component $\mathcal{D}_{\text{res}}$ (i.e. the difference between modelled infrastructure demand and observed (metered) infrastructure demand after removing the effects of longterm trends). The calculation of this daily demand timeseries is shown in Equation (3.4):

$$\mathcal{D}_{\text{res}}(t) = \rho_1 \mathcal{D}_{\text{res}}(t-1) + Z(t) \tag{3.4}$$

$\mathcal{D}_{\text{res}}(t)$, the residual infrastructure demand at step t is related to the previous time step multiplied by residual lag first-order autocorrelation ρ_1. The timeseries is initialised at $\mathcal{D}_{\text{res}}(0) = Z(0)$. The normally distributed random component Z has mean 0 and standard deviation σ_Z related to the standard deviation of the infrastructure demand residual (Chatfield, 2003), and

given in Equation (3.5):

$$\sigma_Z = \sqrt{1 - \rho_1^2} \times \sigma_{\text{res}} \tag{3.5}$$

The residual standard deviation σ_{res} introduces variability equivalent to that of observations minus model (but accounting for longterm trend).

Stochastic realisations are obtained by combining the deterministic and residual stochastic components, described in Equation (3.6):

$$\mathcal{D}^{(r)}(t) = \mathcal{D}(T(t)) + \mathcal{D}_{\text{res}}^{(r)}(t) \tag{3.6}$$

Each stochastic realisation r of modelled demand $\mathcal{D}(t)$ corresponds to a different random sampling of the normally distributed term Z in Equation (3.4). The modelling of the stochastic noise term as normally distributed and lag 1 is justified in the supporting information Figures S3.2 to S3.4 Infrastructure demand $D(t)$ in physical units (kWh) is obtained by applying the inverse of Equation (3.1) to each realisation $\mathcal{D}^{(r)}$ with some minor modifications:

$$D^{(r)}(t) = \left(\mathcal{D}^{(r)}(t) + c_{\text{trend}}(t_{2020}) \right) \times D_{\text{weekday}}^*(t) \tag{3.7}$$

Instead of re-applying the original trend $c(t)$ (which only spans 2016–2020), we apply the static trend coefficient $c_{\text{trend}}(t_{2020})$ evaluated for mid-2020 (1st July) so that the modelled infrastructure demand is relevant to the most recent estimate of infrastructure energy efficiency. Additionally, the stochastic model cycles through different possible combinations of the weekday pattern coinciding on calendar dates: $D_{\text{weekday}}^*(t) = D_{\text{weekday}}(t + (r \bmod 7))$, the modulo offsets the weekday pattern of the realisation by a constant number of days ranging 0 to 6, specific to realisation number r. This ensures that the (non-meteorological) weekday effect is not unfairly suppressing/amplifying particular weather events that happen to overlap particular days of the week.
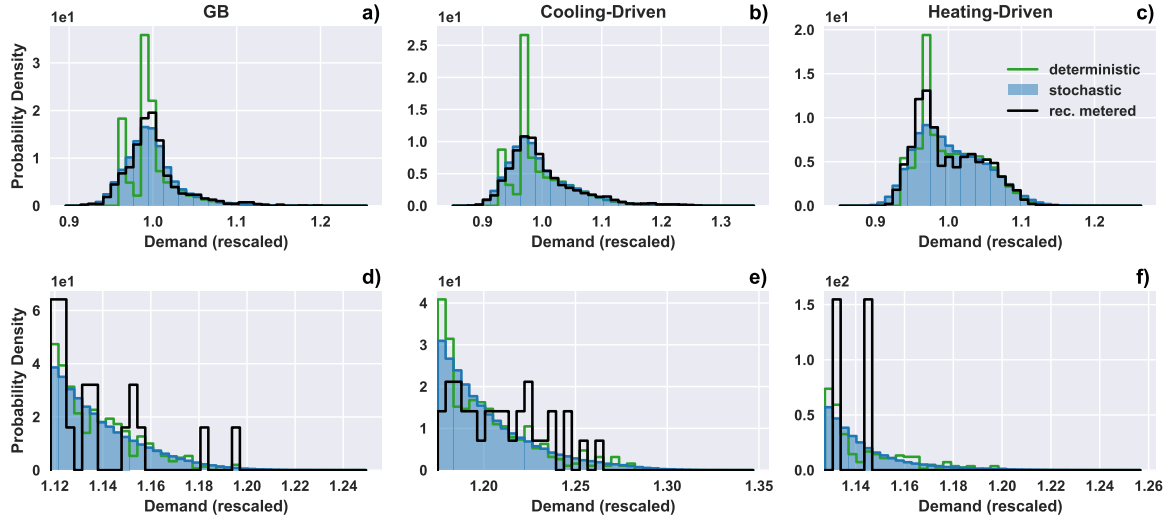
Figure 3.5: Probability distributions of Infrastructure Demand $\mathcal{D}(T)$ in rescaled units, full distribution (a—c) and top 1 % of distribution (d—f). The *reconstructed* metered infrastructure demand is the original metered infrastructure demand rescaled to 2020 (applying a correction for removing the longterm trend c_{trend} by applying Equation (3.1), and then converting back into physical units with a static trend coefficient in Equation (3.7), with $r = 0$ for real calendar days). Scale is hidden in order to protect proprietary information of BT's infrastructure demand data.

The distribution of daily infrastructure demand is shown in Figure 3.5. Histograms are calculated: 41×7 years of daily infrastructure demand deterministic model (from 41 years of `MERRA-2` data and 7 implementations of the weekday cycle); 1750 realisations of the stochastic model (250 of each weekday offset); and 5 years of metered data (reconstructed to remove the underlying long term trend). The probability distribution of the deterministic model is a poor match for the metered data, with two large spikes (corresponding to week-day and weekend infrastructure demand) and unrealistic lower distribution bound cutoff (if the temperature is such that there is no degree day induced demand, and it occurs on a Sunday, then the demand cannot be reduced any further). The stochastic model, however, re-introduces missing variability and provides a very accurate distribution fit for the GB/cooling-driven regions in particular. Whilst the metered data only samples five weather years, the stochastic model has thousands of realisations of 41 weather years, and is therefore a more representative weather-driven infrastructure demand distribution.

Figure 3.5 panels d—f show that, encouragingly, the right-hand tails of the stochastic mod-

els closely match the reconstructed infrastructure demand. The increased sample sizes of the stochastic models yield smoother probability distribution tail-ends than the metered infrastructure demand.

Extreme values are limited by the adopted normal distribution (probability of extreme values of demand are distributed $\sim e^{-D^2}$), and further by first-order correlation of the residual stochastic component (Equation (3.4)). This model, with a large number of realisations ($n = 1750$) and spanning 41 years of weather input, should act as the most complete and accurate dataset from which we can derive estimates of possible infrastructure demand events and implications to reserve power infrastructure.

3.5 Results

3.5.1 INFRASTRUCTURE DEMAND CLIMATOLOGY

Figure 3.6 shows the 41-year climatology of modelled stochastic infrastructure demand, in each of the three regions. Additionally, the grid electricity demand-net-wind (deterministic model) is shown in panel d; 'demand-net-wind' is the shortfall of electricity load to be met by generation after subtracting the windpower generation, calculated by Bloomfield, Brayshaw and Charlton-Perez (2020). We do not explicitly model solar power, which is partially embedded in the grid demand model.

The Heating-Driven region has similar characteristics to the grid demand-net-wind, peaking in winter (cold weather) and suppressed weather-driven variability and low overall demand in summer. Conversely, GB and Cooling-Driven infrastructure demand variability and peaking are most significant in summer months. Given the significant seasonal variation in infrastructure demand, we can also expect to see seasonal variation in the 5-day (or N-day) energy consumption and hence the level of reserve capacity that must be available.
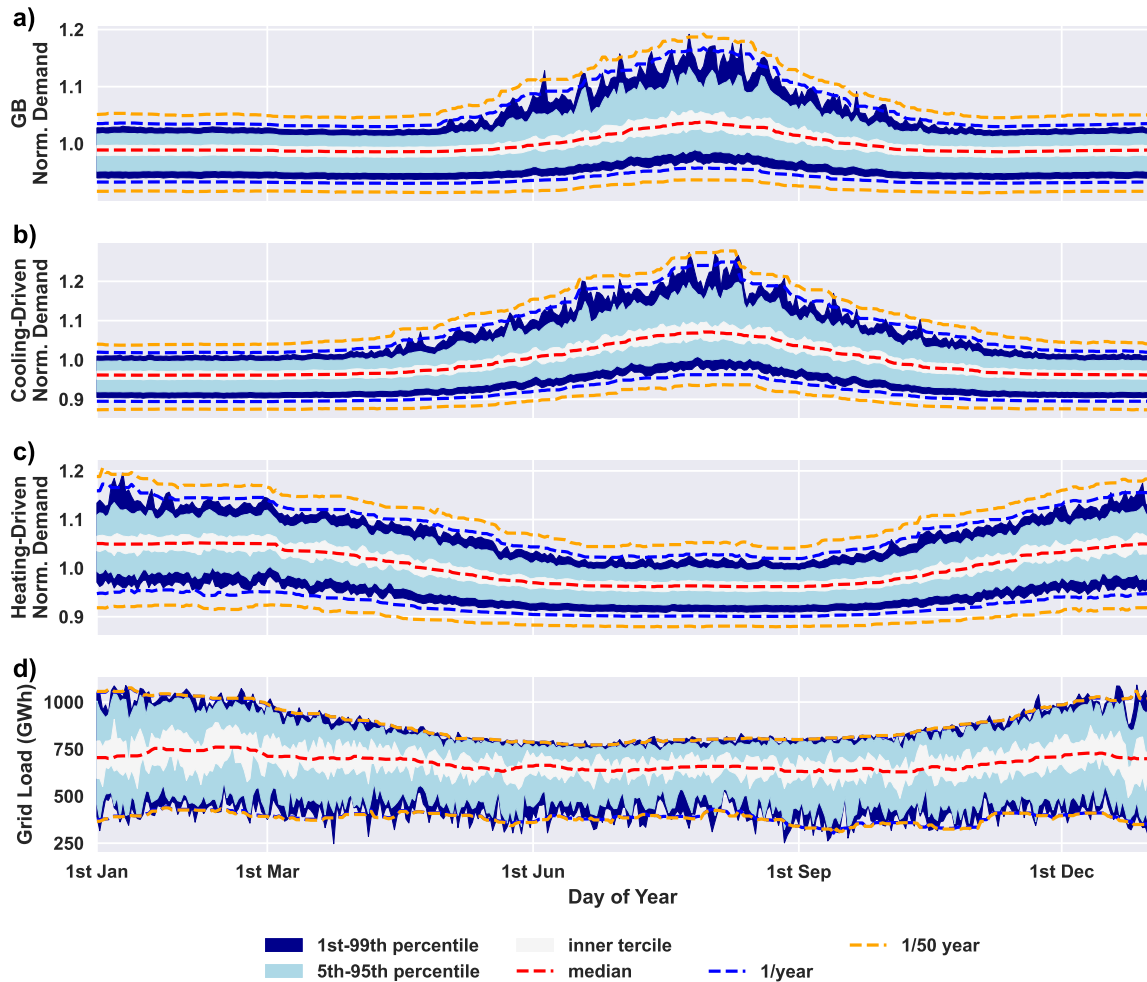
Figure 3.6: Climatology of daily infrastructure demand of GB, Heating-Driven (North Scotland) and Cooling-Driven (London) BT regions, and of the grid demand-net-wind data from (Bloomfield, Brayshaw & Charlton-Perez, 2020). Shaded areas are raw daily-climatology percentiles (sampling 41 weather years and 1750 stochastic realisations for BT infrastructure demand). Dashed lines use 15-day rolling median smoothing.

3.5.2   RESERVE CAPACITY & SEASONAL VARIATION

For critical reserve power infrastructure subject to strict operational time commitments (N-day reserve power), the installation capacity is determined by a small number of infrastructure high-demand events. Simply selecting the highest N-day energy consumption event observed in the original metered infrastructure demand data as a reference for the necessary reserve capacity is precarious since the dataset is limited and unlikely to reflect the most extreme values that could be expected if a longer baseline period was made available. Choosing the highest N-day energy consumption event from the simulated infrastructure demand (Sections 3.3 and 3.4) is an improvement, exposing the data to decades of weather events as well as many different realisations of the 'stochastic' component, ensuring a wide range of plausible outcomes for the combined effects of meteorological and non-meteorological impacts are explored. However, in this latter case, the value of the greatest N-day energy consumption is limited by the number of stochastic realisations, and since the model uses (unbounded) normally distributed noise, there is no upper bound to what the highest N-day energy consumption could be.

Therefore, in order to make a planning decision based on full use of the available weather information, but without arbitrary factors related to the model implementation, we must frame the problem in terms of a risk of exceeding the installed reserve capacity E.

We introduce indicator function $X(t_i)$ to describe whether the infrastructure demand accumulated over N-days (from time t_i to t_{i+N-1}) could have theoretically been supplied (0) or is exceeded (1) if reserve power had been relied upon:

$$X(t_i) = \begin{cases} 1 & \text{if } \sum_{j=0}^{N-1} \left(D_{i+j} \right) > E \\ 0 & \text{otherwise} \end{cases} \tag{3.8}$$

The statement $\sum_{j=0}^{N-1} \left(D_{i+j} \right) > E$ yields true if the N-day infrastructure electricity consumption exceeds the installed reserve capacity E. For convenience, we denote exceedance indicator $X(t_i)$ for a given year y of a given stochastic realisation r as $X_{y,r}(t_d)$ where t_d is the corres-
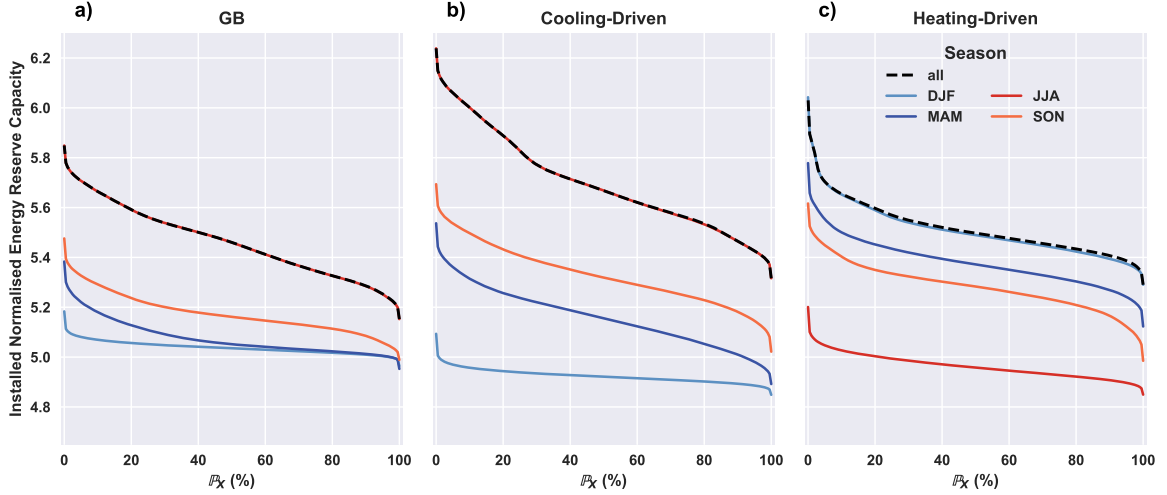
Figure 3.7: Capacity-exceedance relation (see Equation (3.9)) shows the probability that N-day energy consumption exceeds reserve capacity at least once in a given season/year, in the case $N = 5$. Dashed line shows the full-year, whilst other lines correspond to meteorological seasons: December January February (DJF), March April May (MAM), June July August (JJA), and September October November (SON). In the normalised units (y-axis), 1 unit of energy is equal to the mean daily infrastructure demand.

ponding day of the year. With no prior information about the infrastructure demand levels, the likelihood $\mathbb{P}_X$ that in a given year, the N-day energy consumption will exceed the reserve capacity E on one or more occasions is:

$$\mathbb{P}_X = \frac{1}{N_y N_r} \sum_{y=1}^{N_y} \sum_{r=1}^{N_r} \left(1 - \prod_{d=1}^{N_d} \left(1 - X_{y,r}(t_d) \right) \right) \tag{3.9}$$

The probability of exceedance $\mathbb{P}_X$ is defined by averaging over years and realisations the complement to $\prod_{d=1}^{N_d} \left(1 - X_{y,r}(t_d) \right)$ (i.e. the complement to no exceedance events occurring). Subscript r denotes a unique stochastic realisation, and y the calendar year (from 1979 to 2020) for the exceedance indicator X. The limits N_y, N_r, N_d, are the number of years, realisations, and days in a year, respectively. The open script font for $\mathbb{P}_X$ emphasises that it is the probability of one or more instances over a period of time N_d where $X(t_i) = 1$.

The relation between $\mathbb{P}_X$ and E is demonstrated in Figure 3.7, for the three case study regions, with the reserve commitment of $N = 5$. In the normalised units, 1 unit of energy equals the mean daily infrastructure demand, hence 5 units is equal to 5 average days of consumption etc.

In addition to the full-year case (black dashed line), we plot lines corresponding to meteorological seasons. In these cases, Equation (3.9) is revised, so that time indexes 1 to N_d correspond to the respective season.

As risk aversion is relaxed, the installed reserve capacity is reduced whilst the probability of exceedance $\mathbb{P}_X$ increases. For risk-averse behaviour approaching $\mathbb{P}_X = 0$, steeper gradients indicate an increasing cost for more marginal gains in risk reduction. The GB and Cooling-Driven regions experience the maximum energy-consumption events in late July/early August (consecutive days in the upper percentiles of Figure 3.6), hence, the relation between probability of exceedance $\mathbb{P}_X$ and installed capacity E is the same in a given year as it is for a given June July August (shown by the two respective curves matching in Figure 3.7). In the Heating-Driven region, it is December January February (DJF) that closely matches the full-year relation. Demand-inducing low-temperature extremes spread beyond just DJF (see Figure 3.6 Heating-Driven region), so the full-year curve sits slightly above the DJF curve.

As an interpretation of the risk framework for BT's GB region using Figure 3.7, a reserve capacity (given on y-axis) of 5.56 normalised units has 25 % probability $\mathbb{P}_X$ (given on x-axis) of energy consumption exceeding levels that could be supplied by the installed reserve capacity in a given year. Increasing the installed reserve capacity by 2.6 % (to 5.71, slightly higher on the y-axis) reduces the exceedance probability to below 1 % (further left on the x-axis). However, a further reduction in the exceedance probability to below 0.5 % requires an additional 1.2 % to 2.5 % reserve capacity (5.78 to 5.85 units). Off-peak seasons have significantly reduced capacity requirements (corresponding to the overall lower infrastructure demand levels and variability, see Figure 3.6). There is a sizable minimum amount of *surplus* capacity that can be assumed to be available with near-certainty during these off-peak seasons, calculated from the gap between the full-year curve and off-peak season curve.

3.5.3   RESERVE-EXCEEDANCE COINCIDENCE

The hazard faced by operators is not just risk of exceedance but the combination of reserve power being required at the same time. This hazard is sensitive to the total variability in

energy consumption and the installed reserve capacity. To optimise managing the cost of hazard avoidance, the operator may in practice tolerate higher values of $\mathbb{P}_X$, if relying on a low probability of needing N-days of reserve.

This tradeoff can be formulated in terms of the underlying probabilities. First, we introduce indicator function $R(t_i)$, showing when reserve capacity is required for a full N day period starting at day t_i:

$$R(t_i) = \begin{cases} 1 & \text{if reserve required } t_i \text{ to } t_{i+N-1} \\ 0 & \text{otherwise} \end{cases} \tag{3.10}$$

The likelihood of requiring reserve power for N days from a given start day is constant probability $P_R = \mathbb{P}(R(t_i) = 1)$. Each model realisation has a unique corresponding realisation of timeseries $R(t_i)$, and the value of P_R may be adjusted to reflect plausible prevalence. The assumption made of constant P_R is unrealistic, as P_R is likely to have seasonal variability and its own weather-sensitivity, however, modelling a time-dependency for P_R is beyond the scope of our calculations.

The *coincidence* indicator $C(t_i)$ is introduced to mark the hazard of having both reserve requirement $R(t)$ and reserve exceedance $X(t)$:

$$C(t_i) = R(t_i) \cdot X(t_i) \tag{3.11}$$

The hazard probability in a given year without prior knowledge is calculated analogously to Equation (3.9):

$$\mathbb{P}_C = \frac{1}{N_y N_r} \sum_{y=1}^{N_y} \sum_{r=1}^{N_r} \left(1 - \prod_{d=1}^{N_d} \left(1 - C_{y,r}(t_d) \right) \right) \tag{3.12}$$

The probability of coincidence $\mathbb{P}_C$ is defined by averaging the complement to $\prod_{d=1}^{N_d} \left(1 - C_{y,r}(t_d) \right)$ (i.e. the complement to no coincidence events occurring) over timeseries years and realisations.
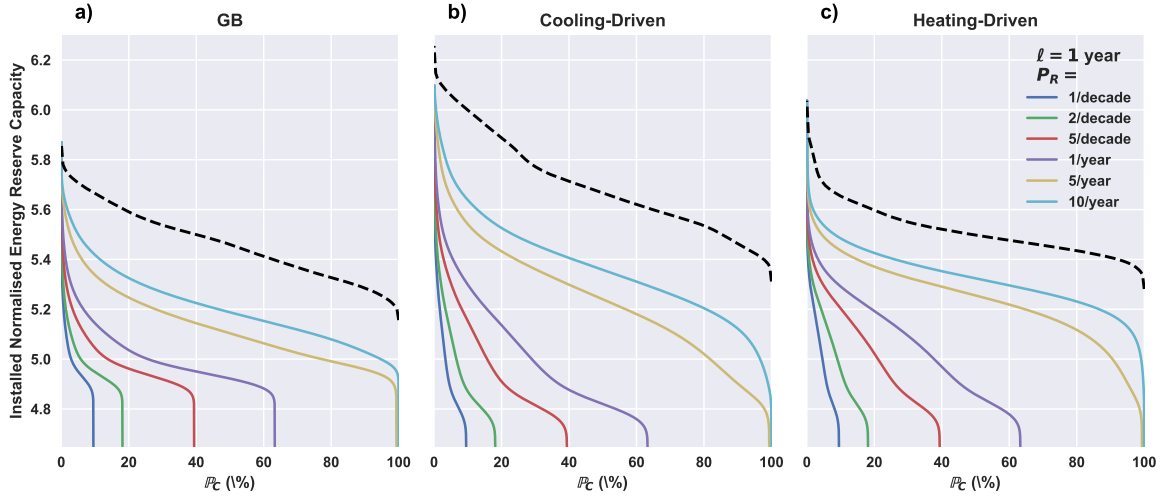
Figure 3.8: Capacity-coincidence hazard relation (see Equation (3.12)). Figure shows the probability that N-day energy consumption ($N = 5$) will exceed the reserve capacity at the same time that N-day's reserve power is required, at least once in a given year. A range of reserve probability, P_R, defined in terms of likelihood of an N-day reserve requirement on any given day, results in adjusted capacity-coincidence curves. An increase in P_R is associated with increase in hazard risk $\mathbb{P}_C$. The dashed line represents hazard risk equal to exceedance risk, i.e. $P_R = 100\%$ and therefore $\mathbb{P}_C = \mathbb{P}_X$. The normalised energy units are as previously described.

Similar to Figure 3.7, but instead demonstrating the capacity-coincidence relation, Figure 3.8 demonstrates how changes in the likelihood (P_R) of a full 5-day reserve event relates the installed reserve capacity to the probability of a coincidence failure.

Most decision-makers will focus on the left side of the plot, where $\mathbb{P}_C$ is low; here, the gradient is strongly impacted by changes to P_R. Being more risk-tolerant (i.e. willing to accept a higher chance $\mathbb{P}_C$ of failure) greatly reduces the reserve requirement, particularly when there is only a small chance (P_R) of needing to draw on the reserve.

Figure 3.8 shows that when taking into account the finite probability of the reserve capacity actually being needed (in addition to the infrastructure demand exceeding the installed capacity), less reserve capacity is needed for a given hazard threshold. The figure also shows the obvious result that a decision-maker assuming lower risk of $R = 1$ has a lower requirement for installed reserve capacity.

However, in the extreme case where the installed capacity is so low as to never meet a full N-days requirement, risk management policy is essentially a bet on the occurrence of $R = 1$.

This lower-limit on the installed capacity corresponds to lines in Figure 3.8 where the $\mathbb{P}_C$—Capacity relation drops off, becoming a vertical line below that point, and this occurs at a $\mathbb{P}_C$ value equal to the probability of reserve, integrated over the year, i.e. $1 - (1 - P_R)^{365}$. This is visible in Figure 3.8 panel a (GB), but too low to be visible in panels b, c.

The Cooling-Driven region again has the highest capacity requirements due to the greater CDD sensitivity, resulting in higher energy consumption during the most extreme events. The Heating-Driven region (which experiences both heating, and to a lesser extent cooling, behaviour) has the steepest gradients, owing to the greater total variability of energy consumption across the full-year (compared to GB and Cooling-Driven where weather-driven variability occurs from exposure to high temperatures primarily in summer months).

3.5.4 SURPLUS VARIABILITY

As discussed previously (Figure 3.6), there is a clear seasonal and meteorological dependence of BT's infrastructure electricity demand, and hence the energy required to meet their 5-day reserve requirement varies similarly (Figures 3.7 and 3.8). Consistent with this, if the installed capacity of the reserve remains constant throughout the year, there are periods where the full installed capacity is not required, referred to here as 'surplus'.

Having developed a framework for linking risk preference to the installed reserve capacity levels, we now seek to quantify how much *surplus* capacity can be exploited for benefits beyond its use as a backup power source. This introduces an additional hazard: if too much surplus is used during a period of low infrastructure demand, there may not be sufficient stored energy for N-day reserve power operation during a subsequent period of higher infrastructure demand.

For a system with a likelihood P_R of having to use the reserve capacity for N-days from a given starting day, there is probability $1 - (1 - P_R)^{365}$ of one or more periods requiring N-day's reserve power in a given year. Consider, for example, a decision-maker operating a system with N-day reserve probability $P_R = 1/365$ on any given starting day, and whose risk tolerance is for up to 1 % probability of at least one coincidence event in a given year (i.e. they
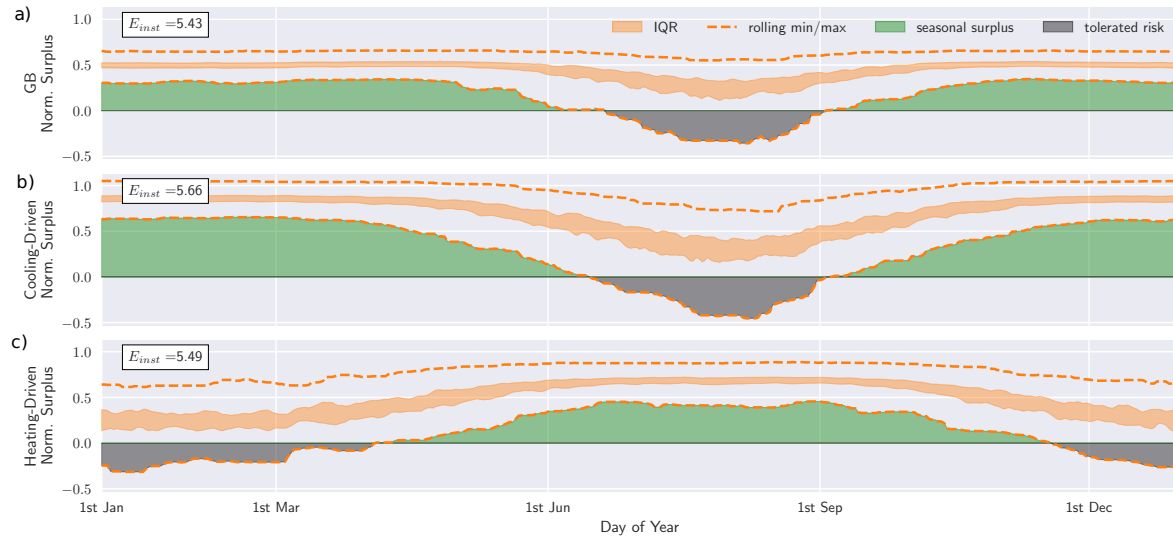
Figure 3.9: For three example systems, reserve capacity installation E_{inst} is set such that the probability $\mathbb{P}_C$ in a given year of failure to meet N-day delivery requirements whilst reserve is in use is 1 %. Green-shaded regions show levels of *surplus* capacity, and grey-shaded regions show tolerated risk concentrated in periods where infrastructure demand is highest. Orange shaded regions show the inter quartile range of N-day ahead surplus capacity. Dashed lines indicated a 15 day rolling window of the climatological minima and maxima (i.e. the highest value to occur on a given day of the year or during the neighbouring 7 days either side).

are aiming for a 99 % assurance of meeting reserve power commitments for an entire year). In the absence of any reserve power system present, the value $P_R = 1/365$ evaluates to a 63 % likelihood of failure in a given year. However, this risk can be mitigated by installing a quantity of reserve power. In the example systems, installing 5.43, 5.66, 5.49 units of reserve power in the GB, Cooling-Driven and Heating-Driven regions, respectively, ensures that $\mathbb{P}_C < 1\%$ (likelihood of a coincidence event where reserve is both required and insufficient for N-day supply) is satisfied, a significant improvement over the 'natural' failure likelihood of 63 % when $P_R = 1/365$.

Given that the installed capacity remains constant, the surplus capacity is calculated by subtracting N-day energy consumption from the installation capacities identified. The annual levels of safe seasonal surplus capacity resulting from the stochastic model are shown in Figure 3.9, as functions of day of the year.

In Figure 3.9, 'worst case' levels of surplus observed in the stochastic model on a given day

of the year (or within 1 week either side) are depicted by the lower dashed curve. For some periods of the year, the 'worst case' levels of safe seasonal surplus still leave a significant baseline amount (shaded green). As long as the 41 years weather data and (1750 realisations of stochastic component) are representative of the full range of infrastructure demand levels that could be experienced, then these shaded green areas give a strong indication of safe levels of reserve almost guaranteed to be available even during the most extreme weather events historically observed for that time of year. Using surplus in excess of the 'safe' levels may sometimes be possible, but induces an additional exceedance hazard (i.e. the overall risk of the reserve not meeting 5-day commitments would be increased). Such operation would require skilful forecasts of infrastructure demand levels at least N-days ahead, to support decisions on how much surplus above safe levels can be utilised for non-reserve purposes.

Periods when the climatological surplus minima crosses below zero indicate that even if dedicating all capacity towards reserve power (setting the amount of surplus to zero), there is the possibility of not meeting the requirements for supplying sufficient reserve capacity. This *tolerated risk* is shaded grey. In this situation of energy consumption exceeding installed reserve, all capacity should be made available for reserve power operation.

3.5.5 SURPLUS ALLOCATION RELATION TO RISK TOLERANCE

Let us consider a decision-maker with access only to climatological information: only the historic weather and infrastructure demand data is known. The climatological decision-maker will base their choices of surplus allocation on the climatological worst-case (i.e. allocating the 'green' levels of surplus capacity shown in Figure 3.9).

We continue with the assumption of $P_R = 1/365$, but now explore a range of risk tolerances in addition to $\mathbb{P}_C = 1\%$.

Surplus accumulated annually for systems installed to meet a variety of different $\mathbb{P}_C$ values are shown in Figure 3.10-a. Increasing $\mathbb{P}_C$ reduces the level of reserve capacity required, which therefore also reduces the annual surplus accumulation. In all three regions, increasing $\mathbb{P}_C$
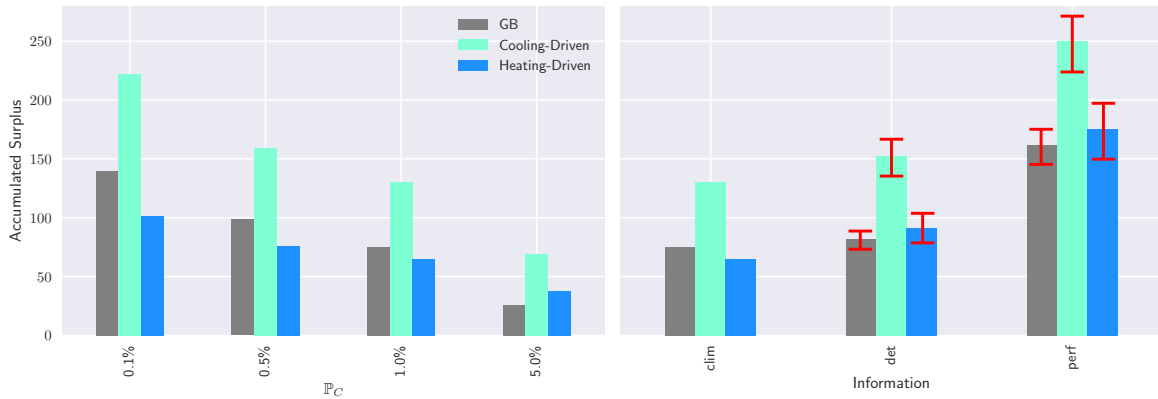
Figure 3.10: Accumulated surplus under different scenarios (for probability of N-day reserve needed $P_R = 1/365$, for $N = 5$). Left: Installed capacity values E (relating to specific coincidence probability tolerances $\mathbb{P}_C$) and resulting accumulated surplus (normalised units). Right: With $E(\mathbb{P}_C = 1\%)$, we explore surplus accumulated under three different decision-making scenarios. Error bars show the 5 % to 95 % range in outcomes across years and realisations.

results in a reduction to the accumulated surplus.

The Cooling-Driven region (with greatest temperature sensitivity) shows the highest levels of accumulated surplus capacity. At lower $\mathbb{P}_C$ values, the Heating-Driven region has the least opportunity in surplus capacity operation, although it does outperform GB at $\mathbb{P}_C = 5\,\%$; tolerated risk in the Heating-Driven region is spread out over a longer period, so an increase to $\mathbb{P}_C$ has comparatively lower impact on the installed capacity E. Most of the change in surplus served relates directly to shifting the green region vertically on the graph by some constant offset, it is only the interface between the surplus and exceedance periods (green and grey) that a minor non-linear contribution to surplus capacity further affects the results.

3.5.6   SURPLUS ALLOCATION RELATION TO FORECAST INFORMATION

A decision-maker with a robust weather-driven model of infrastructure demand should be able to make quite accurate forecasts of the deterministic component, albeit limited to the skill of temperature forecasts up to 5-days ahead, and errors accumulated in model conversion from temperature to infrastructure demand.

Consider two further decision-makers. First, a decision-maker with access to a perfect forecast of the weather-driven infrastructure demand but no information about the stochastic compon-

ent, which we label the *deterministic* decision-maker. Second, a decision-maker with perfect forecast knowledge of both weather-driven and stochastic infrastructure demand components, which we label the *perfect* decision-maker. In this theoretical exercise, these cases can show the potential value, in terms of increased surplus allocation, of using forecast information in the decision-making, and demonstrate the importance of sampling the residual variance in order to estimate upper-bounds to a perfect decision-maker.

In the case of perfect information, a decision-maker knows precisely how much surplus to allocate for the N-days ahead and will maximise the amount of surplus at no risk of exceedance. The deterministic decision-maker has to reduce their forecast allocation of surplus by a constant offset value, matching the upper limit of stochastic-driven energy consumption. Theoretically, this is unbounded, however, we choose a finite value corresponding to 5 σ deviation, so that there is almost no discernible increase in risk. In reality, of course perfect forecast information would not be possible, so this case presents an upper-bound of skill.

In Figure 3.10-b, we see gains in the accumulated surplus when using better forecast information, with the perfect decision-maker benefiting the most. The approach outlined introduces little-to-no risk from increasing surplus operation above seasonally safe levels, demonstrating the potential value of forecast information. Sub-seasonal energy forecasts (derived from meteorological forecasts) may aid decision-makers to exploit this large potential value, by anticipating N-day demand (and hence surplus levels) 1 to 4 weeks ahead (Gonzalez et al., 2021; Goutham et al., 2022). These forecasts could, for example, allow participation in the futures markets, with the amount of surplus capacity traded on the market increased up to realtime as forecast skill improves at shorter leadtimes (Dorrington et al., 2020).

An approach for decision-making under this uncertainty could explore trade-offs of adopting a more risky operational strategy (allowing a small but finite probability of exceedance based on forecast information) in conjunction with a more risk-averse planning strategy (i.e. over-building reserve-capacity). This would more evenly distribute risk across the year, instead of concentrating risk around climatological infrastructure demand highs, and the gains in surplus allocation could further offset building costs.

3.5.7 METEOROLOGICAL DRIVERS OF SURPLUS AND GRID ELECTRICITY LOAD

BT's national "GB" infrastructure demand peaks in summer due to the strong CDD effect, contrasting with the grid demand and demand-net-wind which have strong winter peaking. The Cooling-Driven region has a comparatively stronger CDD dependence and, in fact, no overall HDD effect (instead, the negative coupling coefficient acts to extend the cooling impact to lower temperature ranges). The Heating-Driven region is an outlier from other BT regions, instead acting more in line with the grid demand and demand-net-wind, with strong HDD coupling and a weak cooling effect. As the amount of installed windpower capacity is increased, the grid demand-net-wind is increasingly sensitive to wind, although HDD impacts still play an important role in explaining grid demand-net-wind in Britain (Boßmann & Staffell, 2015).

Having explored the potential role of surplus capacity in the different weather-driven systems (GB/Cooling-/Heating-Driven), we now seek an understanding of the wider electricity-network behaviour in relation to surplus allocation and whether the surplus is available at a time when the wider grid might need it. Using the Bloomfield, Brayshaw and Charlton-Perez (2020) dataset for grid demand-net-wind (MERRA-2, spanning 1979–2017), we compare the deterministic components of the infrastructure *demand* to the wider network.

Grid demand-net-wind is characterised by strong temperature and wind sensitivity (Beerli & Grams, 2019; Bloomfield, Brayshaw & Charlton-Perez, 2020). In winter, there is heightened weather-driven variability (large differences between a cold, low-wind day compared to a mild, windy day). In summer, it is on average lower, has a reduced weather-driven variability, and the distribution of demand-net-wind values is positively skewed. This seasonal difference is seen when comparing panel g in Figures 3.11 and 3.12. Marginal distributions of the three modelled systems' surplus capacity are shown in panels a—c, and the joint probability distributions in panels d—f.

In winter, the GB and Cooling-Driven regions are narrowly concentrated around a high surplus (towards 0.4 to 0.5 and 0.8 to 0.9, respectively). The Heating-Driven region surplus capacity
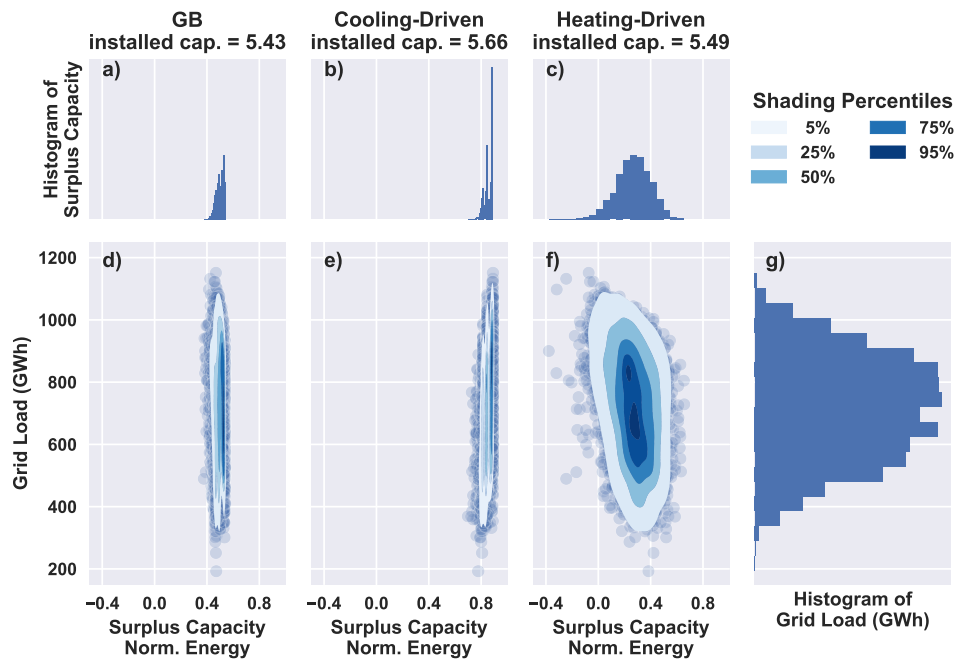
Figure 3.11: Bi-variate distributions (panels d-f) and respective marginal distributions (panels a-c and g) demonstrate how grid demand-net-wind (from Bloomfield, Brayshaw and Charlton-Perez, 2020) relates to infrastructure demand (GB, Cooling-Driven, and Heating-Driven). Data is from the extended winter period (December-March).
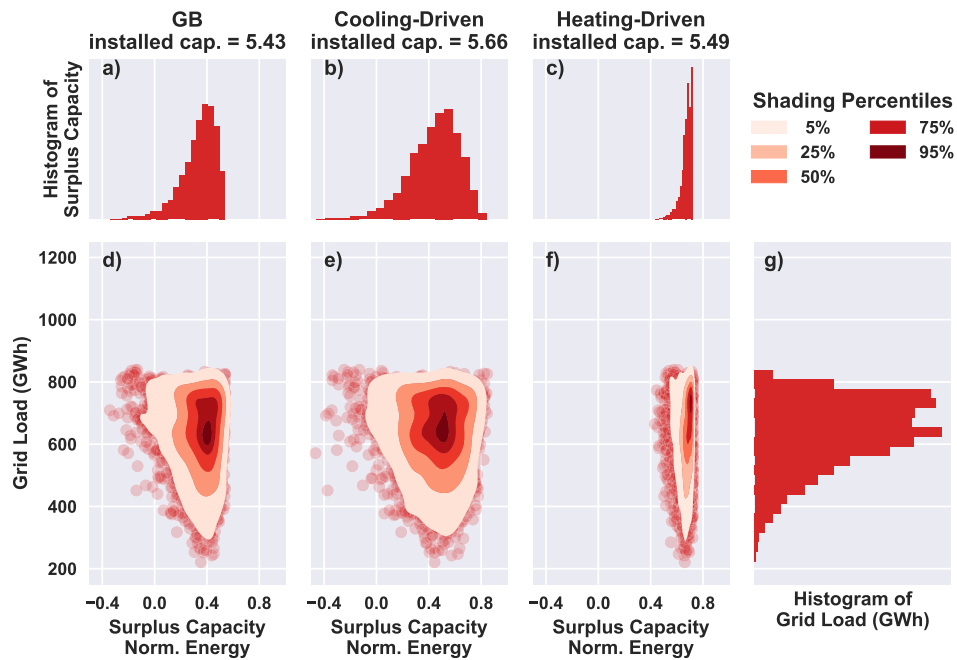
Figure 3.12: As in Figure 3.11, but showing the Extended Summer period (June-September)

has a weak negative correlation to grid demand-net-wind, although this value is not significant at $r = -0.33$.

In summer, the Heating-Driven region is narrowly concentrated at high surplus capacity (similar to the behaviour of GB and Cooling-Driven in the winter period). The grid demand-net-wind doesn't reach near the maximums experienced in winter (during cold, less-windy periods). There is no correlation between grid demand-net-wind and surplus capacity (R^2 is less than 0.02 in each region).

A reserve power system operating in a GB or Cooling-Driven regime has significant potential to provide balancing services to the wider electricity network. Figure 3.11 motivates making surplus available during winter periods, whilst Figure 3.9 shows this to be possible. These non-reserve purposes may involve storing energy during low demand-net-wind periods, and releasing energy during high demand-net-wind periods.

Figure 3.10 indicates that use of forecasts can increase the amount of surplus made available for non-reserve purposes in a given year. Skilful forecasts may also allow Heating-Driven type systems to intermittently provide surplus capacity during the winter period, however, there is no consistent safe level, and Figure 3.11 panel f shows some negative correlation, possibly indicating that the surplus is less likely to be available during high demand-net-wind periods.

3.6   Discussion

In any critical infrastructure, decision-makers will have a dialogue with industry regulators to discuss the cost-risk trade-offs and the extent to which some risks are considered unreasonable to mitigate. We have developed a framework for decision-makers to assess trade-off between installed reserve capacity and risk of failure, using a range of plausible values P_R for the probability of needing N-day reserve capacity, and a range of permissible hazard risks $\mathbb{P}_C$.

This framework makes some simplifying assumptions: we do not discuss the implications of longer (or shorter) periods of reserve power usage. In our case study, we made the assumption that P_R has no time-of-year dependency; it is more likely, however, that in reality, reserve

capacity will be required in grid failures induced by extreme weather such as storms and heat-waves, both of which have a strong seasonal dependence. It is worth considering this context when analysing results: unless correlations between $R(t_i)$ and $X(t_i)$ are explicitly modelled, one should err towards choosing a more risk-averse value for reserve capacity to account for this simplification (or consider increasing the value of P_R to an upper bound).

For some critical infrastructure operators, past occurrences of operating N-day's reserve power may be rare or have never occurred; the event may be considered a *black swan* event, so P_R is unknown. In such cases, it is up to the decision-maker (and regulator) to agree upon appropriate quantities of reserve capacity to be installed, and the resulting exceedance probabilities.

Figure 3.10 shows the high potential value, in terms of surplus allocation, in using extended range forecasts in the decision-making. The theoretical upper limits, described by the deterministic (meteorological forecast only) decision-maker and so-called perfect decision-maker (correctly predicting the precise meteorological and noise impacts to infrastructure demand), are much higher than the baseline climatological yields. Assuming that the infrastructure temperature-demand relation is well modelled, forecast skill in predicting the deterministic component of infrastructure demand should be high in the week ahead, and measurable up to 4 weeks ahead, allowing week-ahead allocation of surplus comparable to the theoretical 'deterministic' decision-maker. Any additional skill in predicting the stochastic component, for example through employment of an ARIMA model (Weisang & Awazu, 2008), could see surplus allocation between the bounds of "deterministic" "perfect" decision-makers. This theoretical exercise demonstrates the value of decision-making to allocate surplus using accurate forecasts, although as no 'perfect' forecast is possible this upper bound is higher than what may be achieved in reality.

Forecast leadtimes from day-ahead to extended range are relevant for applications in the energy sector and across industries (White et al., 2017; Domeisen et al., 2022; Bloomfield, Brayshaw, Gonzalez & Charlton-Perez, 2021b), with extended range allowing participation in trading ancillary service capacity weeks ahead, and shorter-range important for accurately knowing day and week ahead surplus availability. Forecasts can also be used to predict and warn of ex-

ceedance events. Decision-makers may benefit greatly from adopting a risk-tolerant approach, compensated by additional increases in reserve capacity, more evenly distributing risk across the year whilst increasing surplus annual accumulation.

There are multiple possible uses for surplus capacity, including ancillary services such as frequency balancing and peak-load shaving. The added value of surplus capacity can be captured with different metrics relevant to these different use cases.

3.7 Conclusion

The transition to a low-carbon energy system offers challenges and opportunities for rethinking how we plan and use energy. In this paper, we explore the synergies between the need for clean "backup" energy sources for critical infrastructure, and the potential for utilisation of "surplus" capacity in these resources in order to meet other energy needs (particularly ancillary services to the wider national power system).

Weather-driven models of infrastructure electricity demand, including a stochastic representation of residual uncertainty, were developed for three example critical infrastructure systems (based on BT regions). In each case, these models were used to estimate the size of the energy-reserve required to provide 5-day operational capacity in the event of regional power outage or black swan events. Addressing RQ i.1, the size of the store required is dependent on the risk tolerance of the critical infrastructure asset, and is linked to *coincidence risk*; the probability of both having a power system outage *and* having a 5-day infrastructure demand period which exceeds the total reserve capacity.

For the systems examined, a clear seasonal behaviour was observed (corresponding to energy-use driven primarily by heating, cooling, or a mixture of both). This clearly indicates that a reserve energy supply designed to meet 5-days of infrastructure demand during the peak season will have surplus capacity in the off-peak season, answering RQ i.2. For cooling-dominated systems, which describes the bulk of the BT case study and approximately 0.5 % to 1 % of GB grid demand, the greatest surplus occurs at times of greatest value to the wider power system

(i.e. during the winter when the need for generation capacity is greatest on the national power system as a whole), answering RQ i.3.

The existence of clear seasonal variations in energy consumption provide a direct pathway to estimate the "surplus" storage that can be further enhanced by meteorological forecasts. Use of skilful medium to extended range forecasts to identify infrastructure demand levels in advance (i.e. identify periods where the amount of surplus that can be released is greater than that which would be expected on a purely climatological basis alone), may prove highly valuable. For context, a simple test case with a *perfect* forecast doubled the available surplus.

The approaches outlined in this paper employ a weather reanalysis dataset in order to calculate weather- and seasonally-varying impacts to reserve power infrastructure planning and operation. A key observation in developing this analysis is the importance of including a stochastic representation of the residual uncertainty associated with the infrastructure demand. Failing to represent these processes lead to substantial errors in the size of capacity installed with respect to risk-tolerance.

The comparison of decision-making under climatological, deterministic-only and *perfect* forecasts (including the stochastic component) suggest improvements in the amount of surplus that can be allocated. However, it should be emphasised that the weather in the reanalysis should not be considered fully representative of present and near-future events, with the sample range unable to fully explore decadal variations and current climate change impacts. Into the future, impacts of climate and ecological breakdown, and industry response such as heat and transport electrification, will greatly affect weather-drivers of infrastructure demand and what is required from reserve systems, for example driving increased grid demand-net-wind load and variability in winter months (Boßmann & Staffell, 2015; Bloomfield et al., 2016; Peacock et al., 2023). Practical application of the approaches outlined should consider implementing climate impacts into modelling, alongside other projected system changes (such as reductions in the infrastructure temperature-demand sensitivity if more efficient equipment is installed in future).

3.8   Supporting Information

3.8.1   DNO Gridbox boundaries

GSP Group ID	Area ID	Area	lon West	lon East	lat South	lat North
A	10	East England	-1.5	2.0	50.5	53.0
B	11	East Midlands	-2.0	0.0	52.0	53.5
C	12	London UK	-1.0	0.0	51.0	52.0
D	13	North Wales Merseyside and Cheshire	-5.0	-2.5	52.5	53.5
E	14	West Midlands	-3.5	-1.5	51.5	53.0
F	15	North East England	-3.0	0.0	54.0	56.0
G	16	North West England	-4.0	-2.5	53.0	55.0
P	17	North Scotland	-8.0	-1.5	56.0	59.0
N	18	South and Central Scotland	-5.0	-2.5	54.5	56.5
J	19	South East England	-1.0	1.5	50.5	51.5
H	20	Southern England	-2.5	-0.5	50.5	52.0
K	21	South Wales	-5.5	-2.5	51.0	52.5
L	22	South West England	-6.0	-2.5	50.0	51.5
M	23	Yorkshire	-2.5	0.5	53.0	54.0

Table S3.1: Distribution Network Operator (DNO) Gridboxes on MERRA2 grid. These boundaries are shown in Figure 3.2. Adopts standard naming convention: https://www.ofgem. gov.uk/energy-data-and-research/data-portal/energy-network-indicators. GSP is the Group Service Provider. lon_min, lon_max, lat_min, lat_max are the longitudinal and latitudinal domain boundaries respectively.

3.8.2   REGRESSION COEFFICIENTS
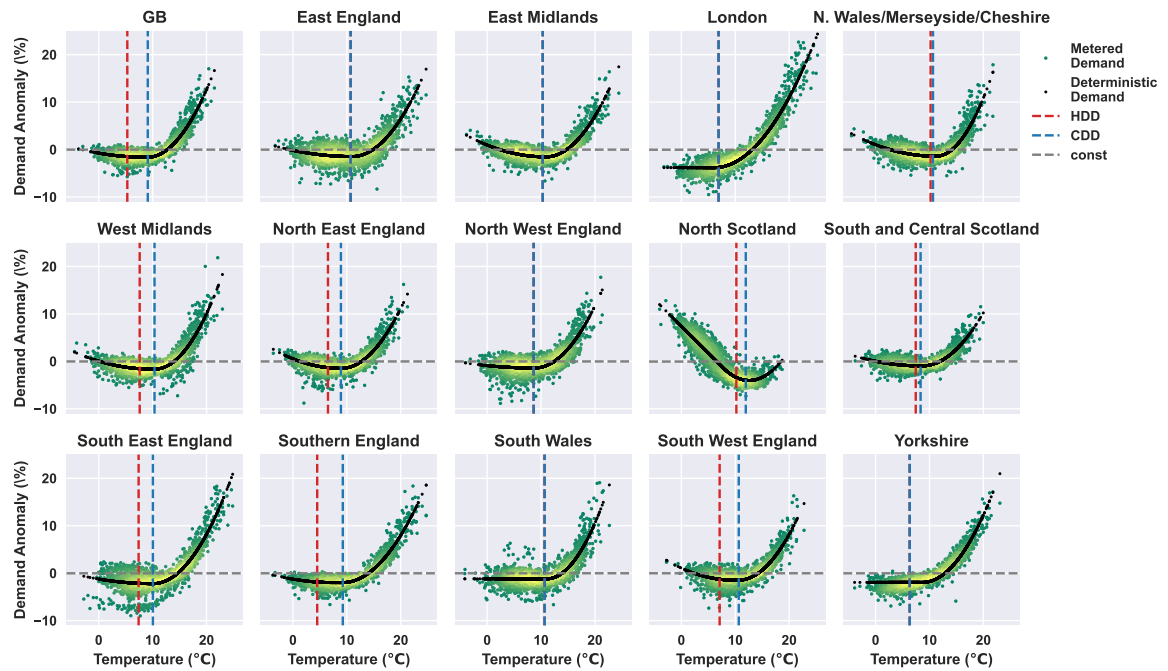
Figure S3.1:   Figure compares metered and deterministic model infrastructure demand fit in each region. Units are in anomaly from average, percent. Black markers are the temperature and corresponding deterministic demand for observations of temperature in the training period 2016 to 2020. Shaded yellow-green markers are metered demand (with detrending and weekday effect removed, i.e. as in Figure 3.2 panel e), with yellow-shaded values indicating high probability density using a Gaussian kernel density estimate. Red and blue dashed lines indicate the HDD and CDD thresholds T_{HDD} and T_{CDD} respectively, and grey dashed lines indicate the intercept value $\mathcal{D}_0$.

Area	T_{HDD} °C	T_{CDD} °C	$\mathcal{D}_0$ %	α_{HDD} % °C^{-1}	α_{CDD} % °C^{-2}
Great Britain	5.30	9.10	-1.58	0.15	0.12
East England	10.70	10.70	-1.65	0.12	0.09
East Midlands	10.30	10.30	-1.87	0.24	0.09
London UK (*Cooling-Driven*)	6.90	6.90	-3.36	-0.20	0.08
North Wales Merseyside and Cheshire	10.20	10.65	-1.72	0.24	0.14
West Midlands	7.60	10.35	-1.66	0.20	0.13
North East England	6.50	8.90	-1.49	0.29	0.10
North West England	8.60	8.65	-1.47	0.06	0.10
North Scotland (*Heating-Driven*)	10.20	11.95	-3.91	1.10	0.07
South and Central Scotland	7.45	8.35	-1.05	0.13	0.08
South East England	7.40	10.05	-2.23	0.14	0.11
Southern England	4.50	9.25	-1.96	0.16	0.09
South Wales	10.65	10.65	-1.46	0.07	0.14
South West England	7.10	10.65	-1.44	0.32	0.11
Yorkshire	6.30	6.35	-2.23	-0.09	0.07

Table S3.2:   Complete table of degree day threshold parameters (°C), extending Table 3.1. The thresholds determine the extent of the *heating* and *cooling* degree day domains. The infrastructure demand when not in either heating or cooling regime has value $\mathcal{D}_0$ (%). The heating and cooling responses are further characterised by gradients, α_{HDD}, α_{CDD}, measured in units, $\%\,°\text{C}^{-1}$, and $\%\,°\text{C}^{-2}$ respectively.

3.8.3 ERROR MODELLING IN THE STOCHASTIC MODEL

Residual error (measurement error in the observed daily infrastructure demand and determ-
inistic model infrastructure demand) in anomaly units (as in Figure 3.2-e), are analysed in
Figures S3.2 to S3.4.
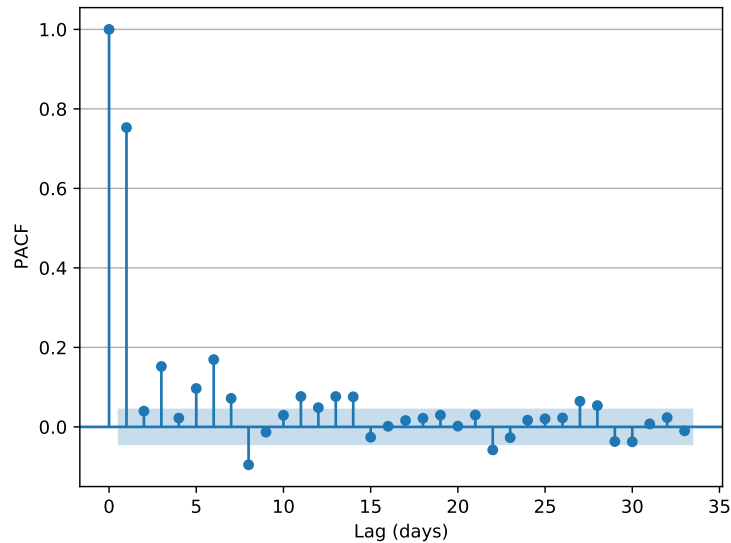
Figure S3.2: Partial Auto-Correlation Function (PACF) of residuals (anomaly reconstructed
metered infrastructure demand against anomaly deterministic model infrastructure demand)

The Partial Auto-Correlation Function, displayed in Figure S3.2, demonstrates the partial cor-
relation of residual error in daily infrastructure demand with its own lagged values, controlling
for other lags (so, for example, the correlation at lag 2 does not double count the correlation
of lag 1). By definition, 100 % correlation is observed at lag 0. A high correlation is shown at
lag 1, indicating that the residual error in model infrastructure demand on neighbouring days
has an underlying relation. This is the basis for including a lag 1 component in the stochastic
model noise term.

The probability distribution of observed errors in daily infrastructure demand, displayed in
Figure S3.3, resembles a normal distribution, although is more sharply formed and outliers
hint at fat distribution tails. The model therefore implements the stochastic noise component
as normally distributed (see Section 3.4).
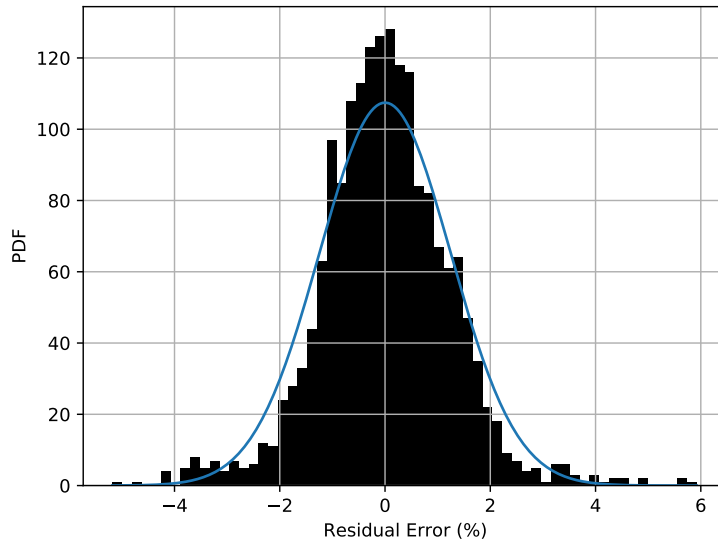
Figure S3.3:   Probability Density Function (PDF) of residuals (anomaly reconstructed metered infrastructure demand against anomaly deterministic model infrastructure demand)
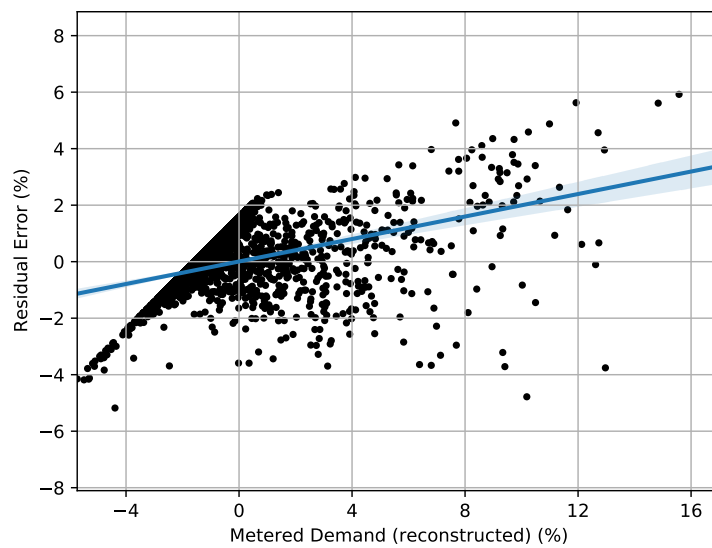
Figure S3.4:   Scatterplot of residuals vs. reconstructed infrastructure demand anomaly. Line of best fit has a positive slope, indicating a slight bias at high demand values. The scale is in normalised units, anomaly percent from mean daily demand.

There is some correlation between observed error and observed infrastructure daily demand, demonstrated in Figure S3.4, with higher demand values having a greater spread and mean error value. Analysis of how errors change with season, comparing the Cooling-Driven and

Heating-Driven regions, indicates that the slight increase in the spread and mean error value is associated with the higher demand values as opposed to an underlying unmodelled seasonal effect. More generally, error distributions are consistent across seasons, allowing the use of a single error model (normal distribution, lag 1) applied individually to each region.

3.8.4   SENSITIVITY TO N=5 CASE

In the following adaptation of Figure 3.8 panel a (GB), we explore how results change when the reserve target window N is set to values other than 5 days.
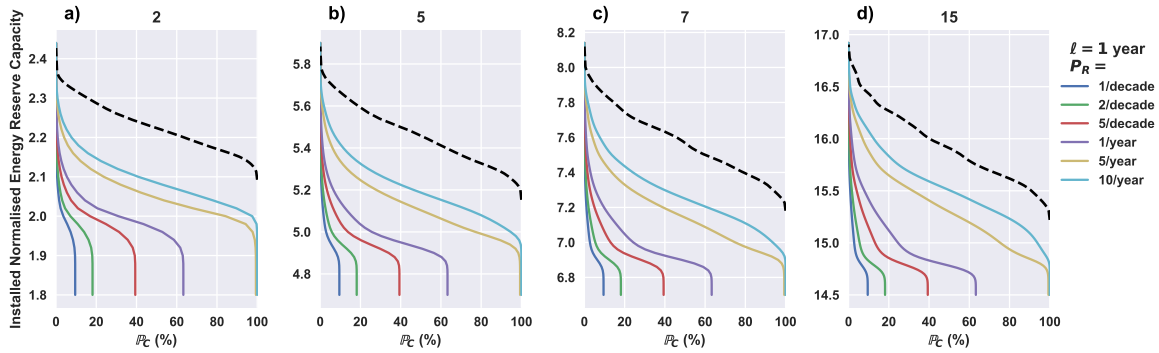
Figure S3.5: Capacity-coincidence hazard relation (see Equation (3.12)). The value of N is shown above each panel.

This adaptation of Figure 3.8 shows that the approaches taken to assessing reserve capacity installation requirements relation to failure rate are valid across a broad range of values for N.

We note that the sensitivity of the installed reserve to $\mathbb{P}_X$ and $\mathbb{P}_C$ does not increase proportionally with N (for example in the case $N = 5$ the relevant range of values for installed energy capacity E is approximately 4.8 to 5.8, whilst in the case $N = 15$ (three times longer) the relevant range is approximately 14.5 to 17.0, less than the three times increase to N. The longer the time window is increased, the more that variance is reduced (a window that was a month or longer would have proportionally much less variance than a window only a small number of days long).

Reserve Power Design in Future Climates: Bias Adjustment Approaches for Regional Climate Projections

This chapter addresses the research question: *To what extent can climate model simulations improve reserve power system design and quantify trends in surplus capacity?* (Thesis RQ ii). The contents of this chapter have also been the prepared for submission to the journal of Meteorological Applications (RMetS), with the provisional reference:

Fallon, J. C., Brayshaw, D. J., Methven, J., Jensen, K., Krug, L., in preparation: Reserve Power Design in Future Climates: Bias Adjustment Approaches for Regional Climate Projections.

Differences between the thesis chapter and prepared manuscript include minor typesetting alterations and newly assigned reference numbers. The introduction has been revised to avoid repetition within the thesis. Two datasets produced for this research have been published on the Reading Research Data Archive; see *Telecoms Electricity Load Model (Re-analysis Delta-shift)* and *Telecoms Electricity Load Model (UKCP18)*, Appendix A.

4.1   Introduction

A model of electricity load and a framework for quantifying risk based on the built energy capacity of a reserve system has been explored in Chapter 3. Additionally, it was demonstrated that periods of predictable surplus capacity are available in cooling-driven infrastructure during periods when the wider grid faces potential energy shortfall.

Following on from this work, the weather-driven impact model is applied to UKCP18 climate model outputs. The UK Climate Projections 2018, UKCP18, is a set of tools for providing insight into how UK climate may change in the future, produced by the UK Met Office (Murphy et al., 2018). A description of this dataset is provided in Supporting Information 4.5.1.

The output variables of climate models (including UKCP18) inevitably contain artefacts of model simplification, error, and bias, which can lead to inconsistency between the climate model and observations. If a climate model is trusted to provide a plausible climate change signal, bias adjustment is a "defensible and potentially powerful approach" (Maraun, 2016; Met Office Hadley Centre et al., 2018).

We investigate how climate model outputs, in this case the global and regional outputs of UKCP18, may complement reanalysis data to better understand the present and future climate risk in reserve power systems, though this in itself introduces a significant form of uncertainty insofar as a wide variety of different bias adjustment schemes have been proposed (Maraun, 2016; Casanueva et al., 2020).

Thesis RQ **ii** is addressed in three sub-questions:

RQ ii.1 Which bias adjustment(s) of temperature should be considered best practice, towards the aim of modelling infrastructure electricity demand using UKCP18 climate model simulations of historic and future periods?

RQ ii.2 To what extent can UKCP18 climate model simulations spanning the recent *historic* period be used to improve the efficient planning of reserve system capacity?

RQ ii.3 To what extent and in what ways will future changes in climate impact **(a)** reserve system capacity planning and **(b)** levels of surplus capacity?

4.2 Methods

4.2.1 NAVIGATING ASSUMPTIONS IN CLIMATE DATA

When presented with climate information, it is not feasible to consider decision-making scenarios that take into account all possible feedbacks and forcing mechanisms in the Earth system climate and all plausible anthropogenic emissions pathways. Rather than focus on the question of "what will happen" to the Earth system climate in its entirety, it is more practical and appropriate for decision-makers to focus on the plausible range of impacts to assets in a definable circumstance with controllable actions (Shepherd, 2019).

The UKCP18 Global Climate Model (GCM) and Regional Climate Model present a wide range of different climate outcomes, known as a Perturbed Physics Ensemble (PPE), that simulates plausible climates from 1900 to present and a diverse spread of future projections.

Scenarios are produced for each of the 12 UKCP18 PPE members with mid-point at a global temperature threshold of Table 4.1. The scenarios are de-trended about the mid-point using the global surface temperature trend, and each spans a total 20-year time period[1].

Δ [°C]	0.78	1.0	1.5	2.0	3.0	4.0
Approx. Era	1981 to 2020	2002 to 2021	2020 to 2039?	Mid-century?	Late-century?	Worst case?
Description	Historic, MERRA2	Recent past	Immin- ent	Paris Accord upper limit	Beyond Paris Accord	IPCC 21st century range

Table 4.1: Table of global temperature increase (Δ) with respect to pre-industrial levels (1850 to 1900). The time span of the 1.0 °C period is derived from reanalysis. The approximate time span for the first era averaging 1.5 °C uses decadal forecast estimates Betts et al. (2023). Qualitative descriptions are used in reference to future time periods.

---

[1]See Supporting Information 4.5.1 for further discussion of these scenarios.
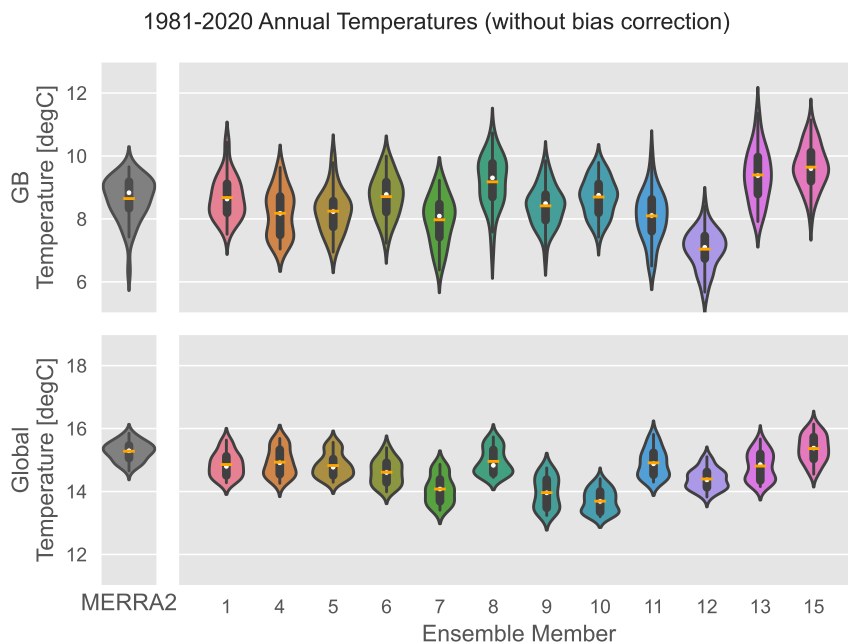
Figure 4.1: Distributions of annual mean GB temperature in `MERRA-2` and in `UKCP18` Regional PPE members (above), and in annual mean global temperature in `MERRA-2` and in `UKCP18` Global PPE members (below). No bias adjustment has been applied. Data spans 1981 to 2021 calendar years (`MERRA-2`) and model years (`UKCP18`). Indicated is distribution mean (orange line markers), quartiles (grey box) and whisker values (lines extending from the box, spanning 1.5× the interquartile range). A Gaussian kernel is used to smooth the distributions.

These scenarios will be used (with appropriate bias adjustment) as input to the electricity load model, to simulate outcomes in plausible historic and future climates.

Figure 4.1 shows annual mean temperature distributions of the GB land surface and global surface (land and sea) without bias adjustment for the calendar/model year 1981 to 2021.

There is greater variability in annual mean temperatures of the GB land surface than in the global surface average, in both the re-analysis and in the PPE members. There is significant variation in the mean values of the PPE members, both in GB (a) and global (b) distributions.

The global biases seen in Figure 4.1 are associated with a persistent bias in future model years. These biases are not strongly correlated with the biases in GB temperature distributions (correlation of Figure 4.1 climate biases is measured to $R^2 = 0.160$.)

The global temperature biases may be explained by climate model error, which if we assume is the leading cause of bias, is a source of epistemic uncertainty that should be corrected. How-

ever, perceived biases arising from plausible decadal variability in climate (either globally, or more localised) should be preserved. In this paper, we consider a range of different approaches to bias adjust model outputs, including approaches that remove the global bias (assumed model error) whilst aiming to preserve plausible variability in the regional model outputs.

4.2.2 BIAS ADJUSTMENT APPROACHES

In Table 4.2, features of three bias adjustment methods are compared, alongside a delta-shift of re-analysis.

Bias Adjustment Feature	Δ	μ	QM	QDM
New dynamical processes Climate model represents new weather configurations, changes to the frequency of certain weather events, etc.		✓	✓	✓
Quantile-correcting Trend-preserving, i.e. an adjustment is made based on historical inconsistency, allowing for changes in distribution shape			✓	✓
Works with unobserved extremes Consistent handling of new values beyond observations range	N/A	✓		✓
Works with limited observations Method performs well even if the re-analysis distribution is affected by low sample size		✓		
Regional climate variability Method aims to preserve regional climate variability	✓	✓		

Table 4.2: A feature comparison of bias adjustment methods. Δ is delta-shift, μ is global mean bias adjustment, QM is Quantile Mapping, and QDM is Quantile Delta Mapping.

The bias adjustments are well established in literature (e.g. Teutschbein & Seibert, 2012; Maraun, 2016; Met Office Hadley Centre et al., 2018; Casanueva et al., 2020; Spuler et al., 2023; Li & Li, 2023), and the implementation of each bias adjustment approach is described in Section 4.5.3. Additionally, the re-analysis delta-shift method is introduced as a counterfactual to using UKCP18 outputs to simulate electricity load: if bias adjustments are applied to *correct* for bias in climate model outputs, can plausible results instead be obtained through intentionally introducing a constant delta offset into re-analysis timeseries to achieve a targeted

level of global temperature increase?

Figure 4.2 highlights methodological differences between delta-shift and mean bias adjustment. The delta-shift is a valid and helpful technique for simulating climate impacts; delta-shift has perfect historical consistency since it makes direct use of re-analysis timeseries (although this may result in overconfidence in the observations, therefore under-representing aleatoric uncertainty). However, since only observations data is used, and climate model outputs are not directly used, future changes in dynamical processes (for example, jet stream position or North Atlantic Oscillation frequency) and the temperature distribution shape (larger distribution tails) are not represented with the delta-shift approach. The delta-shift method is, therefore, a useful comparative approach that can help validate results from bias adjustment of climate data and may indicate sources of uncertainty.

The global mean bias-adjustment identifies the (assumed) climate model error in the global temperature (i.e. the long-term difference between GCM and re-analysis over a reference historic period), and then applies this mean bias adjustment to the regional GB timeseries (thereby preserving regional variability uncorrelated with global variability).

Two trend-preserving bias adjustments to `UKCP18` are considered: Quantile Mapping (QM)
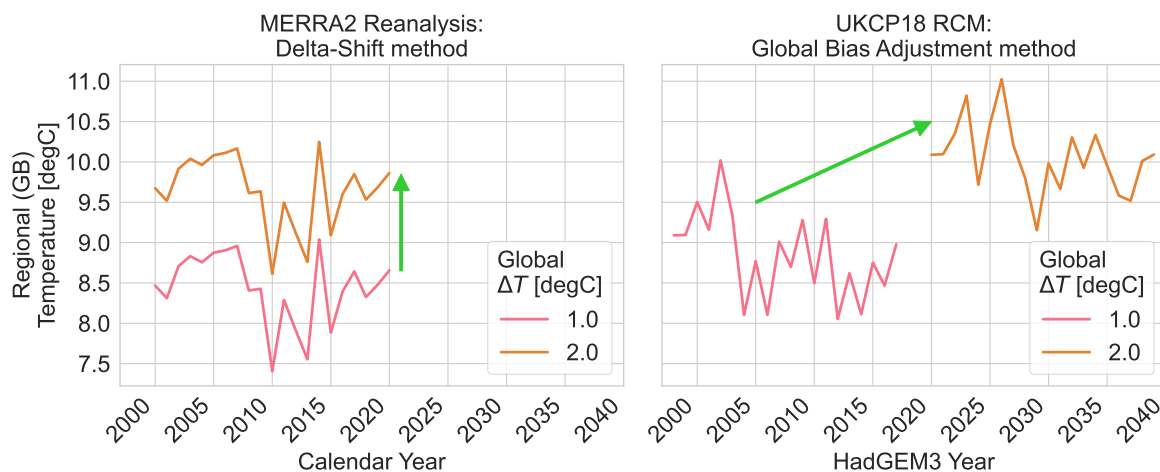
Figure 4.2: Comparison of two impact-driven approaches to generating climate change scenarios: the "delta-shift" method adds a constant value to simulate on-average warmer climate; the "global bias adjustment" method uses global temperature thresholds to define periods where a regional timeseries is extracted. We detrend 20-year windows via linear regression (retaining the respective mean values).

and Quantile Delta Mapping (QDM). However, the QM approach does not provide a plausible correction of unobserved extreme values, (Switanek et al., 2017)[2], whilst QDM achieves a more appropriate correction of (unobserved) extreme values by adjusting data by its perceived bias in quantile rather than absolute temperature. This is demonstrated in Figure 4.3. By applying a "horizontal" correction (less sensitive to the upper quantiles), Figure 4.3 shows that quantile delta mapping can result in a more robust bias adjustment.

If there are problems with the dynamical processes represented in the climate model, then quantile-correcting bias adjustment may not be able to help with this. For example, if weather types are underrepresented, then bias adjustment can inadvertently increase the bias for those weather types. In the presence of substantial errors in the frequency and representation of weather types, bias adjustment may yield implausible future signals (Maraun et al., 2017). However, the findings of McSweeney and Thornton (2020), McSweeney and Yamazaki (2020) and McSweeney and Bett (2020) indicate a good representation of key dynamical processes in the UKCP18 model world, therefore justifying the validity of quantile-correcting approaches.
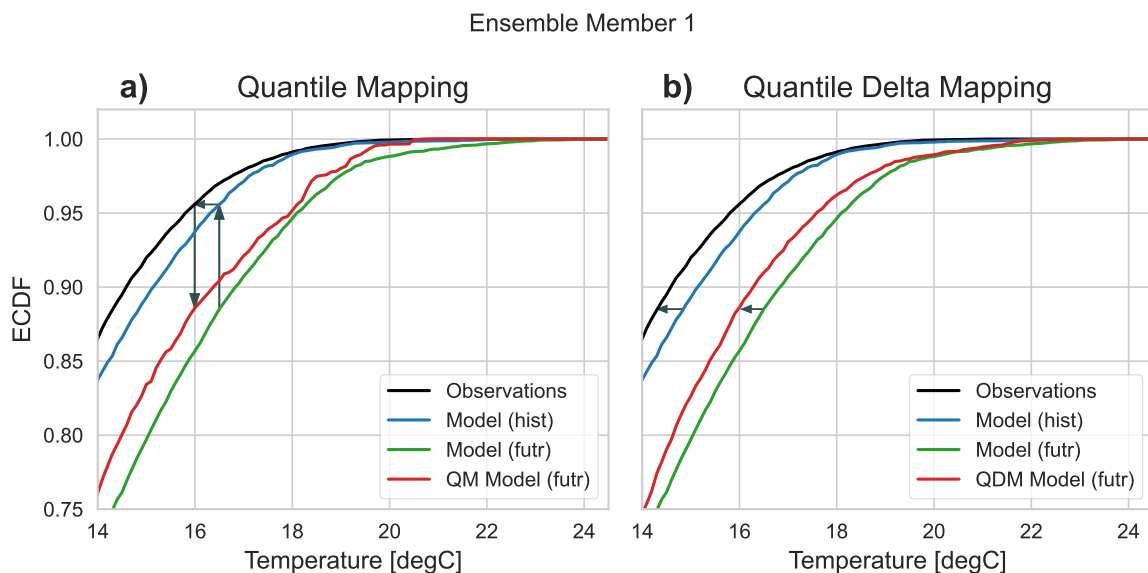
Figure 4.3: Comparison of Quantile Mapping and Quantile Delta Mapping applied to PPE member 1. Figure uses the approach of Switanek et al. (2017, Figure 1). The vertical axis is the Cumulative Distribution Function (CDF).

---

[2]See also supporting information Section 4.5.3.4.

Historic Period (0.779°C)
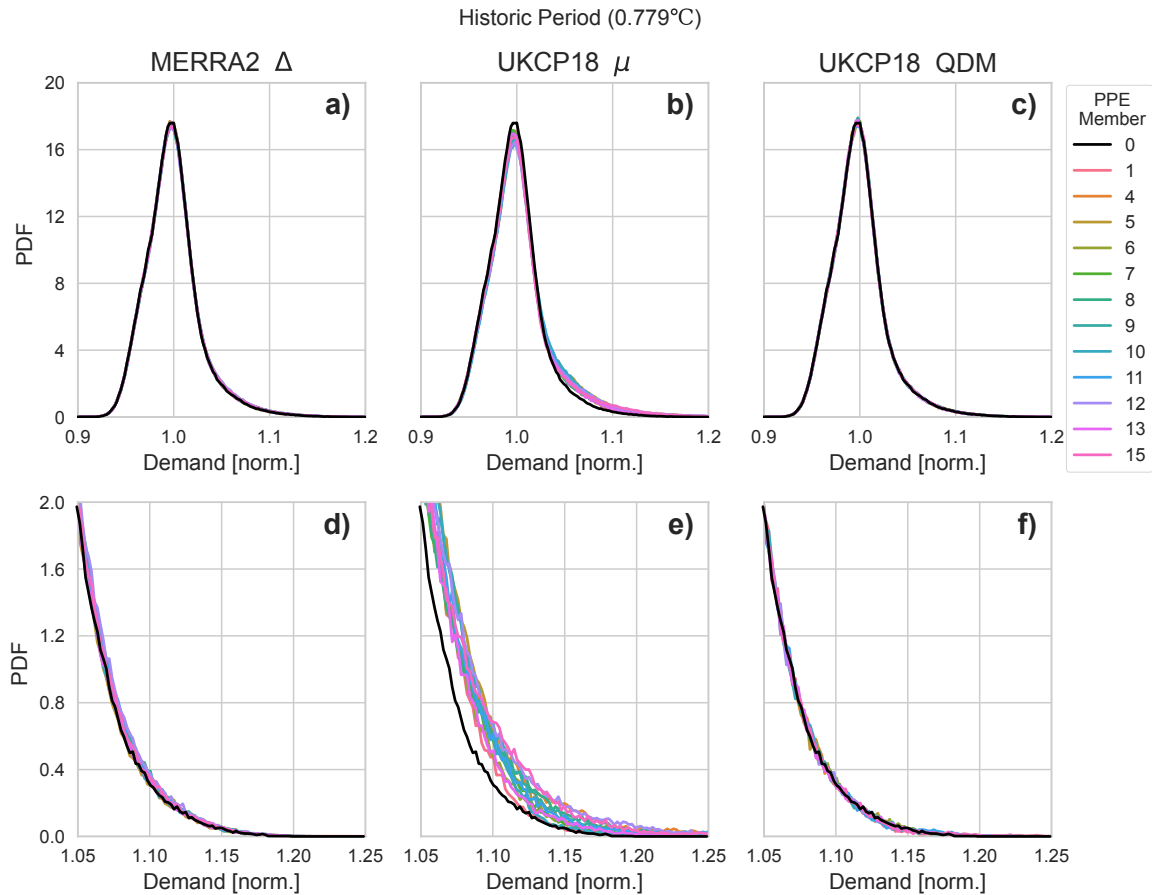
Figure 4.4: Probability distributions of simulated infrastructure electricity demand (350 realisations per PPE member), for a historic period. Colours indicate observations (MERRA-2 in black, label 0) and PPE members (labels ≥ 1). Panels show a) Delta-Shift b) Global Mean Bias Adjustment c) Quantile Delta Mapping. Underneath panels d), e), and f) respectively show enlarged views of the distribution upper tail ends.

4.3 Results

4.3.1 CLIMATE MODELS ON INFRASTRUCTURE ELECTRICITY DEMAND

As discussed above, and summarised in Table 4.2, the different bias adjustment approaches (and delta-shift) offer different trade-offs for managing climate risk. Probability distributions of modelled demand are shown in Figure 4.4, and display how the delta-shift, mean bias adjustment, and QDM impact the simulated electricity load in a *historic* climate (i.e. without a climate change signal with respect to the re-analysis).

An important test for the bias adjustment approach is whether it replicates the distributions of infrastructure electricity demand as calculated from observations, in particular at the distribution upper-tail (since this has a large influence on the dimensioning of reserve capacity infrastructure and risk of energy consumption exceeding installed capacity). The bias adjustments appear to perform well in each case, with probability distributions of demand broadly consistent with the observations derived distribution. However, the mean bias adjustment (panel b, e) is significantly positively skewed and overestimates the frequency of extreme events compared with observations-derived results. There is also a significant spread across different PPE members with mean bias adjustment approach, which is not present with delta-shift or QDM.

In the delta-shift, there is in fact a very small spread in results — in the implemented approach there is not a single 'delta' but in fact a set of 12 delta-shifts corresponding to each PPE member. The average regional response (i.e. the mean of the bias adjust 20-year climate) for each PPE member is used to create a spread in results, which is initially negligible, but grows as discrepancies between PPE members increase in future projections[3].

QDM yields nearly identical temperature distributions to the reanalysis-derived distribution. The stochastic component of simulated demand does not introduce measurable spread in results, and unlike delta-shift and mean bias adjust there is no measurable spread across PPE members.

Whilst delta-shift and QDM achieve historical consistency with reanalysis-derived results of infrastructure electricity demand, the mean bias approach does not (a systematic overestimation of temperature extremes is attributable to climate model error). Any outputs generated from mean bias adjustment can be considered an upper bound of where differences in epistemic uncertainty could shift the demand distribution (perhaps a portion of disagreement in the mean bias approach represents legitimate epistemic uncertainty).

---

[3]From the variability term v_p, see Supporting Information Equation (S4.3). Despite the non-linear form of the demand transfer function (Equations (3.3) and (3.6)), the nudges in v_p are not significant enough to have a noticeable impact on the distribution shape and skew.
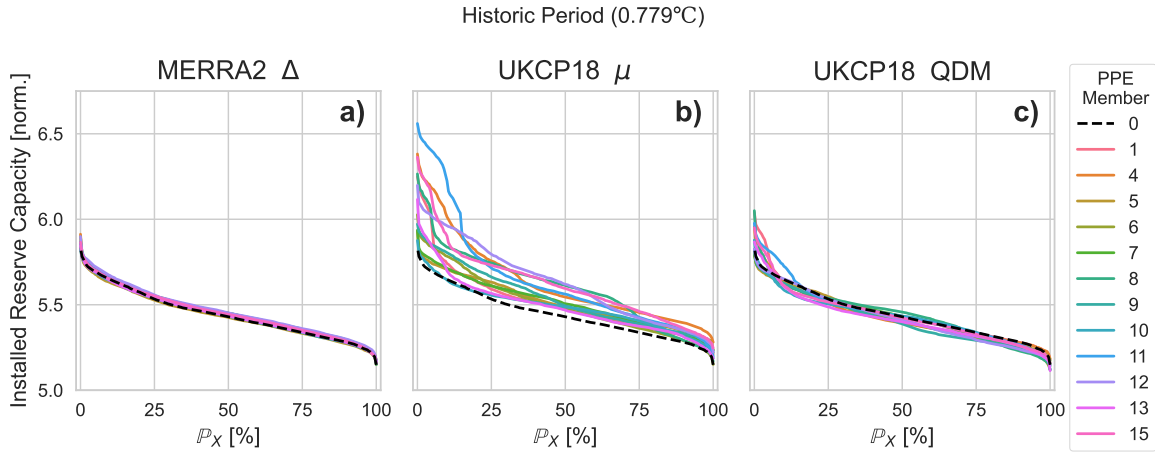
Figure 4.5: The annual risk of failure shows the probability ($\mathbb{P}_X$) that 5 days of BT's GB energy consumption exceeds a given reserve capacity at least once in a given year. The 5-day target used here reflects regulator-set targets for resilience in the case study. Colours indicate observations (MERRA-2 in black, label 0) and PPE members (labels $\geq$ 1).

4.3.2 RESERVE CAPACITY PLANNING: HISTORIC

Section 3.5.2 estimated the annual risk of failure (the probability, $\mathbb{P}_X$, of exceeding built reserve capacity) for the present climate based on reanalysis data. The 40-year reanalysis timeseries is of finite length, and therefore an increase in sample size may improve the weather sample by exposing plausible but unobserved events. Reserve power annual risk of failure (represented by the exceedance indicator X and probability of exceedance $\mathbb{P}_X$, as introduced in Chapter 3) is shown in Figure 4.5 for the historic scenario for each bias adjustment.

Figure 4.5 panels a (delta-shift) and c (QDM) display low spread and a reasonably close match to reanalysis-derived results in this new context of annual risk of failure curves used to support capacity planning decision-making. These results are inline with the effects observed on the electricity load impact model, discussed above in Section 4.3.1. And as in Section 4.3.1, the mean bias adjustment has a significantly larger spread in results and overestimates the annual risk of failure (stemming from the systematic bias in high-temperature extremes).

Whilst in Figure 4.4, delta-shift displays a slightly larger variability than QDM, in Figure 4.5, there is now significantly more disagreement between PPE members when taking the QDM approach. This key result shows that for low probability values which are most relevant to
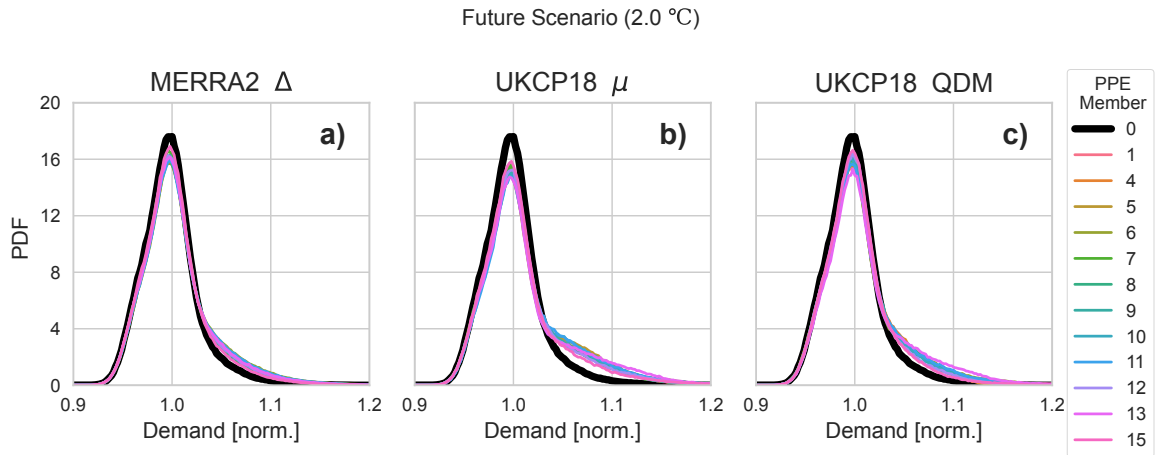
Figure 4.6: Demand probability distributions in the projected scenario of 2.0 °C global temperature rise. Colours indicate observations (MERRA-2 in black, label 0) and PPE members (labels ≥ 1). Panels a-c demonstrate the distribution resulting from the delta-shift approach, global mean bias adjustment, and Quantile Delta Mapping, respectively.

decisions makers[4], results are noticeably more sensitive to the choice of climate model PPE member (disagreement up to 15 %) than would be anticipated using the delta-shift representation of climate variability.

4.3.3 RESERVE CAPACITY PLANNING: FUTURE

In Figure 4.6, infrastructure electricity demand is simulated in the 2.0 °C global temperature rise scenario[5]. The results are again displayed for three bias adjustment approaches: delta-shift (a), mean bias adjustment (b), and Quantile Delta Mapping (c). In each case, the simulation of future infrastructure electricity demand shifts towards a more positively skewed distribution (with a larger distribution tail). In both the bias adjustment methods (mean and QDM), there is a significant increase in the spread of infrastructure electricity demand distributions across PPE members with respect to the historical scenario (Figure 4.4). The spread in demand distributions stems from regional climate variability (the spread in GB temperatures increases across PPE members as global temperatures rise).

From Sections 4.3.1 and 4.3.2, QDM should be considered the best practice method since it

---

[4]Keeping $\mathbb{P}_X$ close to 0 % is desirable for decision-makers.

[5]Corresponding plots for each of the global temperature rise scenarios of Table 4.1 are shown in the supporting information, Figure S4.6
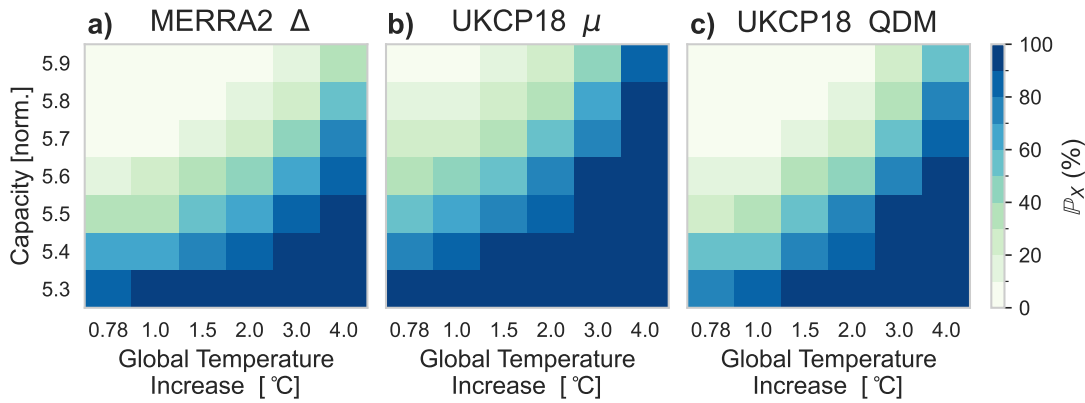
Figure 4.7: The annual risk of failure ($\mathbb{P}_X$) is indicated by colour shading: low risk (white), to high risk (dark blue). Scenarios are split into grids of Global Temperature Anomaly Δ (horizontal axis) and Capacity (vertical axis). Three panels (a-c) show the results obtained by delta-shift, mean bias adjustment, and Quantile Delta Mapping respectively. The risk failure shown is the mean risk result calculated from each PPE member.

captures the changes in dynamical processes (ie. benefits from direct use of climate model outputs) and has strong historical consistency. Whilst QDM may not capture the complete extent of climate uncertainty (the larger decadal variation seen in Figure 4.4, panel a vs. c and potentially valid decadal variability signal encompassed within panel b), the variability observed in Figure 4.4-a is negligible compared to the signals in Figure 4.6. We should remain cautious that climate variability expected in the absence of climate change signal is potentially underrepresented (QDM historical consistency assumes that the reanalysis sample of natural decadal climate variability is sufficient). However, the disagreement between PPE members in Figure 4.6 is now greater in panel c than in b, and therefore, indicates that the identified signal (change in demand distribution) and represented uncertainty (spread between panel c PPE members) is greater than any potentially missing uncertainty.

Figure 4.7 adapts the risk probability framework (used in Figure 4.5), simplifying the display of information by taking the ensemble mean of risk calculated in each ensemble member case. The annual risk of failure probabilities are calculated for each individual ensemble member, for each temperature scenario, and for $N_r = 350$ realisations. However, the information previously represented as curves in the x-y plane is now shown by colour-bar shading[6]. We can

---

[6]Corresponding figures showing the min/max range are displayed in Supporting Information Figures S4.8 to S4.9

interpret that increases in reserve power system capacity requirements are required to maintain an acceptable level of risk; increasing capacity of the reserve system lowers the risk of exceedance, and higher capacity is needed in a warmer climate to achieve the same level of risk. For example, taking QDM (shown in panel-c) as the best practice approach, we observe that what is presently a 0 % to 10 % risk in the 0.78 °C and 1.0 °C scenarios for an installation of 5.7 units of reserve power capacity, subsequently results in increasing risks as global temperatures increase. In the 2.0 °C scenario, the risk is 20 % to 30 %, and in the 4.0 °C scenario, it is 70 % to 80 % (ie. up to eight out of ten years are at risk of one or more events where infrastructure electricity consumption exceeds the reserve capacity).

4.3.4 SURPLUS CAPACITY IN RESERVE POWER SYSTEMS

Section 3.5.4 demonstrated that significant quantities of "surplus" capacity are available when energy consumption is below the maximum designed-for levels. We assume that reserve capacity is installed to some fixed quantity: 5.62 normalised units[7]. The specific value used, 5.62 or otherwise, derives from arbitrary decisions over tolerable levels of risk[8].

Figure 4.8 demonstrates the level of surplus accumulated in a full year (ie. summing the amount of surplus capacity available each day), responding to Table 4.1 global temperature rise scenarios. Longer and hotter future GB summers drive a trend of less surplus capacity in future (the expectation values of each PPE member, indicated by the coloured dot, are reduced in future temperature scenarios). There is a significant increase predicted in the year-to-year variability of how much surplus capacity is made available in total for a given year (the gap between the 5 % to 95 % bars increases for each PPE member). In each of the three approaches, the ensemble spread increases significantly, and the expectation value of some ensemble members is beyond the 5 % to 95 % range of others.

---

[7]This value is the median energy requirement to meet the condition for $\mathbb{P}_C$ =1 %, where $\mathbb{P}_C$ is the coincidence metric used in Chapter 3 with P_R the daily risk of initiating 5-day's running reserve set to 1 %.

[8]For the GB telecommunications case study, with cooling-driven demand, changes to the installed capacity have a non-linear response on the surplus over summer, since it sometimes reaches a minimum value of zero. Changes to the installed capacity have a linear (additive) effect on the *winter* level of surplus as long as values don't fall below zero
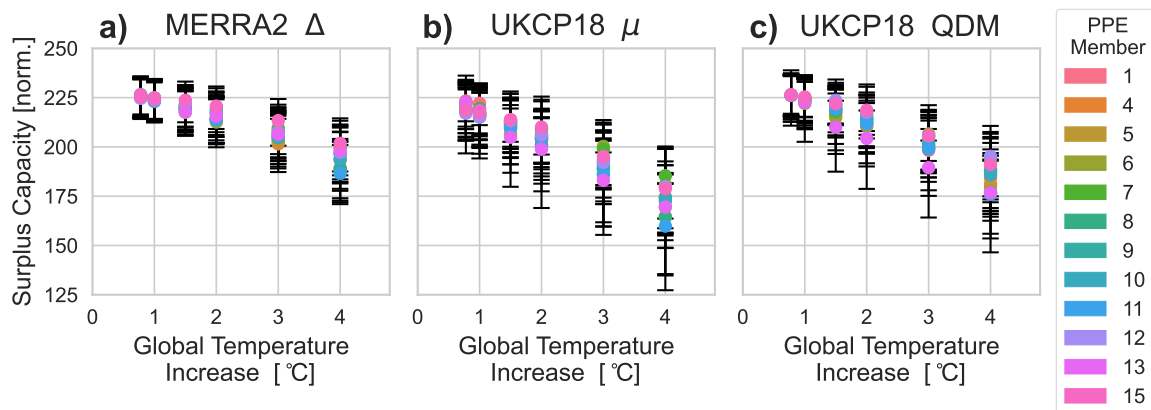
Figure 4.8: The annual yield of surplus capacity (normalised units) is displayed for three alternative bias adjustments (panels a-c) and in the global temperature increase scenarios of Table 4.1. The 5 % to 95 % range of each PPE member is indicated by the black bars.

The mean bias adjustment (with overestimation of high-demand events) will tend to overestimate the reduction in surplus capacity. QDM instead exhibits slightly larger decreases in surplus yield and slightly greater year-to-year variability.

An example PPE member in which annual levels of surplus capacity perform well is member 12, exhibiting typically higher accumulation of surplus annually in each 20-year scenario and with each bias adjustment method compared to other PPE members. In Figure 4.1, the historic mean GB temperature of PPE member 12 is the lowest of all members, whilst the global temperature is close to average — this low-temperature GB climate persists (see plot in supporting information Figure S4.1), and explains the lower Cooling Degree Day energy use / high surplus yield. Conversely, PPE member 11 generally experiences the worst performance; the GB temperature of member 11 rises relatively faster than global temperatures, leading to significantly lower returns in surplus capacity for this PPE member.

In GB, surplus capacity for balancing services and in the capacity market holds greater value during the winter period, where GB national electricity load is most variable and vulnerable to high-demand low-renewables events (Thornton et al., 2016; Coker et al., 2020). Reductions in the number (and severity) of Heating Degree Days drive a small *increase* in the level of surplus demand in future winters, as shown in Figure 4.9. There is a negligible change to the overall year-to-year variability in winter accumulation of surplus capacity — this variability
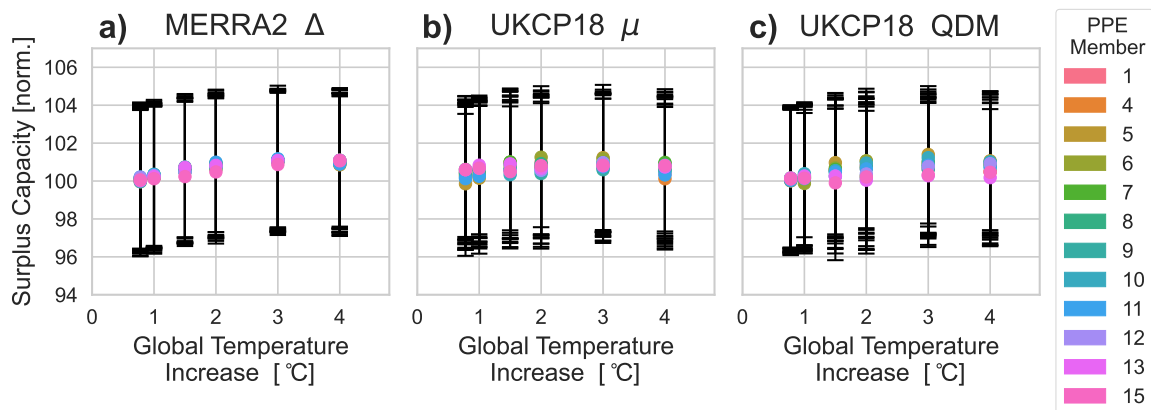
Figure 4.9: As in Figure 4.8, but restricted to the November-March winter yield of surplus capacity.

is small and consistent across methods and PPE members.

4.4 Discussion and Conclusion

This paper demonstrates how decision-makers can implement and interpret climate model outputs towards modelling infrastructure electricity demand and reserve power system design. We have demonstrated that UKCP18 model outputs can be effectively used to support reserve capacity planning and recommend Quantile Delta Mapping (QDM) as a preferable approach (consistent with Qian and Chang (2021) and Li and Li (2023)).

QDM samples new weather that has not occurred historically and in unprecedented new conditions, whilst reducing the risk of climate model biases. The QDM method also facilitates sampling different regional warming responses for a given global warming level, insofar as the change occurs between the modelled 'historic' and 'future' periods. However, using QDM eliminates any initialised signal of natural decadal variability, since the method requires that the historic modelled probability density matches the re-analysis derived results.

In addressing Item RQ ii.2 in Section 4.3.2, we demonstrated that the uncertainty represented as differences between PPE members stemming from dynamical differences and aleatoric uncertainty outweighs the variability simulated using the same representation of regional climate differences under delta-shift, and therefore indicates that the leading sources of uncertainty are

represented in QDM, whilst potentially erased signals of regional decadal variability are only of secondary importance.

The highlighted advantages and trade-offs in bias adjustment and delta-shift conform with studies such as Teutschbein and Seibert (2012) and Hawkins et al. (2013); with delta-shift limited to exactly one single evolution of weather, the dynamics are correctly represented but limited to one realisation of many that could have occurred (a strength for studying the historic period, but a weakness for assessing future risk). Figure 4.5 shows that the delta-shift approach simulating historical regional climate variability has only a slight impact on the annual risk-capacity curves, whereas the QDM approach shows a significant spread across ensemble members for the current risk levels. There is a significant difference between the best- and worst-case PPE members in the 2.0 °C scenario, and therefore decision-makers are urged to consider best and worst cases (or other representations of model disagreement), and not to rely on a single PPE member or ensemble mean.

In relation to RQ ii.1, we have made a detailed comparison of several alternative approaches to interpreting and using UKCP18 model outputs. The advantage of the quantile-correcting methods is the better sampling of weather (no longer restricted to observations); even though the historic distribution under QDM is identical to reanalysis-derived infrastructure electricity demand (Figure 4.4-c), Figure 4.5-c shows greater variation across PPE members than the delta-shift. And for future climate, the quantile-correcting methods offer a representation of natural variability and model uncertainty (Figure 4.6). The primary trade-off in applying QDM is the limitation in fitting to the observations (and therefore, it assumes that any differences between the statistics of a given model realisation and the observation are due to biases we wish to correct, rather than 20-year timescale natural variability). Delta-shift, by contrast, permits variations in the 20-year mean (caused both by perturbed physics and natural variability) but with only a single sample of weather.

As noted in previous studies (e.g. Shepherd (2019)), defining scenarios in terms of global temperature thresholds leapfrogs the issue of choosing a specific emissions concentration pathway and global climate sensitivity that indirectly impact results, and instead presents scenarios in

a policy-relevant framework of global temperature scenarios (1.5 °C, 2.0 °C, 3.0 °C, etc.). The approach we have adopted could be complemented with a set of storylines based on mechanisms that govern the variability of the ocean-climate system and its predictability on decadal timescales. For GB, many climate variables, including temperature, are closely linked with the North Atlantic jet stream. Harvey et al. (2023) propose jet-based storylines, with results presented for combinations of global temperature and jet storyline. Attaining robust results using a jet-based approach necessitates a greater number of climate models, making it unsuitable to use when relying on only the UKCP18 PPE-12 alone. However, using a sufficiently sized climate model ensemble, a jet stream storyline or adaptations of this sort could be used as well as (or instead of) the global-mean temperature approach explored here.

With respect to the specific application for telecommunications, we have demonstrated how surplus levels in reserve capacity respond to future climate change (RQ ii.3—a). Whilst the full-year and summer period returns are expected to decrease (Figure 4.8), the level of surplus available over the critical winter period is expected to have a slight increase (Figure 4.9), responding to a reduction in Heating Degree Days. It is therefore concluded that the concept of surplus reserve capacity for these cooling-dominated systems is robust to likely future climate change in GB (RQ ii.3—b).

4.5   Supporting Information

4.5.1   ABOUT UKCP18

The Met Office UK has published its UKCP18 climate projections covering a range of climate change scenarios, with simulations spanning 1900 to 2100 and exploring different future emissions pathways. Multiple published land projection products are available, including the global and regional projections used in this research, local projections, probabilistic projections, and derived projections.

The UKCP18 *Global* product comprises projections run on a 60 km resolution latitude-longitude grid. 28 projections incorporate 15 members of the HadGEM3-GC3.05 coupled land and ocean-atmosphere PPE, and 13 simulations from the CMIP-5 multi-model ensemble.

The UKCP18 *Regional* product uses a subset of 12 of the HadGEM3-GC3.05 PPE members, applying downscaling over a region of Europe. Two of the 15 PPE members were excluded from the Regional product due to data gaps, and one of a pair of PPEs (each implementing a closely related model) was also excluded (Murphy et al., 2018). The regional climate model downscaling runs at a 12 km resolution on a rotated pole grid without ocean-atmosphere coupling. As a result of the downscaling, temperature on cold winter days and hot summer days is better represented (Met Office Hadley Centre, 2019).

The UKCP18 Probabilistic projections aim to provide uncertainty in future climate change scenarios and use emulators to extend the parameter space. However, issues in the methods used to quantify uncertainty and an overall lack of transparency in the production of the Probabilistic projections can be viewed as a significant quality degradation (Pacchetti et al., 2021). The product design is also poorly suited to the impact modelling use case, as it is preferable to use a timeseries which permits bias adjustments and dynamic/autocorrelated impacts. We therefore rule out using this product type.

We redefine calendar years to span from 1st December through to 30th November, thereby grouping the winter months December January February.

In summary, we use the 12 PPE members present in the Regional products and the corresponding 12 members from the Global product (discarding three members of `HadGEM3-GC3.05` and the 9 alternative model outputs since these are not present in the Regional product).

4.5.2 GLOBAL TEMPERATURE SCENARIO — DATE SPANS

The 20-year date spans (relating to Table 4.1 temperature thresholds) used to define which portions of the climate model we use are indicated in Figure S4.1 by the rectangular blocks spanning the period from start to end. Temperatures are calculated relative to pre-industrial levels using the `HadCRUT5` statistical analysis (Morice et al., 2021). Blue-to-red shading indicates the realised GB climate of each PPE member.

Further into the future, there is increasing divergence in both the window date (model members disagree *when* global temperature thresholds are first crossed) and in the regional warming level of each PPE member at a given threshold (model members disagree on GB climate sensitivity with respect to the level of global temperature rise). The 20-year window timeseries of GB temperature are always detrended to remove the trend around the window centre.
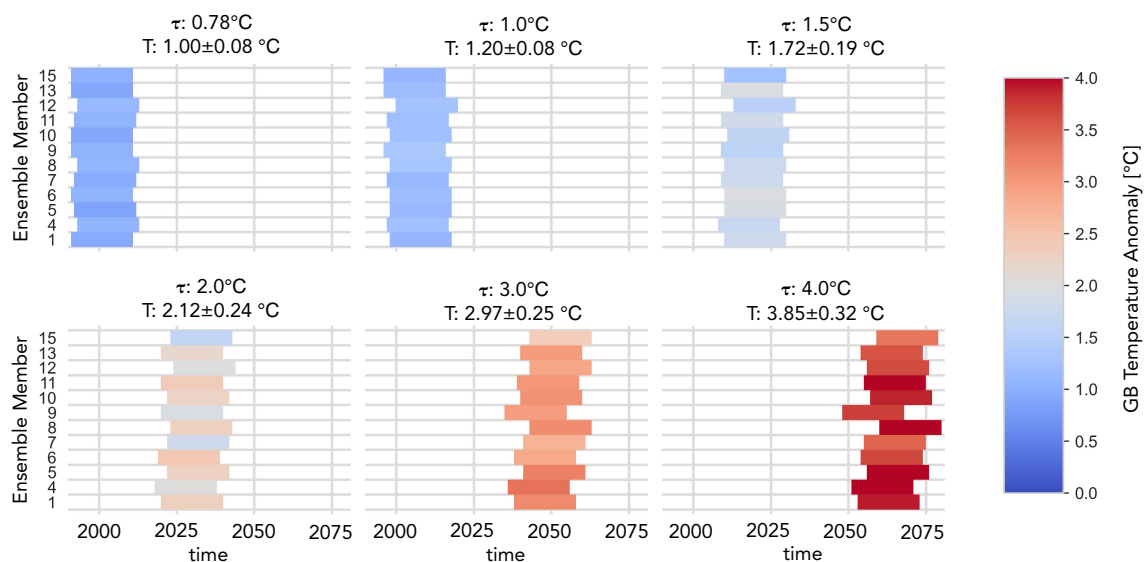
Figure S4.1: Shaded blocks indicate 20-year periods where the global temperature average first crosses a specific threshold. The colour of the shading shows the regional temperature anomaly, and the variation in this colour for a given global threshold demonstrates regional variability to the global climate.

4.5.3   BIAS ADJUSTMENT METHODS

In Section 4.2.2, three bias adjustment approaches are compared alongside delta-shift. The approaches are slight extensions on the standard definitions for each method, reflecting the specific implementation taken for the Perturbed Physics Ensemble. These implementations are described below, and motivated by the need to sensibly interpret the Perturbed Physics Ensemble.

4.5.3.1   GLOBAL MEAN BIAS ADJUSTMENT

Global mean bias adjustment implements a constant offset correction to climate model temperature outputs.

Method 1: Global Mean Bias Adjustment (μ)

A constant offset δ_p^μ, is calculated from the difference between the mean global surface temperature of PPE member p and observations:

$$\delta_p^\mu = \left\langle \tau_p(t) - \tau_{\mathrm{obs}}(t) \right\rangle_{\mathrm{hist}} \tag{S4.1}$$

where τ is the *global* surface temperature, subscript obs refers to observations (the reanalysis product MERRA-2), and $\langle \ldots \rangle_{\mathrm{hist}}$ is the mean taken over the baseline period (1981 to 2018)[a].
The bias adjustment performed on PPE member p is:

$$C_\mu(T_p(t)) = T_p(t) - \delta_p^\mu \tag{S4.2}$$

---
[a]2018 is the latest year available in the HadCRUT5 statistical analysis, used to define warming with respect to pre-industrial temperatures (1850 to 1900)

The effect of global mean bias adjustment C_μ on GB temperature distributions is shown in Figure S4.2. The 20-year temperature trend (centred running mean) is removed from both MERRA-2 and UKCP18 to compare the temperature variability expected in a given year directly.

MERRA-2 and UKCP18 distributions are broadly in agreement, however, in the range of temperatures that induce cooling demand (red-shaded region) a departure is apparent as the range
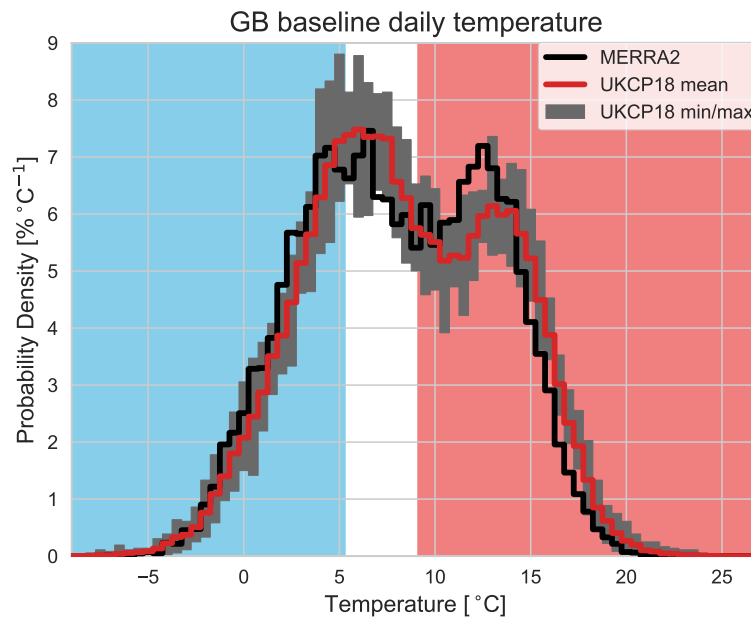
Figure S4.2: GB daily surface temperature probability distribution in MERRA-2 and UKCP18 (with global mean bias adjustment). Blue (red) shading indicates temperatures that induce heating (cooling) demand, respectively, in the case study infrastructure electricity demand. Grey shading shows the minimum/maximum extent of PPE members.

of all PPE member distributions exceeds the upper tail of the observations distribution. This informs us that whilst C_μ provides some consistency between model and observations, the discrepancies are concentrated towards high temperatures and will lead to large errors in modelling extreme cooling-demand events.

4.5.3.2   DELTA-SHIFT

A delta-shift method (Räty et al., 2014; Arnell et al., 2021; Casanueva et al., 2020) simulating global temperature rise and regional climate variability is proposed, allowing a comparison to be made between results derived from direct climate model outputs and the effect of just reanalysis data shifted to have an average temperature change.

Method 2: Delta-Shift (Δ)

The GB reanalysis temperature timeseries $T(t)$ is offset by constant value δ_p^Δ:

$$\delta_p^\Delta = (\Delta - \Delta_{\mathrm{obs}}) + v_p \tag{S4.3}$$

where $\Delta - \Delta_{\mathrm{obs}}$ is the target global temperature increase above pre-industrial levels, Δ, excluding temperature rise already measured up to the reanalysis time period, Δ_{obs}, and v_p is a measure of regional variability (the mean difference between global mean bias-adjusted temperature $C_\mu(T_p)$ of PPE member p, and reanalysis temperature T).
The delta-shift performed on $T(t)$ is:

$$C_\Delta(T(t)) = T(t) + \delta_p^\Delta \tag{S4.4}$$

The delta-shift process is an adjustment of observations and does not directly use the climate model outputs. Instead, it mirrors the climate variability observed in UKCP18 by applying 12 alternative realisations of climate variability v_p (a unique value per PPE member). These delta-shift values are visualised in Figure S4.1, where the global temperature threshold is realised by a slightly different regional warming response in each PPE member..

4.5.3.3 QUANTILE CORRECTING BIAS ADJUSTMENT

Casanueva et al. (2020) assess eight standard and state-of-the-art bias adjustments, finding that quantile trend-preserving methods are better equipped to preserve raw signals in the climate data, given a sufficiently sized observations sample. QM and QDM are bias adjustment methods that can preserve climate change trends independently across the temperature spectrum.

Method 3: Quantile Mapping (QM)

Model temperature timeseries $T_p(t)$ is converted into probability Cumulative Distribution Function (CDF), and then an inverse CDF transforms the probability back into a temperature value, yielding QM bias-adjusted temperature:

$$C_{\text{QM}}(T_p(t)) = \text{CDF}_{\text{obs}}^{-1}\left(\text{CDF}_{\text{HIST}-p}(T_p(t))\right) \tag{S4.5}$$

$\text{CDF}_{\text{HIST}-p}$ is the CDF of the model historic period, $\text{CDF}_{\text{obs}}^{-1}$ is the inverse CDF derived from the observations.

When values of the bias-adjusted variable exceed the range of historic observations, QM is unable to adequately map values (Spuler et al., 2023) and is therefore a poor choice for future scenarios where temperature ranges exceed what has previously been observed. QDM, instead, is a method using a CDF of the future period to map values, and circumvents the issue of previously unobserved events in the historic CDF (Switanek et al., 2017). An adaptation of Figure 1, Switanek et al. (2017), is included in the supporting information (Figure 4.3), demonstrating the different theoretical approaches of Quantile Mapping and Quantile Delta Mapping.

Method 4: Quantile Delta Mapping (QDM)

A temperature correction $\delta_p^{\text{QDM}}(T_p(t))$ is calculated, differencing the inverse CDF of the model historic values and observations, each operating on probability $\text{CDF}_p(T_p(t))$ in the corresponding 20-year period of $T_p(t)$:

$$\delta_p^{\text{QDM}}(T(t)) = \text{CDF}_{\text{HIST}-p}^{-1}\left(\text{CDF}_p(T_p(t))\right) - \text{CDF}_{\text{obs}}^{-1}\left(\text{CDF}_p(T_p(t))\right) \tag{S4.6}$$

Applying this correction of model p at time t yields the QDM bias-adjusted temperature timeseries:

$$C_{\text{QDM}}(T_p(t)) = T_p(t) - \delta_p^{\text{QDM}}(T(t)) \tag{S4.7}$$

$\text{CDF}_{\text{HIST}-p}^{-1}$ is the inverse CDF of the model historic period, $\text{CDF}_{\text{obs}}^{-1}$ is the inverse CDF of the observations.

Trials of additional non-parametric and parametric bias adjustments of UKCP18 temperature

data did not offer measurable performance advantages[9], and therefore QDM is selected as the best practice quantile correcting bias adjustment to use.

4.5.3.4 QUANTILE MAPPING VS. QUANTILE DELTA MAPPING

This section further explores the comparison made between QM and QDM in Figure 4.3.

A large discrepancy is observed between quantile mapping and quantile delta mapping in the upper tail ends. An additional smoothing step eliminates non-monotonicity and reduces sensitivity to low sample-size tails. Although this does not significantly affect derived distribution shapes, the impact on individual (extreme) events can be significant.

Compared to the upper tail end, the lower tail has no significant change between QM and QDM approaches.

---

[9]For example, Scaled Distribution Mapping (Switanek et al., 2017) achieved almost the same adjustment as with QDM, and therefore, the two bias-adjusted timeseries are almost identical, with correlation $R^2 = 0.99991$

Ensemble Member 1
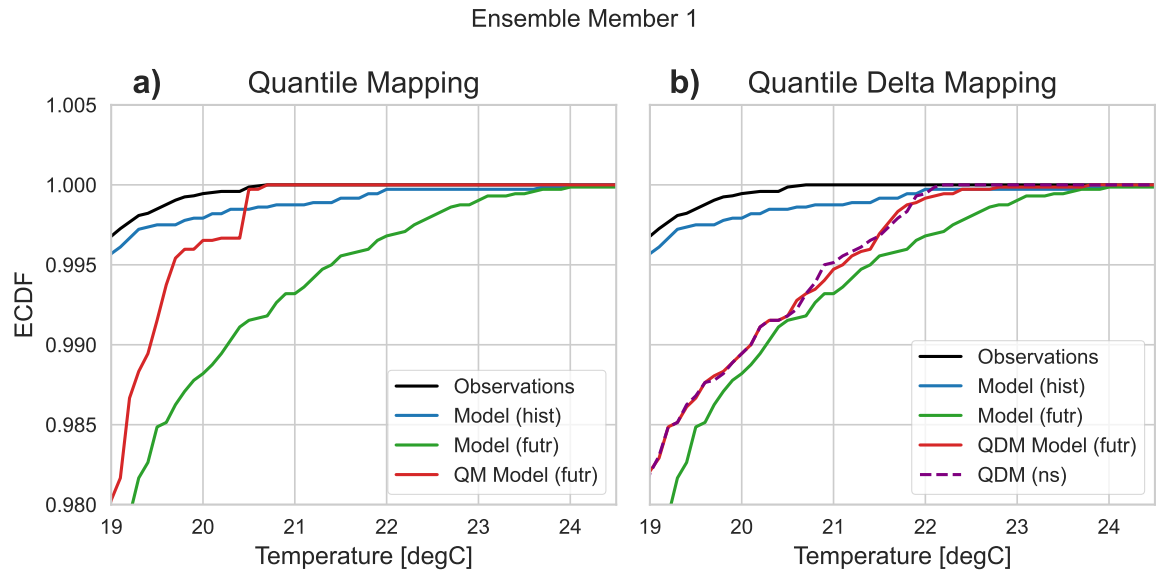
Figure S4.3: Following from Figure 4.3, highlighting upper tail ends in PPE member 1. QDM (ns) shows quantile delta mapping without monotonic smoothing correction.

Ensemble Member 1
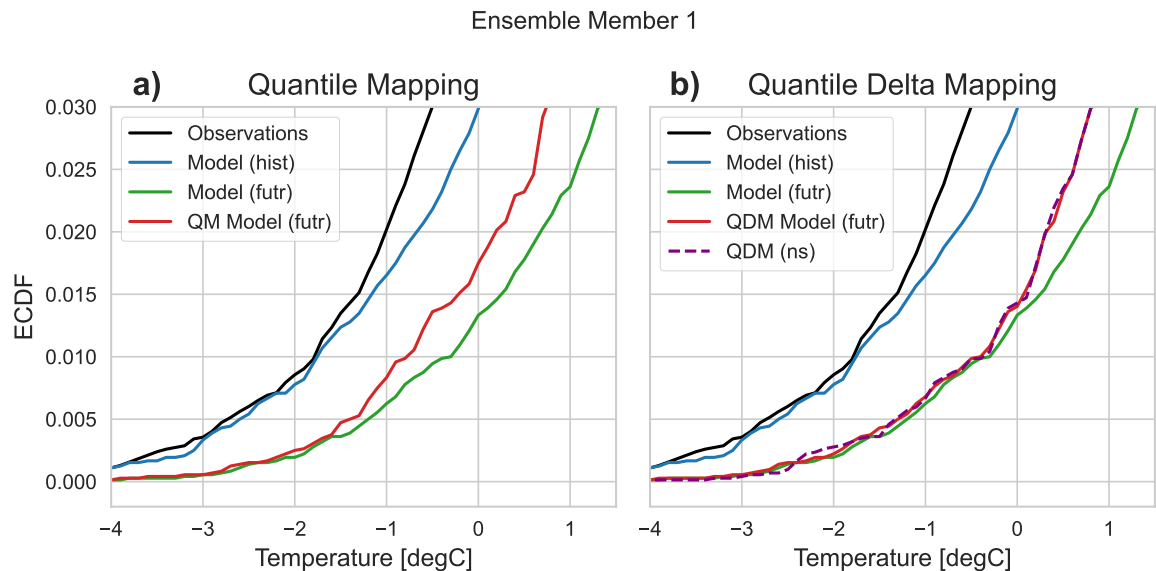
Figure S4.4: Following from Figure 4.3, highlighting lower tail ends in PPE member 1. QDM (ns) shows quantile delta mapping without monotonic smoothing correction.

4.5.3.5 Technique Comparison

Figure S4.5 demonstrates the adjustment applied (in the case of PPE member 1) to the historic period (panel a) and the 2.0 °C scenario (panel b).

Recalling the adopted definition of delta-shift, Equation (S4.3), the temperature values are shifted by the regional climate response to a given global temperature threshold. In Panel a, the delta-shift implements zero global temperature increase, but does result in small positive or negative changes in the climate depending on each PPE member. In panel b, both a target climate change and the regional component are simulated.

The mean bias adjustment does not perfectly match the delta-shift, since although the distribution means are equal, the underlying timeseries and distribution of temperature values differ between the PPE member and observations.

In panel a, both quantile-correcting approaches (QM and QDM) achieve the same result — in the case of QDM being applied to historic data it can be shown that Equation (S4.7) reduces to Equation (S4.5). In panel b, QM and QDM achieve quite different results; of particular note are differences in probability distribution in-between the distribution's bimodal peaks and the
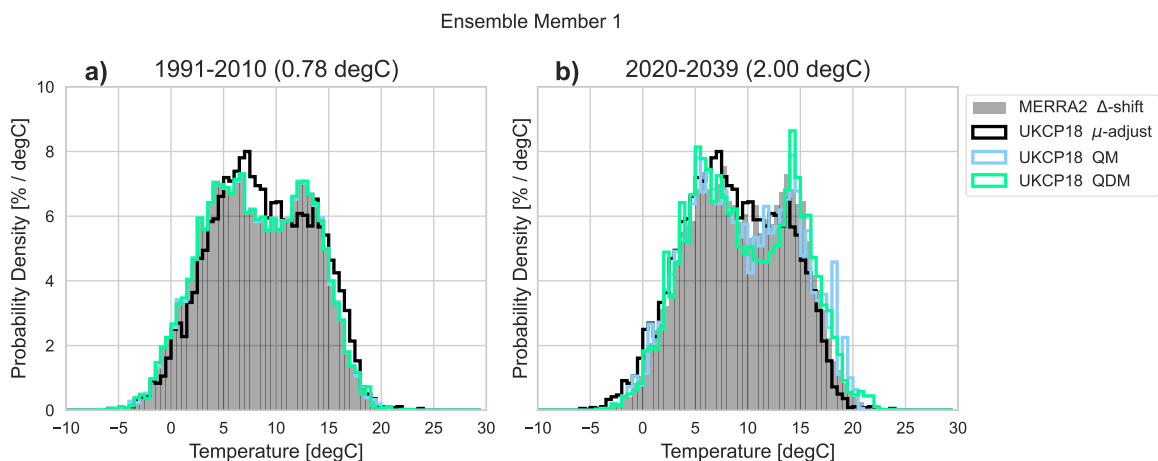
Figure S4.5: Distribution Bias Methods: Daily temperature distribution in the historic period (panel a) and 2.0 °C scenario (panel b). MERRA-2 "observations" (re-analysis) for the historic period and delta-shift applied for the future period 2.0 °C scenario indicated in grey. We show UKCP18 outputs using the global mean bias adjustment approach (μ), Quantile Mapping (QM), and Quantile Delta Mapping (QDM).

fat tail high temperatures in QDM. The QM results are noisier towards the distribution tail end, where low sample sizes disproportionately impact results. The underlying non-bias-adjusted `UKCP18` model exhibits a proportionally larger tail in 2.0 °C than historic, and QDM captures this proportional increase.

There is no single *correct* method to take. Each approach offers different advantages in terms of preserving the climate signals. As QM appears to offer a weaker theoretical basis than QDM (new temperature extremes cannot be sensibly bias-adjusted), we remove it from our toolkit of approaches.

4.5.4 RESERVE CAPACITY PLANNING, ADDITIONAL SCENARIOS

Demand probability distributions in a range of projected scenarios of global temperature rise are shown overpage (Figures S4.6 and S4.7).
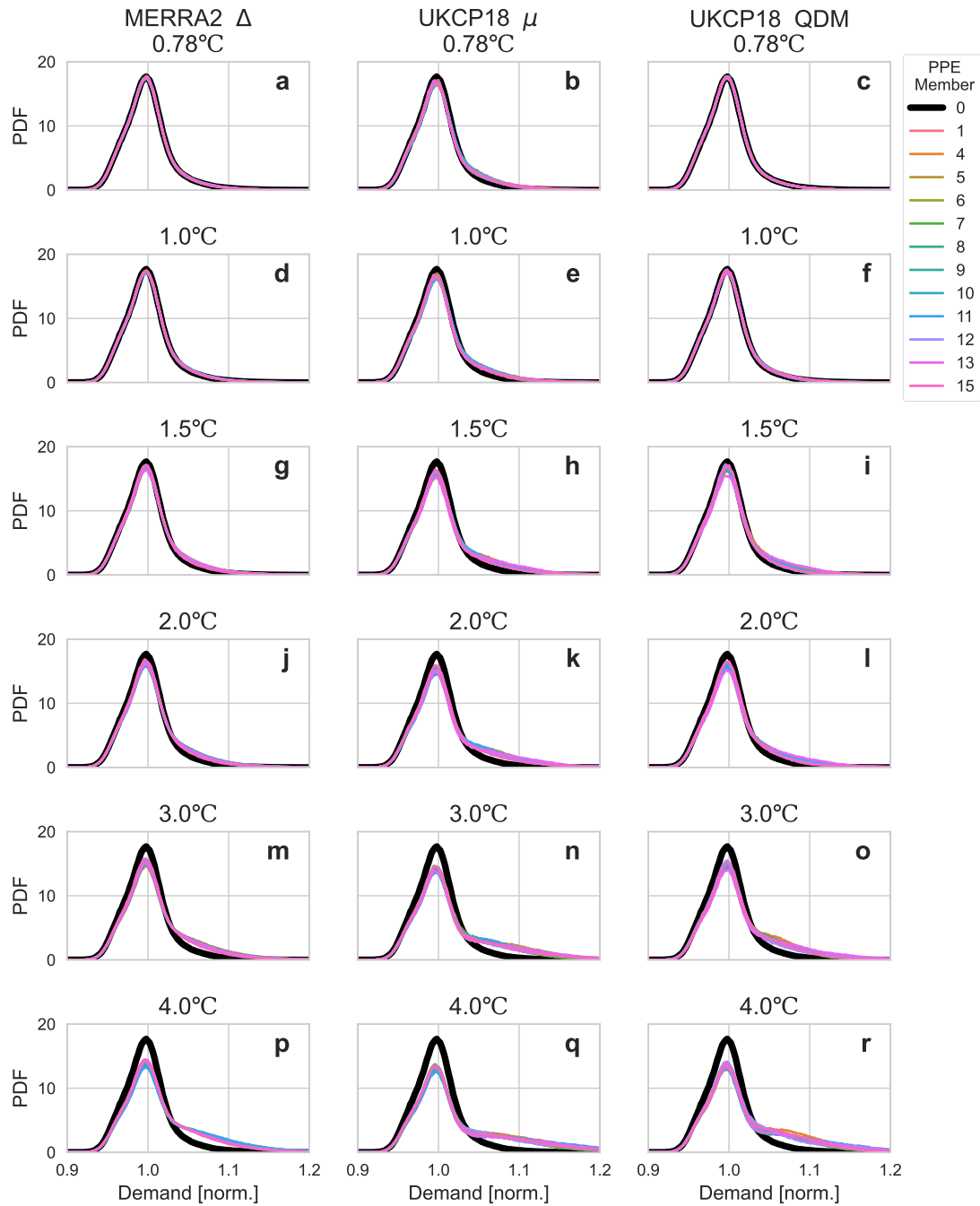
Figure S4.6: Demand probability distributions in the projected scenarios of global temperature rise (Table 4.1). Panels a-c demonstrate the distribution resulting from delta-shift approach, global mean bias adjustment, and quantile delta mapping, respectively.
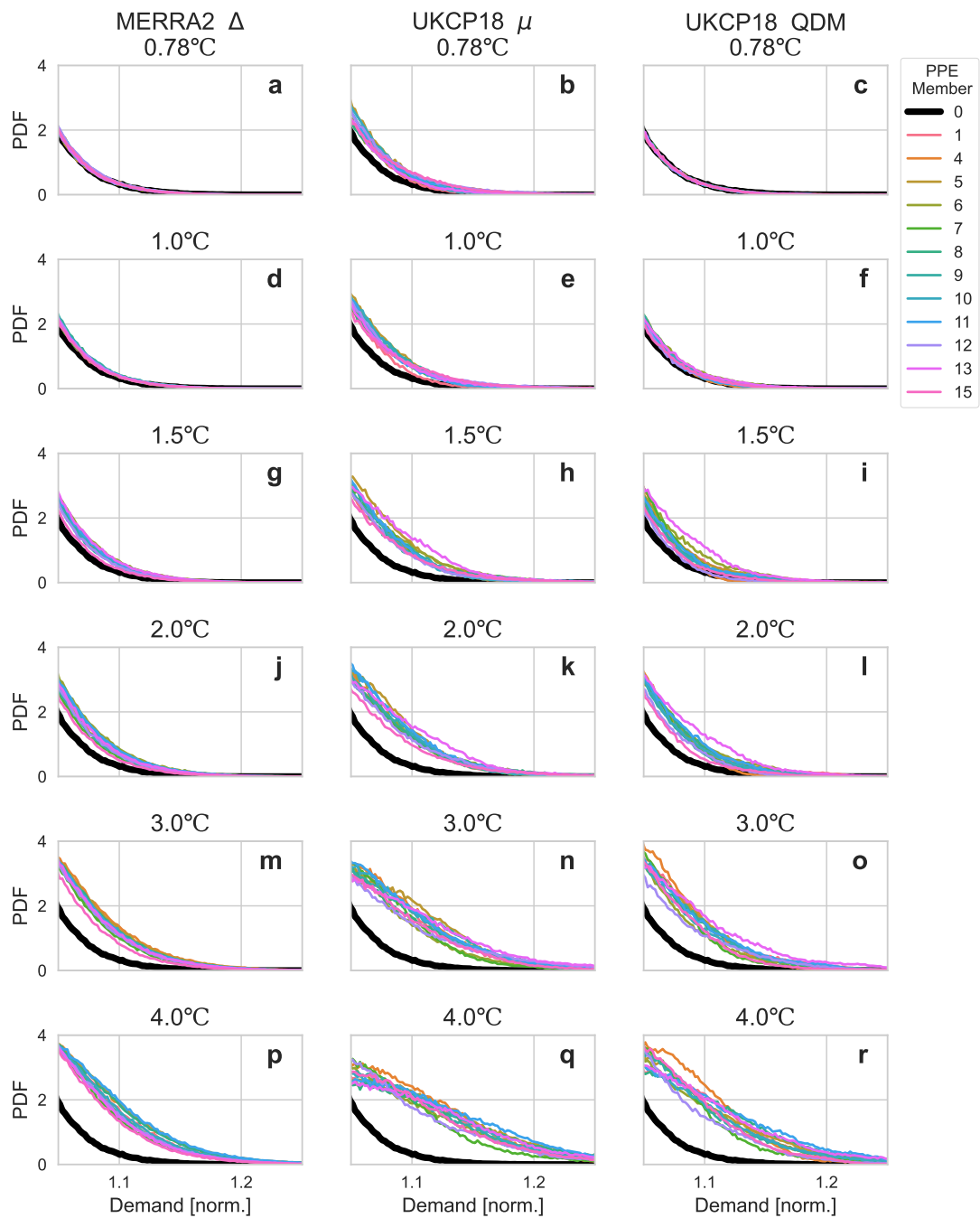
Figure S4.7: Figure S4.6 cropped to the upper tail of distributions.

4.5.5 ANNUAL FAILURE RISK MINIMA-MAXIMA

Figures S4.8 and S4.9 show the range in risk values calculated across PPE members.
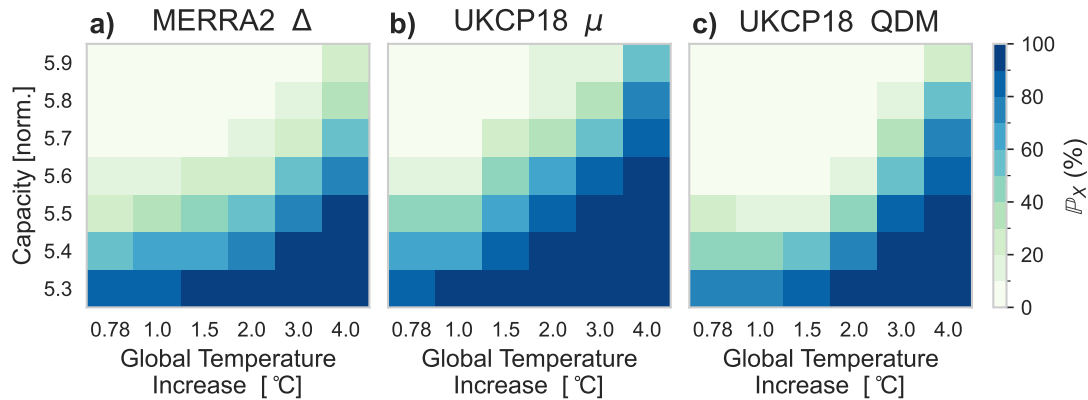
Figure S4.8:   An adaptation of Figure 4.7, showing the PPE minimum risk instead. The colour shading indicates annual risk of failure ($\mathbb{P}_X$): low risk (white), to high risk (dark blue). We split scenarios into grids of Global Temperature Anomaly Δ (horizontal axis) and Capacity (vertical axis). Three panels (a-c) show the results of delta-shift, mean bias adjustment, and quantile delta mapping, respectively. The risk failure shown is the mean risk result calculated from each model member.
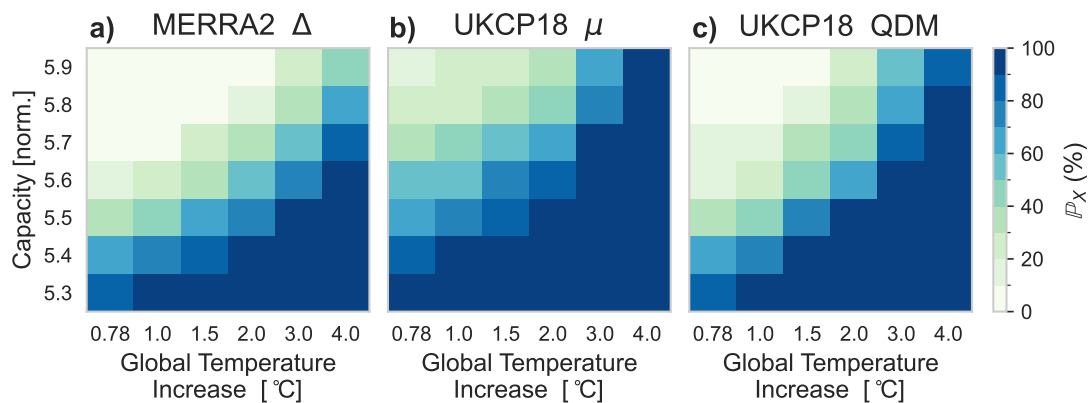
Figure S4.9:   As in Figure S4.8, showing the PPE maximum risk instead.

Weather-driven surpluses in backup energy stores: improving power system adequacy and unlocking the value of decarbonisation

This chapter addresses Thesis RQ iii: *Is it viable to (re)build reserve power systems to have a low carbon impact, paying for this investment through return of surplus power capacity to the wider grid?* The contents of this chapter have also been prepared for submission to Applied Energy (Elsevier), with the provisional reference:

Fallon, J. C., Brayshaw, D. J., Methven, J., Greenwood, D., Jensen, K., Krug, L., in preparation: Weather-driven surpluses in backup energy stores: improving power system adequacy and unlocking the value of decarbonisation.

Supporting information is included in Section 5.5. The delta-shift dataset used in Chapter 4 is used again in this work, and available from the online Reading Research Data Archive (see Appendix A).

5.1   Introduction

5.1.1   RESERVE POWER SYSTEMS

In Great Britain (GB), the combined power capacity of reserve power systems of infrastructure represents a significant fraction of national electricity demand: the contributions from health sector, water treatment plants, telecommunications sector and datacentres each represents around 0.5 % to 1.5 % of GB demand (NHS England, 2022; POST Report 282, 2007; Kotulla et al., 2022; Swabey, 2022; Booth & Wu, 2020). Furthermore, reserve system power capacity is increasing globally with record installations of battery energy storage in recent years (NTESS, 2022). Whilst global data centre energy use is growing steadily (and currently near 1 % of global electricity use), the proportion of energy use of data centres in some countries with low populations but large digital economies is higher, and in some instances projected to reach up to 30 % of national electricity consumption by 2030 (IEA, 2023a). Therefore, reserve power systems represent a significant power capacity that, if leveraged as smart distributed energy resources, could provide valuable balancing services and capacity to the wider power system network.

5.1.2   SURPLUS RESERVES

In Chapter 3, a case study of GB telecommunications assets demonstrated significant seasonal variation in energy requirements ensures that large quantities of surplus capacity become available for the remaining majority of the year. In cooling-driven infrastructure this results in surplus capacity during the winter, a period of peak stress and high variability for the British power system where this surplus capacity could be especially valuable.

The composition of the backup supply can vary, and therefore surplus capacity may represent battery energy storage, compressed air energy storage, generators (such as diesel or fossil gas), or multiple components comprising a combination technologies. There is a potential economic value in making these assets available to support the wider electrical grid, but this

is sensitive to the characteristics of the energy store or generator (Bovera et al., 2018; Mustafa et al., 2021; Hansson, 2022) and the payment mechanism, for example in balancing services revenue (which in recent years has seen significant increases in value (Gianfreda et al., 2018; Blat Belmonte et al., 2023)). Rising balancing costs and a large increase in the projected use of balancing services (60 GW short term flexibility in the UK by 2030, National Infrastructure Commission, 2023) indicate a high potential value for these services.

5.1.3 RESEARCH QUESTIONS

Continuing the case study of GB telecommunications assets (critical infrastructure that consumes approximately 1 % of GB electricity demand (Watson, 2022), we address the research questions:

RQ iii.1 To what extent can surplus in reserve systems be exploited to improve national power system adequacy?

RQ iii.2 What revenue streams are available from the sale of reserve system surplus capacity, and can this revenue yield a return on investment on the capital cost of low carbon reserve systems?

5.2 Methods

5.2.1 POWER SYSTEM ADEQUACY

The system margin of a power transmission network is the spare capacity available to be called upon before an energy shortfall or blackout could potentially occur. In a power system with dispatchable generation capacity X, variable (intermittent) renewable generation Y, and electricity demand D, the system margin Z is defined:

$$Z = X + Y - D \tag{5.1}$$
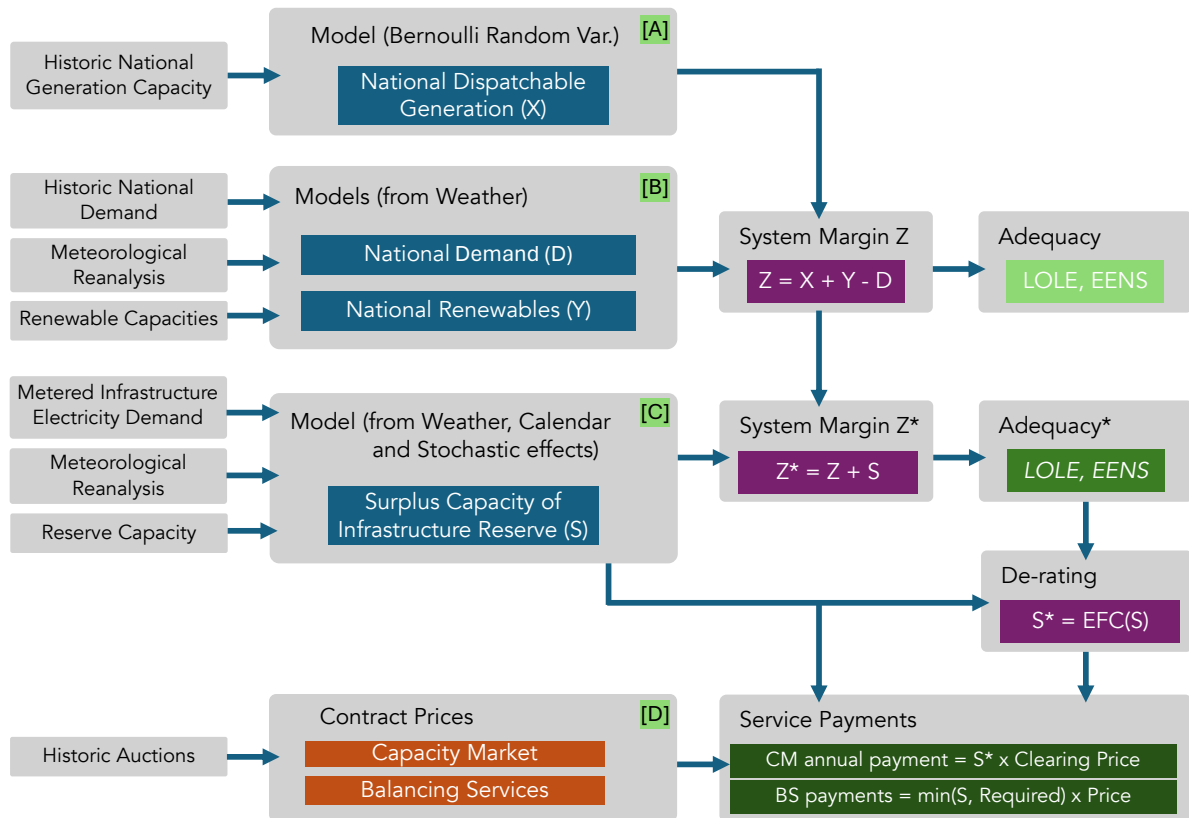
Figure 5.1: High level methods overview. Timeseries (X, D, Y, S) are combined to calculate system margin (Z) and energy shortfall $(Z < 0)$. National power system adequacy is assessed (measured by LOLE, EENS) as well as a simulation of service payments (from the Capacity Market and Balancing Services). Data sources are given: A, Deakin et al. (2022) and Deakin and Greenwood (2022), B, Bloomfield, Brayshaw and Charlton-Perez (2020), C, Fallon et al. (2023) and Fallon, Brayshaw, Methven, Jensen and Krug (2024a), D, National Grid ESO (2024e, 2024d, 2024c).

In the analysis of capacity adequacy, system margin values are usually measured to an hourly or half-hourly resolution. Negative values of Z correspond to an energy shortfall event, known as Loss of Load (LOL), and the missing amount of generation in this shortfall is the Energy Not Served (ENS)[1].

We apply these metrics to simulated scenarios of extended winter GB power system using hourly resolution nationally aggregated energy variables (Bloomfield, Brayshaw et al., 2022), with quantity $D - Y$, the *demand-net-renewables*, sampled as a single covariate (this key energy variable directly relates to the energy shortfall seen by the grid). Generation capacity timeseries (X) is taken from Deakin and Greenwood, 2022[2], with values calibrated tuned to the 2021/22 GB power system, with a base case Loss of Load Expectation (LOLE) of 0.3 h/yr (inline with National Grid ESO, 2021).

Extended multi-decadal reconstruction of self-consistent energy estimates derived from meteorological re-analysis data (rather than recent readings alone) are used in order to achieve a more complete understanding of the impact of climate variations on system behaviours than would be possible sampling only recent years observations (van der Wiel et al., 2019; Bloomfield et al., 2016; Zeyringer et al., 2018).

Figure 5.2 panel a) shows the state of power system variables for a period 1st to 14th December, 2010. In the figure, a single realisation of X is shown which is based on the underlying meteorological conditions. Results are derived comparing many realisations of X to each weather scenario. Panel b) shows the climatological probability distribution of each variable.

From late November to late December 2010, a north-easterly airstream brought bitterly cold air and heavy snow to GB (Prior & Kendon, 2011). The cold weather led to an overall 3 GW (5 %) increase in gas demand compared to levels expected in a typical winter (National Grid ESO, 2011). In the scenario shown by Figure 5.2, the level of GB power system demand (D), and intermittent renewable generation (Y) as built in 2021 is simulated for this weather scenario as an example of a period where low renewables and high demand make the power system

---

[1]Loss of Load and Energy Not Served are also commonly referred to as *lost load* and *energy unserved*.
[2]See original dataset Deakin et al. (2022), `Aggregated Generator Unavailability Data`
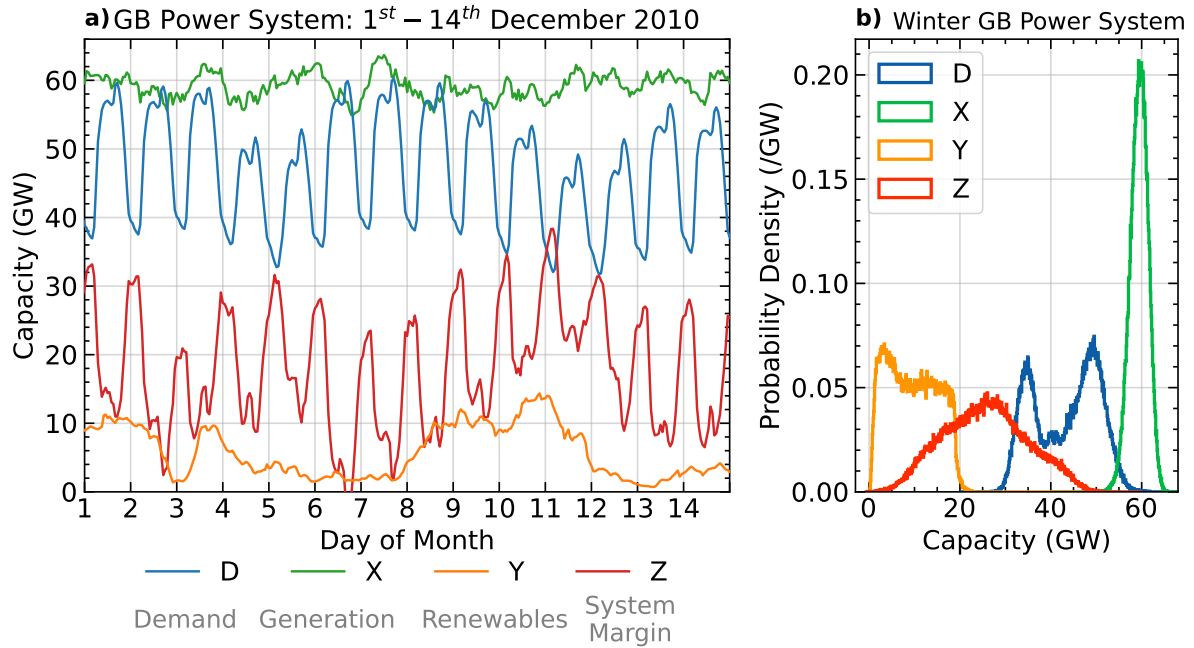
Figure 5.2: GB Power System data for electricity demand (D), dispatchable generation capacity (X), intermittent renewable generation (Y), and derived system margin (Z). Panel a: December 2010 weather scenario. Panel b: Extended winter climatological probability distributions of power system variables.

vulnerable to energy shortfall. For the specific realisation of X shown, the resulting system margin (Z) shows an exceptional 4 h simulated shortfall (6th December 4pm to 8pm)[3].

5.2.2 RESERVE SURPLUS CAPACITY (CASE STUDY)

We introduce a case study simulation of infrastructure electricity load, relating to aggregated GB telecommunications assets. Input to the infrastructure load is a 38-year historical weather record which has been adjusted such that all years are broadly equivalent to present day climate conditions (1.0 °C warming)[4]. Equation (5.2) shows the structure of the modelled infrastructure electricity load. The model construction is described

---

[3]In reality, major power outage did not occur in GB, as the dispatchable generation represented by X is a random variable simulation (not what actually was observed) and $D - Y$ is only the modelled level of demand-net-renewables.

[4]See original datasets Fallon, Brayshaw, Methven, Jensen and Krug (2024a, 2024b); a de-trending and delta-shift to 1.0 °C is performed.
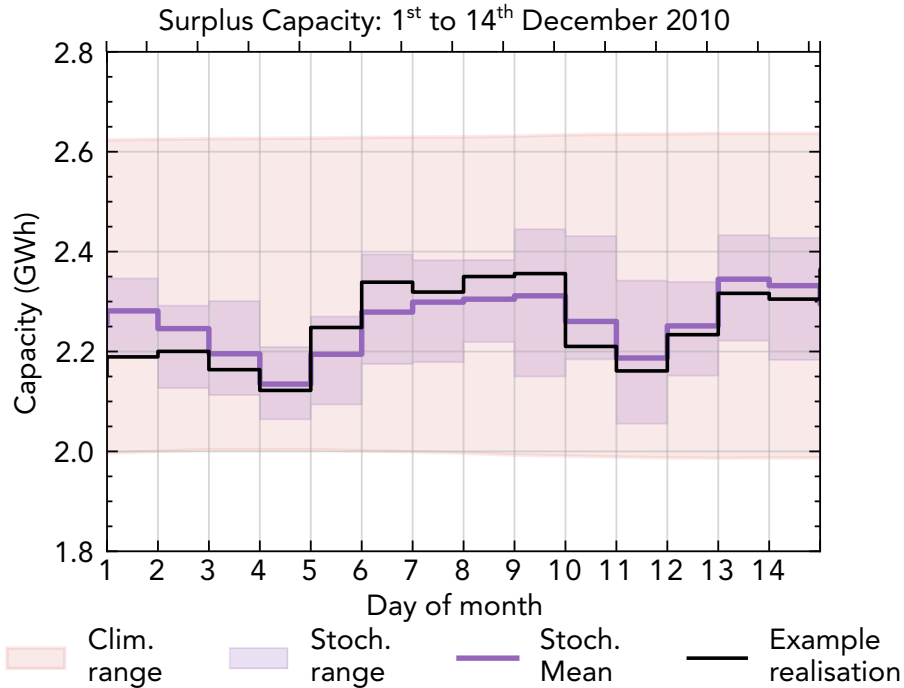
Figure 5.3: Surplus capacity (case study of GB telecommunications assets, BT group plc.): shows the surplus capacity during the December 1st—14th weather scenario (matching Figure 5.2), with the climatological 10-day smoothed min/max (orange), the range of stochastic realisations (purple), mean of stochastic realisations (purple line) and an example of one of the stochastic realisations (black line).

$$\text{infrastructure load} = f(\text{weather}) + \text{stoch. residual} \tag{5.2}$$

in detail in Chapter 3 (Fallon et al., 2023; Fallon, Brayshaw, Methven, Jensen & Krug, 2024c).

Simulated infrastructure load in this case study is particularly sensitive to the need for cooling and thus the peak temperatures in the summer set the size of the installed reserve capacity required to maintain tolerated levels of risk, in this case to ensure a 5-day reserve sufficient to meet the internal load of the telecommunications infrastructure is required to meet mandated security levels. Based on the results of the previous studies (Fallon et al., 2023; Fallon, Brayshaw, Methven, Jensen & Krug, 2024c), a total reserve capacity requirement for the telecommunications infrastructure of GB is set as 15.6 GWh (this amount is sufficient to provide a 1 % annual risk of failure under certain assumptions, refer to Fallon et al., 2023 for further discussion).

Due to the annual cycle, outside of the summer months the need for cooling is much reduced, and thus some level of 'surplus' capacity is almost guaranteed. The amount of day-to-day surplus theoretically available further depends upon (but is not solely determined by) weather conditions, and is determined by the anticipated infrastructure electricity load (Equation (5.2)) subtracted from the total reserve energy capacity (in the case study this is 15.6 GWh).

Surplus capacity is thus modelled as having both a deterministic component (its dependence on daily temperatures) and a stochastic residual (which can be viewed as representing the sum of all influences other than weather). This is demonstrated in Figure 5.3.

For simplicity in this study, we take the climatological minimum as our estimate of the surplus available from the 15.6 GWh total (i.e., approximately 2.0 GWh in the period shown in Figure 5.3). This is, however, clearly a lower bound on the amount of surplus energy potentially available and could of course be increased by using a time-varying estimate of surplus using, e.g., weather forecast methodologies (e.g., Gonzalez et al., 2021).

For the operation of surplus reserve, we consider three different scenarios: *offset*, *export uncapped* and *export capped*.

In the *offset* scenario capacity and balancing services are provided by temporarily switching the power supply for the infrastructure away from external sources (supplied by the Transmission System Operator), instead using the backup supply. The power capacity available to the grid is therefore limited to whatever the infrastructure's electricity load is at a given time.

The *export* scenario is considered in two sub-cases: *capped* and *uncapped*. In the *export uncapped* scenario, there is no constraint on the rate at which energy can be discharged from the store, while the *capped* scenario is rate limited to the designed-for maximum peak instantaneous load of the infrastructure.

These scenarios are summarised in Table 5.1. The order of constraints (from infrastructure load to assumed charge cycle limits) are loosely ordered in terms of the biggest limitation imposed on power output (i.e. the one cycle per day limit only becomes relevant after the other constraints are exhausted). These constraints represent assumptions for how a battery energy

Scenario Power Constraints	Offset	Export (*capped*)	Export (*uncapped*)
Infrastructure load limit	Y	N	N
Built load limit	Y	Y	N
Surplus capacity (climatology)	Y	Y	N
Surplus capacity (actual)	Y	Y	Y
4h supply	Y	Y	Y
One per day charge cycle	Y	Y	Y

Table 5.1: Surplus capacity power constraints. Offset scenario is constrained to the level of infrastructure load, whilst export (capped) is limited by the built infrastructure design (for example maximum power capacity of transmission lines and battery inverters). Both offset and export capped are limited to the climatological minimum level of surplus. The export uncapped is limited to the weekday and temperature driven variations in surplus (allowing slightly greater levels of energy capacity above climatological minimum). In each scenario, (*offset*, *export capped*, *export uncapped*), strict upper limit on power output ensures that 4 h of supply can be met (alternative supply durations accepted by the capacity market / balancing services procurement such as 1 h or 6 h could be substituted instead) and one cycle per day limits are imposed.

store could be used in the surplus capacity context.

5.2.3 IMPROVING POWER SYSTEM ADEQUACY

The two most commonly employed risk metrics in measuring capacity adequacy are the LOLE: the expected quantity of energy shortfall events

$$\text{LOLE} = \sum_{i=0}^{n-1} \mathbb{P}(Z_i < 0) \tag{5.3}$$

and Expected Energy Not Served (EENS): the expected severity of energy shortfall

$$\text{EENS} = \sum_{i=0}^{n-1} \mathbb{E}\left(\max(-Z_i, 0)\right) \tag{5.4}$$

calculated for values of system margin Z_i at hourly time index i (National Grid Electricity Transmission plc, 2018; Zachary et al., 2022).

The benefit to the wider power system is measured by the system margin Z and derived metrics for the system adequacy (including *LOLE*, and *EENS*). Comparison is made between the base

case and the system margin Z^* with the benefit of S, defined:

$$Z^* = Z + S \qquad\qquad (5.5)$$

where Z is previously calculated in Equation (5.1) and S is the power output capability of surplus capacity. Resulting improvements to adequacy metrics are then calculated, LOLE* and EENS*.

Equivalent Firm Capacity (EFC) re-defines a power capacity in terms of its impact towards improved system adequacy. The Equivalent Firm Capacity (EFC) is calculated in two steps: first Z^* is characterised using a reliability metric ρ (usually LOLE, but also alternatively EENS as discussed); and subsequently an optimisation finds the quantity of firm capacity x (positive definite idealised capacity with 100 % reliability) that attains the same improvement to Z^* (Zachary et al., 2022; Greenwood et al., 2022). x is minimised such that $\rho(Z + x) \leq \rho(Z^*)$.

where x is an incremental addition in the capacity (i.e. $x \ll X$), Z is the system margin, Z^* is the system margin with surplus capacity, and ρ is the reliability metric.

Power capacity can be de-rated (reducing its implied contribution to maintaining an adequate system margin), represented instead as the EFC (National Grid ESO, 2023). The EFC (de-rating) is calculated separately for each scenario.

For power systems dominated by dispatchable generation capacity, such as coal plants, nuclear baseload, and gas turbines, the traditional approach to measuring reliability uses the LOLE as the basis for a de-rating factor. However, the penetration of both variable renewable generation and increasing quantities of energy storage capacity is likely to see future procurement de-rated by EENS instead of LOLE (Zachary et al., 2022; Greenwood et al., 2022; Deakin et al., 2021; Mays et al., 2019).

5.2.4 CAPACITY MARKET REVENUE

A capacity market encourages continued investment in generation capacity by paying participants a rate for the de-rated power capacity offered.

The payment made for firm capacity in capacity markets is based on the product of power capacity (kW) and auction price (GBP £/(kW yr)):

$$\text{CM Payment (GBP £/yr)} = \text{Capacity} \times \text{Auction Price} \tag{5.6}$$

We calculate the capacity market payments that could theoretically have been earned through a simulation of recent GB year ahead (T-1) and four years ahead (T-4) auctions (Section 5.3.4). These simulations use auction results published by the Electricity Market Reform delivery body spanning the period 2018 to 2025 (T-1) and 2021 to 2028 (T-4) (National Grid ESO, 2024b).

5.2.5 Balancing Services Revenue

Balancing services relate to frequency containment, frequency restoration, voltage regulation, congestion management, emergency needs and local services (Rancilio et al., 2022). Appropriate services to be provided by surplus capacity are limited by characteristics including strong seasonal variation and a short term variability component, and by the uptime of the energy storage (or generation) being relied upon (Schmidt et al., 2019).

We simulate balancing service revenue with payout:

$$\text{Service Payment (GBP £ h}^{-1}) = S \times P \times \Delta t \tag{5.7}$$

where S is the Surplus Capacity (kW), P is the contract price (GBP £/MW/h), and Δt is the delivery duration (h, usually discretised into 30 min to 4 h blocks).

In the offset and export (capped) scenarios, S is the climatological minimum, and in the export (uncapped) scenario S is the anticipated surplus capacity (with weather and weekday effects).

We shall explore the role of surplus capacity in balancing services provisioned by UK Transmission System Operator, National Grid Electricity System Operator, and in Equation (5.7) this is simulated using results from winter 22/23 National Grid ESO (2024c). The simulated services are: Short Term Operating Reserve (STOR)[5], Demand Flexibility Service (DFS)[6], and Frequency Balancing Service (Dynamic Containment, Dynamic Regulation, and Dynamic Moderation). Note that DFS engagement incurs an exclusion from the capacity market and from other balancing services. The other services can be provided in parallel and also benefit from capacity market payments.

---

[5]Short Term Operating Reserve (STOR) is being phased out and replaced by *Slow Reserve*.
[6]Demand Flexibility Service (DFS) has replaced the legacy Triad service.
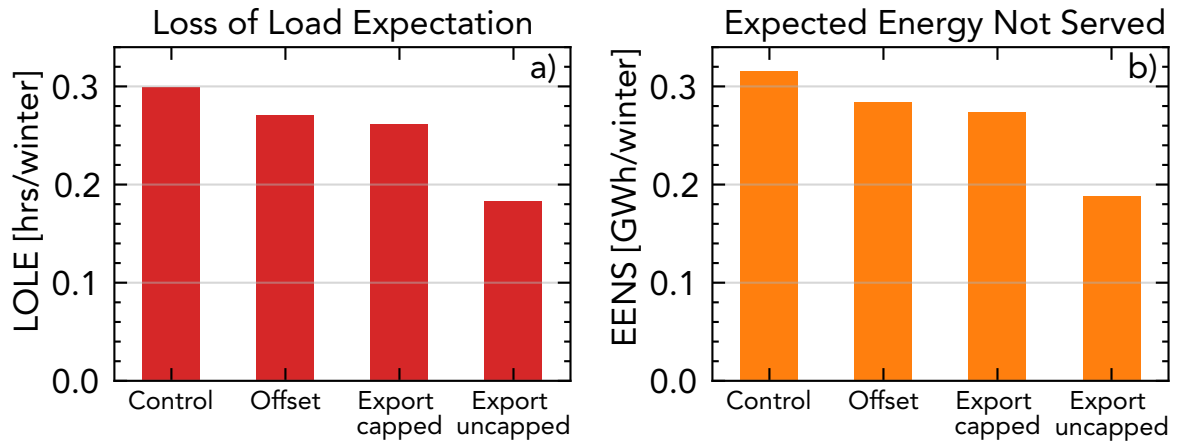
Figure 5.4: The quantity and severity of shortfall (for extended winter period) is indicated by the measure of loss of load expectation (panel a) and expected energy not served (panel b). 4914 Monte Carlo simulations[8] of each weather extended winter scenario are used (exposing different conditions of the dispatchable generation capacity and stochastic component of infrastructure electricity load). The four scenarios explored are control (no additional capacity is secured), and the three scenarios for using surplus capacity: *offset* load, *export capped* and *export uncapped*.

5.3 Results

5.3.1 IMPROVED ADEQUACY USING SURPLUS

Figure 5.4 shows how GB power system adequacy is improved under different scenarios of utilising surplus capacity.

In Figure 5.4-b, we observe that the Expected Energy Not Served is reduced by 10 % in the *offset* scenario. In an *export* scenario where the EENS is further reduced to 13 % below the control. The best outcome is in the *uncapped export* scenario, where the maximum export power output can be arbitrarily high (as long as it meets a 4h minimum delivery period), and the EENS is in this case reduced by 40 %. In Figure 5.4-a, qualitatively similar reductions to the LOLE are observed in each case compared to panel b.

Alternative battery power conversion rates (between 1 h to 8 h) do not affect the EENS result in the control, offset, or export capped scenarios. However, EENS in the export uncapped scenario is highly sensitive to this rate, with a 1 h rate leading to an improved EENS,
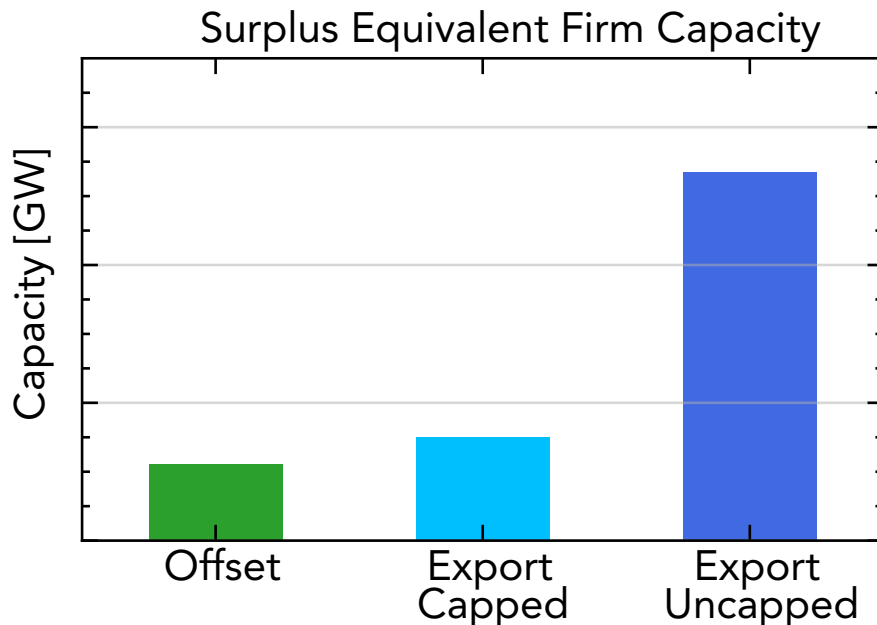
Figure 5.5: The de-rated surplus capacity (Equivalent Firm Capacity (EFC)) in three operational scenarios. EFC is calculated based on the additional firm capacity to secure equal reductions in the Expected Energy Not Served as gained using variable surplus capacity. The error bars in panel a indicate ±1 std. dev. in surplus capacity (see Figure 5.3).

0.127 GWh/winter, and 8 h yielding a higher EENS of 0.242 GWh/winter.

5.3.2 EQUIVALENT FIRM CAPACITY

As shown in Figure 5.5, the export uncapped scenario has an EFC of the surplus capacity (535 MW) is close to the surplus capacity mean (582 MW). The EFC in the *export capped* and *offset* scenarios are however much less, at 151 MW and 111 MW, respectively, due to the restriction on power output, although these are still significant quantities in the context of the GB power system (which has an expected peak winter electricity demand of 58.5 GW (National Grid ESO, 2023)).

5.3.3 LINEARITY OF SURPLUS CONTRIBUTION TO SYSTEM ADEQUACY

In Figure 5.6, the quantity of infrastructure (i.e. both the infrastructure electricity load and installed reserve power assets) is scaled. This could, for example, be considered as a proxy for
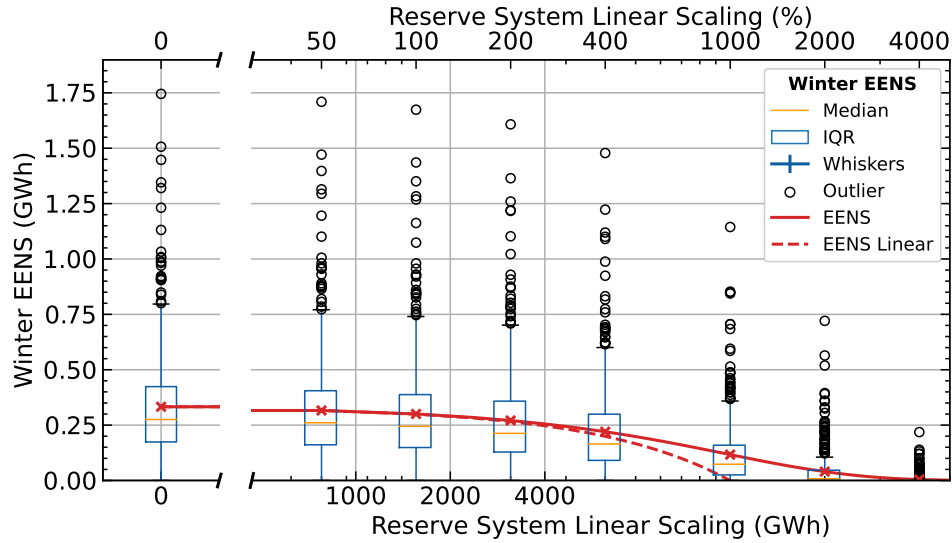
Figure 5.6: Extended Winter Expected Energy Not Served is shown for the energy *offset* scenario, with linear scaling of the total reserve power assets along the (log-scale) x-axis indicated in absolute units (sub axis tick labels) and in relative units (over axis tick labels). Different EENS values are calculated based on 500 different realisations of the dispatchable generation capacity, with the distribution of EENS shown by a whisker plot (box indicates quartile 1 to 3, and whiskers extend beyond the box by 1.5× of the interquartile range). A red curve marks the overall Expected Energy Not Served (EENS) (combining 500 realisations of dispatchable generation capacity), and is compared to (red dashed line) a linear extrapolation around a relative linear scaling 100 %.

incorporating surplus capacity from other infrastructure (for example data centres), assuming that the infrastructure load and reserve systems are broadly similar to the case study of GB telecommunications (i.e. similar temperature sensitives and reserve requirements, which is likely the case for GB data centres). In this experiment, scaling up or down the assets causes a linear change in the EENS — this is demonstrated with a straight line extrapolation (linear regression of surrounding data points) about scaling factor 100 %, indicated by the red dashed line.

At larger scales (400 % and greater scaling increases), the EENS as calculated from our models begins to deviate from the linear trend (red dashed line) with benefits saturating. Even at these higher capacity values, the curve is smooth and continuous, and therefore de-rating factors evolve slowly with large increases in surplus type capacity (and are constant for relatively small changes in the capacity).
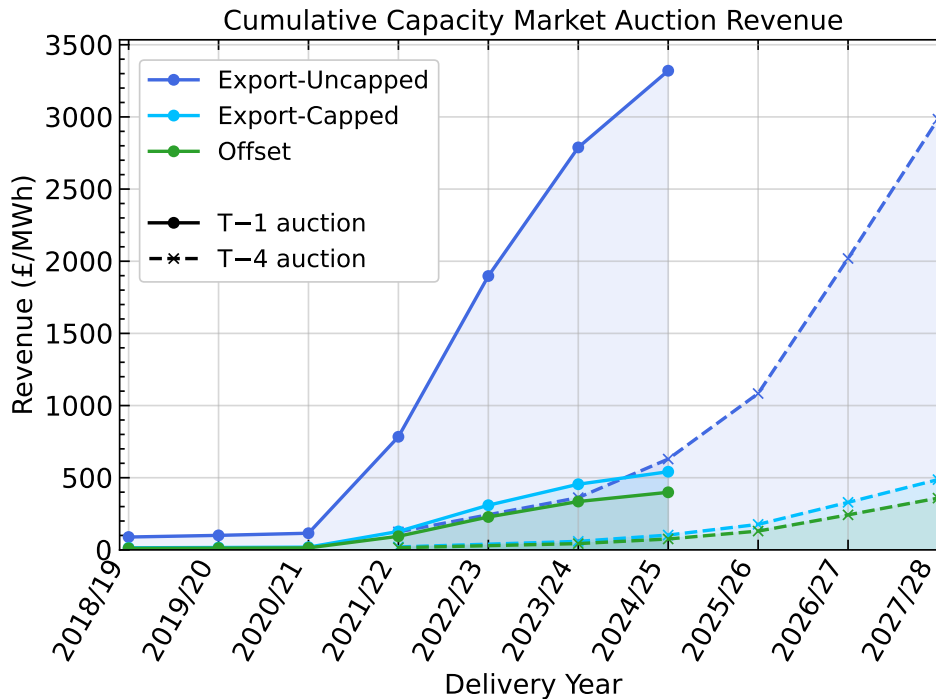
Figure 5.7: The cumulative value of capacity market auctions is simulated for "surplus" capacity in a case study of GB telecommunications assets. The auction value is stated in terms of the revenue (GBP £) with respect to the total of installed reserve capacity (MWh). The delivery year is the auction year +1 (T-1 auctions) and +4 (T-4 auctions). For a reserve power capacity of 15.6 GWh (from the case study), revenue 1000 GBP £/MWh equates to 15.6 GBP £ M.

These results indicate that the de-rating factor of surplus capacity in the case study will not be substantially affected with the introduction of surplus capacity from other sectors (such as health care and data centres and other reserve-protected infrastructure). Therefore, up to a collective total approximately 4 times the size of BT assets (i.e. approximately 4 % GB demand), benefits scale with the size of reserve assets.

5.3.4   CAPACITY MARKET PAYMENTS

In recent years, the clearing price of capacity market auctions has increased significantly, leading to large increases in potential revenue. Figure 5.7 shows the cumulative simulated revenue for bids placed 2018 to 2024 in the three scenarios for BT surplus capacity. The average annual value of capacity in simulated scenarios is given in Table 5.2.

The three simulated scenarios are essentially constant scalings of the recent capacity mar-

Surplus Value	Offset	Export (capped)	Export (capped)
T-1 (GBP £/MWh)	57.0	77.4	474.3
T-4 (GBP £/MWh)	59.8	81.1	497.4
T-1 (GBP £ M/15.6 GWh)	0.890	1.210	7.400
T-4 (GBP £ M/15.6 GWh)	0.930	1.270	7.760

Table 5.2: Annualised revenue from otherwise unutilised "surplus" capacity in reserve power systems, simulated using recent UK Capacity Market auction results (National Grid ESO, 2024b). For the 1-year ahead (T-1) and four year ahead (T-4) auctions, results are displayed both in terms of income GBP £ with respect to reserve system size in MWh, and in alternative units of income GBP £ M with respect to the specific case study reserve capacity installed (15.6 GWh).

ket clearing prices based on the Equivalent Firm Capacity (EFC) of surplus capacity, i.e. Clearing Price × EFC. Hence *export uncapped* and *offset* scenarios (with lower EFC) have smaller returns than the upper bound of achievable revenue from *export uncapped*.

5.3.5 BALANCING SERVICE PAYMENTS

Revenue from balancing services is simulated over extended winter period 2022/23, using recent contract results published by National Grid ESO, 2024c. The simulated revenue accumulation is shown in Figure 5.8. Short Term Operating Reserve (STOR) and Demand Flexibility Service (DFS) offer the highest yields, followed by dynamic containment and dynamic regulation.

The *accepted* value is the total level of revenue generated from all service bids. In many cases, the *export uncapped* scenario is close to or equals the *accepted* value. In the present market, bids would respond to the saturation of the market and the contract price reduce until the supply of services meets the accepted payment price. However, the increasing penetration of renewable generation is increasing the requirement for short term balancing capacity on the grid (60 GW short term flexibility in the UK by 2030, National Infrastructure Commission, 2023), and therefore balancing markets will increase in size. In Dynamic Regulation and Dynamic Moderation, the *offset* and *export uncapped* scenarios also reach market saturation.

Of the three scenarios, the *export uncapped* scenario can be considered an upper bound to what could hypothetically be achieved in a perfectly efficient operation of surplus assets given
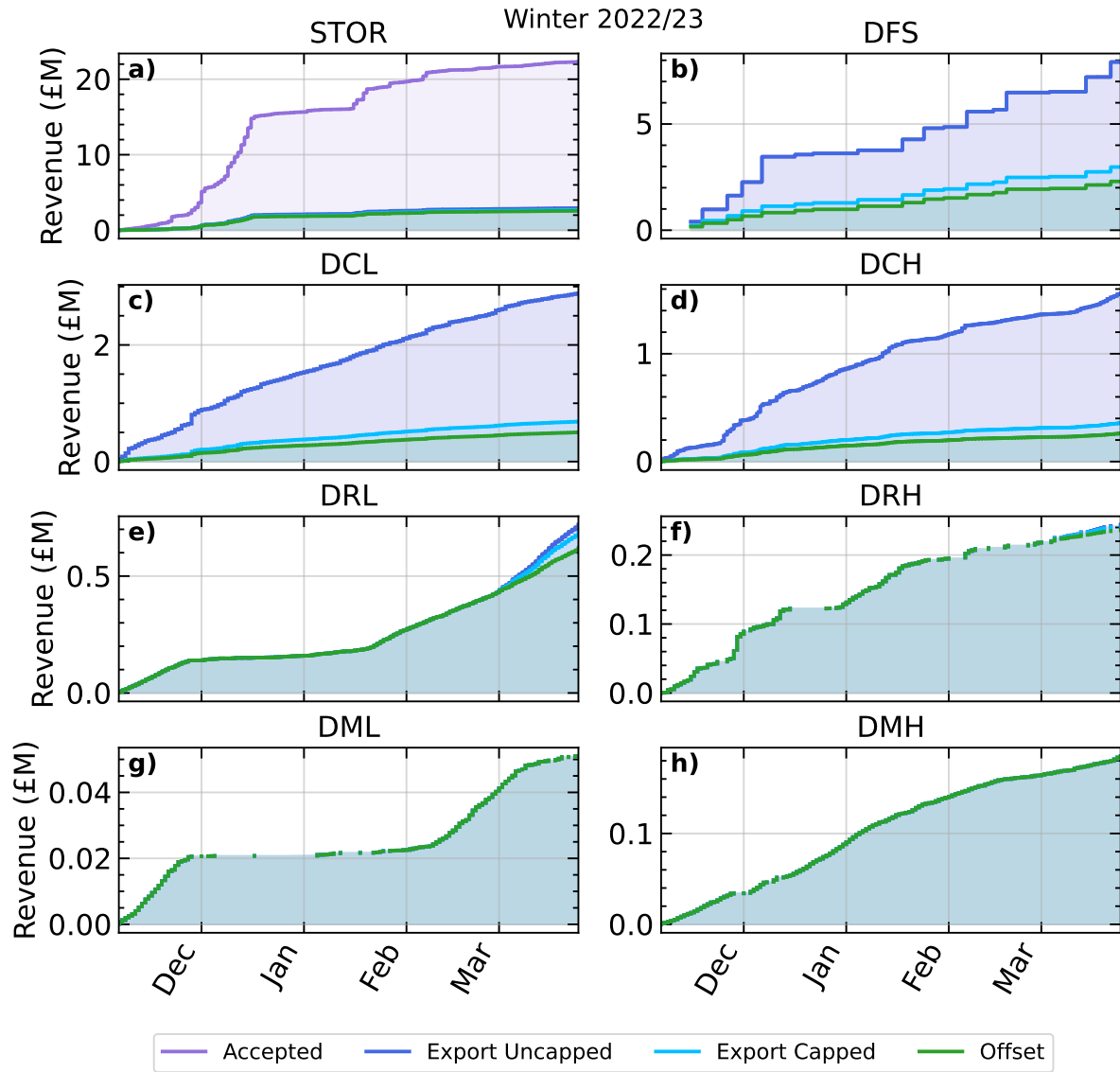
Figure 5.8: The cumulative value of balancing service payments for total capacity accepted at auction (*accepted*), and in separate simulated scenarios of using surplus capacity (*export uncapped*, *export capped*, and *offset*). Bids are simulated for the services: *Short Term Operating Reserve (STOR, panel a), Demand Flexibility Service (DFS, panel b), Dynamic Containment (Low frequency: DCL, panel c, High frequency: DCH, panel d), Dynamic Regulation (Low frequency: DRL, panel e, High frequency: DRH, panel f), and Dynamic Moderation (Low frequency, DML, panel g, High frequency: DRH).*

Surplus Value	Offset (GBP £/MWh)	(GBP £ M/15.6 GWh)	Export (capped) (GBP £/MWh)	(GBP £ M/15.6 GWh)	Export (capped) (GBP £/MWh)	(GBP £ M/15.6 GWh)
STOR	164.2	2.56	173.2	2.70	188.2	2.94
DFS	147.8	2.31	191.4	2.99	509.1	7.94
DCL	16.7	0.26	22.9	0.36	100.3	1.56
DCH	32.32	0.50	44.1	0.69	185.4	2.89
DRL	39.4	0.61	44	0.69	46.3	0.72
DRH	11.9	0.19	11.9	0.19	11.9	0.19
DML	3.3	0.05	3.3	0.05	3.3	0.05
DMH	15.2	0.24	15.6	0.24	15.7	0.24

Table 5.3: Extended Winter 2022/23 balancing service revenue from otherwise unutilised "surplus" capacity in reserve power systems. Simulated using recent UK contract results National Grid ESO (2024c). Results are displayed both in terms of income GBP £ with respect to reserve system size in MWh, and in alternative units of income GBP £ M with respect to the specific case study reserve capacity installed (15.6 GWh). STOR/DRL/DRH/DML/DMH are shaded-in as the simulation reached market saturation.

sufficiently upgraded equipment that facilitates large power export back to the grid.

Balancing services revenue for extended winter 2022/23 is shown in Table 5.3, rescaled with respect to total installed reserve capacity.

The value of surplus capacity represented in Figure 5.8 and Table 5.3 may appear relatively low compared to the cost of energy storage technologies, however, these numbers represent the value with respect to the total reserve system size (not just the surplus capacity). To engage in flexibility services, only a smaller portion of the built reserve system has to be capable of providing balancing services. i.e., due to infrastructure load constraints, or market saturation, there is greater return-on-investment in purchasing smaller quantities of energy storage capable of balancing services; if this capacity has a considerable capital cost (such as circa 350 GBP £/kWh for Lithium-Ion batteries, (Cole & Karmakar, 2023)), then overbuilding has a signifciant trade-off.

Consider a scenario where a reserve system operator is wishing to phase-out its legacy diesel reserve systems for a low carbon alternative. A viable approach could be a hybrid multi-stage phase-out. For example, 10 % of the reserve capacity could be initially built from lithium-ion battery energy storage, with the advantage of lower energy and operational costs, whilst the remaining 90 % is built from a long-term energy store (i.e. for already built reserve systems this could rely on existing legacy fossil fuel generators, with the aim to phase these out for low carbon technologies such as hydrogen fuel cells as technology costs are reduced). A hybrid

	Revenue (GBP £/kWh)	Return Rate (%/yr)
STOR	132.2	37.8
DFS	28.5	8.1
DCL	18.8	5.4
DCH	7.5	2.1
DRL	11.6	3.3
DRH	3.5	1.0
DML	1.9	0.5
DMH	3.9	1.1

Table 5.4: Maximum revenue rate (left column) and annualised return on investment (right colum). Maximum revenue rate is the initial gradient in Figure 5.9, i.e. the revenue with respect to installed capacity before market saturation or infrastructure constraints limit the potential revenue. STOR/DRL/DRH/DML/DMH are shaded-in as the simulation approached market saturation.

scenario brings the advantages of both the long-term energy stores (low-loss storage) and short-term stores (capable of uninterruptible power supply, potentially low-carbon, lower energy cost, and can benefit from surplus capacity revenue).

Figure 5.9 shows how the simulated cumulative revenue over the winter 22/23 period depends on the quantity of built short duration battery energy storage. A quantity (GWh) of 4-hour battery energy storage is built to provide both reserve power, and additionally to provide balancing services (as surplus capacity). This capacity is built in addition to the remaining required quantity of reserve capacity needed to ensure sufficient energy supplies are maintained during power outages. A return on investment (without discounting) can be calculated as ROI = revenue/capital cost, with rates shown in Table 5.4 (assuming a capital cost of 350 GBP £/kWh, Cole and Karmakar, 2023).

DFS achieves the highest return with a simulated annual revenue of 28.5 GBP £/kWh (an estimated 8.1 %/yr annualised return on investment), although in practice additional costs and limits to efficiency make this an upper bound estimate. Whilst STOR achieved significantly higher values, Figure 5.8 demonstrates an early market saturation and therefore these high returns will not be achieved in a competitive market.
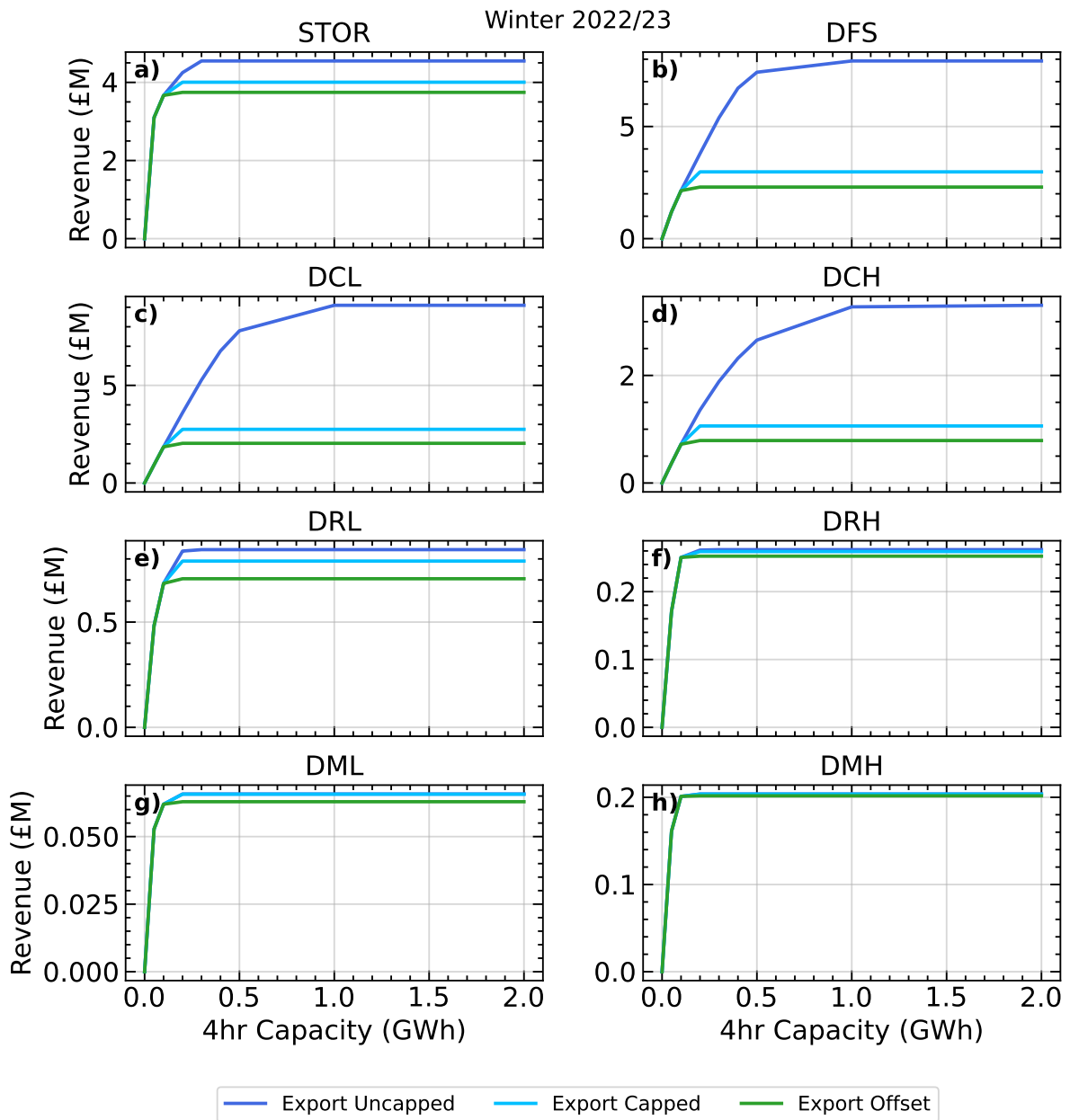
Figure 5.9: The cumulative value of balancing service payments, depending on the quantity of built 4-hour battery energy storage, in simulated scenarios of using surplus capacity (*export uncapped*, *export capped*, and *offset*). Bids are simulated for the services: *Short Term Operating Reserve (STOR, panel a), Demand Flexibility Service (DFS, panel b), Dynamic Containment (Low frequency: DCL, panel c, High frequency: DCH, panel d), Dynamic Regulation (Low frequency: DRL, panel e, High frequency: DRH, panel f), and Dynamic Moderation (Low frequency, DML, panel g, High frequency: DRH).*

5.4   Discussion and Conclusion

Electricity load in infrastructure is typically sensitive to temperature, and therefore in GB and similar mid-high latitude climates demonstrates significant seasonal variation as well as shorter timescale variability. Outside of periods of peak load, large quantities of surplus capacity are available but as yet unutilised. We have for the first time to the authors' knowledge explored the novel application of surplus capacity in reserve systems, using GB power system and infrastructure load modelled on meteorological inputs and a simulation of GB capacity and balancing services markets.

Utilising reserve systems (already required to protect infrastructure, but with significant seasonal variation in energy requirements) could accrue significant payments from both the capacity market (Table 5.2) and balancing services (Table 5.3). In the near future it may no longer be viable to operate legacy generators (including diesel systems), due to a misalignment with business environmental, social, and governance goals and net-zero strategy. Therefore, the return on investment made through surplus capacity represents revenue to recoup this necessary investment into infrastructure, and could also be considered in either investment decisions or by third part financers to support the uptake of low carbon reserve systems.

Compared to traditional *firm* capacity, surplus capacity is an otherwise unutilised asset, and therefore of significant value despite significant de-rating (81 % reduction in the *offset* scenario compared to control, and a lower bound of 8 % reduction in the *export uncapped* scenario), shown in Figure 5.5.

In this work, we have demonstrated that surplus as a capacity resource has a linear effect towards improving power system adequacy, measured through reduction in the quantity and severity of lost load events (Figure 5.6). Since changes are approximately linear (for scaling factors in the range 0 % to 400 %), derived de-rating factors are constant with respect to the size of the reserve system, even in the uptake of surplus capacity across multiple sectors (i.e. a greater than 100 % scaling size).

Therefore, in answer to RQ iii.1, we have demonstrated the value of a 'BT size' contirbution

of surplus capacity to the GB grid (in terms of de-rating factors), and that this result holds for any quantity of surplus capacity added to the GB power system (at least up until a greater than 400 % increase, at which point benefits start to saturate).

The estimated revenue in Figures 5.7 and 5.9 uses a static simulation of the balancing services market. For utility scale additions of surplus capacity (for example 0.5 GWh to 2.0 GWh from BT), engaging in a single balancing service has high return on investment up to a point of market saturation (approximately 0.1 GWh to 1 GWh of battery energy storage), but beyond this, the market is too saturated to bring significantly more revenue. Even though STOR has the highest return rate, the technology reaches market saturation relatively quickly (approximately 0.1 GWh to 0.2 GWh). The revenue gained from DFS, DCH/DCL frequency balancing benefit the most from building 0.5 GWh to 1 GWh, whilst other services provide an optimum return on investment at the lower end 0.1 GWh to 0.4 GWh. To fully benefit from balancing service payments for the present level of balancing services demand, it is necessary to diversify provisioned services.

In relation to RQ iii.2, we have shown the potential for high return on investment, from investment into surplus capacity up until market saturation. In the future, the market for flexibility services will be significantly larger (National Infrastructure Commission, 2023). The export-uncapped scenario is primarily limited by the balancing service market requested capacity (not physical constraints, as is the case in export-capped and offset). Therefore, in a hypothetical future market with larger capacity requirements, potential revenue scales linearly with built battery energy storage, up to market saturation (shown in Supporting Information, Figures S5.1 and S5.2).

The increasing weather sensitivity of national electricity demand due to electrification of heating is leading to greater inter- and intra-seasonal demand variability (Deakin et al., 2021; Peacock et al., 2023). The role of surplus capacity in improving system adequacy could be explored in future work in the context of heating electrification and other changes resulting from the decarbonisation of energy. Another pertinent area to study is the application of surplus capacity in alternative energy markets (that have different energy mixes) and in simulated future

scenarios (with increasing energy sector renewable energy penetration). As existing energy storage technologies are further developed and reduce in cost, and new technologies become available, further inspection of the technical characteristics constraints on surplus capacity and the potential return on investment of upgrading and decarbonising reserve systems could be investigated.

5.5 Supporting Information

5.5.1 BALANCING SERVICES RETURNS — INCREASED MARKET SIZE

A coarse simulation of surplus value in *future* markets is conducted using a scaled version of the 22/23 winter balancing bids, repeating Figure 5.9 for two hypothetical scenarios. With large projected increases in balancing capacity in energy markets, this simple demonstration can highlight the value constraints caused by a comparatively restricted flexibility services market.

Figures S5.1 and S5.2 shows the relationship between built capacity (of 4 h battery energy storage) and winter revenue, based on a scaled winter 22/23 scenario. The *offset* and *export-capped* scenarios are both constrained by infrastructure limitation. However, the *export-uncapped* scenario provides the most value, and revenue is expected to scale linearly up to a point of market saturation. For the DFS, and DCH frequency response, market saturation is increased from circa 0.5 GWh in Figure 5.9, doubling to 1.0 GWh in Figure S5.1, and is unconstrained in Figure S5.2.
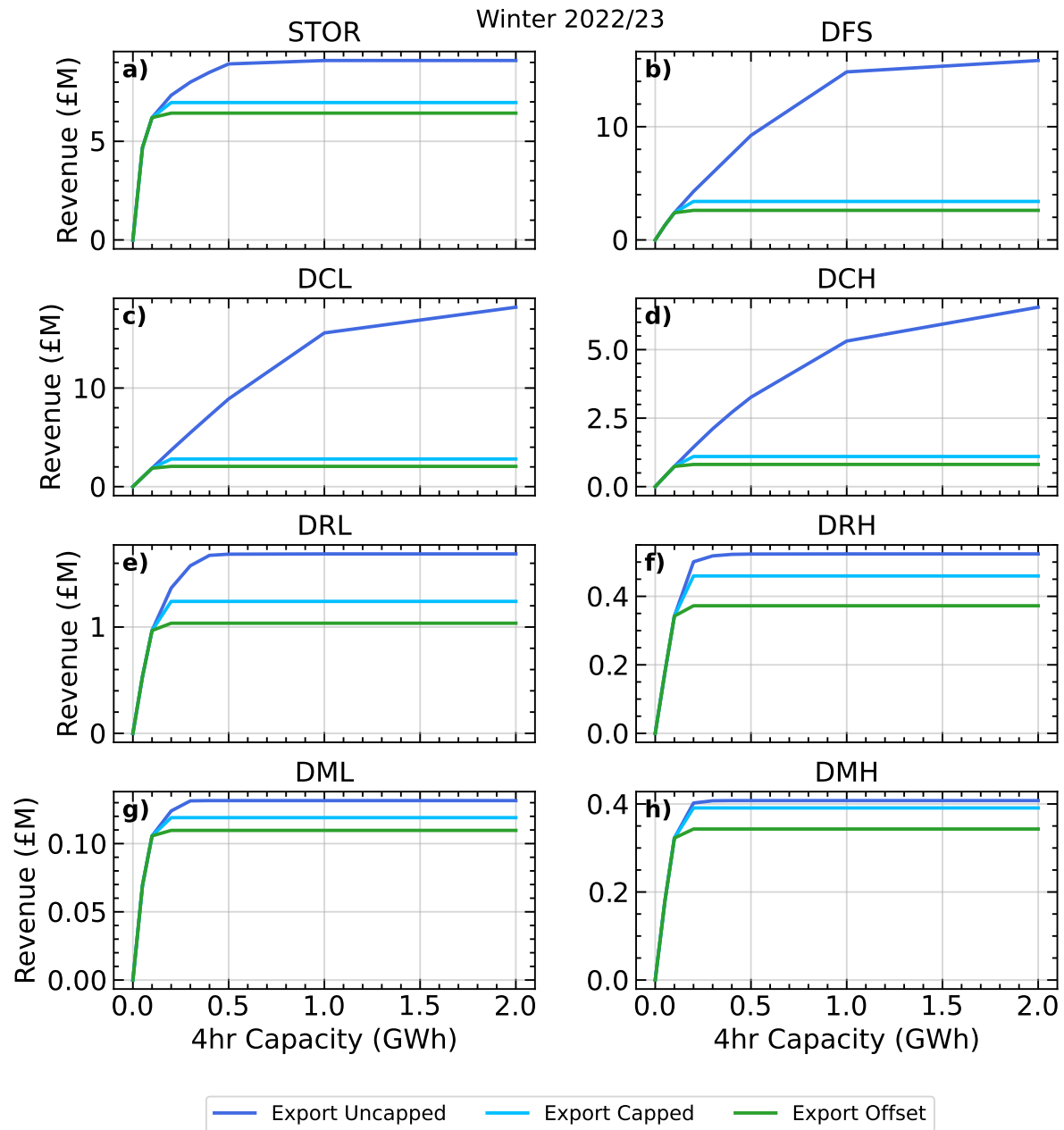
Figure S5.1:   The cumulative value of balancing service payments, depending on the quantity of built 4-hour battery energy storage. As in Figure 5.9, except the simulated winter 22/23 market size (procured capacity) has been doubled.
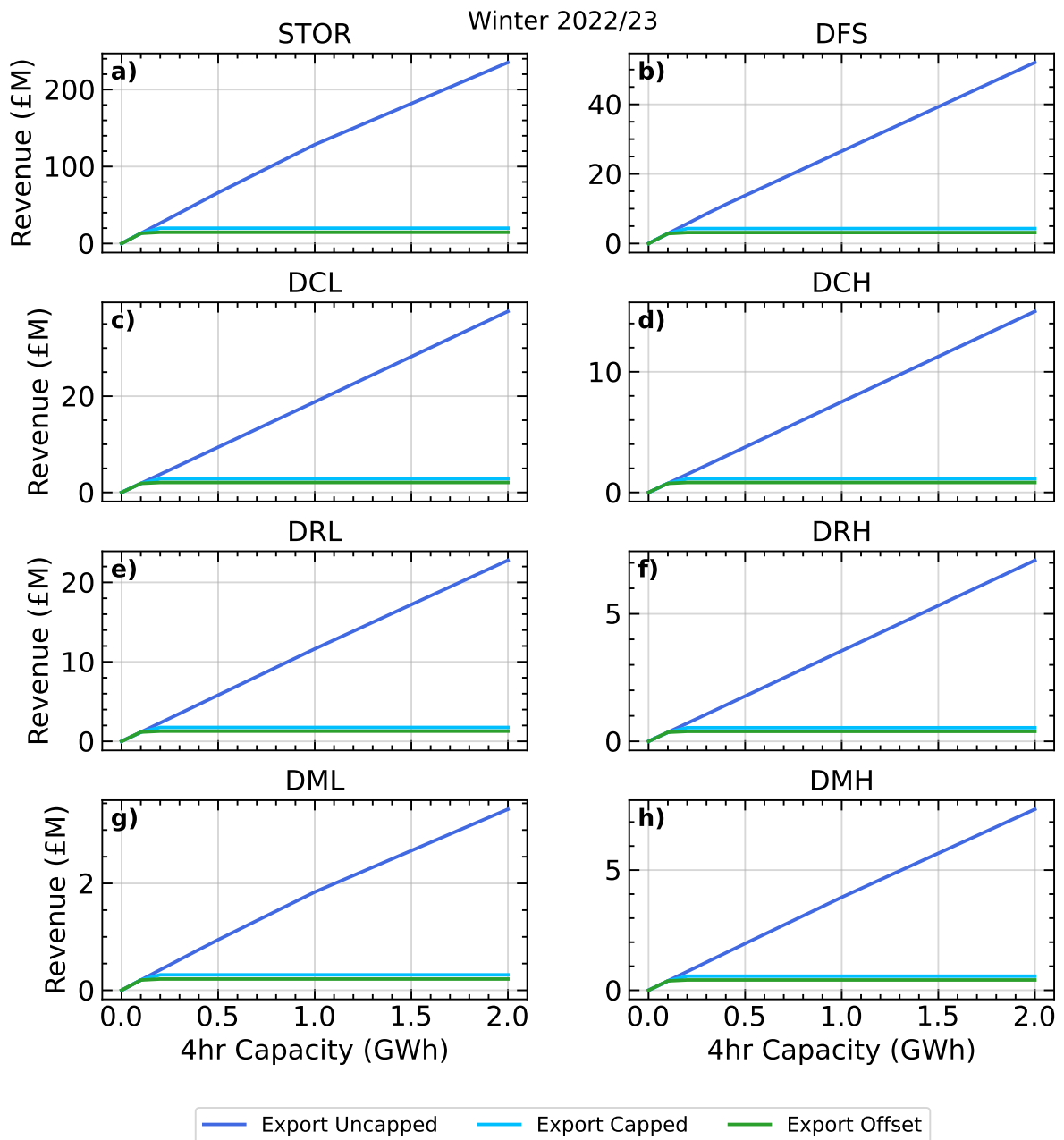
Figure S5.2: The cumulative value of balancing service payments, depending on the quantity of built 4-hour battery energy storage. As in Figure 5.9, except the simulated winter 22/23 market size (procured capacity) has been increased by factor 200 (a coarse upper estimate proxy for reaching a 60 GW scale flexibility services market).

Conclusion

6.1   Research Findings

Whilst the practice of modelling electricity demand with meteorological inputs is well established (as covered in Section 2.2.2), the application of infrastructure-specific models towards reserve power system design and operation has limited developed literature.

Identifying this gap, this thesis explores how meteorological datasets can support reserve system operators in meeting the challenges of resilient design. We address this both with the view towards managing weather-risk and climate-risk, and with an investigation into the potential role of surplus capacity being used to offset the capital cost of reserve system upgrade and support decarbonisation.

This investigation is divided into three research questions (as introduced in Section 1.1):

i Can weather-sensitive simulation of reserve power systems support resilient system design and furthermore characterise periods of surplus capacity? (Chapter 3)

ii To what extent can climate model simulations improve reserve power system design and quantify trends in surplus capacity? (Chapter 4)

iii Is it viable to (re)build reserve power systems to have a low carbon impact, paying for this investment through return of surplus power capacity to the wider grid? (Chapter 5)

A case study of BT GB infrastructure is used to explore temperature-driven electricity load modelled with different meteorological dataset inputs. Diverse weather sensitivities are explored for the data aggregated into Distribution Network Operator (DNO) regions. The case study is considered comparable to many other infrastructure and critical infrastructure including data centres and hospitals, and results hold relevance towards other similarly developed national electricity grids in countries with mid-latitude climates. Research findings using this model and case study are summarised in the sections below.

6.1.1 THESIS RQ I

The re-analysis driven simulation of electricity load reveals the probability distribution of electricity load across 14 DNO regions and in the GB region. We find that the size of the reserve capacity required in a given region, in order to ensure that 5-day (or other N-day) requirements can be met, is highly sensitive to the specified risk tolerance. This 'exceedance' risk is generally determined by weather in the warmest few months (peaking in July and August) in all but one region; the opposite behaviour is demonstrated in the North Scotland region, which exhibits predominantly heating-driven demand (and hence is sensitive to cold periods).

It was demonstrated that the strong temperature dependence in electricity load leads to predictable periods of surplus capacity (using only climatological knowledge). The quantity of surplus capacity that can be safely used can be further increased when periods of lower electricity load can be anticipated, requiring forecast knowledge of the temperature-driven and stochastic components of electricity load (although in practice, the latter may be difficult to anticipate).

A reserve power system operating in GB and with cooling-driven demand has significant potential to make surplus capacity available to the wider grid, for example, to provide balancing services. It is demonstrated that during winter periods, surplus can be stored up during low demand-net-wind periods and released during high demand-net-wind periods (i.e. making use of energy surpluses in the grid, and releasing power during periods of stress).

6.1.2 THESIS RQ II

The `UKCP18` Perturbed Physics Ensemble (PPE) is used to explore a representation of physical process uncertainty in climate. By conditioning results on the degree of global-mean warming (Shepherd, 2019; Mindlin et al., 2020), a set of physically self-consistent scenarios corresponds to a given global warming threshold (1.5 °C, 2.0 °C, etc.). This framing of model outputs constrains the representation of uncertainty to the regional dynamical response to climate change (and does not directly involve emissions pathways).

Another important aspect of interpreting climate model outputs is to identify possible inconsistency between the model world and real world. Three alternative bias adjustment approaches are compared alongside a delta-shift of re-analysis, to explore trade-offs and benefits in each case.

Quantile Delta Mapping (QDM) is a trend-preserving bias adjustment that corrects historical inconsistency in climate models. It is shown to provide a more convincing correction of historical inconsistency in `UKCP18`, compared with Quantile Mapping or mean bias adjustment.

A delta-shift approach is also applied to re-analysis, presented as a counter-factual pathway to plausible results and allowing us to distinguish between the results affected solely by 'average temperature shift' and the dynamical changes and new realisation of weather within each `UKCP18` PPE member. The delta-shift implements a representation of regional variability to mirror the `UKCP18` PPE (i.e. a collection of 12 shifts compound the global temperature rise with the different regional climate responses observed in each PPE member).

Delta-shift and QDM yield similar probability distributions of temperature and electricity load in the historic period. However, calculating the capacity requirements (a non-linear impact) yields significant differences with the different methods. Delta-shift generally gives results that closely match the re-analysis derived results used in Thesis RQ i, whilst the QDM methods results in significant differences across PPE members and greater overall capacity requirements.

This key finding highlights the sensitivity of the result to methodological choice, and to realised climate. It implies that relying only upon re-analysis as input may underestimate historic

weather and climate variability and its impact on reserve system design.

Scenarios of 1.5 °C, 2.0 °C, etc. global temperature rise share qualitatively consistent trends irrespective of method or PPE member: greater reserve power capacity is required in future to maintain currently tolerated levels of risk, although the exact level of capacity is sensitive to bias adjustment method and PPE member.

During the critical extended winter period (where grid demand-net-wind is highest), without upgrades to increase reserve system capacity the expected level of surplus capacity is maintained (slightly increasing due to a reduction in future Heating Degree Days). Levels of surplus capacity in other months (and especially summer months) are, however, expected to significantly reduce (due to a greater number and strength of Cooling Degree Days).

6.1.3   THESIS RQ III

The primary motivation for reserve power systems is to support infrastructure resilience. However, the capital cost of reserve systems can act as a barrier to building or upgrading. It is desirable to expand the use of reserve power systems to protect critical infrastructure and other valuable assets, especially in regions that experience frequent interruptions to power supply. To align with decarbonisation and air quality targets, new and existing systems should ideally be built using low carbon technologies, although this can increase capital costs.

Chapter 5 examines whether it would be viable to (re)build reserve systems now so that they have a low carbon impact and can pay for themselves through surplus capacity. Continuing with the case study of BT assets, we examine both the value of surplus capacity to the GB grid, and calculate a return on investment using simulated earnings from balancing services and the capacity market.

The benefit to the GB grid is determined by the de-rated capacity. The Transmission System Operator (TSO) will only make capacity market payments based on how the capacity performs if called upon to avert energy shortfall. The Energy Not Served (ENS) acts as a measure of energy shortfall, and we demonstrate that surplus capacity achieves significant improvement

to system adequacy indicated by a reduction in ENS.

The potential value of surplus capacity to the asset owner is simulated in the capacity market using a de-rating factor based on the Expected Energy Not Served, and recent capacity market auction results. Additional revenue from the balancing services market is also simulated, showing the greatest potential value in short term operating reserve and demand flexibility services. Balancing services revenue is limited by the finite size of the existing market and by scenario constrains (such as the offset constraint), although the value cap is anticipated to increase as the flexibility market expands.

Total revenue from capacity market and balancing service income is presented in terms of a return on investment, based on the assumption of a 4 h Lithium-Ion battery being purchased at current market value. Plausible returns of up to 8 % are estimated, however, this value is sensitive to assumptions on the future value and size of the balancing market.

Surplus capacity in reserve systems offers a desirable opportunity to asset owners and to the wider grid. Without increasing the risk to the asset owner, new revenue streams can be made available to support building and upgrading reserve systems, offsetting capital cost to investment and therefore supporting upgrades and a transition to low carbon technologies.

6.2 Synthesis

The use of large (multi-decade) datasets of meteorological variables supports an improved assessment of weather risk. Meteorological re-analyses used as an input to impact models are a good first step towards improving this assessment of risk, as demonstrated in Chapter 3 where the use of the gridded MERRA-2 surface temperature product supported modelling BT infrastructure load across 14 DNO regions. Application of climate models can improve the representation of climate variability (past) and support planning for future climate risk. We have established key methodological considerations for decision-makers, and the sensitivity of results to these choices. The value of surplus capacity has been assessed in the context of both the TSO and reserve owner. Rethinking the role of reserve power systems — using surplus

capacity — represents a win-win scenario.

Beyond the immediate applications to reserve systems, this research demonstrates the value of weather and climate information which can help inform long term planning and decision-making. This can support enhanced risk assessment, and therefore motivate infrastructure upgrades to mitigate risk, and support efficient infrastructure design. The costs of transitioning to low-carbon infrastructure (whether in the energy sector, agriculture, health care, or otherwise) and building climate resilience can be supported through these design efficiency improvements, and by identifying areas for win-win repurposing of assets (such as the surplus capacity concept).

Weather and climate information can bring significant value to many infrastructure operators, and this thesis has demonstrated this case for reserve power systems using meteorological re-analyses and climate models for data aggregated at DNO or national level. The value of meteorological information is dependent on the quality of observations, analysis, and predictions, and furthermore dependent upon our capabilities to correctly interpret, apply appropriate methods, and produce understandable, reliable results.

6.3 Future Investigations

6.3.1 IMPROVED MODEL AND DOWNSCALING

Whilst the model constructed in this thesis has been derived on aggregated data (DNO regions), the characteristics of electricity load at a smaller scale (smaller districts or individual asset locations) may differ. For practical application of the methods outlined in this thesis (for reserve system design, and identifying surplus capacity), a decision-maker must consider the effect of downscaling on results.

Gridded weather and climate data products could be used to construct a high-spatial-resolution impact model of infrastructure electricity load, allowing assessment of downscaling effects and exploring more localised problems (such as congestion management by DSOs). However,

even using very high-resolution re-analyses, some level of bias is likely to persist (including from collocation error, grid-box resolution constraints, urban effects) and needs to be treated appropriately.

Constructing models on site-resolved datasets may enable improved fitting of the model parameters, and incorporating additional variables (such as enthalpy latent heat, thermal inertia, wind chill, Section 2.2.2). Machine learning methods may be able to identify complex drivers of electricity load (for example taking on board qualities such as the type of server hardware, or office heating/cooling equipment in use).

With model improvements, it may be possible to reduce the magnitude of the stochastic model component (explaining some of the residual error through explainable meteorological or non-meteorological effects). If the additional variables contain some co-dependency (beyond the lag-1 autocorrelation already measured and accounted for), this could alter the probability distribution tail end of modelled electricity load, impacting the risk-capacity sensitivity and therefore affecting system design results.

6.3.2 EXTREME VALUES

Statistical downscaling may support an improved assessment of extreme event risk for infrastructure (Katz et al., 2002) for gridded or site-specific impact models.

To anticipate climate change impacts, Chapter 4 uses bias-adjusted climate model PPE outputs to simulate future reserve system operation and design requirements under physically consistent scenarios relating to a given planning decision and global temperature threshold. Climate models present different ranges of climate sensitivity, an uncertainty that has been intentionally circumvented using the temperature threshold scenarios. However, the sample of model members could be increased by repeating Chapter 4 results using datasets such as EURO-CORDEX and CMIP6, and could affect results by expanding (or constraining) the perceived risk-uncertainty for a given planning decision and temperature threshold.

PPE or multi-model approaches do not permit a probabilistic assessment of extreme values

across model members (only within each model member). To increase the sample of extreme events, one could implement a single model large ensemble (Section 2.3.2.5). For critical infrastructure with low risk-tolerance, it could be valuable to model these upper-tail events and the impact on reserve system design.

6.3.3 STORYLINES

The UKCP18 PPE projections exhibit substantial uncertainty. The approaches employed in Chapter 4 permit decision-makers to consider plausible outcomes for a given decision and a global scale thermodynamic climate indicator (global temperature threshold). However, introducing more degrees of freedom into the storyline could be beneficial to decision-makers (with the increased complexity of decision-making when considering more scenarios compensated by a constrained uncertainty in each considered storyline).

For example, Harvey et al. (2023) introduce the North Atlantic jet storyline, associated with dynamical changes of atmospheric circulation instead of the thermodynamic changes considered by the global temperature thresholds. This approach can facilitate a more focussed communication of uncertainty for UK and northern-Europe climate impacts under a range of global temperature scenarios.

The risk assessments conducted in this thesis are univariate and sensitive to temperature. However, many hazardous situations relate to compound events (for example, the risk of a reserve power system failing could overlap with a wildfire event). Therefore, risk assessments should be conducted to resolve compound extreme weather and climate events, for example, by applying this model in parallel with simulations of other events that present hazards to a decision-maker (Zscheischler et al., 2018).

Some infrastructure asset owners may operate over a large (multi-national) domain. Regional climate responses could vary with latitude and may not be zonally symmetric (Mindlin et al., 2020). Therefore, the potential co-variability in regional climate impacts be considered.

6.3.4 INDUSTRY TRIALS

This research work has established the theoretical science basis for reserve system design and operating surplus capacity. A useful next step is to establish case studies and support adoption by industry.

An initial starting point would be to establish potential industry partner needs, decision-making practices, and risk-reward approaches (Halford, 2019). In order to convince an industry partner to adopt these methods, it is necessary to communicate benefits (i.e. improved weather-risk assessment, or new revenue streams from surplus capacity), and establish trust and confidence in results.

Additional market simulations of balancing services revenue (with site-specific models, Section 6.3.1) could help constrain near-future and long-term estimates for the value of surplus capacity. The impact of increased Heating Degree Day effect in future winters (due to heat electrification) could be explored for the effect on increasing the value of surplus capacity (Deakin et al., 2021; Peacock et al., 2023).

Chapter 3 demonstrated that greater quantities of surplus capacity can be provisioned using weather forecast information (instead of relying on climatology). Supporting reserve owners with estimated reserve requirements days to weeks ahead (using operational and S2S forecasts, introduced in Section 2.3.2) could increase confidence both towards maintaining the primary function of the reserve system (ensuring that expendable supplies are maintained for the determined target length of time) and additionally by maximising the value of the surplus capacity. Research into the feasibility of operational and S2S decision-making could employ hindcasts to investigate both the skill and value.

Epilogue

Earth is on fire. Ocean acidification, desertification, biodiversity loss, nitrogen and phosphorous loading, and climate change are some symptoms of a rift between self-sustaining ecosystems and an extractive industrialised society. The sixth mass extinction has already started, and it is too late to entirely reverse much of the damage already caused to our home. However, stabilising the climate, reversing land conversion trends, eliminating pollutants, and fostering the restoration of nature remains within reach, if we as a society want it.

The research explored in this PhD thesis relates to climate impact modelling, and towards more efficiently using energy infrastructure. This work is motivated by the aim to provide benefits to society, as well as contribute to scientific knowledge. This epilogue chapter is a follow-up to the thesis research chapters, and explores the assumptions that we may hold on how academia does and should function.

7.1   System Change?

In a world with such incredible scientific advances and technological developments, society should be enjoying a shared wealth and prosperity. So why are communities needing to band together donations so that fewer people miss meals? Why are fossil fuel companies receiving tax breaks whilst they break climate accords? Why are the rich getting richer, whilst almost one billion people have no reliable access to electricity?

Ingrained in discussions addressing climate change is the notion that this is a problem that "we"

must address. However, this seemingly innocuous use of the word "we" has a powerful effect on shaping the climate change narrative. It draws attention away from the actually powerful people and corporations, absolving them of responsibility for causing climate change, and directs our efforts inwards to individual actions.

In neoliberal ideology, people and communities get redefined as consumers and demographics. Terms such as "the market" sound natural and unquestionable — like the laws of thermodynamics — but work to diminish corporate responsibility.

In this framing, market forces are inevitable flows of finance that deliver value to society. Profit made by 'rational' investors is a fair reimbursement for investment risk, and will anyway trickle down to the rest of society. The language of the free market is reinforced as a dominant social paradigm by the communications teams and think tanks that represent its beneficiaries. In this ideological framework we lose our own capacity to take collective responsibility and action. We think of our role in an individualistic and apolitical sense: we should have faith in our social leaders (including politicians) to act in good faith. To prevent climate collapse, we just need to 'do our bit' to help planet Earth (e.g. recycle more and cycle to work).

Saltmarsh (2021) describes how green capitalism adopts individualistic messaging and makes ideas such as the carbon footprint central to advertising campaigns so that consumers can feel good purchasing their product. Green capitalism follows in the footsteps of rainbow capitalism, feminist capitalism, and anti-racist capitalism in co-opting slogans and the feel-good power of doing something whilst taking no active part in addressing ongoing struggles and campaigns. Bode (2013) discusses inadequacies in models for corporate responsibility programmes for people employed in the garment industry: corporations claim to be producing clothes 'ethically', but to actually address and improve the social and economic situations of their employees there is a need to address structural power imbalances and confront neoliberalism.

It is not exactly a coincidence that the 'carbon footprint' was first introduced by fossil fuel giant BP (Kaufman, 2020). Of course, our own individual role in society and our interactions with the natural world do matter (and this is part of the reason the carbon footprint is such a successful idea), but the intention of the messaging is always to place responsibility on the

individual, whilst large businesses and multinationals continue to plunder our planet for natural resources and exploit communities (much more so in the Global South) for short-term profit.

Adjusting our 'consumer' behaviour is not going to by itself fix systemic issues that underpin environmental breakdown, social injustices, and other crises of the modern era. Real change from our society, approaching anything close to proportionate levels of scale and urgency, requires confronting our economic systems, and to ask what an actually democratic, equitable, and sustainable society should look like.

At the policy level, intervention into climate and ecological collapse, and building progress towards sustainable development, is hindered by an unwillingness to engage in open, scientific monitoring and modelling of progress.

Some attempts to engage communities in decision-making processes and social monitoring are met with growing dissent, dissatisfaction, and disagreement. Progress monitoring is often marred by unequal power structures and an unwillingness to adjust what kinds of assessments are made (Kaika, 2017). Economic models of climate change and development frequently employ a reductionist neoliberal understanding of social change, instead prioritising technological and market-based solutions (Forster et al., 2020), and make unjustified simplifications that have drastically underestimated the potential impact of climate change to economies (Keen, 2021).

Over 400 academics and organisations have signed an open letter calling for a post-growth 'well-being' cooperation (Parrique et al., 2023). There is no empirical basis to believe that economic growth can be decoupled from environmental pressures; instead alternative economic models should be explored (Hickel, 2021). Raworth (2017) proposes a framework to meet social well-being without exceeding planetary boundaries. Slameršak et al. (2024) find that lower growth scenarios make it more feasible to achieve the Paris accord's $1.5\,^\circ$C to $2.0\,^\circ$C limit, although acknowledge that this would still require an extremely ambitious and rapid decarbonisation effort and scaling up of efficiency improvements, equivalent to the whole world adopting and achieving European Union Green Deal decarbonisation targets.

So in the face of overlapping crises and the urgent need for political intervention, how do we overhaul society and reach our aims of an equitable and a post-growth, sustainable future?

Luckily, we are not starting from square one. There are many people globally who are actively engaged in building community resilience.

The youth-led Fridays for Future (FFF) network breaks away from environmental movements led by adults, which typically focus on policy reform. The 'Friday strikes for climate' learn from the activism of previous movements, including the Student Nonviolent Coordinating Committee of the US civil rights movement in the 1960s and 1970s. FFF highlight the voices of the most affected people and areas and young people, who will bear the brunt of climate change.

"

1. *Keep the global temperature rise below* 1.5 °C
   compared to pre-industrial levels.

2. *Ensure climate justice and equity.*

3. *Listen to the best united science currently available.*

"

400 climate activists from 38 countries, *Fridays for Future Declaration of Lausanne*, August 2019

The three demands of the FFF movement are rooted in decolonialism and therefore demand climate justice and equity. The reference to 1.5 °C is based on the stated aims of the Paris Agreement (UNFCCC. Secretariat, 2016). The final demand states explicitly that the first two demands should be reached through informed decision-making, based on scientific consensus.

These demands should not be seen as radical, but rather the bare minimum for a rational response to climate and ecological collapse.

7.2   Academia in the Climate Emergency

Studying for my PhD, I have experienced great unease attempting to rationalise my work as a researcher in a society that simultaneously supports a thriving class of millionaires and billionaires whilst poverty and injustice is not only rife but increasing (Christensen et al., 2023).

Foodbank use in the UK has risen 50 % since I began my PhD, now reaching almost 3 million people a year[1], and globally 122 million more people were pushed into hunger[2].

Energy prices have reached record highs, forcing some to choose between heating and eating, whilst generating record-breaking profits for fossil fuel companies. 675 million people lack access to electricity, and the annual access growth rate has fallen to stagnant levels of 0.6 %.

Many mental and physical health problems are on the rise, exacerbated by poverty. Many countries including the UK face an epidemic of political corruption. Misinformation, misogyny, and xenophobia are flourishing on various media platforms. Uncountable numbers of war crimes take place every day, war and genocide are live streamed around the world. A new acronym WCNSF introduced in Gaza describes a "wounded child, no surviving family". This should not be normal, and none of this is inevitable.

The role of the researcher is multi-faceted. A key task is communication; without disseminating knowledge into the wider scientific community and beyond, the value of research is diminished (and so are opportunities to apply for new funding).

Academics are usually motivated to ensure that academia benefits society, especially in cases where research has been publicly funded. Academia does not operate with an explicit theory of change, however, there is a prevailing assumption among academics that the information we produce will lead to society's leaders using this information effectively and for the public good.

A theory of change is a framework to understand how a series of actions can contribute to a

---

[1]https://www.statista.com/statistics/382695/uk-foodbank-users
[2]https://www.who.int/news/item/12-07-2023-122-million-more-people-pushed-into-hunger-since-2019-due-to-multiple-crises--reveals-un-report

series of results and intended impacts (Rogers, 2014). There are different ways of designing and representing a theory of change, dependent upon the context and scale being considered. A theory of change should be reviewed and revised in line with data collection, so that we can better achieve desired results and impacts. Several different 'levels' of theory of change analysis may be relevant to us (Stein & Valters, 2012), with macro theories (developing perspectives and thinking that influence us) to targeted or project-specific theories of change.

We may not always consider the implicit assumptions that motivate our work — space for these discussions might open up in more casual settings such as coffee break chats, if brought up at all. But in the work that we are actually funded to do there is not usually scope for this introspective work.

Without provisioned opportunity to consider the efficacy of the science-to-decision-making pathway, we are susceptible to our own wishful thinking and may hold biased views of our actions as academics aligning with our desire for public good, without evidence to support this.

Two implicit theories of change that might describe assumptions commonly held by academics on the interaction between science and society are given below:

1. Disseminating information (to social leaders) will result in effective action (Gardner et al., 2021)

2. Warning society of dangers posed by not acting on this information will generate sufficient public pressure to force leaders to take action

Gardner et al. (2021) identify that academia appears to operate under an assumption: that if academics generate information, then societal leaders will take evidence-based effective action for public benefit. The second theory of change is an extension of this belief; that should the first process fail for some reason, then it is simply a matter of informing the public of the resulting danger which will in turn lead to sufficient public pressure to force leaders to act.

Both of these theories take the naïve view that the decision-making of societal leaders is always solely evidence based. Societal leaders, however, do not always listen to scientists. In social

democracies, policy and political decision-making can be affected by lobbying, election-cycle pacification, corruption, misinformation, and other confounding factors.

Lobbying by oil and gas companies is so commonplace as to appear as an entirely normal and acceptable practice (Carlile, 2023; *Fossil Fuels*, 2024). A more powerful and troublesome disruption to the efficacy of scientific knowledge dissemination as an intervention is the potential for state capture, (Dávid-Barrett, 2023), that is, political corruption in which private capital significantly influences state decision-making. The Democracy Index 2022 identifies almost half of the world population as living in nations with political leaders pursuing state capture (Economist Intelligence Unit, 2023).

In the absence of effective leadership in theory of change 1, a democracy relies on the public to intervene. In this theory, scientists appeal to the wider public and communicate the urgency of an issue, in order to generate pressure that catalyses action.

This second theory is reliant upon the media to disseminate scientific findings to society, ensuring that urgent issues are picked up on. The influence of capital and incumbent powers can take the form of an explicit intervention, for example, misinformation disruption tactics of denial and delay have been used by fossil fuel companies (and their think tanks) (Supran et al., 2023). But even without overt coercion, modern mass media can support an 'effective and powerful' system-supportive propaganda function (Herman & Chomsky, 1988). e.g. A news programme that is part of a billionaire-owned media conglomerate and supported by ad breaks for SUVs and weekend airline getaways is not well positioned to communicate the climate and ecological emergency.

So academics should consider how our work is used by policy-makers (theory of change 1) and by society (theory of change 2). If we want our work to support equitable, democratic decision-making, we must understand our implicit theories of change and re-evaluate how we want our work to be acted upon.

Attempting to hold onto the false theories of change may not just be ineffective (towards our aims of academia benefiting society); it makes us complicit in political failings.

Considering socially and politically ambitious futures, such as post-growth scenarios, could play an important role in addressing the root causes of climate and global justice issues. A more capable spectrum of radical interventions must complement palliative measures and hopeful messaging. This requires us to consciously position our expertise and our research within the context of capitalist, exploitative and extractive systems that are root drivers of climate change (Morrison et al., 2022). In other words, *ask not what you can do for academia, but what academia can do for the world.*

Accompanying Published Datasets

Telecoms Electricity Load Model (Re-analysis)

A dataset to accompany Chapter 3 containing model code and coefficients for use with re-analysis has been published on the University of Reading Research Data Archive and may be referenced with the following citation:

Fallon, J. C., Brayshaw, D. J., Methven, J., Jensen, K., Krug, L., 2024: MERRA2 derived time series of GB telecommunications infrastructure electricity load, using historical daily surface temperature. *University of Reading, Dataset,* 10.17864/1947.000533

Telecoms Electricity Load Model (Re-analysis Delta-shift)

A dataset to accompany Chapter 4 and Chapter 5 for using re-analysis with delta-shift to simulate climate impacts to infrastructure electricity load has been published on the University of Reading Research Data Archive and may be referenced with the following citation:

Fallon, J. C., Brayshaw, D. J., Methven, J., Jensen, K., Krug, L., 2024: Model of GB telecommunications electricity load using meteorological re-analysis and temperature delta-shift. *University of Reading, Dataset,* 10.17864/1947.001338

Telecoms Electricity Load Model (UKCP18)

A dataset to accompany Chapter 4 for using UKCP18 climate model outputs to simulate infrastructure electricity load has been published on the University of Reading Research Data Archive and may be referenced with the following citation:

Fallon, J. C., Brayshaw, D. J., Methven, J., Jensen, K., Krug, L., 2024: Model of GB telecommunications electricity load using meteorological UKCP18 climate projections. *University of Reading, Dataset,* 10.17864/1947.001339

TEMPERATURE CORRELATION
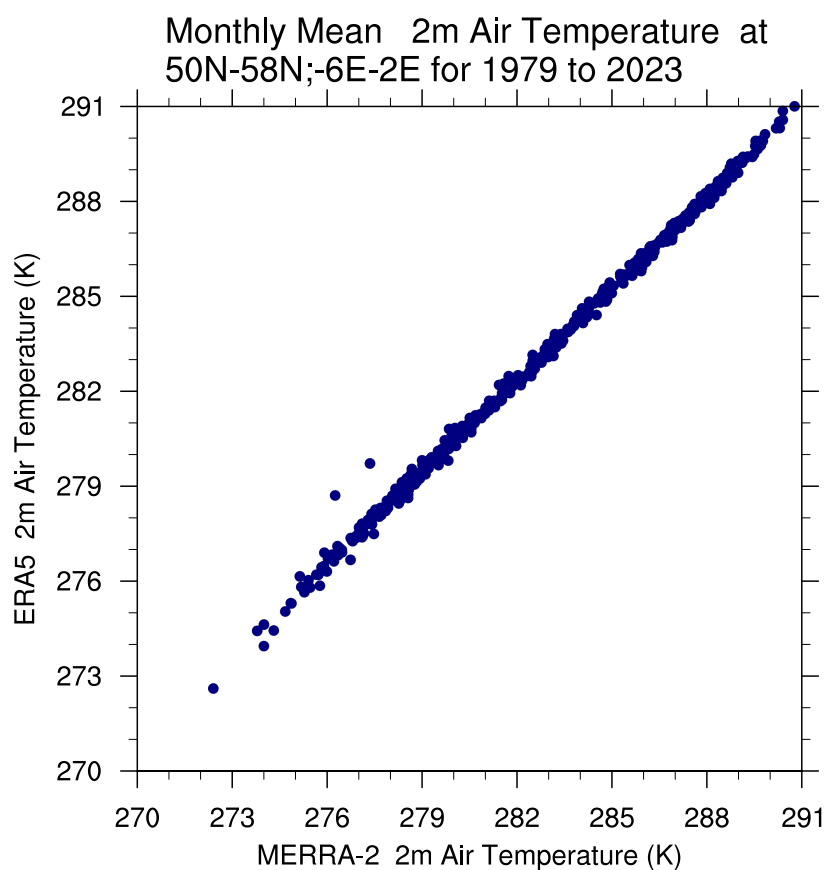
Figure B.1: Monthly Mean surface temperature (2 m air temperature) over a GB grid-box, comparing `MERRA-2` and `ERA5`. Correlation is 0.99890 and RMS Difference is 0.4281. Image provided by the NOAA-ESRL Physical Sciences Laboratory, Boulder Colorado from their Web site at https://psl.noaa.gov.

Bibliography

Abbe, C. (1901). The physical basis of long-range weather forecasts. *Monthly Weather Review*, *29*(12), 551–561.

Abbott, P., Rafaeli, G., Shazar, Y., & Cherpak, E. (2018, November 6). *European Resilience Management Guidelines*. Retrieved March 15, 2024, from https://cordis.europa.eu/project/id/653260/results

Aldersey-Williams, J., & Rubert, T. (2019). Levelised cost of energy – A theoretical justification and critical assessment. *Energy Policy*, *124*, 169–179. https://doi.org/10.1016/j.enpol.2018.10.004

Andrews, J., & Jelley, N. (2022). *Energy science: Principles, technologies, and impacts*. Oxford university press.

Añel, J. A., Pérez-Souto, C., Bayo-Besteiro, S., Prieto-Godino, L., Bloomfield, H. C., Troccoli, A., & Torre, L. D. L. (2024). Extreme weather events and the energy sector in 2021. *Weather, Climate, and Society*. https://doi.org/10.1175/WCAS-D-23-0115.1

Antweiler, W., & Müsgens, F. (2024, January 22). *The New Merit Order: The Viability of Energy-Only Electricity Markets With Only Intermittent Renewable Energy Sources and Grid-Scale Storage*. https://doi.org/10.2139/ssrn.4702939

Arnell, N. W., Freeman, A., Kay, A. L., Rudd, A. C., & Lowe, J. A. (2021). Indicators of climate risk in the UK at different levels of warming. *Environmental Research Communications*, *3*(9), 095005. https://doi.org/10.1088/2515-7620/ac24c0

Avgerinou, M., Bertoldi, P., & Castellazzi, L. (2017). Trends in Data Centre Energy Consumption under the European Code of Conduct for Data Centre Energy Efficiency. *Energies*, *10*(10), 1470. https://doi.org/10.3390/en10101470

Bauer, P., Thorpe, A., & Brunet, G. (2015). The quiet revolution of numerical weather prediction. *Nature*, *525*(7567), 47–55. https://doi.org/10.1038/nature14956

Baur, F. (1949). Musterbeispiele europäscher Großwetterlagen. Einführung in die Großwetterkunde (H. Flohn). *Zeitschrift Naturforschung Teil A*, *4*, 79.

Beccali, M., Cellura, M., & Ardente, D. (1998). Decision making in energy planning: The ELECTRE multicriteria analysis approach compared to a FUZZY-SETS methodology. *Energy Conversion and Management*, *39*(16), 1869–1881. https://doi.org/10.1016/S0196-8904(98)00053-3

Beerli, R., & Grams, C. M. (2019). Stratospheric modulation of the large-scale circulation in the Atlantic–European region and its implications for surface weather events. *Quarterly Journal of the Royal Meteorological Society*, *145*(725), 3732–3750. https://doi.org/10.1002/qj.3653

Bessec, M., & Fouquau, J. (2008). The non-linear link between electricity consumption and temperature in Europe: A threshold panel approach. *Energy Economics*, *30*(5), 2705–2721. https://doi.org/10.1016/j.eneco.2008.02.003

Bessembinder, J., Terrado, M., Hewitt, C., Garrett, N., Kotova, L., Buonocore, M., & Groenland, R. (2019). Need for a common typology of climate services. *Climate Services*, *16*, 100135. https://doi.org/10.1016/j.cliser.2019.100135

Betts, R. A., Belcher, S. E., Hermanson, L., Klein Tank, A., Lowe, J. A., Jones, C. D., Morice, C. P., Rayner, N. A., Scaife, A. A., & Stott, P. A. (2023). Approaching 1.5 °C: How will we know we've reached this crucial warming mark? *Nature*, *624*(7990), 33–35. https://doi.org/10.1038/d41586-023-03775-z

Bevacqua, E., Suarez-Gutierrez, L., Jézéquel, A., Lehner, F., Vrac, M., Yiou, P., & Zscheischler, J. (2023). Advancing research on compound weather and climate events via large ensemble model simulations. *Nature Communications*, *14*(1), 2145. https://doi.org/10.1038/s41467-023-37847-5

Billington, N. S. (1966). Estimation of annual fuel consumption. *Journal of the Institution of Heating Ventilating Engineers*, *34*(5), 253–256.

Bjerknes, V. (1904). Das Problem der Wettervorhersage, betrachtet vom Standpunkte der Mechanik und der Physik. *Meteorologische Zeitschrift*, *21*, 1–7.

Blat Belmonte, B., Mouratidis, P., Franke, G., & Rinderknecht, S. (2023). Developments in the cost of grid balancing services and the design of the European balancing market. *Energy Reports*, *10*, 910–931. https://doi.org/10.1016/j.egyr.2023.07.045

Bloomfield, H. C., Brayshaw, D. J., Shaffrey, L. C., Coker, P. J., & Thornton, H. E. (2016). Quantifying the increasing sensitivity of power systems to climate variability. *Environmental Research Letters*, *11*(12), 124025. https://doi.org/10.1088/1748-9326/11/12/124025

Bloomfield, H. C., Gonzalez, P. L. M., Lundquist, J. K., Stoop, L. P., Browell, J., Dargaville, R., Felice, M. D., Gruber, K., Hilbers, A., Kies, A., Panteli, M., Thornton, H. E., Wohland, J., Zeyringer, M., & Brayshaw, D. J. (2021). The Importance of Weather and Climate to Energy Systems: A Workshop on Next Generation Challenges in Energy–Climate Modeling. *Bulletin of the American Meteorological Society*, *102*(1), E159–E167. https://doi.org/10.1175/BAMS-D-20-0256.1

Bloomfield, H. C., Brayshaw, D. J., & Charlton-Perez, A. J. (2020). Characterizing the winter meteorological drivers of the European electricity system using targeted circulation types. *Meteorological Applications*, *27*(1), e1858. https://doi.org/10.1002/met.1858

Bloomfield, H. C., Brayshaw, D. J., & Charlton-Perez, A. J. (2020). *MERRA2 derived time series of European country-aggregate electricity demand, wind power generation and solar power generation*. University of Reading. https://doi.org/10.17864/1947.239

Bloomfield, H. C., Brayshaw, D. J., Deakin, M., & Greenwood, D. (2022). Hourly historical and near-future weather and climate variables for energy system modelling. *Earth System Science Data*, *14*(6), 2749–2766. https://doi.org/10.5194/essd-14-2749-2022

Bloomfield, H. C., Brayshaw, D. J., Gonzalez, P. L. M., & Charlton-Perez, A. J. (2021a). Sub-seasonal forecasts of demand and wind power and solar power generation for 28 European countries. *Earth System Science Data*, *13*(5), 2259–2274. https://doi.org/10.5194/essd-13-2259-2021

Bloomfield, H. C., Brayshaw, D. J., Gonzalez, P. L. M., & Charlton-Perez, A. J. (2021b). Pattern-based conditioning enhances sub-seasonal prediction skill of European national energy variables. *Meteorological Applications*, *28*(4), e2018. https://doi.org/10.1002/met.2018

Bloomfield, H. C., Wainwright, C. M., & Mitchell, N. (2022). Characterizing the variability and meteorological drivers of wind power and solar power generation over Africa. *Meteorological Applications*, *29*(5), e2093. https://doi.org/10.1002/met.2093

Bode, N. (2013). *Global Actors, Local Governance: Corporate Social Responsibility In The Indian Garment Industry* [BA thesis]. Leiden University. https://studenttheses.universiteitleiden.nl/access/item%3A2605128/view

Boorman, P., Troccoli, A., Bertocco, E., Boyer, W., Dubus, L., Cordeddu, S., Contreras, B., Correa, N., Hibbert, S., Nielsen, K., Obahoundje, S., Saravanan, S., Turrisi, G., & Walker, S. (2022). *Teal: A visualisation tool for non-expert users to explore climate data* (EMS2022-431). Copernicus Meetings. https://doi.org/10.5194/ems2022-431

Booth, J., & Wu, H. (2020). *UK Data Centres – Carbon Neutral by 2030?* UKERC. Retrieved March 22, 2024, from https://ukerc.ac.uk/news/uk-data-centres-carbon-neutral-by-2030

Boßmann, T., & Staffell, I. (2015). The shape of future electricity demand: Exploring load curves in 2050s Germany and Britain. *Energy*, *90*, 1317–1333. https://doi.org/10.1016/j.energy.2015.06.082

Bovera, F., Delfanti, M., & Bellifemine, F. (2018). Economic opportunities for Demand Response by Data Centers within the new Italian Ancillary Service Market. *2018 IEEE International Telecommunications Energy Conference (INTELEC)*, 1–8. https://doi.org/10.1109/INTLEC.2018.8612440

Box, G. E. P. (1979). Robustness in the Strategy of Scientific Model Building. In R. L. Launer & G. N. Wilkinson (Eds.), *Robustness in Statistics* (pp. 201–236). Academic Press. https://doi.org/10.1016/B978-0-12-438150-6.50018-2

Box, G. E. P., Jenkins, G. M., Reinsel, G. C., & Ljung, G. M. (2015). *Time Series Analysis: Forecasting and Control* (5th ed.). Wiley. Retrieved January 13, 2024, from https:

//www.wiley.com/en-us/Time+Series+Analysis%3A+Forecasting+and+Control%2C+5th+Edition-p-9781118675021

Brayshaw, D. J. (2018). Weather, Climate and the Nature of Predictability. In A. Troccoli (Ed.), *Weather & Climate Services for the Energy Industry* (pp. 85–95). Springer International Publishing. https://doi.org/10.1007/978-3-319-68418-5_6

Brayshaw, D. J., Halford, A., Smith, S., & Jensen, K. (2020). Quantifying the potential for improved management of weather risk using sub-seasonal forecasting: The case of UK telecommunications infrastructure. *Meteorological Applications*, *27*(1), e1849. https://doi.org/10.1002/met.1849

Brayshaw, D. J., Hoskins, B., & Blackburn, M. (2011). The Basic Ingredients of the North Atlantic Storm Track. Part II: Sea Surface Temperatures. *Journal of the Atmospheric Sciences*, *68*(8), 1784–1805. https://doi.org/10.1175/2011JAS3674.1

Brayshaw, D. J., Troccoli, A., Fordham, R., & Methven, J. (2011). The impact of large scale atmospheric circulation patterns on wind power generation and its potential predictability: A case study over the UK. *Renewable Energy*, *36*(8), 2087–2096. https://doi.org/10.1016/j.renene.2011.01.025

Büeler, D., Beerli, R., Wernli, H., & Grams, C. M. (2020). Stratospheric influence on ECMWF sub-seasonal forecast skill for energy-industry-relevant surface weather in European countries. *Quarterly Journal of the Royal Meteorological Society*, *n/a*(n/a). https://doi.org/10.1002/qj.3866

Buizza, R., Milleer, M., & Palmer, T. N. (1999). Stochastic representation of model uncertainties in the ECMWF ensemble prediction system. *Quarterly Journal of the Royal Meteorological Society*, *125*(560), 2887–2908. https://doi.org/10.1002/qj.49712556006

Buontempo, C., Hutjes, R., Beavis, P., Berckmans, J., Cagnazzo, C., Vamborg, F., Thépaut, J.-N., Bergeron, C., Almond, S., Amici, A., Ramasamy, S., & Dee, D. (2020). Fostering the development of climate services through Copernicus Climate Change Service (C3S) for agriculture applications. *Weather and Climate Extremes*, *27*, 100226. https://doi.org/10.1016/j.wace.2019.100226

Burpee, H., & McDade, E. (2014). Comparative Analysis of Hospital Energy Use: Pacific Northwest and Scandinavia. *HERD: Health Environments Research & Design Journal*, *8*(1), 20–44. https://doi.org/10.1177/193758671400800104

Bush, M., Allen, T., Bain, C., Boutle, I., Edwards, J., Finnenkoetter, A., Franklin, C., Hanley, K., Lean, H., Lock, A., Manners, J., Mittermaier, M., Morcrette, C., North, R., Petch, J., Short, C., Vosper, S., Walters, D., Webster, S., … Zerroukat, M. (2020). The first Met Office Unified Model–JULES Regional Atmosphere and Land configuration, RAL1. *Geoscientific Model Development*, *13*(4), 1999–2029. https://doi.org/10.5194/gmd-13-1999-2020

Cabinet Office (UK). (2014). *Sector resilience plan 2014*. GOV.UK. Retrieved March 18, 2024, from https://www.gov.uk/government/publications/sector-resilience-plan-2014

Cabinet Office (UK). (2023). *National Risk Register 2023*. Retrieved March 18, 2024, from https://www.gov.uk/government/publications/national-risk-register-2023

Carlile, C. (2023). *Transparency Watchdog Calls on EU to Strengthen its Lobbying Rules After DeSmog Investigation*. DeSmog. Retrieved February 11, 2024, from https://www.desmog.com/2023/07/20/consumer-choice-center-eu-transparency-lobbying-rules

Casanueva, A., Herrera, S., Iturbide, M., Lange, S., Jury, M., Dosio, A., Maraun, D., & Gutiérrez, J. M. (2020). Testing bias adjustment methods for regional climate change applications under observational uncertainty and resolution mismatch. *Atmospheric Science Letters*, *21*(7), e978. https://doi.org/10.1002/asl.978

Cassou, C. (2008). Intraseasonal interaction between the Madden-Julian Oscillation and the North Atlantic Oscillation. *Nature*, *455*(7212), 523–527. https://doi.org/10.1038/nature07286

Chantry, M., Christensen, H., Dueben, P., & Palmer, T. (2021). Opportunities and challenges for machine learning in weather and climate modelling: Hard, medium and soft AI. *Philosophical Transactions of the Royal Society A: Mathematical, Physical and Engineering Sciences*, *379*(2194), 20200083. https://doi.org/10.1098/rsta.2020.0083

Charlton-Perez, A. J., Dacre, H. F., Driscoll, S., Gray, S. L., Harvey, B., Harvey, N. J., Hunt, K. M. R., Lee, R. W., Swaminathan, R., Vandaele, R., & Volonté, A. (2024, February

19). *Do AI models produce better weather forecasts than physics-based models? A quantitative evaluation case study of Storm Ciarán*. arXiv: 2312.02658 [physics]. https://doi.org/10.48550/arXiv.2312.02658

Charney, J. G., Fjörtoft, R., & Neumann, J. V. (1950). Numerical Integration of the Barotropic Vorticity Equation. *Tellus*. https://doi.org/10.3402/tellusa.v2i4.8607

Charney, J. G. (1948). On the scale of atmospheric motions. In *The Atmosphere—A challenge: The science of jule gregory charney* (pp. 251–265). Springer.

Chatfield, C. (2003). *The analysis of time series: An introduction*. Chapman and hall/CRC.

Chawla, S., Kurani, S., Wren, S. M., Stewart, B., Burnham, G., Kushner, A., & McIntyre, T. (2018). Electricity and generator availability in LMIC hospitals: Improving access to safe surgery. *Journal of Surgical Research*, *223*, 136–141. https://doi.org/10.1016/j.jss.2017.10.016

Chen, D., Rojas, M., Samset, B. H., Cobb, K., Diongue Niang, A., Edwards, P., Emori, S., Faria, S. H., Hawkins, E., Hope, P., Huybrechts, P., Meinshausen, M., Mustafa, S. K., Plattner, G.-K., & Tréguier, A.-M. (2021). Technical Summary. In *Climate Change 2021 – The Physical Science Basis: Working Group I Contribution to the Sixth Assessment Report of the Intergovernmental Panel on Climate Change*. Cambridge University Press. https://www.cambridge.org/core/books/climate-change-2021-the-physical-science-basis/framing-context-and-methods/1F59D76B1C6876F25902D09A74C34634

Christensen, M.-B., Hallum, C., Maitland, A., Parrinello, Q., Putaturo, C., Abed, D., Brown, C., Kamande, A., Lawson, M., & Ruiz, S. (2023). *Survival of the Richest: How we must tax the super-rich now to fight inequality*. Oxfam. https://doi.org/10.21201/2023.621477

CISA. (2022). *Fact Sheet for Resilient Power Best Practices*. Retrieved March 23, 2024, from https://www.cisa.gov/sites/default/files/publications/Fact%20Sheet%20for%20Resilient%20Power%20Best%20Practices%20CISA%20v2.pdf

Clò, S., Cataldi, A., & Zoppoli, P. (2015). The merit-order effect in the Italian power market: The impact of solar and wind generation on national wholesale electricity prices. *Energy Policy*, *77*, 79–88. https://doi.org/10.1016/j.enpol.2014.11.038

Cludius, J., Hermann, H., Matthes, F. C., & Graichen, V. (2014). The merit order effect of wind and photovoltaic electricity generation in Germany 2008–2016: Estimation and distributional implications. *Energy Economics*, *44*, 302–313. https://doi.org/10.1016/j.eneco.2014.04.020

Coker, P. J., Bloomfield, H. C., Drew, D. R., & Brayshaw, D. J. (2020). Interannual weather variability and the challenges for Great Britain's electricity market design. *Renewable Energy*, *150*, 509–522. https://doi.org/10.1016/j.renene.2019.12.082

Cole, W., & Karmakar, A. (2023). *Cost Projections for Utility-Scale Battery Storage: 2023 Update* (NREL/TP-6A40-85332). Golden, CO: National Renewable Energy Laboratory. https://www.nrel.gov/docs/fy23osti/85332.pdf

Contreras, J., Espinola, R., Nogales, F., & Conejo, A. (2003). ARIMA models to predict next-day electricity prices. *IEEE Transactions on Power Systems*, *18*(3), 1014–1020. https://doi.org/10.1109/TPWRS.2002.804943

CPNI. (2021). *Critical National Infrastructure | Centre for the Protection of National Infrastructure*. Retrieved June 20, 2022, from https://www.cpni.gov.uk/critical-national-infrastructure-0

Craig, M. T., Wohland, J., Stoop, L. P., Kies, A., Pickering, B., Bloomfield, H. C., Browell, J., De Felice, M., Dent, C. J., Deroubaix, A., Frischmuth, F., Gonzalez, P. L., Grochowicz, A., Gruber, K., Härtel, P., Kittel, M., Kotzur, L., Labuhn, I., Lundquist, J. K., … Brayshaw, D. J. (2022). Overcoming the disconnect between energy system and climate modeling. *Joule*, *6*(7), 1405–1417. https://doi.org/10.1016/j.joule.2022.05.010

Cramton, P., Ockenfels, A., & Stoft, S. (2013). Capacity Market Fundamentals. *Economics of Energy & Environmental Policy*, *2*(2). https://doi.org/10.5547/2160-5890.2.2.2

Dávid-Barrett, E. (2023). State capture and development: A conceptual framework. *Journal of International Relations and Development*, *26*(2), 224–244. https://doi.org/10.1057/s41268-023-00290-6

De Felice, M., Alessandri, A., & Catalano, F. (2015). Seasonal climate forecasts for medium-term electricity demand forecasting. *Applied Energy*, *137*, 435–444. https://doi.org/10.1016/j.apenergy.2014.10.030

De Felice, M., Alessandri, A., & Ruti, P. M. (2013). Electricity demand forecasting over Italy: Potential benefits using numerical weather prediction models. *Electric Power Systems Research*, *104*, 71–79. https://doi.org/10.1016/j.epsr.2013.06.004

Deakin, M., Bloomfield, H. C., Greenwood, D., Sheehy, S., Walker, S., & Taylor, P. C. (2021). Impacts of heat decarbonization on system adequacy considering increased meteorological sensitivity. *Applied Energy*, *298*, 117261. https://doi.org/10.1016/j.apenergy.2021.117261

Deakin, M., & Greenwood, D. (2022). *Aggregated Generator Unavailability Data for Northwest European Countries*. Newcastle University. https://doi.org/10.25405/data.ncl.18393971.v1

Deakin, M., Greenwood, D., Brayshaw, D. J., & Bloomfield, H. C. (2022). Comparing Generator Unavailability Models with Empirical Distributions from Open Energy Datasets. *2022 17th International Conference on Probabilistic Methods Applied to Power Systems (PMAPS)*, 1–6. https://doi.org/10.1109/PMAPS53380.2022.9810629

Dempsey, H., & White, E. (2023). *China's battery plant rush raises fears of global squeeze*. Financial Times. Retrieved February 15, 2024, from https://www.ft.com/content/b6038e51-7b5b-4f97-a5da-9202e71562fc

Department for Business, Energy & Industrial Strategy. (2020). *Electricity Generation Costs 2020*. London.

Department for Business, Energy & Industrial Strategy. (2022). Historical electricity data: 1920 to 2021.

Department for Business, Energy & Industrial Strategy & Ofgem. (2021). *Transitioning to a net zero energy system: Smart Systems and Flexibility Plan 2021*. London.

Department for Business, Energy & Industrial Strategy & Ofgem. (2022). *Smart Systems & Flexibility Plan Forum - March 2022*. Retrieved January 25, 2024, from https://www.ofgem.gov.uk/publications/smart-systems-flexibility-plan-forum-march-2022

Department for Energy Security & Net Zero. (2023). *Capacity Market 2023: Phase 2 proposals and 10 year review*. GOV.UK. Retrieved November 19, 2023, from https://www.gov.uk/government/consultations/capacity-market-2023-phase-2-proposals-and-10-year-review

Department of Homeland Security. (2013). *National Infrastructure Protection Plan*. Retrieved March 15, 2024, from https://www.cisa.gov/resources-tools/resources/2013-national-infrastructure-protection-plan

Domeisen, D. I. V., White, C. J., Afargan-Gerstman, H., Muñoz, Á. G., Janiga, M. A., Vitart, F., Wulff, C. O., Antoine, S., Ardilouze, C., Batté, L., Bloomfield, H. C., Brayshaw, D. J., Camargo, S. J., Charlton-Pérez, A. J., Collins, D., Cowan, T., Chaves, M. d. M., Ferranti, L., Gómez, R., … Tian, D. (2022). Advances in the Subseasonal Prediction of Extreme Events: Relevant Case Studies across the Globe. *Bulletin of the American Meteorological Society*, *103*(6), E1473–E1501. https://doi.org/10.1175/BAMS-D-20-0221.1

Dorrington, J., Finney, I., Palmer, T., & Weisheimer, A. (2020). Beyond skill scores: Exploring sub-seasonal forecast value through a case-study of French month-ahead energy prediction. *Quarterly Journal of the Royal Meteorological Society*, *146*(733), 3623–3637. https://doi.org/10.1002/qj.3863

Dreidy, M., Mokhlis, H., & Mekhilef, S. (2017). Inertia response and frequency control techniques for renewable energy sources: A review. *Renewable and Sustainable Energy Reviews*, *69*, 144–155. https://doi.org/10.1016/j.rser.2016.11.170

Dubus, L., Saint-Drenan, Y.-M., Troccoli, A., De Felice, M., Moreau, Y., Ho-Tran, L., Goodess, C., Amaro e Silva, R., & Sanger, L. (2023). C3S Energy: A climate service for the provision of power supply and demand indicators for Europe based on the ERA5 reanalysis and ENTSO-E data. *Meteorological Applications*, *30*(5), e2145. https://doi.org/10.1002/met.2145

Dupačová, J., Hurt, J., & Štěpán, J. (2005). *Stochastic Modeling in Economics and Finance*. Springer Science & Business Media.

Dyer, M., Dyer, R., Weng, M.-H., Wu, S., Grey, T., Gleeson, R., & Ferrari, T. G. (2019). Framework for soft and hard city infrastructures. *Proceedings of the Institution of Civil Engineers - Urban Design and Planning*, *172*(6), 219–227. https://doi.org/10.1680/jurdp.19.00021

ECMWF. (2024). *Lead time of anomaly correlation coefficient reaching multiple thresholds (High resolution 500 hPa height forecasts)*. ECMWF | Charts. Retrieved July 30, 2024, from https://charts.ecmwf.int/products/plwww_m_hr_ccaf_adrian_ts?single_product=latest

Economist Intelligence Unit. (2023). *Democracy Index 2022: Frontline democracy and the battle for Ukraine*. London. Retrieved February 11, 2024, from https://www.eiu.com/n/wp-content/uploads/2023/02/Democracy-Index-2022_FV2.pdf

Edmunds, C., Galloway, S., Elders, I., Bukhsh, W., & Telford, R. (2020). Design of a DSO-TSO balancing market coordination scheme for decentralised energy. *IET Generation, Transmission & Distribution*, *14*(5), 707–718. https://doi.org/10.1049/iet-gtd.2019.0865

ENTSO-E. (2019). *Mid-term Adequacy Forecast 2019*. Brussels. Retrieved March 23, 2024, from https://www.entsoe.eu/outlooks/midterm

ENTSO-E. (2023). ENTSO-E Future of our Grids: Accelerating Europe's energy transition. Retrieved March 28, 2024, from https://www.entsoe.eu/eugridforum

Eskeland, G. S., & Mideksa, T. K. (2010). Electricity demand in a changing climate. *Mitigation and Adaptation Strategies for Global Change*, *15*(8), 877–897. https://doi.org/10.1007/s11027-010-9246-x

European Commission Internal Energy Market. (2018). *Study on the quality of electricity market data of transmission system operators, electricity supply disruptions, and their impact on the European electricity markets*. Retrieved August 3, 2024, from https://energy.ec.europa.eu/document/download/3fc39813-cd94-4f65-8697-974f168b470a_en

Fallon, J. C., Brayshaw, D. J., Methven, J., Jensen, K., & Krug, L. (2023). A new framework for using weather-sensitive surplus power reserves in critical infrastructure. *Meteorological Applications*. https://doi.org/10.1002/met.2158

Fallon, J. C., Brayshaw, D. J., Methven, J., Jensen, K., & Krug, L. (2024a). *MERRA2 derived time series of GB telecommunications infrastructure electricity load, using historical daily surface temperature* (Dataset). Dataset. https://doi.org/10.17864/1947.000533

Fallon, J. C., Brayshaw, D. J., Methven, J., Jensen, K., & Krug, L. (2024b). *Model of GB telecommunications electricity load using meteorological re-analysis and temperature delta-shift*. University of Reading. https://doi.org/10.17864/1947.001338

Fallon, J. C., Brayshaw, D. J., Methven, J., Jensen, K., & Krug, L. (2024c). *Reserve Power Design in Future Climates: Bias Adjustment Approaches for Regional Climate Projections*.

Fallon, J. C., Brayshaw, D. J., Methven, J., Jensen, K., Krug, L., & Greenwood, D. (2024). *Weather-driven surpluses in backup energy stores: Improving power system adequacy and unlocking the value of decarbonisation*.

Farquharson, D., Jaramillo, P., & Samaras, C. (2018). Sustainability implications of electricity outages in sub-Saharan Africa. *Nature Sustainability*, *1*(10), 589–597. https://doi.org/10.1038/s41893-018-0151-8

Feynman, R. P., Leighton, R. B., & Sands, M. (2011). *The Feynman Lectures on Physics, Vol. I: The New Millennium Edition: Mainly Mechanics, Radiation, and Heat*. Basic Books.

Findlater, K., Webber, S., Kandlikar, M., & Donner, S. (2021). Climate services promise better decisions but mainly focus on better data. *Nature Climate Change*, *11*(9), 731–737. https://doi.org/10.1038/s41558-021-01125-3

Forster, J., Vaughan, N. E., Gough, C., Lorenzoni, I., & Chilvers, J. (2020). Mapping feasibilities of greenhouse gas removal: Key issues, gaps and opening up assessments. *Global Environmental Change*, *63*, 102073. https://doi.org/10.1016/j.gloenvcha.2020.102073

Fossil Fuels: Lobbying. Retrieved February 11, 2024, from https://hansard.parliament.uk/Commons/2024-01-30/debates/B50D7B80-FBFE-4C13-9C37-116699E059E0/FossilFuelsLobbying#contribution-4CF60282-B260-41CB-8CA8-C9C5F0029F93

Fröhlich, K., Bittner, M., Müller, W., & Baehr, J. (2015). Seasonal predictability over Europe arising from El Niño and stratospheric variability in the MPI-ESM seasonal prediction system. *J. Climate*, (28), 256–271. https://doi.org/10.1175/JCLI-D-14-00207.1

Furbank, L. (2023). *Carbon Capture and Storage (CCS): Frequently Asked Questions*. Center for International Environmental Law. Retrieved February 15, 2024, from https://www.ciel.org/carbon-capture-and-storage-ccs-frequently-asked-questions

Gardner, C. J., Thierry, A., Rowlandson, W., & Steinberger, J. K. (2021). From Publications to Public Actions: The Role of Universities in Facilitating Academic Advocacy and Activism in the Climate and Ecological Emergency. *Frontiers in Sustainability*, *2*, 679019. https://doi.org/10.3389/frsus.2021.679019

Gelaro, R., McCarty, W., Suárez, M. J., Todling, R., Molod, A., Takacs, L., Randles, C. A., Darmenov, A., Bosilovich, M. G., Reichle, R., Wargan, K., Coy, L., Cullather, R., Draper, C., Akella, S., Buchard, V., Conaty, A., Silva, A. M. da, Gu, W., … Zhao, B. (2017). The Modern-Era Retrospective Analysis for Research and Applications, Version 2 (MERRA-2). *Journal of Climate*, *30*(14), 5419–5454. https://doi.org/10.1175/JCLI-D-16-0758.1

Gerard, H., Rivero Puente, E. I., & Six, D. (2018). Coordination between transmission and distribution system operators in the electricity sector: A conceptual framework. *Utilities Policy*, *50*, 40–48. https://doi.org/10.1016/j.jup.2017.09.011

Gianfreda, A., Parisio, L., & Pelagatti, M. (2018). A review of balancing costs in Italy before and after RES introduction. *Renewable and Sustainable Energy Reviews*, *91*, 549–563. https://doi.org/10.1016/j.rser.2018.04.009

Giorgi, F., Jones, C., & Asrar, G. R. (2009). Addressing climate information needs at the regional level: The CORDEX framework. *World Meteorological Organization (WMO) Bulletin*, *58*(3), 175.

Gonzalez, P. L. M., Brayshaw, D. J., & Ziel, F. (2021). A new approach to extended-range multimodel forecasting: Sequential learning algorithms. *Quarterly Journal of the Royal Meteorological Society*, *147*(741), 4269–4282. https://doi.org/10.1002/qj.4177

Goutham, N., Plougonven, R., Omrani, H., Parey, S., Tankov, P., Tantet, A., Hitchcock, P., & Drobinski, P. (2022). How Skillful Are the European Subseasonal Predictions of Wind Speed and Surface Temperature? *Monthly Weather Review*, *150*(7), 1621–1637. https://doi.org/10.1175/MWR-D-21-0207.1

Grams, C. M., Beerli, R., Pfenninger, S., Staffell, I., & Wernli, H. (2017). Balancing Europe's wind-power output through spatial deployment informed by weather regimes. *Nature Climate Change*, *7*(8), 557–562. https://doi.org/10.1038/nclimate3338

Green, M. A., Dunlop, E. D., Yoshita, M., Kopidakis, N., Bothe, K., Siefer, G., & Hao, X. (2024). Solar cell efficiency tables (Version 63). *Progress in Photovoltaics: Research and Applications*, *32*(1), 3–13. https://doi.org/10.1002/pip.3750

Greenwood, D. M., Deakin, M., Sarantakos, I., Brayshaw, D. J., & Bloomfield, H. C. (2022). Capacity Value of Interconnectors for Resource Adequacy Assessment in Multi-Region Systems. *2022 17th International Conference on Probabilistic Methods Applied to Power Systems (PMAPS)*, 1–6. https://doi.org/10.1109/PMAPS53380.2022.9810649

Grochowicz, A., van Greevenbroek, K., & Bloomfield, H. C. (2024). Using power system modelling outputs to identify weather-induced extreme events in highly renewable systems. *Environmental Research Letters*. https://doi.org/10.1088/1748-9326/ad374a

Groenemeijer, P., Becker, N., Djidara, M., Gavin, K., Hellenberg, T., Holzer, A. M., Juga, I., Jokinen, P., Jylhä, K., Lehtonen, I., et al. (2015). Past cases of extreme weather impact on critical infrastructure in Europe. *Risk Analysis of Infrastructure Networks in Response to Extreme Weather (RAIN), European Union Project*.

Gudmundsson, L., Bremnes, J. B., Haugen, J. E., & Engen-Skaugen, T. (2012). Technical Note: Downscaling RCM precipitation to the station scale using statistical transformations – a comparison of methods. *Hydrology and Earth System Sciences*, *16*(9), 3383–3390. https://doi.org/10.5194/hess-16-3383-2012

Guerrero, J. M., Garcia De Vicuna, L., & Uceda, J. (2007). Uninterruptible power supply systems provide protection. *IEEE Industrial Electronics Magazine*, *1*(1), 28–38. https://doi.org/10.1109/MIE.2007.357184

Halford, A. P. (2019). *Forecasting weather impacts on the United Kingdom telecommunication network* [engd]. University of Reading. https://doi.org/10.48683/1926.00085058

Hall, J. W., Thacker, S., Ives, M. C., Cao, Y., Chaudry, M., Blainey, S. P., & Oughton, E. J. (2017). Strategic analysis of the future of national infrastructure. *Proceedings of the Institution of Civil Engineers - Civil Engineering*, *170*(1), 39–47. https://doi.org/10.1680/jcien.16.00018

Hamilton, S. H., Fu, B., Guillaume, J. H. A., Badham, J., Elsawah, S., Gober, P., Hunt, R. J., Iwanaga, T., Jakeman, A. J., Ames, D. P., Curtis, A., Hill, M. C., Pierce, S. A., & Zare, F. (2019). A framework for characterising and evaluating the effectiveness of environmental modelling. *Environmental Modelling & Software*, *118*, 83–98. https://doi.org/10.1016/j.envsoft.2019.04.008

Hansen, J., Johnson, D., Lacis, A., Lebedeff, S., Lee, P., Rind, D., & Russell, G. (1981). Climate Impact of Increasing Atmospheric Carbon Dioxide. *Science*, *213*(4511), 957–966. https://doi.org/10.1126/science.213.4511.957

Hansson, J. (2022). *The Potential of Data Centre Participation in Ancillary Service Markets in Sweden*.

Harris, C. R., Millman, K. J., van der Walt, S. J., Gommers, R., Virtanen, P., Cournapeau, D., Wieser, E., Taylor, J., Berg, S., Smith, N. J., Kern, R., Picus, M., Hoyer, S., van Kerkwijk, M. H., Brett, M., Haldane, A., del Río, J. F., Wiebe, M., Peterson, P., … Oliphant, T. E. (2020). *Array programming with NumPy*. https://doi.org/10.1038/s41586-020-2649-2

Harvey, B., Hawkins, E., & Sutton, R. (2023). Storylines for future changes of the North Atlantic jet and associated impacts on the UK. *International Journal of Climatology*, *n/a*(n/a). https://doi.org/10.1002/joc.8095

Hausfather, Z., Drake, H. F., Abbott, T., & Schmidt, G. A. (2020). Evaluating the Performance of Past Climate Model Projections. *Geophysical Research Letters*, *47*(1). https://doi.org/10.1029/2019GL085378

Hawkins, E., Brohan, P., Burgess, S. N., Burt, S., Compo, G. P., Gray, S. L., Haigh, I. D., Hersbach, H., Kuijjer, K., Martínez-Alvarado, O., McColl, C., Schurer, A. P., Sliv-

inski, L., & Williams, J. (2023). Rescuing historical weather observations improves quantification of severe windstorm risks. *Natural Hazards and Earth System Sciences*, *23*(4), 1465–1482. https://doi.org/10.5194/nhess-23-1465-2023

Hawkins, E., Osborne, T. M., Ho, C. K., & Challinor, A. J. (2013). Calibration and bias correction of climate projections for crop modelling: An idealised case study over Europe. *Agricultural and Forest Meteorology*, *170*, 19–31. https://doi.org/10.1016/j.agrformet.2012.04.007

Hawkins, E., & Sutton, R. (2009). The Potential to Narrow Uncertainty in Regional Climate Predictions. *Bulletin of the American Meteorological Society*, *90*(8), 1095–1108. https://doi.org/10.1175/2009BAMS2607.1

Hegyi, B., Stackhouse, P. W., Taylor, P., & Patadia, F. (2024). *NASA POWER: Providing Present and Future Climate Services Based on NASA Data for the Energy, Agricultural, and Sustainable Buildings Communities*. Retrieved April 1, 2024, from https://ntrs.nasa.gov/citations/20240000860
    NTRS Author Affiliations: Analytical Mechanics Associates (United States), Langley Research Center
    NTRS Meeting Information: 104th American Meteorological Society (AMS) Annual Meeting ; 2024-01-29 to 2024-02-01; undefined
    NTRS Document ID: 20240000860
    NTRS Research Center: Langley Research Center (LaRC).

Herman, E. S., & Chomsky, N. (1988). *Manufacturing Consent: The Political Economy of the Mass Media*. Random House.

Hersbach, H., Bell, B., Berrisford, P., Hirahara, S., Horányi, A., Muñoz-Sabater, J., Nicolas, J., Peubey, C., Radu, R., Schepers, D., Simmons, A., Soci, C., Abdalla, S., Abellan, X., Balsamo, G., Bechtold, P., Biavati, G., Bidlot, J., Bonavita, M., … Thépaut, J.-N. (2020). The ERA5 global reanalysis. *Quarterly Journal of the Royal Meteorological Society*, *146*(730), 1999–2049. https://doi.org/10.1002/qj.3803

Hewitt, C. D., Guglielmo, F., Joussaume, S., Bessembinder, J., Christel, I., Doblas-Reyes, F. J., Djurdjevic, V., Garrett, N., Kjellström, E., Krzic, A., Costa, M. M., & Clair,

A. L. S. (2021). Recommendations for Future Research Priorities for Climate Modeling and Climate Services. *Bulletin of the American Meteorological Society*, *102*(3), E578–E588. https://doi.org/10.1175/BAMS-D-20-0103.1

Hickel, J. (2021). *Less is More*. Random House Publishing Group. Retrieved February 11, 2024, from https://www.penguin.co.uk/books/441772/less-is-more-by-jason-hickel/9781786091215

Hitchin, E. R. (1981). Degree-days in britain. *Building Services Engineering Research and Technology*, *2*(2), 73–82.

Hong, Y.-Y., Apolinario, G. F. D., & Cheng, Y.-H. (2023). Week-ahead Daily Peak Load Forecasting Using Hybrid Convolutional Neural Network. *IFAC-PapersOnLine*, *56*(2), 372–377. https://doi.org/10.1016/j.ifacol.2023.10.1596

Hor, C.-L., Watson, S., & Majithia, S. (2005). Analyzing the impact of weather variables on monthly electricity demand. *IEEE Transactions on Power Systems*, *20*(4), 2078–2085. https://doi.org/10.1109/TPWRS.2005.857397

Houthakker, H. S., & Taylor, L. D. (1970). Consumer demand in the United States: Analyses and projections. *(No Title)*.

Hoyer, S., & Hamman, J. (2017). Xarray: N-D labeled arrays and datasets in Python. *Journal of Open Research Software*, *5*(1). https://doi.org/10.5334/jors.148

Hunter, J. D. (2007). Matplotlib: A 2D graphics environment. *Computing in Science & Engineering*, *9*(3), 90–95. https://doi.org/10.1109/MCSE.2007.55

Hurrell, J. W., Delworth, T. L., Danabasoglu, G., Drange, H., Drinkwater, K., Griffies, S., Holbrook, N. J., Kirtman, B., Keenlyside, N., Latif, M., Marotzke, J., Murphy, J., Meehl, G. A., Palmer, T., Pohlmann, H., Rosati, T., Seager, R., Smith, D., Sutton, R., … Visbeck, M. (2010). Decadal climate prediction: Opportunities and challenges. *OceanObs' 09: Sustained Ocean Observations and Information for Society*, 521–533.

IEA. (2018). *World Energy Outlook 2018 – Analysis*. Paris. Retrieved January 25, 2024, from https://www.iea.org/reports/world-energy-outlook-2018

IEA. (2019). *Battery storage is (almost) ready to play the flexibility game – Analysis*. Paris. Retrieved March 19, 2024, from https://www.iea.org/commentaries/battery-storage-is-almost-ready-to-play-the-flexibility-game

IEA. (2022). *World Energy Outlook 2022*. Paris. https://www.iea.org/reports/world-energy-outlook-2022

IEA. (2023a). *Tracking Clean Energy Progress*. Paris. Retrieved March 24, 2024, from https://www.iea.org/reports/tracking-clean-energy-progress-2023

IEA. (2023b). *Tracking SDG7: The Energy Progress Report, 2023*. IEA. Paris. Retrieved September 27, 2023, from https://www.iea.org/reports/tracking-sdg7-the-energy-progress-report-2023

IEA. (2024). *Electricity 2024*. Retrieved March 5, 2024, from https://www.iea.org/reports/electricity-2024

Ilbahar, E., Cebi, S., & Kahraman, C. (2019). A state-of-the-art review on multi-attribute renewable energy decision making. *Energy Strategy Reviews*, *25*, 18–33. https://doi.org/10.1016/j.esr.2019.04.014

International Organization for Standardization. (2015). *ISO 9000:2015(en), Quality management systems — Fundamentals and vocabulary*. Geneva, CH. https://www.iso.org/obp/ui/#iso:std:iso:9000:ed-4:v1:en

International Organization for Standardization. (2019). *ISO 37123:2019, Sustainable cities and communities — Indicators for resilient cities*. Geneva, CH. https://www.iso.org/obp/ui/#iso:std:iso:37123:ed-1:v1:en

International Organization for Standardization. (2021). *ISO 22300:2021, Security and resilience — Vocabulary*. Geneva, CH. https://www.iso.org/obp/ui/#iso:std:iso:22300:ed-3:v1:en

IRENA. (2020). *Innovation landscape brief: Co-operation between transmission and distribution system operators*. International Renewable Energy Agency. Abu Dhabi. https://www.irena.org/Publications/2020/Jul/System-Operation-Innovation-Landscape-briefs

IRENA. (2023). *Renewable power generation costs in 2022*. https://www.irena.org/Publicati ons/2023/Aug/Renewable-power-generation-costs-in-2022

Jacobs, K. L., & Street, R. B. (2020). The next generation of climate services. *Climate Services*, *20*, 100199. https://doi.org/10.1016/j.cliser.2020.100199

Jamasb, T., & Pollitt, M. (2005). Electricity Market Reform in the European Union: Review of Progress toward Liberalization & Integration. *The Energy Journal*, *26*, 11–41. https: //doi.org/10.5547/ISSN0195-6574-EJ-Vol26-NoSI-2

Jasiński, T. (2020). Use of new variables based on air temperature for forecasting day-ahead spot electricity prices using deep neural networks: A new approach. *Energy*, *213*, 118784. https://doi.org/10.1016/j.energy.2020.118784

Jeevanjee, N., Held, I., & Ramaswamy, V. (2022). Manabe's Radiative–Convective Equilibrium. *Bulletin of the American Meteorological Society*, *103*(11), E2559–E2569. https: //doi.org/10.1175/BAMS-D-21-0351.1

Joskow, P., & Tirole, J. (2007). Reliability and competitive electricity markets. *The RAND Journal of Economics*, *38*(1), 60–84. https://doi.org/10.1111/j.1756-2171.2007. tb00044.x

Jülch, V. (2016). Comparison of electricity storage options using levelized cost of storage (LCOS) method. *Applied Energy*, *183*, 1594–1606. https://doi.org/10.1016/j.apenergy. 2016.08.165

Kaika, M. (2017). *'Don't Call Me Resilient Again!'* : The New Urban Agenda as immunology … or … what happens when communities refuse to be vaccinated with 'smart cities' and indicators. *Environment and Urbanization*, *29*(1), 89–102. https://doi.org/10. 1177/0956247816684763

Kalnay, E., Kanamitsu, M., Kistler, R., Collins, W., Deaven, D., Gandin, L., Iredell, M., Saha, S., White, G., Woollen, J., Zhu, Y., Chelliah, M., Ebisuzaki, W., Higgins, W., Janowiak, J., Mo, K. C., Ropelewski, C., Wang, J., Leetmaa, A., … Joseph, D. (1996). The NCEP/NCAR 40-Year reanalysis project. *Bulletin of the American Meteorological Society*, *77*(3), 437–472. https://doi.org/10.1175/1520-0477(1996)077%3C0437: TNYRP%3E2.0.CO;2

Kamigauti, L. Y., Perez, G. M. P., Martin, T. C. M., Andrade, M. d. F., & Kumar, P. (2024). Enhancing spatial inference of air pollution using machine learning techniques with low-cost monitors in data-limited scenarios. *Environmental Science: Atmospheres*, *4*(3), 342–350. https://doi.org/10.1039/D3EA00126A

Kappes, M. S., Keiler, M., von Elverfeldt, K., & Glade, T. (2012). Challenges of analyzing multi-hazard risk: A review. *Natural Hazards*, *64*(2), 1925–1958. https://doi.org/10.1007/s11069-012-0294-2

Katz, R. W., Parlange, M. B., & Naveau, P. (2002). Statistics of extremes in hydrology. *Advances in Water Resources*, *25*(8), 1287–1304. https://doi.org/10.1016/S0309-1708(02)00056-8

Kaufman, M. (2020). *The devious fossil fuel propaganda we all use*. Mashable. Retrieved February 11, 2024, from https://mashable.com/feature/carbon-footprint-pr-campaign-sham

Kaya, T., & Kahraman, C. (2011). Multicriteria decision making in energy planning using a modified fuzzy TOPSIS methodology. *Expert Systems with Applications*, *38*(6), 6577–6585. https://doi.org/10.1016/j.eswa.2010.11.081

Keen, S. (2021). The appallingly bad neoclassical economics of climate change. *Globalizations*, *18*(7), 1149–1177. https://doi.org/10.1080/14747731.2020.1807856

Kennedy-Asser, A. T., Andrews, O., Mitchell, D. M., & Warren, R. F. (2021). Evaluating heat extremes in the UK Climate Projections (UKCP18). *Environmental Research Letters*, *16*(1), 014039. https://doi.org/10.1088/1748-9326/abc4ad

Knuth, D. E., & Bibby, D. (1986). *The texbook* (Vol. 1993). Addison-Wesley Reading, MA.

Kobayashi, S., Ota, Y., Harada, Y., Ebita, A., Moriya, M., Onoda, H., Onogi, K., Kamahori, H., Kobayashi, C., Endo, H., Miyaoka, K., & Takahashi, K. (2015). The JRA-55 Reanalysis: General Specifications and Basic Characteristics. *Journal of the Meteorological Society of Japan*, *93*(1), 5–48. https://doi.org/10.2151/jmsj.2015-001

Koolen, D., De, F. M., & Busch, S. (2022). *Flexibility requirements and the role of storage in future European power systems*. JRC Publications Repository. https://doi.org/10.2760/384443

Kotulla, M., Goňo, M., Goňo, R., Vrzala, M., Leonowicz, Z., Kłosok-Bazan, I., & Boguniewicz-Zabłocka, J. (2022). Renewable Energy Sources as Backup for a Water Treatment Plant. *Energies*, *15*(17), 6288. https://doi.org/10.3390/en15176288

Kozlova, M., & Overland, I. (2022). Combining capacity mechanisms and renewable energy support: A review of the international experience. *Renewable and Sustainable Energy Reviews*, *155*, 111878. https://doi.org/10.1016/j.rser.2021.111878

Kruyt, B., van Vuuren, D. P., de Vries, H. J. M., & Groenenberg, H. (2009). Indicators for energy security. *Energy Policy*, *37*(6), 2166–2181. https://doi.org/10.1016/j.enpol.2009.02.006

Kumar, A., Schei, T., Ahenkorah, A., Rodriguez, R. C., Devernay, J.-M., Freitas, M., Hall, D., Killingtveit, Å., Liu, Z., Branche, E., & et al. (2011). Hydropower. In O. Edenhofer, R. Pichs-Madruga, Y. Sokona, K. Seyboth, S. Kadner, T. Zwickel, P. Eickemeier, G. Hansen, S. Schlömer, C. von Stechow & et al. (Eds.), *Renewable energy sources and climate change mitigation: Special report of the intergovernmental panel on climate change* (pp. 437–496). Cambridge University Press.

Lang, A. L., Pegion, K., & Barnes, E. A. (2020). Introduction to Special Collection: "Bridging Weather and Climate: Subseasonal-to-Seasonal (S2S) Prediction". *Journal of Geophysical Research: Atmospheres*, *125*(4), e2019JD031833. https://doi.org/10.1029/2019JD031833

Leal Filho, W., Viera Trevisan, L., Simon Rampasso, I., Anholon, R., Pimenta Dinis, M. A., Londero Brandli, L., Sierra, J., Lange Salvia, A., Pretorius, R., Nicolau, M., Paulino Pires Eustachio, J. H., & Mazutti, J. (2023). When the alarm bells ring: Why the UN sustainable development goals may not be achieved by 2030. *Journal of Cleaner Production*, *407*, 137108. https://doi.org/10.1016/j.jclepro.2023.137108

Lee, S. H., Charlton-Perez, A. J., Furtado, J. C., & Woolnough, S. J. (2020). Representation of the Scandinavia–Greenland pattern and its relationship with the polar vortex in S2S forecast models. *Quarterly Journal of the Royal Meteorological Society*, *146*(733), 4083–4098.

Li, X., & Li, Z. (2023). Evaluation of bias correction techniques for generating high-resolution daily temperature projections from CMIP6 models. *Climate Dynamics*, *61*(7), 3893–3910. https://doi.org/10.1007/s00382-023-06778-8

Liu, B., Siu, Y. L., & Mitchell, G. (2016). Hazard interaction analysis for multi-hazard risk assessment: A systematic classification based on hazard-forming environment. *Natural Hazards and Earth System Sciences*, *16*(2), 629–642. https://doi.org/10.5194/nhess-16-629-2016

Longden, T., Beck, F. J., Jotzo, F., Andrews, R., & Prasad, M. (2022). 'Clean' hydrogen? – Comparing the emissions and costs of fossil fuel versus renewable electricity based hydrogen. *Applied Energy*, *306*, 118145. https://doi.org/10.1016/j.apenergy.2021.118145

Lorenz, E. N. (1963). Deterministic Nonperiodic Flow. *Journal of the Atmospheric Sciences*, *20*(2), 130–141. https://doi.org/10.1175/1520-0469(1963)020<0130:DNF>2.0.CO;2

Lowe, J. A., Bernie, D., Bett, P., Bricheno, L., Brown, S., Calvert, D., Clark, R., Edwards, T., Fosser, G., Fung, F., Gohar, L., Good, P., Gregory, J., Harris, G., Howard, T., Kaye, N., Kendon, E., Krijnen, J., Maisey, P., … Belcher, S. (2018). UKCP18 Science Overview Report.

Lynch, K. J., Brayshaw, D. J., & Charlton-Perez, A. J. (2014). Verification of European Sub-seasonal Wind Speed Forecasts. *Monthly Weather Review*, *142*(8), 2978–2990. https://doi.org/10.1175/MWR-D-13-00341.1

Maia-Silva, D., Kumar, R., & Nateghi, R. (2020). The critical role of humidity in modeling summer electricity demand across the United States. *Nature Communications*, *11*(1), 1686. https://doi.org/10.1038/s41467-020-15393-8

Maraun, D. (2016). Bias Correcting Climate Change Simulations - a Critical Review. *Current Climate Change Reports*, *2*(4), 211–220. https://doi.org/10.1007/s40641-016-0050-x

Maraun, D., Shepherd, T. G., Widmann, M., Zappa, G., Walton, D., Gutiérrez, J. M., Hagemann, S., Richter, I., Soares, P. M. M., Hall, A., & Mearns, L. O. (2017). Towards process-informed bias correction of climate change simulations. *Nature Climate Change*, *7*(11), 764–773. https://doi.org/10.1038/nclimate3418

Marcheggiani, A., Robson, J., Monerie, P.-A., Bracegirdle, T. J., & Smith, D. (2023). Decadal Predictability of the North Atlantic Eddy-Driven Jet in Winter. *Geophysical Research Letters*, *50*(8), e2022GL102071. https://doi.org/10.1029/2022GL102071

Mavromatidis, G., Orehounig, K., & Carmeliet, J. (2018). Uncertainty and global sensitivity analysis for the optimal design of distributed energy systems. *Applied Energy*, *214*, 219–238. https://doi.org/10.1016/j.apenergy.2018.01.062

Mays, J., Morton, D. P., & O'Neill, R. P. (2019). Decarbonizing electricity requires re-evaluating capacity mechanisms. *Nature Energy*, *4*(11), 912–913. https://doi.org/10.1038/s41560-019-0502-3

McSweeney, C., & Bett, P. (2020). UKCP European Circulation Indices: Jet Stream Position and Strength. *UKCP Factsheet*. Retrieved December 7, 2023, from https://www.metoffice.gov.uk/binaries/content/assets/metofficegovuk/pdf/research/ukcp/ukcp18_factsheet_jet_stream.pdf

McSweeney, C., & Thornton, H. (2020). European Circulation Indices: Weather Patterns. *UKCP18 Factsheet*. Retrieved November 29, 2023, from https://www.metoffice.gov.uk/binaries/content/assets/metofficegovuk/pdf/research/ukcp/ukcp18_factsheet_weather_patterns.pdf

McSweeney, C., & Yamazaki, K. (2020). UKCP European Circulation Indices: Winter Atlantic Pressure Gradient (North Atlantic Oscillation – NAO). *UKCP Factsheet*. Retrieved November 29, 2023, from https://www.metoffice.gov.uk/binaries/content/assets/metofficegovuk/pdf/research/ukcp/ukcp18_factsheet_nao.pdf

McVicker, I. F. G. (1946). The calculation and use of degree-days. *Journal of the Institution of Heating and Ventilating Engineers*, *14*, 256–283.

Meehl, G. A., Richter, J. H., Teng, H., Capotondi, A., Cobb, K., Doblas-Reyes, F., Donat, M. G., England, M. H., Fyfe, J. C., Han, W., Kim, H., Kirtman, B. P., Kushnir, Y., Lovenduski, N. S., Mann, M. E., Merryfield, W. J., Nieves, V., Pegion, K., Rosenbloom, N., … Xie, S.-P. (2021). Initialized Earth System prediction from subseasonal to decadal timescales. *Nature Reviews Earth & Environment*, *2*(5), 340–357. https://doi.org/10.1038/s43017-021-00155-x

Met Office Hadley Centre. (2019). *UKCP18 Factsheet: UKCP Local (2.2km) Projections*. Retrieved December 7, 2023, from https://www.metoffice.gov.uk/binaries/content/assets/metofficegovuk/pdf/research/ukcp/ukcp18-factsheet-local-2.2km.pdf

Met Office Hadley Centre, Department for Environment Food & Rural Affairs, Department for Business, Energy & Industrial Strategy & Environment Agency. (2018). *UKCP18 Guidance: How to bias correct*. Met Office. Retrieved May 10, 2023, from https://www.metoffice.gov.uk/binaries/content/assets/metofficegovuk/pdf/research/ukcp/ukcp18-guidance---how-to-bias-correct.pdf

Michelangeli, P.-A., Vautard, R., & Legras, B. (1995). Weather regimes: Recurrence and quasi stationarity. *Journal of Atmospheric Sciences*, *52*(8), 1237–1256.

Mindlin, J., Shepherd, T. G., Vera, C. S., Osman, M., Zappa, G., Lee, R. W., & Hodges, K. I. (2020). Storyline description of Southern Hemisphere midlatitude circulation and precipitation response to greenhouse gas forcing. *Climate Dynamics*, *54*(9), 4399–4421. https://doi.org/10.1007/s00382-020-05234-1

Moreno-Chamarro, E., Caron, L.-P., Loosveldt Tomas, S., Vegas-Regidor, J., Gutjahr, O., Moine, M.-P., Putrasahan, D., Roberts, C. D., Roberts, M. J., Senan, R., Terray, L., Tourigny, E., & Vidale, P. L. (2022). Impact of increased resolution on long-standing biases in HighResMIP-PRIMAVERA climate models. *Geoscientific Model Development*, *15*(1), 269–289. https://doi.org/10.5194/gmd-15-269-2022

Morice, C. P., Kennedy, J. J., Rayner, N. A., Winn, J. P., Hogan, E., Killick, R. E., Dunn, R. J. H., Osborn, T. J., Jones, P. D., & Simpson, I. R. (2021). An Updated Assessment of Near-Surface Temperature Change From 1850: The HadCRUT5 Data Set. *Journal of Geophysical Research: Atmospheres*, *126*(3), e2019JD032361. https://doi.org/10.1029/2019JD032361

Morrison, T. H., Adger, W. N., Agrawal, A., Brown, K., Hornsey, M. J., Hughes, T. P., Jain, M., Lemos, M. C., McHugh, L. H., O'Neill, S., & Van Berkel, D. (2022). Radical interventions for climate-impacted systems. *Nature Climate Change*, *12*(12), 1100–1106. https://doi.org/10.1038/s41558-022-01542-y

Moyer, J. D., & Hedden, S. (2020). Are we on the right path to achieve the sustainable development goals? *World Development*, *127*, 104749. https://doi.org/10.1016/j.worlddev.2019.104749

Murphy, J. M., Harris, G. R., Sexton, D. M. H., Kendon, E. J., Bett, P. E., Clark, R. T., Eagle, K. E., Fosser, G., Fung, F., Lowe, J. A., McDonald, R. E., McInnes, R. N., McSweeney, C. F., Mitchell, J. F. B., Rostron, J. W., Thornton, H. E., Tucker, S., & Yamazaki, K. (2018). UKCP18 Land Projections: Science Report.

Mustafa, M. B., Keatley, P., Huang, Y., Agbonaye, O., Ademulegun, O. O., & Hewitt, N. (2021). Evaluation of a battery energy storage system in hospitals for arbitrage and ancillary services. *Journal of Energy Storage*, *43*, 103183. https://doi.org/10.1016/j.est.2021.103183

National Grid Electricity Transmission plc. (2018). *National Grid EMR Electricity Capacity Report*. https://www.emrdeliverybody.com/Lists/Latest%20News/Attachments/189/Electricity%20Capacity%20Report%202018_Final.pdf

National Grid ESO. (2011). *Winter Outlook 2011/12*. Retrieved March 21, 2024, from https://www.nationalgrid.com/sites/default/files/documents/12191-WinterOutlook_201112.pdf

National Grid ESO. (2020). *GIS boundaries for GB DNO license areas*. Retrieved May 1, 2022, from https://data.nationalgrideso.com/system/gis-boundaries-for-gb-dno-license-areas

National Grid ESO. (2021). *Winter Outlook 2021/22*. Retrieved March 25, 2024, from https://www.nationalgrideso.com/document/289136/download

National Grid ESO. (2023). *Winter Outlook 2023/24*. Retrieved March 21, 2024, from https://www.nationalgrideso.com/document/289136/download

National Grid ESO. (2024a). *Balancing Services*. ESO. Retrieved April 3, 2024, from https://www.nationalgrideso.com/industry-information/balancing-services

National Grid ESO. (2024b). *EMR Portal - Published-Round-Results*. EMR Delivery Body. Retrieved March 2, 2024, from https://www.emrdeliverybody.com/CM/Published-Round-Results.aspx

National Grid ESO. (2024c). *National Grid ESO Data Portal*. Retrieved March 2, 2024, from

   https://www.nationalgrideso.com/data-portal

National Grid ESO. (2024d). *Provisional Auction Report 2023 Four Year-Ahead Capacity
   Auction (T-4) Delivery year 2027/28*. Warwick. Retrieved February 26, 2024, from
   https://www.emrdeliverybody.com/Capacity%20Markets%20Document%20Library/
   T-4%20DY%2026-27%20Final%20Auction%20Results%20Report%20v1.0.pdf

National Grid ESO. (2024e). *Provisional Auction Report 2023 One Year-Ahead Capacity Auc-
   tion (T-1) Delivery year 2024/25*. Warwick. Retrieved February 26, 2024, from https:
   //www.emrdeliverybody.com/Capacity%20Markets%20Document%20Library/T-
   1%20DY%202024-25%20Provisional%20Results%20v1.0.pdf

National Infrastructure Commission. (2023). *The Second National Infrastructure Assessment*.
   London. Retrieved March 13, 2024, from https://nic.org.uk/studies-reports/national-
   infrastructure-assessment/second-nia

Neal, R., Fereday, D., Crocker, R., & Comer, R. E. (2016). A flexible approach to defining
   weather patterns and their application in weather forecasting over Europe. *Meteorolo-
   gical Applications*, *23*(3), 389–400. https://doi.org/10.1002/met.1563

Nelder, J. A., & Wedderburn, R. W. (1972). Generalized linear models. *Journal of the Royal
   Statistical Society Series A: Statistics in Society*, *135*(3), 370–384.

NHS England. (2022). *Estates Returns Information Collection, Summary page and dataset for
   ERIC 2021/22*. NHS England Digital. Retrieved March 22, 2024, from https://digital.
   nhs.uk/data-and-information/publications/statistical/estates-returns-information-
   collection/england-2021-22

NTESS. (2022). *DOE Global Energy Storage Database*. National Technology & Engineering
   Sciences of Sandia, LLC (NTESS). Retrieved March 24, 2024, from https://www.
   sandia.gov/ess-ssl/gesdb/public/statistics.html

Ofgem. (2022). *Decision on accelerating onshore electricity transmission investment*. London.
   Retrieved March 28, 2024, from https://www.ofgem.gov.uk/publications/decision-
   accelerating-onshore-electricity-transmission-investment

O'Reilly, C. H., Heatley, J., MacLeod, D., Weisheimer, A., Palmer, T. N., Schaller, N., & Woollings, T. (2017). Variability in seasonal forecast skill of Northern Hemisphere winters over the twentieth century. *Geophysical Research Letters*, *44*(11), 5729–5738. https://doi.org/10.1002/2017GL073736

Oró, E., Depoorter, V., Garcia, A., & Salom, J. (2015). Energy efficiency and renewable energy integration in data centres. Strategies and modelling review. *Renewable and Sustainable Energy Reviews*, *42*, 429–445. https://doi.org/10.1016/j.rser.2014.10.035

Pacchetti, M. B., Dessai, S., Stainforth, D. A., & Bradley, S. (2021). Assessing the quality of state-of-the-art regional climate information: The case of the UK Climate Projections 2018. *Climatic Change*, *168*(1), 1. https://doi.org/10.1007/s10584-021-03187-w

Palmer, T. N., Buizza, R., Doblas-Reyes, F., Jung, T., Leutbecher, M., Shutts, G. J., Steinheimer, M., & Weisheimer, A. (2009). Stochastic parametrization and model uncertainty.

Parrique, T., Raworth, K., & May, V. L. (2023). Post-Growth Europe: 400+ Experts Call for Wellbeing Economy. https://znetwork.org/znetarticle/post-growth-europe-400-experts-call-for-wellbeing-economy

Peacock, M., Fragaki, A., & Matuszewski, B. J. (2023). The impact of heat electrification on the seasonal and interannual electricity demand of Great Britain. *Applied Energy*, *337*, 120885. https://doi.org/10.1016/j.apenergy.2023.120885

Pickering, B., & Choudhary, R. (2019). District energy system optimisation under uncertain demand: Handling data-driven stochastic profiles. *Applied Energy*, *236*, 1138–1157. https://doi.org/10.1016/j.apenergy.2018.12.037

Pohekar, S. D., & Ramachandran, M. (2004). Application of multi-criteria decision making to sustainable energy planning—A review. *Renewable and Sustainable Energy Reviews*, *8*(4), 365–381. https://doi.org/10.1016/j.rser.2003.12.007

Pollitt, M. G. (2012). The role of policy in energy transitions: Lessons from the energy liberalisation era. *Energy Policy*, *50*, 128–137. https://doi.org/10.1016/j.enpol.2012.03.004

POST Report 282. (2007). *Energy and Sewage* (postnote No. 282). Retrieved March 22, 2024, from https://www.parliament.uk/globalassets/documents/post/postpn282.pdf

Prior, J., & Kendon, M. (2011). The disruptive snowfalls and very low temperatures of late 2010. *Weather*, *66*(12), 315–321. https://doi.org/10.1002/wea.874

Pursiainen, C., & Kytömaa, E. (2023). From European critical infrastructure protection to the resilience of European critical entities: What does it mean? *Sustainable and Resilient Infrastructure*, *8*, 85–101. https://doi.org/10.1080/23789689.2022.2128562

Qian, W., & Chang, H. H. (2021). Projecting Health Impacts of Future Temperature: A Comparison of Quantile-Mapping Bias-Correction Methods. *International Journal of Environmental Research and Public Health*, *18*(4), 1992. https://doi.org/10.3390/ijerph18041992

Rancilio, G., Rossi, A., Falabretti, D., Galliani, A., & Merlo, M. (2022). Ancillary services markets in europe: Evolution and regulatory trade-offs. *Renewable and Sustainable Energy Reviews*, *154*, 111850. https://doi.org/10.1016/j.rser.2021.111850

Rantanen, M., Lee, S. H., & Aalto, J. (2023). Asymmetric warming rates between warm and cold weather regimes in Europe. *Atmospheric Science Letters*, *24*(10), e1178. https://doi.org/10.1002/asl.1178

Räty, O., Räisänen, J., & Ylhäisi, J. S. (2014). Evaluation of delta change and bias correction methods for future daily precipitation: Intermodel cross-validation using ENSEMBLES simulations. *Climate Dynamics*, *42*(9), 2287–2303. https://doi.org/10.1007/s00382-014-2130-8

Raworth, K. (2017). *Doughnut economics: Seven ways to think like a 21st-century economist*. Chelsea Green Publishing.

Rezvan, A. T., Gharneh, N. S., & Gharehpetian, G. B. (2013). Optimization of distributed generation capacities in buildings under uncertainty in load demand. *Energy and Buildings*, *57*, 58–64. https://doi.org/10.1016/j.enbuild.2012.10.031

Rinaldi, S., Peerenboom, J., & Kelly, T. (2001). Identifying, understanding, and analyzing critical infrastructure interdependencies. *IEEE Control Systems Magazine*, *21*(6), 11–25. https://doi.org/10.1109/37.969131

Ritchie, H., Roser, M., & Rosado, P. (2022). Energy. *Our World in Data*.

Rogers, P. (2014). *Theory of Change: Methodological Briefs - Impact Evaluation No. 2*. UNICEF Office of Research - Innocenti. Florence. Retrieved February 11, 2024, from https://www.unicef-irc.org/publications/747-theory-of-change-methodological-briefs-impact-evaluation-no-2.html

Royal Society. (2018). Options for producing low-carbon hydrogen at scale. Retrieved February 15, 2024, from https://royalsociety.org/low-carbon-energy-programme

Royal Society. (2020). Ammonia: Zero-carbon fertiliser, fuel and energy store. Retrieved February 15, 2024, from https://royalsociety.org/green-ammonia

Rummukainen, M. (2016). Added value in regional climate modeling. *WIREs Climate Change*, *7*(1), 145–159. https://doi.org/10.1002/wcc.378

Ryan-Christensen, A. (2022). The rise and rise of data centres in Ireland. Retrieved March 24, 2024, from https://www.rte.ie/brainstorm/2022/0815/1315804-data-centres-ireland-electricity-energy-resources-climate-change

Saltmarsh, C. (2021). *Burnt: Fighting for climate justice*. Pluto Press. https://www.plutobooks.com/9780745341828/burnt

Schmidt, O., Melchior, S., Hawkes, A., & Staffell, I. (2019). Projecting the Future Levelized Cost of Electricity Storage Technologies. *Joule*, *3*(1), 81–100. https://doi.org/10.1016/j.joule.2018.12.008

Seabold, S., & Perktold, J. (2010). Statsmodels: Econometric and statistical modeling with python. *Proceedings of the 9th Python in Science Conference*, *57*(61), 10–25080.

Shaw, Z. A. (2017). *Learn python 3 the hard way: A very simple introduction to the terrifyingly beautiful world of computers and code*. Addison-Wesley Professional. https://learnpythonthehardway.org

Shepherd, T. G. (2019). Storyline approach to the construction of regional climate change information. *Proceedings of the Royal Society A: Mathematical, Physical and Engineering Sciences*, *475*(2225), 20190013. https://doi.org/10.1098/rspa.2019.0013

Short, A., C., Guthrie, P., Soulti, E., & Macmillan, S. (2015). *Health Technical Memorandum 07-02: EnCO2de 2015 – making energy work in healthcare* (No. 07-02). Department of Health, gov.uk.

Siegert, S., & Stephenson, D. B. (2019). Chapter 15 - Forecast Recalibration and Multimodel Combination. In A. W. Robertson & F. Vitart (Eds.), *Sub-Seasonal to Seasonal Prediction* (pp. 321–336). Elsevier. https://doi.org/10.1016/B978-0-12-811714-9.00015-2

Singh, C., Daron, J., Bazaz, A., Ziervogel, G., Spear, D., Krishnaswamy, J., Zaroug, M., & Kituyi, E. (2018). The utility of weather and climate information for adaptation decision-making: Current uses and future prospects in Africa and India. *Climate and Development*, *10*(5), 389–405. https://doi.org/10.1080/17565529.2017.1318744

Slameršak, A., Kallis, G., O'Neill, D. W., & Hickel, J. (2024). Post-growth: A viable path to limiting global warming to 1.5°C. *One Earth*, *7*(1), 44–58. https://doi.org/10.1016/j.oneear.2023.11.004

Slingo, J., & Palmer, T. (2011). Uncertainty in weather and climate prediction. *Philosophical Transactions of the Royal Society A: Mathematical, Physical and Engineering Sciences*, *369*(1956), 4751–4767. https://doi.org/10.1098/rsta.2011.0161

SmartNet. (2019). *TSO-DSO co-ordination for acquiring ancillary services from distribution grids: The Smartnet project final results*. EU Horizons 2020 project. Retrieved January 25, 2024, from https://smartnet-project.eu/wp-content/uploads/2019/05/SmartNet-Booktlet.pdf

Smith, D. M., Scaife, A. A., Eade, R., Athanasiadis, P., Bellucci, A., Bethke, I., Bilbao, R., Borchert, L. F., Caron, L.-P., Counillon, F., Danabasoglu, G., Delworth, T., Doblas-Reyes, F. J., Dunstone, N. J., Estella-Perez, V., Flavoni, S., Hermanson, L., Keenlyside, N., Kharin, V., … Zhang, L. (2020). North Atlantic climate far more predictable than models imply. *Nature*, *583*(7818), 796–800. https://doi.org/10.1038/s41586-020-2525-0

Smith, M. D. (2011). An ecological perspective on extreme climatic events: A synthetic definition and framework to guide future research. *Journal of Ecology*, *99*(3), 656–663. https://doi.org/10.1111/j.1365-2745.2011.01798.x

Soret, A., Torralba, V., Cortesi, N., Christel, I., Palma, L., Manrique-Suñén, A., Lledó, L., González-Reviriego, N., & Doblas-Reyes, F. J. (2019). Sub-seasonal to seasonal cli-

mate predictions for wind energy forecasting. *Journal of Physics: Conference Series*, *1222*(1), 012009. https://doi.org/10.1088/1742-6596/1222/1/012009

Sovacool, B. K. (2012). The political economy of energy poverty: A review of key challenges. *Energy for Sustainable Development*, *16*(3), 272–282. https://doi.org/10.1016/j.esd.2012.05.006

Spry, W. (2023). *Energy Trends: UK renewables*. Retrieved May 24, 2023, from https://www.gov.uk/government/statistics/energy-trends-section-6-renewables

Spuler, F. R., Wessel, J. B., Comyn-Platt, E., Varndell, J., & Cagnazzo, C. (2023). *Ibicus: A new open-source Python package and comprehensive interface for statistical bias adjustment and evaluation in climate modelling (v1.0.1)* (preprint). Climate and Earth system modeling. https://doi.org/10.5194/egusphere-2023-1481

Staffell, I., Pfenninger, S., & Johnson, N. (2023). A global model of hourly space heating and cooling demand at multiple spatial scales. *Nature Energy*, 1–17. https://doi.org/10.1038/s41560-023-01341-5

Stein, D., & Valters, C. (2012). *Understanding theory of change in international development*. Retrieved February 11, 2024, from http://www.lse.ac.uk/internationalDevelopment/research/JSRP/jsrp.aspx

Supran, G., Rahmstorf, S., & Oreskes, N. (2023). Assessing ExxonMobil's global warming projections. *Science*, *379*(6628), eabk0063. https://doi.org/10.1126/science.abk0063

Swabey, P. (2022). *UK blackouts: Data centres should withstand "organised" power outages*. Retrieved March 22, 2024, from https://techmonitor.ai/technology/data-centre/uk-blackouts-data-centres-organised

Switanek, M. B., Troch, P. A., Castro, C. L., Leuprecht, A., Chang, H.-I., Mukherjee, R., & Demaria, E. M. C. (2017). Scaled distribution mapping: A bias correction method that preserves raw climate model projected changes. *Hydrology and Earth System Sciences*, *21*(6), 2649–2666. https://doi.org/10.5194/hess-21-2649-2017

Taleb, N. N. (2007). *The Black Swan: The Impact of the Highly Improbable*. Random House Publishing Group.

Taszarek, M., Pilguj, N., Allen, J. T., Gensini, V., Brooks, H. E., & Szuster, P. (2021). Comparison of Convective Parameters Derived from ERA5 and MERRA-2 with Rawinsonde Data over Europe and North America. *Journal of Climate*, *34*(8), 3211–3237. https://doi.org/10.1175/JCLI-D-20-0484.1

Taylor, J. W., & Buizza, R. (2003). Using weather ensemble predictions in electricity demand forecasting. *International Journal of Forecasting*, *19*(1), 57–70. https://doi.org/10.1016/S0169-2070(01)00123-6

Teutschbein, C., & Seibert, J. (2012). Bias correction of regional climate model simulations for hydrological climate-change impact studies: Review and evaluation of different methods. *Journal of Hydrology*, *456–457*, 12–29. https://doi.org/10.1016/j.jhydrol.2012.05.052

The pandas development team. (2020). *Pandas-dev/pandas: Pandas* (Version latest). https://doi.org/10.5281/zenodo.3509134

Thompson, V., Dunstone, N. J., Scaife, A. A., Smith, D. M., Slingo, J. M., Brown, S., & Belcher, S. E. (2017). High risk of unprecedented UK rainfall in the current climate. *Nature Communications*, *8*(1), 107. https://doi.org/10.1038/s41467-017-00275-3

Thornton, H. E., Hoskins, B. J., & Scaife, A. A. (2016). The role of temperature in the variability and extremes of electricity and gas demand in Great Britain. *Environmental Research Letters*, *11*(11), 114015. https://doi.org/10.1088/1748-9326/11/11/114015

Tripathi, O. P., Charlton-Perez, A. J., Sigmond, M., & Vitart, F. (2015). Enhanced long-range forecast skill in boreal winter following stratospheric strong vortex conditions. *Environmental Research Letters*, *10*(10), 104007. https://doi.org/10.1088/1748-9326/10/10/104007

UN Department of Economic and Social Affairs. (2023). *The Sustainable Development Goals Report 2023: Special Edition*. United Nations. https://doi.org/10.18356/9789210024914

UN Office for Disaster Risk Reduction. (2022). *Principles for resilient infrastructure*. Retrieved March 18, 2024, from http://www.undrr.org/publication/principles-resilient-infrastructure

UNFCCC. Secretariat. (2016). *Report of the Conference of the Parties on its twenty-first session, held in Paris from 30 November to 13 December 2015. Addendum. Part two: Action taken by the Conference of the Parties at its twenty-first session. | UNFCCC* (Session and meeting reports). Paris Climate Change Conference - November 2015. Retrieved February 11, 2024, from https://unfccc.int/documents/9097

US EPA, O. P. (2014). *Economics of Biofuels*. Retrieved March 24, 2024, from https://www.epa.gov/environmental-economics/economics-biofuels

van der Wiel, K., Bloomfield, H. C., Lee, R. W., Stoop, L. P., Blackport, R., Screen, J. A., & Selten, F. M. (2019). The influence of weather regimes on European renewable energy production and demand. *Environmental Research Letters*, *14*(9), 094010. https://doi.org/10.1088/1748-9326/ab38d3

van der Wiel, K., Selten, F. M., Bintanja, R., Blackport, R., & Screen, J. A. (2020). Ensemble climate-impact modelling: Extreme impacts from moderate meteorological conditions. *Environmental Research Letters*, *15*(3), 034050. https://doi.org/10.1088/1748-9326/ab7668

van Leeuwen, P. J. (2020). A consistent interpretation of the stochastic version of the Ensemble Kalman Filter. *Quarterly Journal of the Royal Meteorological Society*, *146*(731), 2815–2825. https://doi.org/10.1002/qj.3819

Vitart, F. (2014). Evolution of ECMWF sub-seasonal forecast skill scores. *Quarterly Journal of the Royal Meteorological Society*, *140*(683), 1889–1899. https://doi.org/10.1002/qj.2256

Vitart, F., & Robertson, A. W. (2018). The sub-seasonal to seasonal prediction project (S2S) and the prediction of extreme events. *npj Climate and Atmospheric Science*, *1*(1), 1–7. https://doi.org/10.1038/s41612-018-0013-0

Vitart, F., & Takaya, Y. (2021). Lagged ensembles in sub-seasonal predictions. *Quarterly Journal of the Royal Meteorological Society*, *147*(739), 3227–3242. https://doi.org/10.1002/qj.4125

Wang, Y., Hu, Q., Li, L., Foley, A. M., & Srinivasan, D. (2019). Approaches to wind power curve modeling: A review and discussion. *Renewable and Sustainable Energy Reviews*, *116*, 109422. https://doi.org/10.1016/j.rser.2019.109422

Watson, H. (2022). *How BT Group is making our networks more energy efficient*. BT Group Newsroom. Retrieved May 19, 2023, from https://newsroom.bt.com/how-bt-group-is-making-our-networks-more-energy-efficient/

Weber, J., Wohland, J., Reyers, M., Moemken, J., Hoppe, C., Pinto, J. G., & Witthaut, D. (2018). Impact of climate change on backup energy and storage needs in wind-dominated power systems in Europe (V. Magar, Ed.). *PLOS ONE*, *13*(8), e0201457. https://doi.org/10.1371/journal.pone.0201457

Weisang, G., & Awazu, Y. (2008). Vagaries of the Euro: An introduction to ARIMA modeling. *Case Studies In Business, Industry And Government Statistics*, *2*(1), 45–55.

Wells, E. M., Boden, M., Tseytlin, I., & Linkov, I. (2022). Modeling critical infrastructure resilience under compounding threats: A systematic literature review. *Progress in Disaster Science*, *15*, 100244. https://doi.org/10.1016/j.pdisas.2022.100244

Werner, P. C., & Gerstengarbe, F.-W. (2010). Katalog der Großwetterlagen Europas nach Paul Hess und Helmuth Brezowsky:(1881-2009). *Potsdam Intitute for Climate Impact Research*, (7). Retrieved July 17, 2024, from https://d-nb.info/100775043X/34

White, C. J., Carlsen, H., Robertson, A. W., Klein, R. J. T., Lazo, J. K., Kumar, A., Vitart, F., Perez, E. C. de, Ray, A. J., Murray, V., Bharwani, S., MacLeod, D., James, R., Fleming, L., Morse, A. P., Eggen, B., Graham, R., Kjellström, E., Becker, E., … Zebiak, S. E. (2017). Potential applications of subseasonal-to-seasonal (S2S) predictions. *Meteorological Applications*, *24*(3), 315–325. https://doi.org/10.1002/met.1654

WHO, the World Bank, IRENA & SEforALL. (2023). *Energizing health: Accelerating electricity access in health-care facilities*. World Health Organization, the World Bank, Sustainable Energy for All and the International Renewable Energy Agency. Retrieved January 25, 2024, from https://www.who.int/publications-detail-redirect/9789240066960

Wilkinson, D. J. (2018). *Stochastic Modelling for Systems Biology, Third Edition* (3rd ed.). Chapman and Hall/CRC. https://doi.org/10.1201/9781351000918

Wilks, D. S. (2008). Effects of stochastic parametrization on conceptual climate models. *Philosophical Transactions of the Royal Society A: Mathematical, Physical and Engineering Sciences*, *366*(1875), 2475–2488. https://doi.org/10.1098/rsta.2008.0005

Wood, S. N. (2017). *Generalized Additive Models: An Introduction with R, Second Edition* (2nd ed.). Chapman and Hall/CRC. https://doi.org/10.1201/9781315370279

World Meteorological Organization. (2023). *Global Framework for Climate Services (GFCS)*. World Meteorological Organization. Retrieved February 12, 2024, from https://wmo.int/site/global-framework-climate-services-gfcs

Zachary, S., Wilson, A., & Dent, C. (2022). The Integration of Variable Generation and Storage into Electricity Capacity Markets. *The Energy Journal*, *43*(4). https://doi.org/10.5547/01956574.43.4.szac

Zeyringer, M., Price, J., Fais, B., Li, P.-H., & Sharp, E. (2018). Designing low-carbon power systems for Great Britain in 2050 that are robust to the spatiotemporal and inter-annual variability of weather. *Nature Energy*, *3*(5), 395–403. https://doi.org/10.1038/s41560-018-0128-x

Zhang, X., Shahidehpour, M., Alabdulwahab, A., & Abusorrah, A. (2016). Hourly Electricity Demand Response in the Stochastic Day-Ahead Scheduling of Coordinated Electricity and Natural Gas Networks. *IEEE Transactions on Power Systems*, *31*(1), 592–601. https://doi.org/10.1109/TPWRS.2015.2390632

Zscheischler, J., Westra, S., van den Hurk, B. J. J. M., Seneviratne, S. I., Ward, P. J., Pitman, A., AghaKouchak, A., Bresch, D. N., Leonard, M., Wahl, T., & Zhang, X. (2018). Future climate risk from compound events. *Nature Climate Change*, *8*(6), 469–477. https://doi.org/10.1038/s41558-018-0156-3

Datasets

`BT meter readings` Fibre to the Cabinet and Buildings metered demand data for the British Telecommunications PLC (BT) estate spanning April 2015 to July 2021. Half-hourly interval data aggregated, to Distribution Network Operator zones, covers the majoirty of consumption but excludes non-half-hourly and unmetered supplies.

Proprietary Dataset: confidential dataset sourced by agreement with BT. 72

`ERA5` The European Centre for Medium-Range Weather Forecasts atmospheric reanalysis of the global climate, version 5 (ERA5) spanning 1940 to present.

Available from: Copernicus Climate Data Store

(Hersbach et al., 2020) 57, 59, 185

`MERRA-2` The Modern-Era Retrospective analysis for Research and Applications, version 2 (MERRA-2), is a global reanalysis product spanning 1980 to present, produced by NASA's Global Modeling and Assimilation Office (GMAO).

Available from: Goddard Earth Sciences Data and Information Services Center

(Gelaro et al., 2017) 57, 59, 74–76, 81, 94, 110, 114, 116, 117, 126, 127, 132, 185

`UKCP18` The UK Climate Projections (UKCP) is a set of tools and data designed to help decision-makers assess their risk exposure to climate published by the UK Met Office. The 2018 release (UKCP18) uses cutting-edge climate science to provide climate change projections out to 2100 in the UK and globally.

Available from: UK Climate Projections User Interface

(Lowe et al., 2018) 61–63, 108–113, 121–124, 126–129, 132, 133, 167, 172

Bloomfield et al. (2020), `MERRA-2 derived demand, wind and solar power` The `MERRA-2` reanalysis data (1980-2018) has been used to calculate the hourly, country aggregated

wind and solar power generation for 28 European countries based on a distribution of wind and solar farms which is considered to be representative of the current situation (2017). In addition a corresponding daily time series of nationally aggregated electricity demand is provided. The data sets have been produced to investigate the inter-annual variability of the three weather-dependent power system components.

Available from: University of Reading Research Data Archive

(Bloomfield, Brayshaw & Charlton-Perez, 2020) 28

Deakin et al. (2022), `Aggregated Generator Unavailability Data` This dataset compiles estimated generator unavailability for eight countries in Northwest Europe, plus Spain. The advantages and limitations of the data are described in detail in the paper submitted to the PMAPS 2022 (Manchester) conference, "Comparing Generator Unavailability Models with Empirical Distributions from Open Energy Datasets" (submitted); the code used to generate the csvs in this dataset are provided at https://github.com/deakinmt/entsoe_outage_models.

Available from: Newcastle University data.ncl

(Deakin & Greenwood, 2022) 141

SOFTWARE

python A versatile and powerful general-purpose programming language.

Available from: https://python.org (Shaw, 2017)

numpy The fundamental package for scientific computing with Python.

Available from: https://numpy.org (Harris et al., 2020)

xarray A Python library that supports labelled multi-dimensional arrays.

Available from: https://xarray.dev (Hoyer & Hamman, 2017)

pandas A tool for data analysis and manipulation, built on top of Python.

Available from: https://pandas.pydata.org (The pandas development team, 2020)

statsmodels A Python module that provides classess and functions for the estimation of many different statistical models and tests.

Available from: https://statsmodels.org (Seabold & Perktold, 2010)

matplotlib A graphics package for data visualisation in Python.

Available from: https://matplotlib.org (Hunter, 2007)

LaTeX A high-quality typesetting system that produces technical and scientific documents.

Available from: The Comprehensive TeX Archive Network (Knuth & Bibby, 1986)

Vim A highly configurable text editor built to make creating and changing any kind of text very efficient.

Available from: https://www.vim.org

Zotero Free, easy-to-use tool to collect, organise, annotate, cite, and share research.

Available from: https://www.zotero.org

GLOSSARY

Capacity Market Renumeration mechanism that provides payment for reliable sources of capacity, alongside electricity revenues to improve national security of supply. 3, 6, 41–44, 147, 148, 152, 168, 169

Critical Infrastructure Systems and assets that are deemed vital for the functioning of a society, economy, or nation. 1, 2, 5, 19, 20, 23, 24, 35, 68, 70, 96–98, 166, 168, 172

Electricity load The total electrical power demand that must be balanced by dispatchable generation. Sometimes refers to the electricity demand alone, or may refer to the demand-net-renewables. 35, 48

Energy Science Interdisciplinary study of energy production, conversion, distribution and utilisation. 5, 7, 11

Merit Order A way of ranking available sources of energy based on ascending operational cost. 26, 40

Primary Energy Energy found in nature in its original, unprocessed form. This can be from renewable or non-renewable sources. 7

Re-analysis Archived observations are used in forecast models and data assimilation systems, creating global datasets of the historic atmosphere, land surface, and oceans conditions. 3, 5, 15, 16, 27, 32, 57–59, 66, 110–112, 114, 121, 132, 166, 167, 169–171

Acronyms and Abbreviations

Calendar

DJF December January February 85, 86

JJA June July August 85

MAM March April May 85

SON September October November 85

Meteorological

CDD Cooling Degree Day 28, 29, 77, 78, 89, 94, 101, 102, 120, 230

GCM Global Climate Model 59–62, 109, 112

HDD Heating Degree Day 28, 29, 77, 78, 94, 101, 102, 120, 123, 173, 230

NAO North Atlantic Oscillation 48, 54

NWP Numerical Weather Prediction 16, 27, 51–54, 57, 63, 68

PPE Perturbed Physics Ensemble 62, 109, 110, 114–128, 131, 132, 136, 167, 168, 171, 172

RCM Regional Climate Model 61–63

S2S Sub-seasonal to Seasonal 50, 53–56, 173

Methods

EENS Expected Energy Not Served 140, 145, 146, 149–151

EFC Equivalent Firm Capacity 146, 150, 153

ENS Energy Not Served 141, 168, 169

LCoE Levelised Cost of Electricity 9–11, 35, 36, 68

LCoS Levelised Cost of Storage 35, 36

LOL Loss of Load 141

LOLE Loss of Load Expectation 140, 141, 145, 146, 149

NPV Net Present Value 9, 35, 36

Organisations

BT British Telecommunications PLC 1, 3, 24, 29, 70, 72, 76, 78, 79, 86, 89, 94, 98, 116, 143, 152, 158, 159, 166, 168, 169, 223

C3S Copernicus Climate Change Service 29, 30

ECMWF European Centre for Medium-Range Weather Forecasts 53, 55, 57

ENTSO-E European Network of Transmission System Operators 16, 29, 30, 34

Met Office Met Office 50, 53, 54, 57, 60, 63

National Grid ESO National Grid Electricity System Operator 43, 44, 76, 148

Policy

EU European Union 34, 44

GB Great Britain 1, 3, 24, 26, 32, 34, 43, 70, 76, 78, 81–83, 86, 89, 90, 92, 94–96, 98, 106, 110, 112, 116, 117, 119, 120, 123, 125–128, 138, 139, 141–143, 147, 149–152, 158, 159, 166, 168

NDC Nationally Determined Contribution 21

SDG Sustainable Development Goal 18–20

UK United Kingdom of Great Britain and Northern Ireland 20, 30, 34, 35, 42–44, 46, 53, 61, 63, 72, 108, 139, 148, 153, 155, 172, 179

UN United Nations 18, 22

Power System Operation

DER Distributed Energy Resource 26, 33, 43–46

DFS Demand Flexibility Service 148, 153, 154, 156, 157, 159, 161

DNO Distribution Network Operator 32–34, 72, 74, 100, 166, 169, 170

DSO Distribution System Operator 26, 32–34, 44–46, 170

ESO Electricity System Operator 26, 32–34, 43, 44

li-ion Lithium-Ion 36–38, 68

PV Photovoltaic 8, 10

STOR Short Term Operating Reserve 148, 153, 154, 157, 159

TSO Transmission System Operator 3, 6, 32–35, 44–46, 55, 76, 144, 148, 168, 169

Statistical

SYMBOLS

Sign	Description	Unit
α	Demand-Temperature Coupling Coefficient	$\%\,°\mathrm{C}^{-1}$
C	Coincident reserve-exceedance indicator	—
$\mathcal{D}$	Electricity demand (anomaly)	$\%$
D	Electricity demand	kW
E	Electricity energy consumption	kWh
P_R	Probability of reserve, $\langle R \rangle$	$\%$
$\mathbb{P}_C$	Probability of coincidence, $\langle C \rangle$	$\%$
$\mathbb{P}_X$	Probability of exceedance, $\langle X \rangle$	$\%$
R	Reserve indicator	—
S	Surplus capacity	kWh
T_{CDD}	Cooling Degree Day temperature threshold	$°\mathrm{C}$
T_{HDD}	Heating Degree Day temperature threshold	$°\mathrm{C}$
T	Temperature	$°\mathrm{C}$
X	Reserve-exceedance indicator (Chapters 3 and 4)	—
X	Dispatchable Generation Capacity (Chapter 5)	GWh
Y	Instantaneous Renewable Generation Capacity	GWh
Z	System Margin	GWh

Copyright